Medical University of South Carolina

MEDICA

MUSC Theses and Dissertations

2003

Structure and Functional Effects of Age-Related Posttranslational Modifications of Aquaporin 0 in the Normal Human Lens

Lauren Elizabeth Smith-Ball
Medical University of South Carolina

Follow this and additional works at: https://medica-musc.researchcommons.org/theses

Recommended Citation

Smith-Ball, Lauren Elizabeth, "Structure and Functional Effects of Age-Related Posttranslational Modifications of Aquaporin 0 in the Normal Human Lens" (2003). *MUSC Theses and Dissertations*. 79.
https://medica-musc.researchcommons.org/theses/79

This Dissertation is brought to you for free and open access by MEDICA. It has been accepted for inclusion in MUSC Theses and Dissertations by an authorized administrator of MEDICA. For more information, please contact medica@musc.edu.

STRUCTURE AND FUNCTIONAL EFFECTS OF AGE-RELATED POSTTRANSLATIONAL MODIFICATIONS OF AQUAPORIN 0 IN THE NORMAL HUMAN LENS

By

Lauren Elizabeth Smith Ball

A dissertation submitted to the faculty of the Medical University of South Carolina in partial fulfillment of the requirement for the degree of Doctor of Philosophy in the College of Graduate Studies

Department of Pharmacology, 2003

Approved by:

Chairman, Advisory Committee

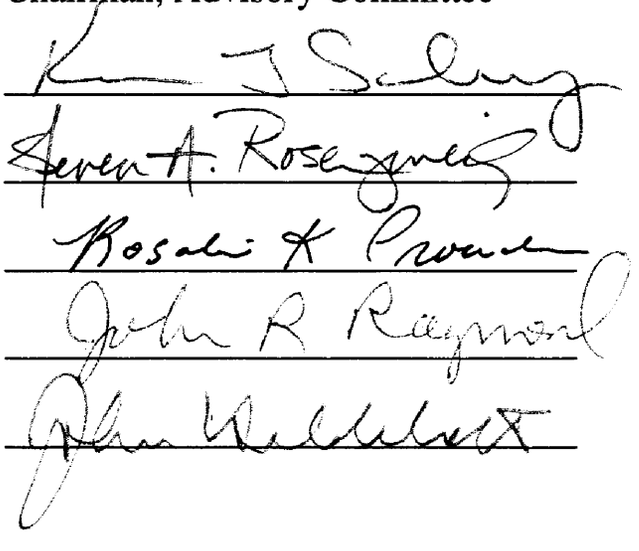

ACKNOWLEDGEMENTS

There are so many people to thank for the experiences and training I have had during my graduate career. I express my sincerest appreciation to my mentor Dr. Kevin Schey. Through his guidance, encouragement, and enthusiasm he stimulated self-motivation and scientific curiosity. His honesty, patience, and kindness contributed to an enjoyable work environment conducive to learning and open scientific discussion. I would also like to thank Dr. Rosalie Crouch for her valuable suggestions and encouraging words. Her gentle persistence coupled with enthusiasm for discovery is truly inspiring. I will never forget the "just try it one more time" that finally worked! Dr. John Hildebrandt for his dedication to teaching and training and for his encouragement of critical thinking while also sparking the imagination. Dr. Mark Nowak for his generous assistance with the molecular biology and *Xenopus* work. Dr. John Raymond for his critical evaluation and valuable suggestions at committee meetings. I would also like to express my gratitude to Dr. Dan Knapp for introducing me to the power of mass spectrometry and to the department of pharmacology. His creativity inspires one to keep an open mind and look beyond the present. I would also like to thank other faculty members of the pharmacology department for excellent instruction and past and present members of the department including Laura Bolchoz, Ryan Carnegie, Lana Cook, Kuruppu Dharmasiri, Eric Finley, Rick Francis, Kristen French, Cliff Harvey, Kristie Lindsey, John Oatis, Severine Patat, Nicole Redmond, Xin Wang, and Chris Wells for their help, support, and friendship through the years.

Scientists and technical experts who contributed materials or their expertise to this work include Dr. Donna Garland, Dr. Kirsten Lampi, Mark Little, Dr. Swamy-Mruthini, Jim Nicholson, Dr. Craig Crosson, Dr. Jim McLaughlin, Dr. Rebbeca Ettling, Dr. John Zhang, and Margaret Romano.

I am very grateful for the support and encouragement of my family, Nat IV, Patrick, Beverly, Paul, Star, Nat III, Jane, Janie, Anthony, Betty, and George. My husband Nat has sacrificed in many ways to enable me to pursue my goal of a career in scientific research. He coached me through many hard times always focusing my attention and efforts on the immediate task at hand. I know he learned more about mass spectrometry, water channels, and raising frogs than he had ever anticipated! Thank you Nat, I love you so much. A special thanks also goes to my mother for her encouragement and belief in us. She always taught us to persevere and finish what we started which came in especially handy during my graduate training!

TABLE OF CONTENTS

ACKNOWLEDGEMENTS.....ii

LIST OF TABLES.....vii

LIST OF FIGURES.....viii

ABBREVIATIONS.....xi

ABSTRACT.....xiii

CHAPTER 1- LITERATURE REVIEW.....1

I. Introduction.....2

II. Lens.....3

A. Anatomy of the Eye and General Properties of the Lens.....3

B. Development of the Lens.....4

1. Lens Anatomy.....4

2. Formation of the Organelle Free Zone.....6

3. Changes in Cell Morphology with Fiber Cell Age.....7

C. Lens Physiology and Transport within the Lens.....8

1. Glucose Requirements.....8

2. An Active Internal Circulatory System.....9

3. Movement of Water within the Lens and Development of a Barrier to Transport.....13

4. Components of the Circulatory System.....14

D. Age-Related Changes in Fiber Cell Membrane Lipid Composition...19

E. Age-Related Changes in Lens Protein Structure and Function.....20

1. Backbone cleavage (Enzymatic).....21

a. Proteases in the lens.....22

2. Spontaneous Age-related Posttranslational Modifications.....23

a. Deamidation.....24

b. Isomerization and Racemization of Aspartic acid.....24

c. Spontaneous Backbone Cleavage.....28

3. Detection of Age-related Posttranslational Modifications.....28

E. Diseases of the Lens.....30

1. Cataract.....30

2. Presbyopia.....33

III. The Aquaporins 35

A. Discovery of Aquaporins 35

B. Sequence and Structure of the Aquaporins and AQP0 36

1. Sequence Similarities and the Aquaporin Family 36

2. Tissue Distribution and Physiological Significance.....37

3. Aquaporin Structure 41

4. Pore of the Channel.....43

5. Regulation of Aquaporin Water Permeability.....45

IV. Aquaporin 0.....49

A. General Introduction 49

B. Cataractogenic Mutations linked to Mouse and Human AQP0.....50

C. Postulated Roles of AQP0 in the Lens.....53

1. Water Transporting Properties of AQP0.....53

2. Structural Role of AQP0.....56

3. Ion Channel.....58

4. Transport of Small Neutral Molecules.....58

D. Posttranslational Modifications of AQP0 59

1. Phosphorylation.....59

2. Age-Related Deamidation.....60

3. Age-Related Protein Truncation.....60

4. Truncation of AQP0 in Animal Models of Cataract and in Opaque Regions of Human Lenses..... 66

CHAPTER 2 HYPOTHESIS AND SPECIFIC AIMS 69

CHAPTER 3 The Distribution Of Posttranslationally Modified Products of AQP0 within the Human Lens.....72

INTRODUCTION.....73

EXPERIMENTAL METHODS.....76

RESULTS.....80

DISCUSSION.....110

CHAPTER 4 The Water Permeability of Human AQP0.....118

INTRODUCTION.....119

EXPERIMENTAL METHODS.....124

RESULTS.....138

DISCUSSION.....151

CHAPTER 5 The Effect of Posttranslational Modifications on

the Water Permeability of Human AQP0.....156

INTRODUCTION..... 157

EXPERIMENTAL METHODS.....161

RESULTS.....165

DISCUSSION.....175

CHAPTER 6 DISCUSSION.....178

CHAPTER 7 FUTURE DIRECTIONS.....193

APPENDIX 1: Labview Program.....201

LIST OF REFERENCES.....222

LIST OF TABLES

1.1 Distribution of Aquaporins in the Eye 40

3.1 Mass Measurements of Intact and Truncated Forms of AQP0 by MALDI-MS.....86

3.2 Changes in the Percent Phosphorylation of Serine Residues 235, 229, and 231 With Fiber Cell Age in Sections of a 34 Year Old Lens 95

3.3. Changes in the Relative Abundance of Truncated Forms of the C-terminal Peptide 239-263 with Fiber Cell Age in Sections of a 34 Year Old Lens.....99

3.4. Changes in the Relative Abundance of Truncated Forms of the C-terminal Peptide 239-263 with Fiber Cell Age in Sections of a 35 Year Old Lens 100

3.5. Changes in the Relative Abundance of Truncated Forms of the C-terminal Peptide 239-263 with Fiber Cell Age in Sections of a 38 Year Old Lens 101

3.6 Changes in the Relative Levels of Isomerized and Racemized Aspartic acid 243 in the Truncated Peptide 239-244 with Fiber Cell Age in 34, 35, and 38 Year Old Lens Sections.....109

3.7 Summary Table of Previously Identified and Novel Sites of Posttranslational Modifications Observed in the C-terminus of Human AQP0.....112

4.1 Comparison of Osmotic Membrane Water Permeability Measurements with Literature Values.....152

6.1. Summary of Posttranslational Modifications Identified in AQP0 and the Effects of Particular Modifications on Water Channel Activity.....181

LIST OF FIGURES

1.1. Diagrammatic Sections of the Eye and Lens.....5

1.2 Proposed Model of Circulation through the Lens.....11

1.3 Proposed Model of Circulation through the Lens Fiber Cells.....12

1.4 Proposed Protein Components of the Internal Circulatory System of the Lens.....15

1.5 Isomerization and Racemization of Aspartic Acid 26

1.6 Deamidation and Spontaneous Truncation of Asparagine 27

1.7 Sequence Alignment of Mammalian Aquaporins.....38

1.8 Human Aquaporin Gene Family 39

1.9 The Monomeric Structure of AQP1.....42

1.10 Sequence and Previously Identified Posttranslational Modifications of Human AQP0.....61

1.11 MALDI-Mass Spectra of an HPLC Fraction Containing C-terminal Peptides of AQP0 from Human Lenses Ranging in Age from 7 to 86..... 64

1.12 MALDI-Mass Spectra of C-terminal Peptides of AQP0 from a 27 Year Old Lens.....65

1.13 Sequence Alignment of Aquaporin 0 from Different Species.....68

3.1 MALDI-MS of Membrane Protein Isolated from Four Concentric Sections of a 35 year old lens.....83

3.2 MALDI-MS of Membrane Protein Isolated from Four Concentric Sections of a 38 year old lens.....84

3.3 MALDI-MS of Membrane Protein Isolated from Three Concentric Sections of a 34 year old lens.....85

3.4 Expected Tryptic Peptides Released from Membrane Embedded AQP0.....88

3.5 MALDI-MS Of Membrane Protein Isolated from the Outer Cortical Section of a 34 Year Old Lens Before and After Trypsin Digestion 89

3.6 Chromatographic Separation of Tryptic Peptides from AQP0 C-Terminus.....93

3.7 Mass Spectrum and Tandem Mass Spectrum of Phosphorylated AQP0 229-233.....94

3.8 Changes in the Relative Abundance of Truncated Forms of the C-terminal Peptide 239-263 with Fiber Cell Age in 34, 35, and 38 Year old Lenses.....98

3.9 *In vitro* Spontaneous Truncation of a Synthetic Peptide of AQP0 239-263 on the C-terminal Sides of Asn 246 and Asn 259.....103

3.10 Chromatographic Separation of Isomerized and Racemized Aspartic acid 243 with Fiber Cell Age in the 34, 35, and 38 Year Old Lens Sections 106

3.11 Tandem Mass Spectrum of Isomerized Aspartic acid 243 in the Truncated Peptide 239-244 m/z 586.3.....107

3.12 Age-Related Isomerization and Racemization of Aspartic acid 243 in the 34 Year Old Lens and Chromatographic Separation of Isomerized and Racemized Synthetic Peptide 239-244.....108

3.13 Primary Sequence and Newly Identified Sites of Posttranslational Modifications of Human AQP0.....111

4.1 Design of the Human AQP0 Vector Construct.....126

4.2 Anti-AQP0 Polyclonal Antibody Generation.....137

4.3 Permeability of Bovine AQP0 as Measured in the *Xenopus* Oocyte Swelling Assay.....139

4.4 Relative Increase in Oocyte Volume and Osmotic Membrane Permeability of Oocytes Expressing Bovine AQP0.....140

4.5 Human AQP0 cDNA Sequence Results.....142

4.6 Human AQP0 cDNA and Translated Amino Acid Sequence.....143-144

4.7 Relative Increase in Oocyte Volume and Osmotic Membrane Permeability of Oocytes Expressing Human AQP0.....146

4.8 Effect of the Amount of Human AQP0 RNA Injected on Osmotic Membrane Permeability and Protein Expression.....147

4.9 Permeability of Human AQP0 and Human AQP1.....149

4.10 Effect of a Reduced pH on the Permeability of Human AQP0.....150

5.1 Permeability of Wild Type and Mutant AQP0.....166

5.2 Immunofluorescence Staining of Xenopus Oocytes Injected with 10 ng of Wild Type or Mutant AQP0 RNA.....169

5.3 Permeability and Total Protein Expression of Wild Type and Truncated AQP0 1-243.....171

5.4 Expression of Wild Type AQP0 Protein and 1-243 Protein at the Oocyte Surface as Determined by ^{125}I Labeled Antibody Binding.....173

5.5 Effect of Substitution of a Phosphorylation Site on the Water Permeability of AQP0.....174

ABBREVIATIONS

MIP	Major Intrinsic Protein of the lens, also known as MIP26, MP26, Aquaporin 0, AQP0
AQP	Aquaporin
GLUT	Glucose transporter
Cx	Connexin
TFA	Trifluoroacetic acid
HFBA	Heptafluorobutyric acid
MALDI-MS	Matrix Assisted Laser Desorption Ionization mass spectrometry
ESI-MS	Electro-Spray Ionization mass spectrometry
MS/MS	Tandem mass spectrometry
TPA	12-O-tetradecanoyl phorbol-13-acetate

Ala	Alanine (A)
Arg	Arginine (R)
Asn	Asparagine (N)
Asp	Aspartic acid (D)
Cys	Cysteine (C)
Glu	Glutamic acid (E)
Gln	Glutamine (Q)
Gly	Glycine (G)
His	Histidine (H)
Ile	Isoleucine (I)

Leu	Leucine (L)
Lys	Lysine (K)
Met	Methionine (M)
Phe	Phenylalanine (F)
Pro	Proline (P)
Ser	Serine (S)
Thr	Threonine (T)
Trp	Tryptophan (W)
Tyr	Tyrosine (Y)
Val	Valine (V)

Iso-Asp	iso or β-aspartic acid
Asx	Aspartic acid or asparagine
Glx	Glutamic acid or glutamine

Lauren Elizabeth Smith Ball. Structure and functional effects of age-related posttranslational modifications of Aquaporin 0 in the normal human lens. (Under the direction of Kevin L. Schey)

Aquaporin 0 (AQP0, MIP), a water channel protein found in the ocular lens fiber cells, has been proposed to maintain osmotic homeostasis by contributing to an internal circulatory system within the avascular lens. The formation of cataracts in patients with mutations in the AQP0 gene and in heterozygous AQP0 deficient mice suggests that AQP0 is necessary for establishing and preserving lens transparency. Previous structural characterization of AQP0 revealed that the C-terminus, a putative regulatory domain, is subject to many age-related posttranslational modifications. The goal of the present study was to map the spatial distribution of posttranslationally modified forms of AQP0 within normal human lenses and determine the effects of the posttranslational modifications on AQP0 membrane water permeability. Mass spectrometric analysis of AQP0 isolated from concentrically dissected human lenses ages 34, 35, and 38 revealed novel sites of phosphorylation at serines 229 and 231, backbone cleavage at residues 249, 260, 261, and 262, and isomerization/racemization of L-Asp 243 to D-iso-Asp. As anticipated the extent of truncation and isomerization/racemization increased as a function of fiber cell age, whereas the level of phosphorylation was highest in the inner cortex and decreased in the lens nucleus. The water permeability of AQP0 was not affected by substitution of phosphorylation site 231, incorporation of a negative charge at sites of deamidation 246 and 259, nor removal of the C-terminal twenty amino acid residues. These findings suggest that within the human lens modified AQP0 in aged fiber

cells may retain the ability to transport water. Elucidation of the sites and extent of posttranslational modifications of AQP0 revealed that truncation at residues 246 and 259, the most abundant sites of backbone cleavage detected, may occur through a spontaneous truncation event. Identification of an age-related increase in racemized/isomerized D-iso-Asp 243 provides evidence for the presence of protein L-isoaspartate O-methyl transferase, a potentially active protein repair enzyme in the human lens. The results obtained and methods developed in this study provide the groundwork for understanding the structure and function of AQP0 in the normal human lens and future investigation of the role of AQP0 in the development of cataract.

CHAPTER 1

LITERATURE REVIEW

I. Introduction

Aquaporin 0 (AQP0), the most abundant membrane protein in the ocular lens, is crucial for maintaining the transparent nature of the lens. Mutations or a deficiency of the AQP0 protein result in the loss of the focusing ability of the lens and the development of congenital cataracts in humans and mice (1, 2). The role of AQP0, cloned in 1984 (3), remained elusive until the discovery of homologous water permeable proteins, the aquaporins in 1992 (4). AQP0, the only water channel protein found in the lens fiber cells, has been proposed to contribute to the circulation of water and nutrients through the avascular lens (5). The heterogeneous distribution of pumps, ion channels, aquaporins, and gap junctions are thought to generate the driving force and provide a path for circulation through the lens (5). In the human lens, the rate of diffusion of water into the lens nucleus decreases with the age of the lens (6). Likewise, fiber cell membrane water permeability decreases with fiber cell age (7). These changes in fiber cell membrane water permeability correlate with an accumulation of age-related posttranslational modifications in the AQP0 protein (8). The C-terminus of AQP0, a putative regulatory domain, is phosphorylated and undergoes age-related deamidation and extensive truncation (8). The functional consequences of these changes in structure on AQP0 membrane water permeability are not known. Determination of the effects of posttranslational modifications on AQP0 function and characterization of the distribution posttranslationally modified products of AQP0 spatially within a normal human lens may provide insights into the role of AQP0 in maintaining lens transparency.

As an overview, this literature review is aimed at providing a basis for reaching an understanding of the role of aquaporin 0 in the normal aging human lens. First, the

anatomy and physiology of the ocular lens, including the current proposed model of circulation and the potential protein components involved in the internal circulatory system, are described. Second, the biochemical changes observed in aging fiber cells and common age-related posttranslational modifications that accrue in long-lived lens proteins are discussed. Then the discovery, structure, function, and mechanisms of regulation of proteins in the Major Intrinsic Protein/Aquaporin family of transmembrane water channels are introduced. Lastly while the relevance of the presented topics to understanding of the role of AQP0 are addressed throughout the review, details specific to AQP0 are provided in the final section.

II. The Lens

A. Anatomy of the Eye and General Properties of the Lens

Situated behind the iris, the ocular lens is a simple tissue comprised of epithelial cells and fiber cells encased in a collagenous capsule. The lens is suspended between the aqueous and vitreous humors by ligaments that are attached to the capsule (Fig 1.1). The primary function of the lens is to focus and transmit light onto the retina where an image is formed. While the cornea provides the majority of the refractive power to focus light onto the retina, the lens has the ability to accommodate and focus images that are at variable distances. During accommodation, the curvature of the convex lens increases thereby increasing the refractive power of the lens. Under normal resting conditions, the lens is pulled flat by ligaments that are attached to the lens capsule and inserted at the ciliary muscle. As the ciliary muscle contracts, the tension on the lens is released and the

lens becomes more spherical. This increased the refractive index allows one to focus on objects that are nearer the eye (9).

The transparent nature of the lens is compromised by the absorption, reflection-refraction, and/or scattering of light as it passes through the lens (10). The normal human lens is not perfectly transparent. About 5% of the incident light is scattered, which has been attributed to the fiber cell membranes (11). The high protein concentration of the lens crystallins in the lens fiber cells is thought to contribute to the transparency of the cytoplasm. The fiber cells within are densely packed with proteins such that there is not a change in refractive index as light travels through the cytoplasm (11). The fiber cells themselves are tightly packed so as not to scatter light, thus cell volume regulation is crucial for maintaining lens clarity (12).

B. Development of the Lens

1. Lens Anatomy

The avascular lens is a relatively simple tissue comprised of just two cell types. A single layer of epithelial cells lines the anterior surface of the lens and the bulk of the lens is comprised of lens fiber cells (Fig 1.1). The lens develops from embryonic ectoderm and continues to grow throughout one's lifetime. During embryogenesis, primary fiber cells are laid down forming the core of the lens or the embryonic nucleus. As the lens grows, epithelial cells at the lens equator differentiate giving rise to secondary fiber cells that elongate posteriorly and anteriorly covering the lens core. The ends of the long fiber cells meet at the anterior and posterior poles of the lens forming sutures. As the lens grows the branching pattern of the sutures changes resulting in distinct patterns that are

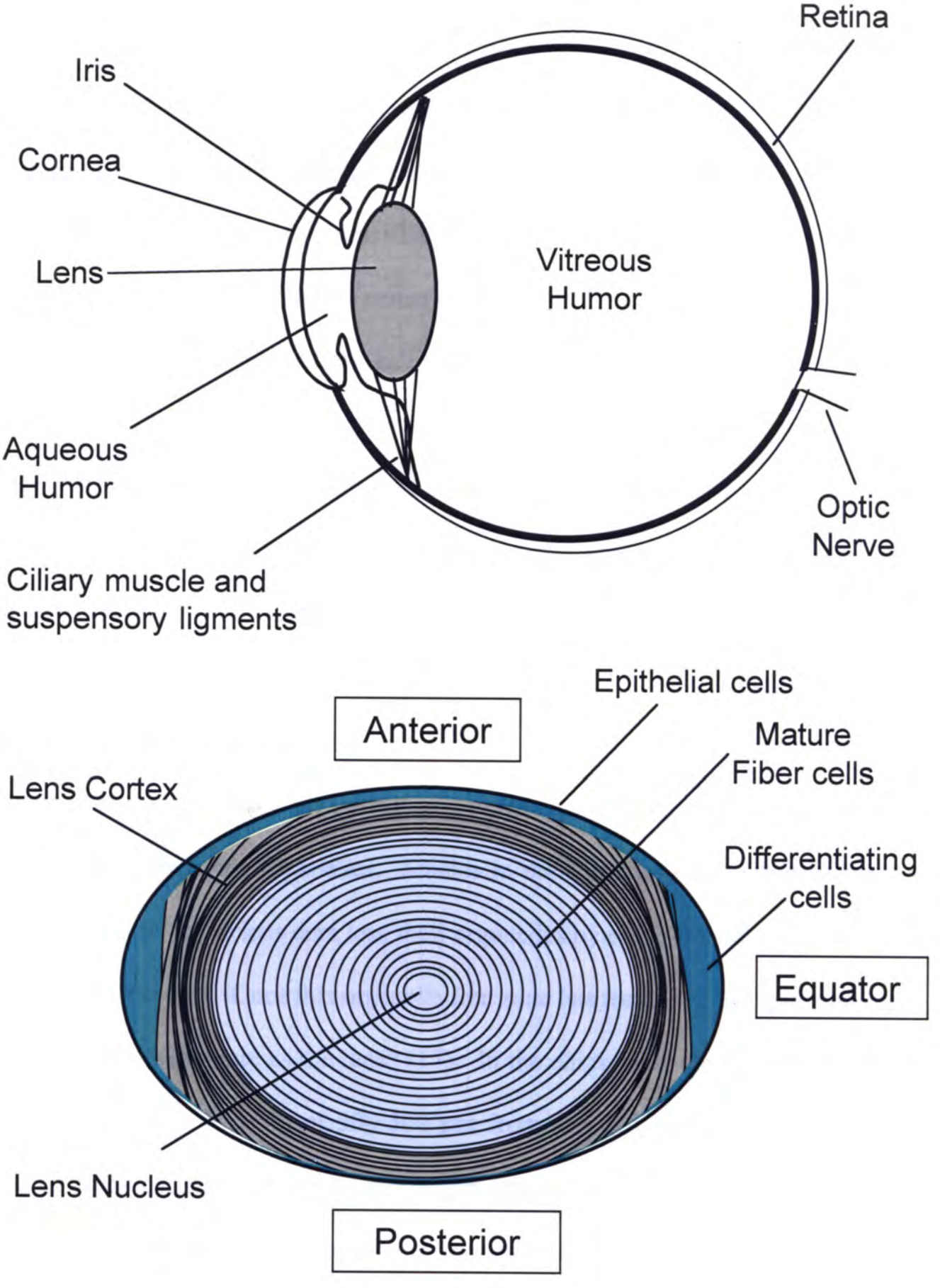

Figure 1.1. Diagrammatic sections of the eye and lens. In the equatorial regions of the lens epithelial cells differentiate into lens fiber cells which elongate toward the anterior and posterior regions of the lens.

associated with the age of the fiber cells (13). As newly differentiated lens fiber cells are deposited on top of existing fiber cells, the older fiber cells are not shed or turned over but compressed toward the center of the lens (14). Since all of the fiber cells formed throughout one's lifetime are retained, the fiber cells within the lens represent various stages of differentiation and maturation. The newly differentiated cells are in the lens periphery and the oldest cells are in the center of the lens. The layers of cells, stacked in concentric shells, result in the "onion-like" appearance of the lens upon cross-section. The human lens is about 9 mm in diameter along the equatorial axis (24). Although the human lens does not grow appreciably in the equatorial dimension, along the visual axis the lens increases about 0.02 mm per year in diameter from ~4 mm at age 10 to ~6 mm at age 90 (15).

2. Formation of the Organelle Free Zone

To maintain transparency the optical axis of the lens is devoid of light scattering elements such as cytoplasmic organelles. Studies in the chick lens have demonstrated that primary fiber cells in the lens core lose their organelles by embryonic day 12 forming an organelle free zone (16). Once this organelle free zone has formed it "increases in size at approximately the same rate as the lens" (17). In the chick lens, the boundary of the organelle free zone is at a depth of 300-500 μm from the lens surface and as newly differentiated fiber cells are buried to this depth they abruptly lose their nuclei and membrane bound organelles. The programmed removal of organelles occurs within 1-2 fiber cell layers (16) and shares characteristics with apoptosis (18). The triggers responsible for organelle degradation are not known. However, the activation of caspases

(19, 20), nucleases, and calpains (21) is thought to be involved. In the normal lens this process appears to be precisely controlled and specific. For instance while organelles are abruptly removed, the actin cytoskeleton remains intact (16). Disruption of the programmed removal of nuclei and organelles from differentiating fiber cells has been associated with the development of congenital cataract in humans and animal models (21, 22).

3. Changes in Cell Morphology with Fiber Cell Age

Upon slit-lamp examination of intact adult lenses, typically four concentric zones of discontinuity within the lens are observed. These zones correspond to fiber cells of the embryonic/fetal nucleus, juvenile nucleus, adult nucleus, and the cortex (23). Along the equatorial axis, the diameters of the embryonic nucleus, fetal nucleus, juvenile nucleus, adult nucleus and cortex observed in a typical 40 year old human lens are 1.5 mm, 4 mm, 5 mm, 7 mm, 9 mm, respectively (24). Each of these zones coincides with a distinct suture pattern permitting the concentric dissection of the regions of the lens (13, 24). Comparisons of the morphology of fiber cells within the deep cortex, adult, juvenile, embryonic and fetal nuclei demonstrate that the cells within each region have different shapes, cross-sectional areas, and interlocking membrane digitations (25). Cortical fiber cells are long, flat, and hexagonal in shape, whereas embryonic and fetal fiber cells are rounded (25). The fiber cells within the adult nucleus have the smallest cross-sectional area suggesting that fiber cell compaction may occur in this zone (25).

C. Lens Physiology and Transport within the Lens

The removal of light scattering organelles and the lack of blood vessels, both prerequisites for maintaining transparency, pose unique physiological problems to the lens. With the elimination of mitochondria and the electron transport chain, mature fiber cells rely on the metabolism of glucose by glycolysis for energy (11). The lens requires an internal circulatory system to facilitate the exchange of solutes, ions, and nutrients to maintain osmotic balance. Since the protein of interest, AQP0, has been proposed to play a role in lens circulation (5, 12), the current models of an internal circulatory system within the lens and the spatial distribution of components of this circulatory system will be discussed.

1. Glucose Requirements

Metabolism of glucose by glycolysis provides about two-thirds of the energy generated in the lens, while the remaining ATP is generated by oxidative phosphorylation in the epithelial cells and outer fiber cells (11). With glucose as the primary source of energy, several mechanisms have been proposed to describe how glucose is transported to the inner fiber cells. The aqueous humor provides glucose at blood glucose concentration, to the epithelial cells, which are equipped with GLUT1 for glucose uptake (26). The transport of glucose from the anterior lens surface to the fiber cells has been suggested to occur by passive diffusion or active transport through paracellular and/or transcellular routes. Based on the size of the lens and the rate of glucose uptake, calculations predict that if glucose were transported by simple diffusion alone the glucose would be depleted within the outer 10% of the lens (27). Therefore, paracellular

diffusion of glucose alone would not be adequate to supply the inner fiber cells with glucose. An alternative mechanism of glucose transport was proposed based on the observation of extensive gap junctional coupling within the lens. Transcellular transport of glucose from epithelial cells to the lens fiber cells was predicted to occur through the gap junctions (28). However, studies have since shown that the anterior epithelial cells are not coupled to the fiber cells by gap junctions (29). In addition, the identification of GLUT3, a high affinity glucose transporter, in inner lens fiber cells indicates that these cells are not dependent on the epithelial cells for glucose uptake (26). Proposed models of active transport of nutrients and glucose through the lens are discussed below.

2. An Active Internal Circulatory System

More recently, proposed hypotheses involve an active internal circulatory system that moves nutrients and glucose through the lens in a paracellular (27) or a combination of paracellular and transcellular pathways (5). There have been several hypotheses of active transport describing how nutrients, carried by the bulk flow of water, are transported from the metabolically active, peripheral fiber cells to the central fiber cells. One hypothesis suggested an anterior to posterior trans-lens flux of water and nutrients from the aqueous humor to the vitreous humor (30). This model, once questioned since the flux, as measured in a Ussing chamber, may have been induced by the experimental apparatus (12) is consistent with results obtained recently in a trans-lens flux assay (27). In this experiment, an anterior to posterior trans-lens flux of similar magnitude was observed in a rabbit lens regardless of the direction of the hydrostatic pressure head (27). The trans-lens flux was observed in the absence of an osmotic gradient and could be

blocked by mercurials, nonspecific but potent inhibitors of AQP1. Based on the rate of flux through the lens, a complete exchange of extracellular fluid every 2 hours was estimated (27). This estimation is supported by the rate of water transport into young (27 year old) human lenses observed by magnetic resonance imaging (6).

Observations that ionic currents circulating around the lens were directed inward at the anterior and posterior poles and outward at the equator led to an alternative hypothesis (31). Put forth by Mathias *et al*, this model is based on electrophysiological measurements recorded in different regions of the lens and the asymmetric spatial distribution of ion pumps, ion channels, and gap junctions in the lens. The model implies that ion pumps and channels in the epithelial cells and cortical fiber cells establish an electromotive potential for flow and that gap junctions and aquaporins create a path for flow resulting in an influx of water at the anterior and posterior poles of the lens and efflux at the equatorial poles of the lens (Fig 1.2) (for reviews see (5, 12)). In this model an ionic current primarily carried by sodium convects water and nutrients through the lens (5). The current enters the lens at the anterior and posterior poles and travels paracellularly toward the center of the lens. Eventually it traverses the fiber cell membrane through sodium and chloride leak channels into the fiber cells (5). The current then moves toward the equator through the extensive network of gap junctions that connect the fiber cells (5) (Fig 1.3). This process is thought to be driven by Na/K ATPases and facilitated by gap junctions, both of which are concentrated at the lens equator. In this model, the extracellular flow of water delivers nutrients to the deeper-lying fiber cells, while the intracellular flow removes metabolic wastes (Fig 1.4). Studies by Zampighi *et al* characterizing the spatial distribution of gap junctions, tight junctions,

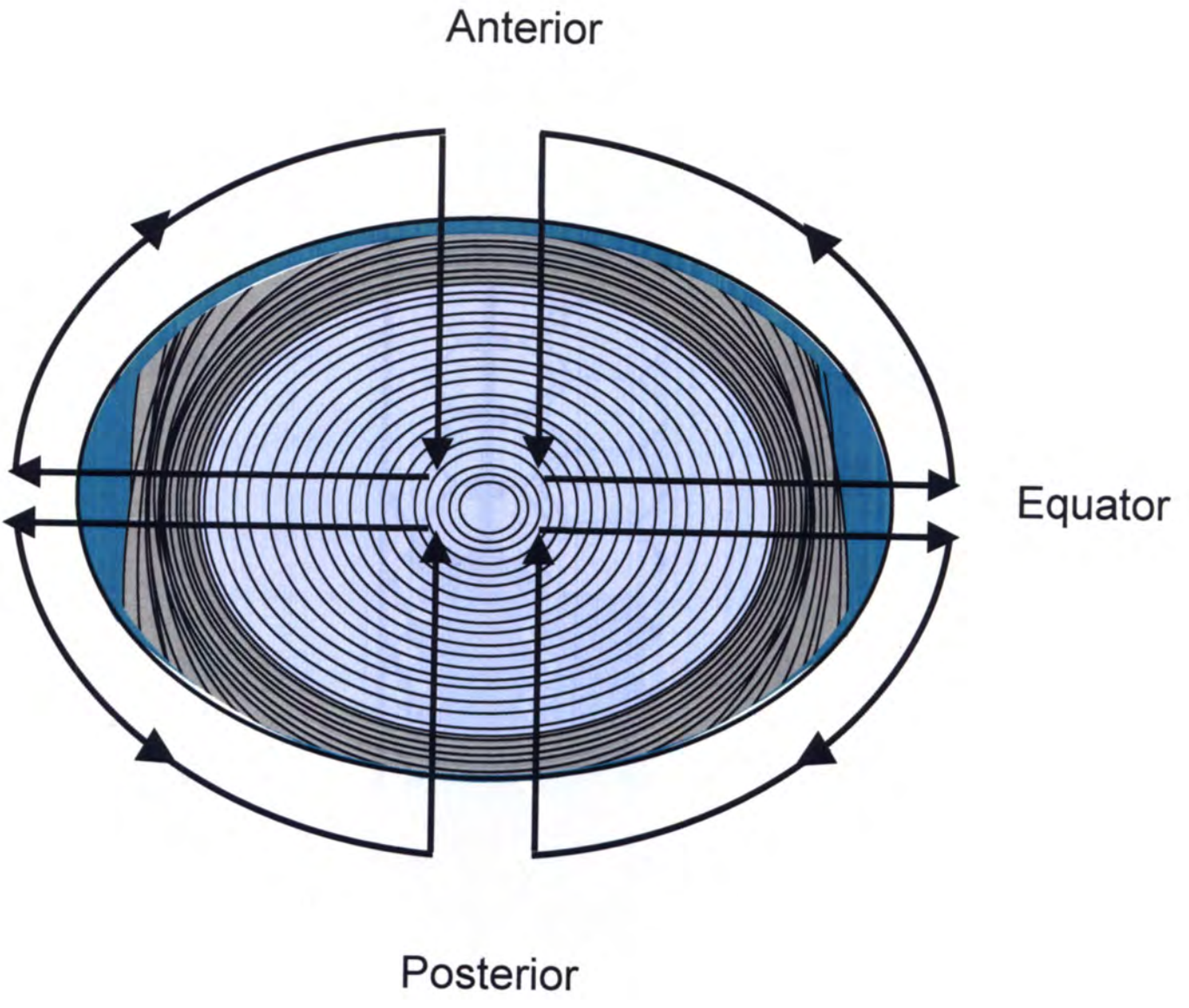

Figure 1.2. Proposed model of circulation through the lens. Structure of the mammalian lens showing the architecture of the lens with epithelial cells, differentiating fiber cells, and mature fiber cells in the center of the lens. The proposed direction of flow through the lens is superimposed. Based on a figure from reference #43.

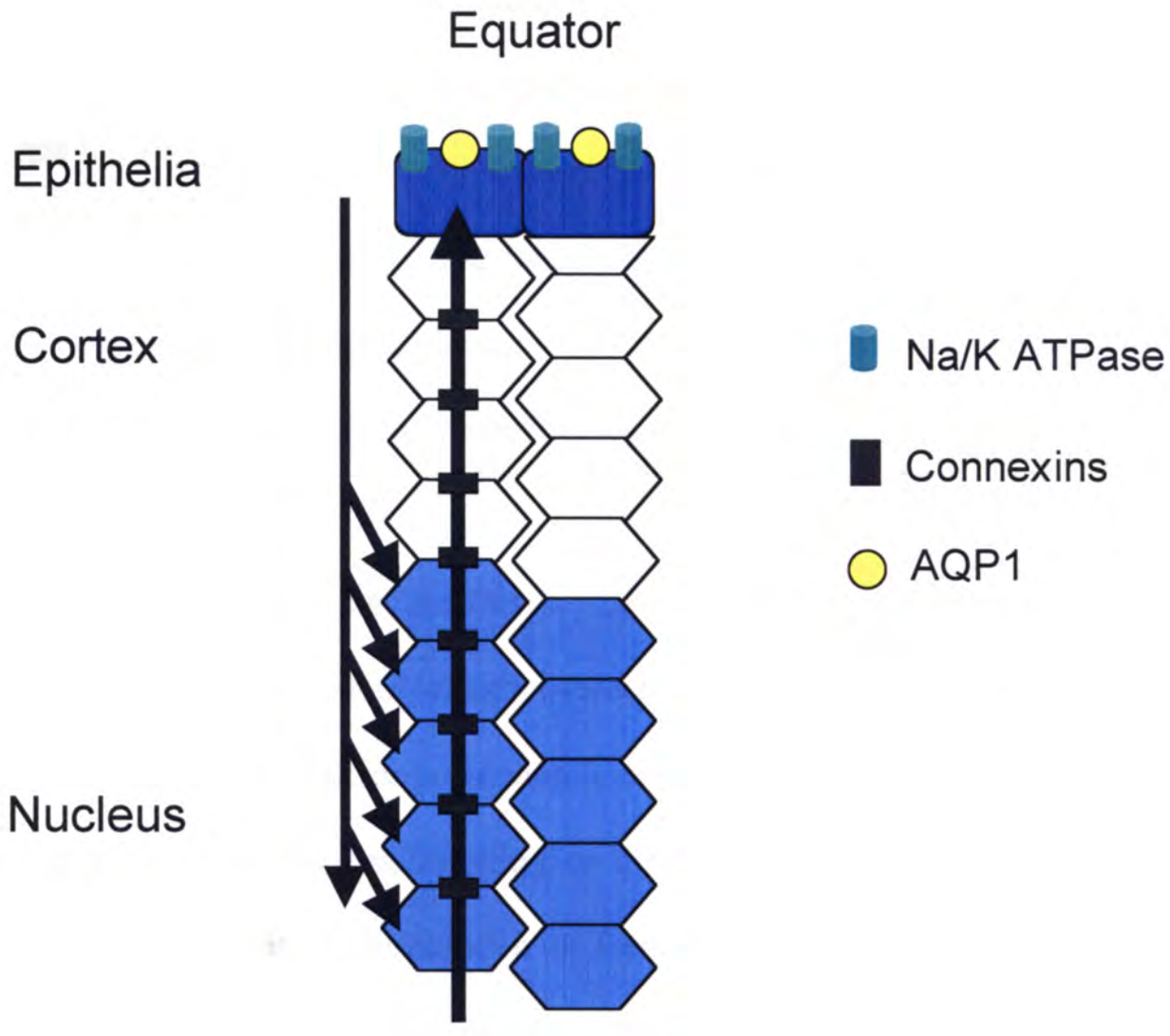

Figure 1.3. Proposed model of circulation through the lens fiber cells. Cross-section through fiber cells illustrating the paracellular and transcellular path of sodium that is actively transported out of the epithelial cells by Na/K ATPases. The model predicts that water and nutrients follow sodium paracellularly into the lens, the sodium leaks through mature fiber cell membranes, then moves transcellularly through the gap junctions connecting the differentiating fiber cells toward the epithelial cells. AQP0, distributed throughout cortical and nuclear fiber cell membranes, would permit the flow of water into and out of the cell. The Na/K ATPase pumps, concentrated in the equatorial region of the lens, provide the driving force for circulation. Based on a figure from reference #5.

and AQP0 within the lens, are consistent with this model. In addition, they postulate that paracellular influx occurs along the anterior suture lines (32).

The models of anterior to posterior trans-lens flux (27) and axial to equatorial flux (5) are different in the predicted routes of water efflux. The apparatus used to measure anterior to posterior flux, however, does not address the movement of water into or out of the equatorial regions of the lens (27). The models of circulation remain controversial and investigators are beginning to test these models and to assess the distribution and function of protein components potentially contributing to transport.

3. Movement of Water in the Lens and the Development of a Physiological Barrier

Regardless of the mechanism of water movement in the lens, maintaining osmotic balance within the lens is essential for preserving lens transparency since the disruption of the fiber cell architecture by cell swelling or dilation of the extracellular space increases light scattering potentially resulting in the formation of opacities (33). The total amount of water in the lens is tightly controlled and the proportion of extracellular water is less than 5% of the total water in the lens (34). In bovine, rabbit, and rat lenses the total water in the lens nucleus gradually decreases with age (35). However in the human lens, Raman spectroscopy studies suggest that rather than a decrease in nuclear water content with age that in the human lens there is actually about a 5% increase in nuclear water content (36).

Compounding the complexity of the models of an internal circulatory system are data suggesting the development of a physiological barrier that becomes increasingly defined with age. This barrier blocks the transport of water (6) and nutrients, such as

glutathione (37), to nuclear fiber cells. Using magnetic resonance imaging, Moffat *et al.* found that the rate of diffusion of deuterium oxide (D_20) from the cortex to the nucleus of a human lens decreases with age (6). In a 26 year old lens, a weak barrier to water transport was observed and within ~3 hours the water within the lens had completely exchanged with the deuterium oxide. However, after incubating a noncataractous 79 year old lens in artificial aqueous humor with D_20 for ~3 hours, exchange had only occurred in a concentric zone corresponding to the cortex (6). These data are consistent with the formation of concentric barrier to the transport of water into the nucleus. The formation of a barrier to flow into the nucleus was observed by a different group analyzing rabbit lenses by magnetic resonance imaging (38). These results are also consistent with examination of the total level of water in the human lens by Raman spectroscopy. Raman spectroscopy revealed that along the visual axis, the total level of water decreases abruptly in the first 0.5 mm and in the equatorial axis the drop occurs over the first millimeter (36). The boundary of the barrier, measured along the visual axis using magnetic resonance imaging, remained the same in human lenses of from age 15-80 (15). The biochemical nature of the barrier is not known, nor is it known whether the barrier to water movement is a protective mechanism (15) or the result of degraded protein function predisposing the lens to the development of cataract (39).

4. Components of the Transport System and Their Distribution

The model of circulation through the lens is based on electrophysiological measurements and the asymmetric distribution of aquaporins, ion channels, pumps, and gap junctions (Fig. 1.4) (5). With regard to the internal circulatory system many

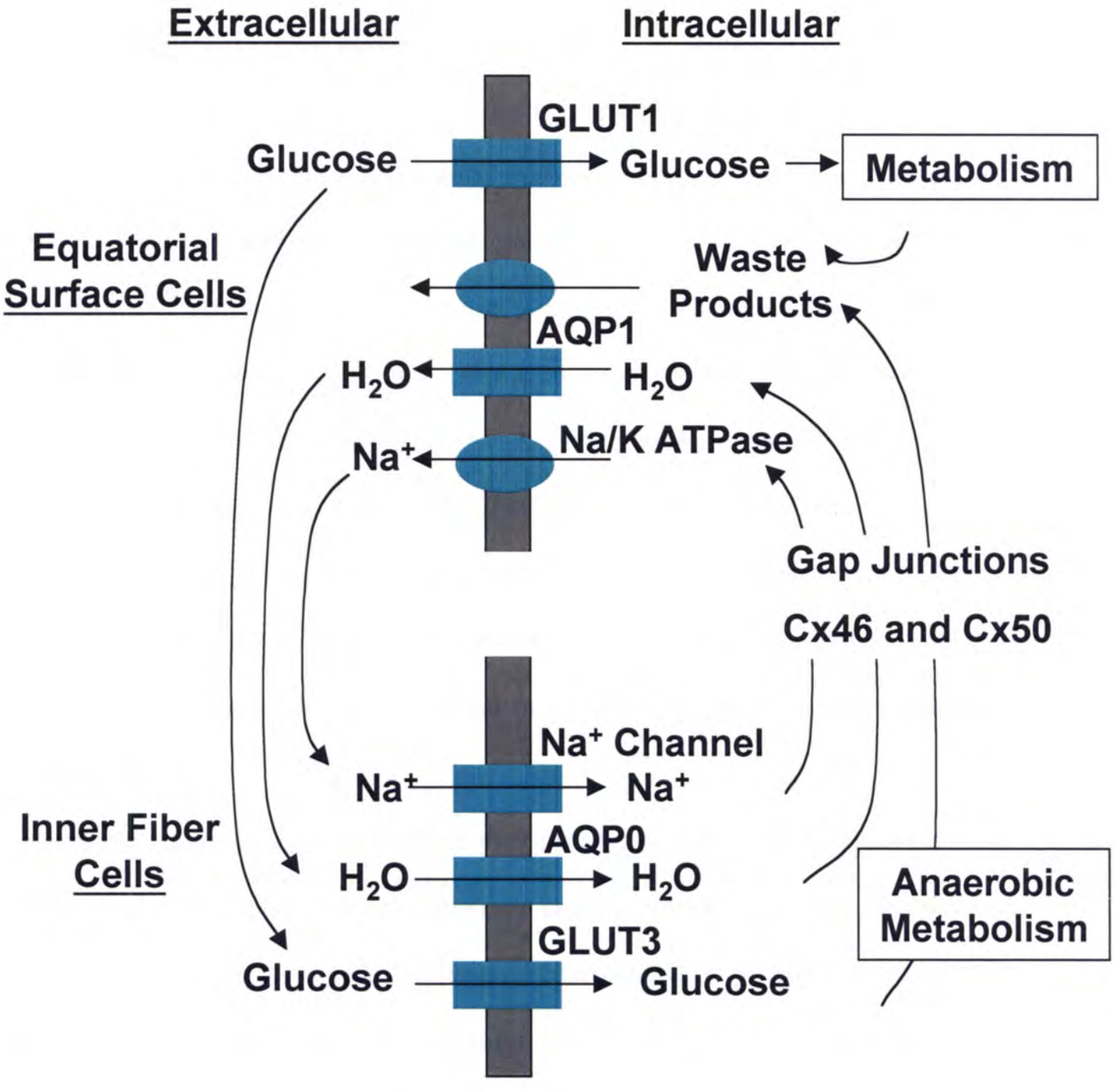

Figure 1.4. Proposed protein components of the internal circulatory system of the lens. The model provides a mechanism for the delivery of nutrients and removal of metabolic waste products from the inner lens fiber cells. Based on a figure from reference #5.

questions remain, including the identity of channels, pumps, and junctions that contribute to the system, and how age-related posttranslational modifications affect the function and distribution of these potential players. The distribution of aquaporins, Na/K ATPases, gap junctions, and ion channels within different regions of the lens is reviewed.

Two aquaporin transmembrane water channels are found in the lens. Aquaporin 1 (AQP1) is restricted to the lens epithelial cells at the anterior surface of the lens while Aquaporin 0 (AQP0), the protein of interest, is found in the lens fiber cells comprising the bulk of the lens. The movement of water in an anterior to posterior direction through cultured lens epithelial cells grown on transwells and through an intact lens in a transwell apparatus can be blocked by mercurials (27). This suggests that the mercury sensitive AQP1, which has a much higher water permeability than AQP0 (40), may control the rate at which water enters the lens. As is seen in other tissues which express multiple aquaporins, the aquaporins most likely act in a concerted manner to maintain water balance (41).

AQP0 comprises over 50% of the total membrane protein in the lens (42). The distribution of AQP0 in the fiber cell membrane changes with the age of the fiber cell and location within the lens. The recent systematic characterization of AQP0 distribution by Zampighi *et al* indicates that AQP0 is found in the lateral (narrow) membranes of fiber cells (32). As the fiber cells mature and lose their hexagonal shape, AQP0 is dispersed throughout the fiber cell membrane. Interestingly, the association of AQP0 with fiber cell junctions also changes with fiber cell age and location within the lens (32). In the young cortical fiber cells, AQP0 is evenly distributed throughout single plasma membranes. As the fiber cells age there is a gradual transition from localization in single

membranes to the association of AQP0 with fiber cell junctions. In the nuclear fiber cells AQP0 is found only in fiber cell junctions (32). Studies have also shown that AQP0 imparts water permeability to the fiber cell membranes and that the fiber cell membrane water permeability decreases with the age of the fiber cell and the age of the protein (7). Vesicles prepared with membranes from younger cortical fiber cells from a rabbit lens had a higher water permeability than those from inner fiber cells (7). The functional significance of the altered distribution of AQP0 in the membrane and the age-related changes that affect water permeability are not known.

The Na/K ATPases, which pump $3Na^+$ out and $2K^+$ into the cell per ATP expended, are found in the lens epithelial cells and in differentiating fiber cells and are crucial for establishing the currents required for transport through the lens (43). The α-2 and α-1 isoforms of the Na/K pump, both found in lens epithelial cells, are distributed differently within these cells. The α-2 isoform is located in the anterior epithelial cells and the α-1 isoform is found in the equatorial epithelial cells and differentiating cells (43). The α-1 isoform is thought to generate the current for efflux at the equator by constantly pumping sodium out of these cells (5). Uncontrolled tissue hydration in the lens, as is seen in osmotic cataract, can be experimentally induced by inhibition of Na/K ATPases (33). In the mature nuclear fiber cells, Na/K ATPase activity is not observed and these cells are thought to rely on gap junctional coupling to peripheral cells to maintain a negative resting membrane potential (12). Age-related modifications have been implicated in the loss of Na/K ATPase activity in the lens fiber cells (12).

Gap junctions are clusters of intercellular channels or connexins that permit communication between adjacent cells. The connexins (Cxs) are hexameric structures

composed of connexon monomers that have four transmembrane spanning domains. The interaction of connexins between adjacent cells forms a channel through which molecules up to 1,000 Da can pass. Of the 13 connexins described in humans, Cx46 (α3) and Cx50 (α8), are expressed in the lens (28). Gap junctions composed of Cx43 are concentrated in the equatorial regions of the lens. Cx43 has been found in the epithelial cells and localized in the apical and lateral membranes of differentiating fiber cells (32). Cx50 (α8), which is cleaved from Cx70, has been observed only on the lateral (narrow) sides of the inner fiber cells (32). The size and distribution of gap junctional plaques change with fiber cell age. Large gap junctional plaques are localized on the broad faces of the lens fiber cells in the lens periphery and smaller plaques are found on the narrow sides of the cells (44). As the fiber cells age and lose their hexagonal shape, the plaques become smaller, are dispersed throughout the cell membrane and it remains to be determined whether connexins deep within the lens align to form cell-to-cell junctions (44).

The role of transporters in maintaining lens homeostasis is supported by the consequences observed following mutation or inhibition of the membrane transporters. Animal models of cataract formation, such as the diabetic rat, demonstrate that disruption of equatorial tissue occurs with uncontrolled increase in tissue hydration or osmotic cataract (45). The phenotypic characteristics of an osmotic cataract include the development of intra- and extracellular pools of water in the cortical regions of the lens. This can also be induced experimentally by disturbing the internal circulation by inhibiting Na/K pumps or Cl channels (33, 43). The anterior to posterior trans-lens flux can be inhibited by the effect of quinidine on K+ channels and mercurials presumably on AQP1 (27). Mutations in potential components of the circulatory system have been

shown to result in cataract formation. Mutations in Cx43 and Cx50 result in dominant zonular pulverant (dust-like specks) cataract (46, 47). Human AQP0 mutations, as will be discussed later, result in pulverant opacities distributed throughout the lens or opacities along the sutures (48).

D. Age-Related Changes in Fiber Cell Membrane Lipid Composition

As fiber cells differentiate, the membrane lipid composition changes and continues to change as the fiber cells mature. The level of phosphotidylcholine is higher in epithelial cells than cortical or nuclear fiber cells, whereas the levels of phosphatidylglycerol and lysophosphatidylglycerol are higher in the fiber cells (49). Lens fiber cell plasma membranes are rich in cholesterol and sphingomyelin and as a result have a low fluidity as compared to other membranes (50). The levels of both dihydrosphingomyelin, which comprises over 50% of the lens lipid, and sphingomyelin increase with fiber cell age in cortical and nuclear membranes (49, 51). These lipids decrease membrane fluidity and increase membrane order (49, 52). By reconstituting lipids isolated from inner and outer cortical fiber cells into vesicles, Mathias *et al* showed that the permeability of the lipid membranes to water was very low and did not appear to change much with fiber cell age (7). This may result from the high levels of cholesterol and sphingomyelin which have been shown to have a low water permeability in reconstituted bilayers (53). Lipid bilayers composed of phosphotidylcholine have a water permeability of about 20-50 x 10^{-4} cm/sec, whereas bilayers composed of mostly sphingomyelin and cholesterol have a permeability of 2.3 x 10^{-4} cm/sec at 25°C (54).

E. Age-Related Changes in Lens Protein Structure and Function

As epithelial cells in the lens equator differentiate, there is a rise in protein synthesis and ubiquitin-dependent protein turnover shifting the complement of proteins from that of an epithelial cell to that of a fiber cell (55). As the fiber cells mature, lose their organelles and concomitantly the ability to synthesize new proteins, a decrease in protein ubiquitinylation and protein turnover is observed (16). Consequently, in the mature lens, there is a gradient of the newly synthesized protein in the lens periphery and protein as old as the individual in the lens nucleus. At various stages of fiber cell maturation some proteins are degraded and no longer detectable (17), whereas other proteins, such as AQP0, are retained throughout the lifetime of the individual. Lens proteins that are not turned over accumulate many age-related posttranslational modifications, including, backbone cleavage or truncation, oxidation, deamidation, racemization, isomerization, glycation, crosslinking, and acetylation (56). The effects of these modifications on protein function and regulation of function are currently being addressed in a number of laboratories. Many questions remain as to whether the modified proteins are incorporated into normal physiological functioning of the lens, if they predispose the lens to the onset of cataract, or if they are nonfunctional vestigial protein remnants. General mechanisms, examples, and the functional effects of enzymatic truncation, deamidation, isomerization, racemization, and spontaneous truncation are discussed below.

1. Backbone cleavage/Truncation

A number of membrane, cytoskeletal, and cytosolic lens proteins such as, AQP0 (3, 57), spectrin (58), ankyrin (58), connexin 50 (59), and the crystallins (24), undergo truncation or backbone cleavage with fiber cell age. Proteolysis is thought to begin in the zone of denucleation in the outer cortex and continue as the fiber cell ages (58) and has been observed in normal human lenses as early as age 7 (8). Analyses of the nuclear regions from lenses of many ages indicate that the sites of protein truncation of the crystallins are consistent, suggesting that truncation is not a random event (24). Indeed, not all lens proteins are truncated, tropomodulin, tropomyosin and F-actin remain intact in the aging lens (58). Lee *et al* suggest that backbone cleavage of specific cytoskeletal elements, such as α-spectrin, may play an important role in cytoskeletal remodeling as the fiber cells age, implying that truncation is a normal programmed process in the lens (58).

Upon cleavage of the gap junctional protein, connexin 50, the sensitivity to changes in extracellular pH is lost (59). Furthermore, the loss of regulation of connexins by changes in pH, voltage, and calcium results in gap junctions that remain coupled (12). The cytosolic crystallin proteins also undergo backbone cleavage. Truncation at particular sites within the C-terminus of αA-crystallin, a molecular chaperone within the lens, results in a partial loss of function (60). Although extensive truncation has been observed in human AQP0 (8), the effects of truncation on protein function and regulation have not been tested.

a. Proteases in the Lens

Truncation of aged proteins is thought to occur through the action of proteolytic enzymes and/or through a spontaneous backbone cleavage event. Exopeptidases and endoproteases have been isolated and characterized from bovine and human lenses. Exopeptidases identified include leucine amino-peptidase and aminopeptidase III (61) and based on observed cleavage of single residues from the C-termini of lens proteins, the presence of an unidentified carboxypeptidase has been proposed (62). Endoproteases found in the lens include serine proteases, cysteine proteases, and a 700 kDa neutral endoproteinase with trypsin-like activity (11, 63). Two serine proteases, a 25 kDa endoprotease that cleaves after Lys, Arg, and Asn (64) and a 17 kDa membrane associated protease that cleaves at Arg (65, 66) and multiple cysteine proteases, such as the calpains and caspases, have also been identified in the lens.

Many proteins within the lens are substrates for the intracellular calcium-dependent calpains (67). Calpain 1 (μ-calpain) and calpain 2 (m-calpain) are activated at low (10μm) and high (1mM) calcium concentrations, respectively (11). Unlike the calcium dependent calpains 1-3, calpain 10, recently identified in human, rat, and mouse lenses (68), does not contain calcium binding EF hands (69). Calpains 1, 2, 10, and lens specific variants of calpain 3, Lp82 and Lp85 are abundant in rat lenses (69). Although Lp82 and Lp85 are absent from the human lens, calpain 2 (70) is found predominately in the epithelial and cortical fiber cells and calpain 10 is concentrated in the water insoluble fraction of differentiating fiber cells in the human lens (68). A calpain inhibitor, calpastatin, has been observed in high levels in the human lens especially in the lens nucleus (70). *In vitro* cleavage of rat AQP0 (71), α-crystallin (72), spectrin (58), and

connexin 50 (67) with calpain results in cleavage products that are identical to those detected in normal lenses.

Lens calpains may also proteolytically activate caspases within the lens (69). The involvement of caspases in fiber cell differentiation and organelle loss (20) has led to the suggestion that caspases may also be responsible for the proteolytic processing of lens proteins that are not completely degraded. Caspases cleave on the C-terminal side of aspartic acid residues and known consensus sequences may prove useful in predicting sites of cleavage (73). In the developing chick lens at embryonic day 16, caspase 1 was found throughout the lens, whereas caspases 2, 3, 4, and 6 were only observed in cortical lens fiber cells (19). Thus far, spectrin is the only lens protein shown to be susceptible to cleavage by caspase (58).

2. Spontaneous Age-related Posttranslational Modifications

Since proteins within the lens are not turned over they are subject to spontaneous changes in structure at labile regions of the protein. The most prevalent spontaneous reactions that affect proteins at physiological pH and temperature are succinimide-linked reactions (74). The formation and hydrolysis of an unstable succinimide ring at susceptible residues results in deamidation, isomerization, and racemization (74). Asparagine (Asn) and glutamine (Gln) can be deamidated to aspartic acid (Asp) and glutamic acid (Glu), respectively. Aspartic acid can be isomerized to isoaspartic acid (β-Asp) and/or racemized from an L-amino acid to a D-amino acid. While a number of factors, such as steric constraints imposed by adjacent residues, secondary and tertiary structure, temperature, and pH, affect the rate of succinimide ring formation, typically

asparagine and aspartic acid residues are more susceptible to these reactions than glutamine and glutamic acid (74). Age-related deamidation has been proposed to serve as molecular clock, signaling protein turnover or imparting a new protein function at a specific time prior to protein turnover (75).

a. Deamidation

Many lens proteins, including the crystallins (76) and AQP0 (8) are deamidated. During deamidation of asparagine or glutamine the main chain nitrogen of the succeeding residue attacks the carbonyl carbon of the Asn or Gln side chain. A succinimide ring is hydrolyzed giving rise to α-linked or β-linked aspartic acid isomers in a ratio of about 1:3 (Fig. 1.6) (76). Deamidation results in the incorporation of a negative charge at the deamidated site, a gain of 1Da in mass, and incorporation of an additional carbon into the peptide backbone of the iso-(β-)aspartic acid. The aspartic acid resulting from deamidation can be further subject to isomerization and racemization as discussed below.

b. Isomerization and Racemization of Aspartic Acid

Isomerization and racemization of aspartic acid residues is commonly observed in aged proteins of the lens, teeth, erythrocytes, and brain (77) and was first observed in lens proteins in the 1970's (78). These isomers arise through spontaneous formation of succinimide ring (74). Hydrolysis of the succinimide ring results in four products, L-Asp, L-iso-Asp, D-Asp, and D-iso-Asp. During isomerization to iso-Asp, the peptide backbone is transferred to the side chain of the aspartic acid thereby incorporating an additional carbon in the peptide backbone. During racemization of L-Asp to D-Asp, the

configuration around the α-carbon is inverted (Fig. 1.6) (74). The age-dependent increase in the amount of D-Asp in particular tissues has enabled the use of the ratio of L-Asp to D-Asp for estimation of age in forensic analysis (77).

Although the formation of isomers of aspartic acid following racemization, isomerization and deamidation have been observed in lens proteins, such as α-A crystallin (79, 80), the effects on function and regulation of function have not yet been elucidated. To demonstrate the potential effects of asparagine deamidation and aspartic acid isomerization on protein function, examples are given for non-lens proteins (for reviews see (76, 81) (77)). Deamidation may completely abolish enzyme activity. This has been observed for a phosphocarrier protein, which completely lost transferase activity following deamidation (81). In addition, the products of deamidation may have different activities as was the case for calbindin, a calcium binding protein. Upon deamidation of asparagine to an iso-aspartyl residue, the affinity of calbindin for calcium decreased by 10 fold, whereas generation of an aspartyl residue increased calbindin affinity for calcium by 50% (81). Isomerization of aspartic acid to iso-aspartate has also been shown to affect protein-protein interactions and protein function. For instance, following isomerization of aspartic acid, the affinity of lysozyme for substrate is reduced (81). In addition, to altering protein function by affecting enzyme-substrate interactions these modifications have also been implicated in protein aggregation observed in Alzheimer's disease and cataract (82-84). It has been proposed that the incorporation of negative charges and alterations in structure can lead to protein unfolding, exposure of hydrophobic domains that promote the aggregation of proteins and disulfide bond formation (85).

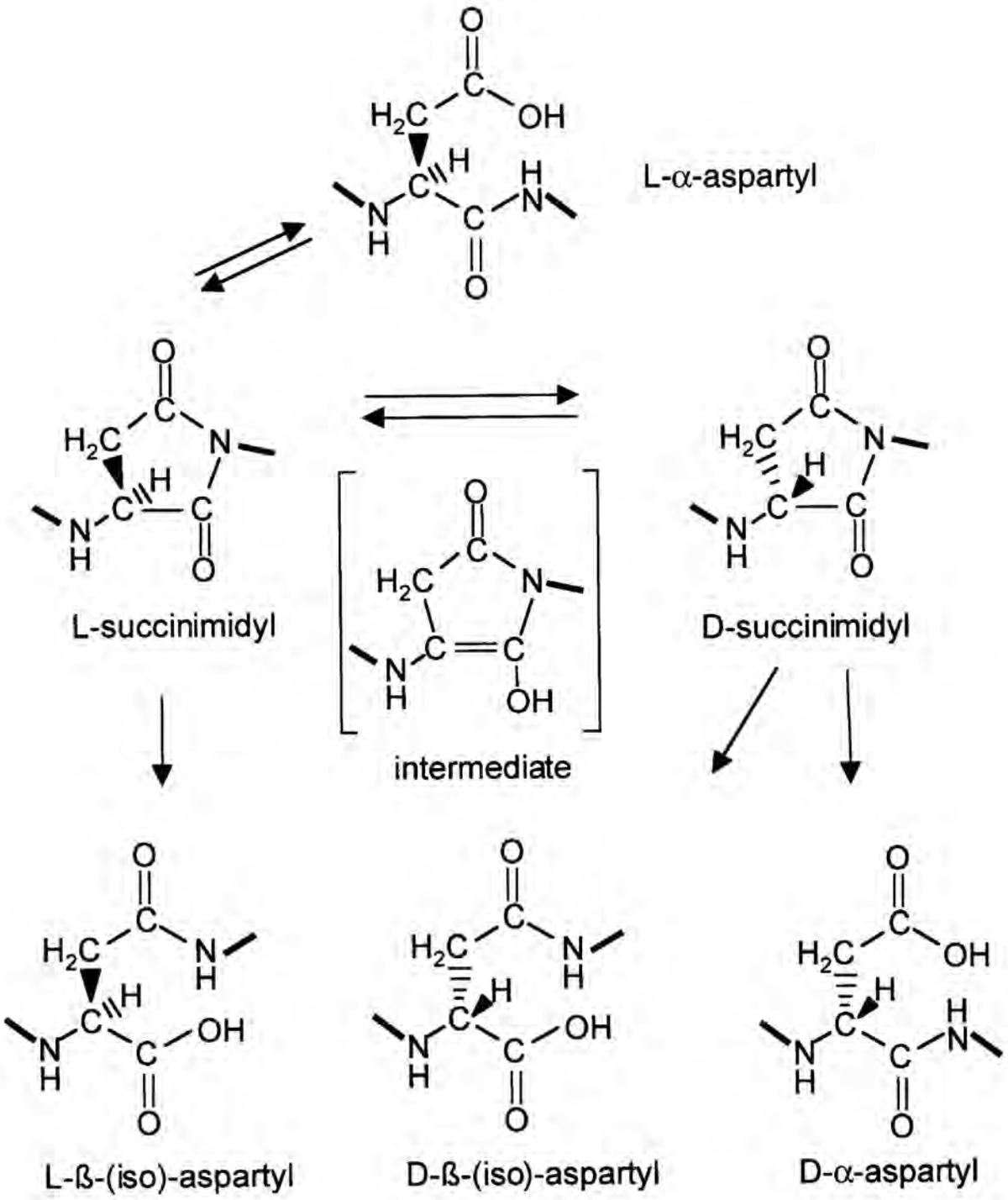

Figure 1.5. Isomerization and racemization of aspartic acid. Formation of isomerized (α or ß) and racemized (L or D) aspartic acid through the spontaneous formation of a succinimide ring intermediate. Based on a figure from reference #80.

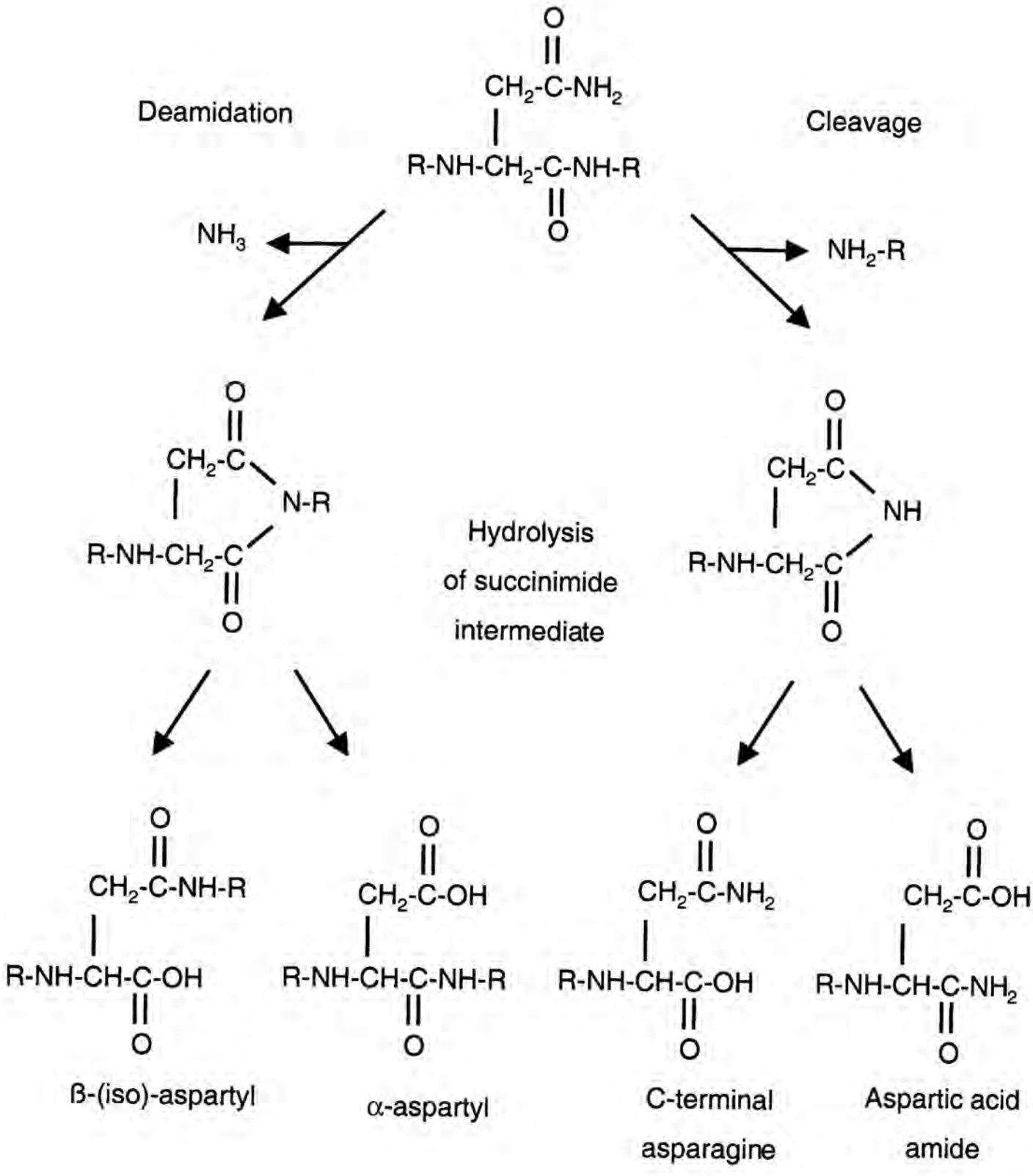

Figure 1.6. Deamidation and spontaneous truncation of asparagine. Formation and hydrolysis of a succinimide ring yeilding isomers of aspartic acid following deamidation of asparagine. An aspartic acid amide or C-terminal asparagine results from spontaneous backbone cleavage of asparagine. Based on a figure from reference #86.

c. Spontaneous Backbone Cleavage

In addition to the action of the proteolytic enzymes discussed previously, aging peptides (74) and proteins (86) are subject to spontaneous backbone cleavage at residues that can form a succinimide intermediate. A mechanism proposed by Voorter *et. al.* suggests that the β-amide nitrogen of an asparagine side chain attacks the backbone carbonyl resulting in the succinimide ring (86). Hydrolysis of the ring then produces a penultimate asparagine or an aspartic acid amide in the truncated peptide (Fig. 1.6) (86). Although asparagine, aspartic acid, glutamine, and glutamic acid residues are susceptible to the formation of a succinimide ring, truncation was predominately observed after asparagine residues (74). Spontaneous truncation has been proposed to result in the age-related truncation of α-A crystallin after Asn 101 (86). This is the only case cited in the literature for *in vivo* age-related spontaneous truncation of a lens protein.

3. Detection of Age-related Posttranslational Modifications

Deamidation of Asn or Gln to Asp or Glu results in a 1Da increase in molecular weight, incorporation of a negative charge, and an additional carboxylic acid. The heterogeneity in charge can be detected by nondenaturing SDS-PAGE, ion exchange chromatography, and 2D-gel electrophoresis. The 1Da shift in molecular weight can be detected by high resolution mass spectrometry (75, 87), alternatively the carboxylic acids can be chemically derivatized to increase the shift in molecular weight (88) facilitating mass spectrometric detection. The sites of deamidation can be elucidated by tandem mass spectrometry. Since deamidation partially results in iso-aspartic acid, which is not

amenable to Edman sequencing, an abrupt drop in the sequencing results can indicate the presence of a deamidated residue.

Detection of isomerized and racemized aspartic acid is more difficult since it does not change the charge or molecular weight of the peptide or protein. The relative levels of L and D amino acids in a tissue or purified protein can be quantified by amino acid analysis. However, amino acid analysis does not distinguish between normal (α) and iso- (β) aspartic acid isomers, aspartic acid and asparagine, nor glutamic acid and glutamine. Enzymatic incorporation of radiolabeled methyl groups using protein isoaspartate methyl transferase (PIMT) has been used to detect accessible L-iso-Asp and D-Asp residues (89). However, this enzyme cannot distinguish between L-iso-Asp and D-Asp nor does it recognize D-iso-Asp (89). Tandem mass spectrometric methods have been developed to identify isomerized Asp (α) and iso-Asp (β) however, this requires prior characterization of a synthetic peptide standard and these methods do not distinguish racemized L- and D-Asp (90, 91). The most commonly used approaches to distinguish between L-Asp, L-iso-Asp, D-Asp, or D-iso-Asp, are immunological methods (77) and chromatographic separation (79, 80, 92).

Age-related truncation of lens proteins and AQP0 was first observed using gel electrophoresis techniques during the late 1970's (93, 94). Edman degradation has been utilized to elucidate sites of N-terminal protein truncation, however is not as amenable to determination of the sites of C-terminal truncation. N- and C-terminal protein truncation was evaluated using antisera generated against different regions of the protein (57, 95-98). One problem with this approach is that a decrease in antibody binding may reflect protein truncation or a different modification. Utilization of mass spectrometry has

permitted identification of the nature and the exact sites of protein truncation and posttranslational modification of cytosolic soluble proteins (99) and integral membrane proteins (8). Recent application of a proteomic approach using mass spectrometry, has enabled the identification of the sites and nature of posttranslational modifications in many lens soluble proteins simultaneously (100).

E. Diseases of the Lens

1. Cataract

The most common disease associated with the lens is the formation of opaque regions within the lens or cataract. Depending on the severity and location of the opacity, the transmission of light to the retina may be obstructed impairing vision. Cataracts can be classified based on their location within the lens; nuclear, cortical, posterior subcapsular, mixed or by their etiology; maturity-onset (senile, age-related), congenital, traumatic, associated with intraocular or systemic disease, or drug induced (101). Most congenital cataracts are non-syndromal autosomal dominant cataracts due to an isolated abnormality (47). Thus far, mutations in nine lens proteins have been linked to the development of congenital cataract in humans. These include αA-crystallin, βB2-crystallin, βA3-crystallin, γC-crystallin, γD-crystallin, connexin 46, connexin 50, PITX3, and aquaporin 0 (46, 48, 102). Candidate genes for human congenital cataract include other transcription factors, crystallins, phakinin, MP20 (LIM2), and filensin (46). The remaining congenital cataracts are a secondary feature of almost 200 genetic syndromes (103). The genes implicated in congenital cataract formation could potentially play a role in the susceptibility to age-related cataracts.

The most prevalent type of cataract is maturity-onset cataract. Age-related cataracts affect nearly 20.5 million Americans age 40 and older, or about one in every six people in this age range. By age 80, more than half of all Americans will develop cataract. Age-related cataracts are found in all regions of the lens with the highest percentage located in the center, or nucleus, of the lens. The Beaver Dam Eye study, performed in the United States on 4,926 subjects between 1988-1990, found that in patients ages 55-64, 65-74, and 75-84 the prevalence of nuclear cataract was 6.6%, 27.4%, and 57.0%, the prevalence of cortical cataract was 10.9%, 25.4%, and 42.4%, and the prevalence of posterior subcapsular cataract was 4.3%, 8.4%, and 14.3%, respectively (101). Similar results were obtained in the Blue Mountain Eye Study performed on 3,654 subjects in Australia. In this study, performed between 1992-1994, in patients ages 55-64, 65-74, and 75-84 the prevalence of nuclear cataract was 3.9%, 21.8%, and 48.5%, the prevalence of cortical cataract was 13.1%, 28.4%, and 46.7%, and the prevalence of posterior subcapsular cataract was 3.8%, 6.5%, and 11.7%, respectively (101). Although slightly different classification systems were used, these studies demonstrate that the formation of maturity-onset cataracts is a common problem in industrialized countries (101).

A number of risk factors have been proposed to increase the likelihood of developing cataract although it is not conclusive if any of these risk factors actually cause cataract. Age, female gender, smoking, diabetes, and steroids have been reproducibly associated with cataract formation, whereas sunlight, socio-economic factors, height, weight, body mass, alcohol consumption, severe dehydration, and hypertension have been implicated but studies have yielded inconsistent results as to whether these are risk

factors for cataract (101). Particular risk factors have also been associated with cataracts within different regions of the lens. Risk factors associated with the development of cataract in the lens cortex include age, female gender, ultraviolet light, and Afro-Carribean ethnicity. The development of nuclear cataracts is associated with age, smoking, and diet, whereas the development of posterior subcapsular cataracts is associated with diabetes and steroid treatment (101). The relationships among initiating factors, their molecular effects in the lens, and the development of opacities have not been elucidated.

The development of age-related cataract is thought to be the result of a multi-factorial process that ends in protein aggregation, pooling of water inside or outside of cells, and/or cell membrane damage (11, 82). Lens proteins are subject to age-related oxidation, glycation, disulfide formation, cross-linking, deamidation, backbone cleavage (56). These changes in protein structure may impair protein function and alter protein conformation. Unfolding and changes in protein conformation may expose hydrophobic domains that interact, or may reveal sites that interact by disulfide or crosslinking (56). These scenarios could lead to protein aggregation and precipitation. Another result of protein aggregation proposed to alter lens transparency is syneresis. As proteins aggregate the hydration state of the protein is altered and water that was once protein bound becomes free water (35).

Protective mechanisms in the lens include anti-oxidants, protein chaperones, and protein degradation pathways. Anti-oxidants found in the lens include, glutathione, vitamin C (ascorbate), vitamin E (tocopherol), and carotenoids and anti-oxidative enzymes such as superoxide dismutase, catalase, and glutathione reductase/peroxidase

(104). A protective role of dietary supplements of antioxidant vitamins has been suggested; however, studies correlating the use of dietary supplements and cataract formation are inconsistent (104) and recent clinical trials did not show a protective effect of supplements on cataract formation (105).

According to the World Health Organization, cataract is the leading cause of blindness in the world. Presently, there are no pharmacological means for the prevention, delay, or treatment of cataracts. Cataracts are treated by surgically removing the cloudy lens and replacing it with an artificial intraocular lens. This surgery has become routine and is one of the most commonly performed surgical procedures in the United States. With more than a million cataract surgeries performed per year, the estimated cost to the Federal government through the Medicare program is $3.4 billion per year.

2. Presbyopia

Another common age-related problem associated with the lens is presbyopia. Presbyopia is the loss the ability to focus from far to near or accommodate and necessitates the use of bifocals. The mechanism of accommodation is not fully understood and this has been attributed to the lack of an easily obtainable animal model (106). The spherical mouse lens has negligible accommodative ability while rabbit and rat lenses have minimal accommodative amplitude (10). Monkey and other primate lenses have similar accommodative amplitude to the human lens (10). The age-related changes responsible for the loss of accommodation are not known, and there are many hypotheses concerning the role of the lens, capsule, as well as extra-lenticular structures in the development of presbyopia (107). Focusing the lens requires a pliable lens and

capsule and adequate function of the muscles responsible for changing the tension applied to the collagenous lens capsule. With age, the capsule loses its elastic properties and the lens grows thicker and becomes less elastic decreasing the ability of the lens to change shape (106). While aged ciliary muscle retains the ability to contract, dysfunction of the muscle anchor may decrease the effect of contracted ciliary muscle (106). The ability of the lens to accommodate usually begins to fail in the mid-forties and progressively worsens with age until the lens has completely lost the ability to accommodate.

An understanding of normal lens physiology and how the normal lens changes with age is an essential basis for elucidating the mechanisms underlying the formation of cataract and the loss of accommodative ability.

III. The Aquaporins

A. Discovery of Aquaporins

Ten years ago, the pore forming protein responsible for cell membrane water permeability was discovered. Although the existence of membrane water channels was predicted prior to the 1950's (108), the identity of these proteins, now known as aquaporins, remained elusive until 1992 (4). In a comprehensive review published in 1987, Finkelstein compiled evidence, obtained by a number of investigators, for the presence of water permeable pores in particular cell membranes. These observations included the following; the variability in the permeability of renal epithelia in comparison to other epithelia, the fact that differences in membrane water permeability could not solely be attributed to differences in membrane lipid composition, the low Arrhenius activation energy of water flux across erythrocyte membranes, and the reduction in red cell membrane permeability by sulfhydryl reagents (53). The activation energy for the diffusion of water across a lipid membrane is >10 kcal/mol, whereas the activation energy of the diffusion of water in bulk solution is <3 kcal/mol. The activation energy of water transport across membranes containing aquaporin water channels approaches the rate of diffusion of water in bulk solution (109).

AQP1 (formerly known as CHIP28) was the first protein demonstrated to function as a water channel. AQP1 was cloned from an erythrocyte cDNA library (110) and the protein expressed in *Xenopus leavis* oocytes (4). After subjecting the oocytes to a hypotonic buffer, the oocytes expressing AQP1 rapidly swelled and ruptured. As observed with erythrocyte membranes, the water permeability of the oocyte membrane could be reversibly inhibited by mercury (4). The activation energy of water transport

across oocyte membranes in oocytes expressing AQP1 was similar to that of the diffusion of water in a bulk solution (4). This was consistent with the presence of water permeable membrane channels. The ability of AQP1 to increase membrane water permeability was further confirmed by experiments performed in proteoliposome vesicles. The permeability of vesicles, reconstituted with pure AQP1 protein, was measured and found to have a low Arrhenius activation energy and to be reversibly inhibited by mercurial sulfhydryl reagents (111).

B. Sequence and Structure of the Aquaporins and AQP0

1. Sequence Similarities and the Aquaporin Family

While AQP1 was the first member of this family demonstrated to have water channel activity (4), AQP0 (formerly known as the Major Intrinsic Protein of the lens, MIP) was the first member of this protein family to be cloned and identified (3). As a result, this now very large family of proteins is referred to as the Major Intrinsic Protein/Aquaporin family. AQP0 shares ~45% sequence identity with AQP1 (112). The aquaporins have several highly conserved motifs, two asparagine- proline- alanine- (NPA) repeats, "AEFL" and "HW[V/I]]F/Y]WXGP" (113). A sequence alignment of mammalian aquaporins is shown in Figure 1.7. Further sequence analysis indicates that the first three transmembrane domains are homologous to transmembrane domains 4-6 suggesting evolution of the aquaporin gene by an intragenic duplication event (114). Based on sequence alignment and transport specificity, the proteins in the major intrinsic protein family can be subdivided into two subfamilies, the aquaporins (AQP0, AQP1, AQP2, AQP4, AQP5, AQP6, AQP8), and aquaglyceroporins (AQP3, AQP7, AQP9,

AQP10) (Fig. 1.8) (113, 115). Aquaglyceroporins, also known as glycerol facilitators, transport water at a slower rate than the aquaporins and can transport small neutral molecules such as glycerol. The remaining discussion will primarily pertain to the aquaporins proper which transport water.

2. Tissue Distribution and Physiological Significance

Aquaporins are ubiquitously found in bacteria, plants, and animals and exhibit a diverse tissue distribution in mammals (for review see (116)). Of the eleven mammalian aquaporins identified thus far, six are expressed in the eye (Table 1.1) (117). Multiple aquaporins expressed in a single cell type often exhibit different membrane localization. For instance in renal collecting duct principal cells, AQP's 3 and 4 are localized in the basolateral membrane, whereas AQP2 is routed to the apical membrane permitting the transcellular transport of water across the epithelial layer and the reabsorption of water (118). In addition to maintaining osmotic balance, aquaporins found in hepatocytes and salivary glands are thought to play a role in secretion (119, 120). To further investigate the physiological role of the aquaporins, transgenic animals have been engineered with deficiencies in the genes encoding AQP0 (121), AQP1, AQP3, AQP4, AQP5 (122). Impairment of aquaporin function results in a wide spectrum of pathologies including nephrogenic diabetes insipidus (118), deafness (123), Sjogren's syndrome (124), and cataract (1). The involvement of AQP0 in cataract formation will be discussed further in section IV.

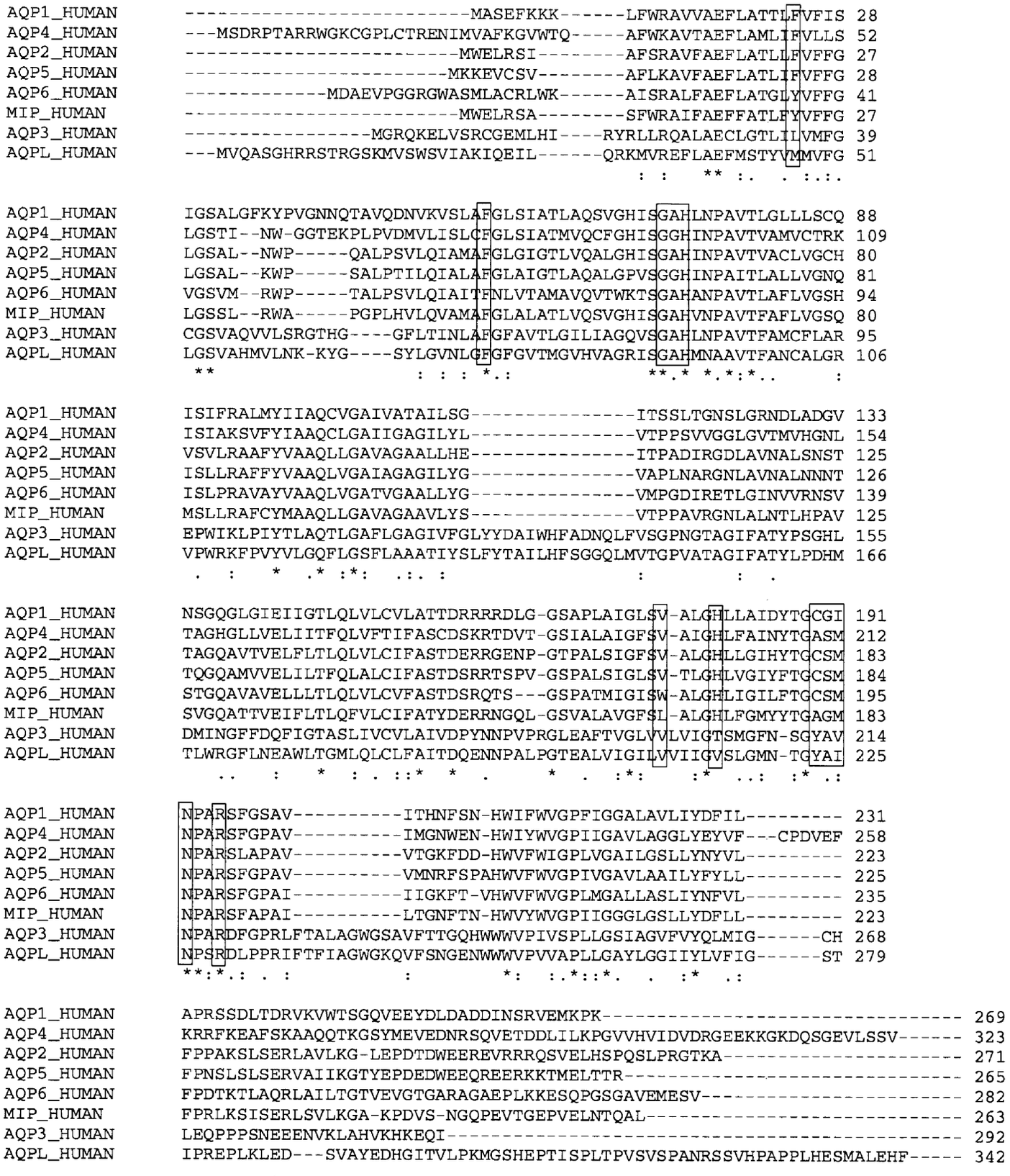

Figure 1.7. Sequence alignment of mammalian aquaporins. Boxed residues line the AQP1 monomer channel. MIP has been renamed AQP0 and AQPL renamed AQP7.

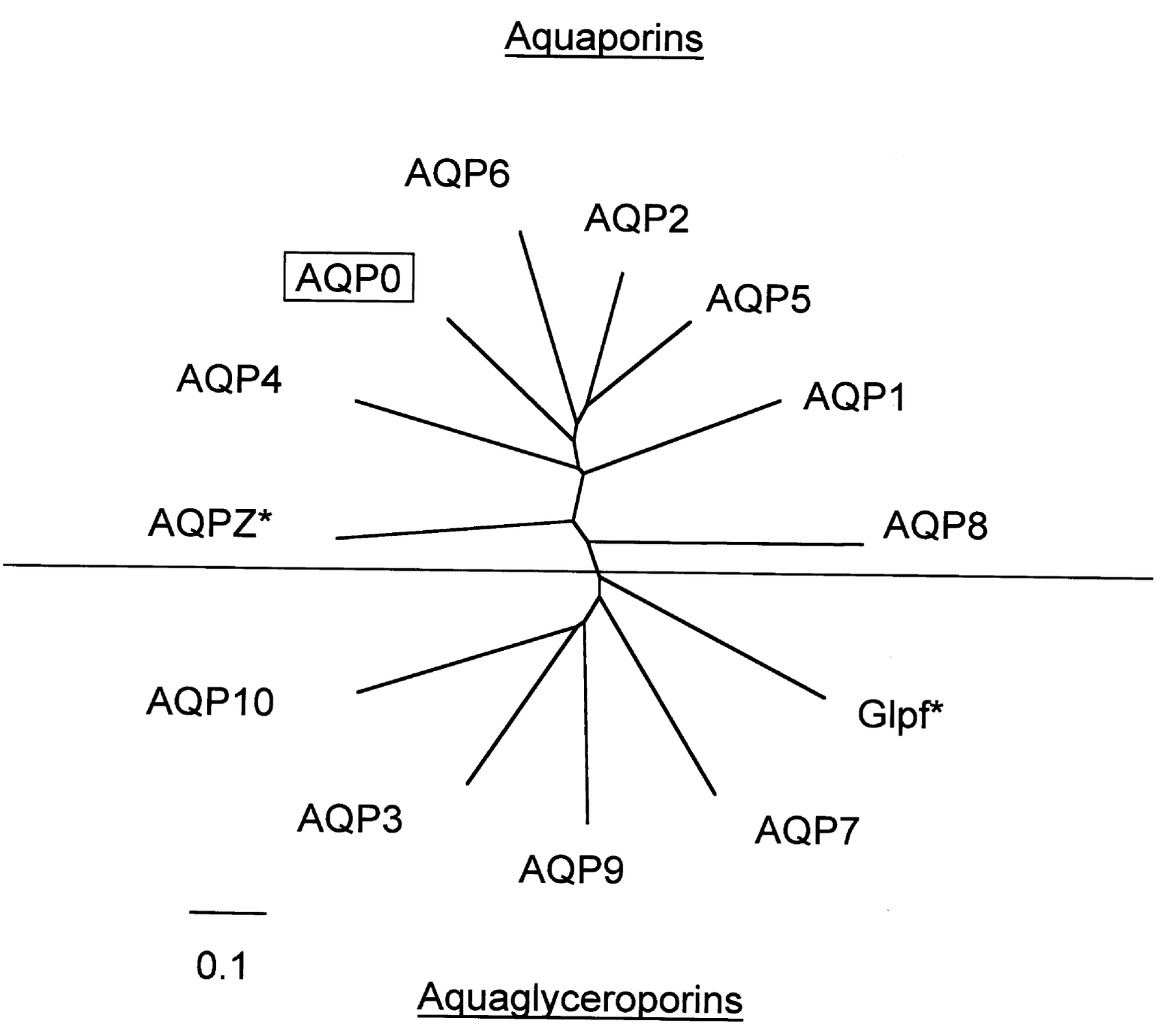

Figure 1.8. Human aquaporin gene family. Phylogram of human AQPs and bacterial AQPz and GLPf. Based on sequence similarity and substrate specificity, members of the Major Intrinsic Protein Family can be divided into two subfamilies, the aquaporins and aquaglyceroporins. Scale bar represents genetic distance between homologs. Based on a figure from reference #115. Based on a BLAST query of human AQP0 the percent identity and similarity of other aquaporins to human AQP0 are, respectively: AQP2 (54%; 71%), AQP5 (48%; 65%), AQP6 (50%; 63%), AQP4 (40%; 61%), AQP1 (43%; 60%), AQP8 (30%; 47%), AQP7 (27%; 39%), AQP9 (23%; 37%), AQP3 (25%; 37%), AQP10 (24%; 36%).

AQP0	Lens fiber cells
AQP1	Lens epithelial cells, corneal epithelium, nonpigmented epithelium, trabecular meshwork
AQP3	Conjuctiva
AQP4	Retinal glia (Müller cells)
AQP5	Lacrimal gland, corneal epithelium

Table 1.1. Distribution of aquaporins in the eye. While several aquaporins have been found in the eye, AQP0 is the only aquaporin that has been identified in the lens fiber cells. Multiple aquaporins localized in the same cells or tissues are thought to act in a concerted manner to maintain osmotic homeostasis. Based on a figure from reference #117.

3. Aquaporin Structure

The aquaporins are small integral membrane proteins ranging in molecular weight from 26 to 34 kDa. Hydropathy profiles of AQP0 are consistent with six α-helical transmembrane domains (3). The surface topology of extramembranous domains of AQP0 have been probed by atomic force microscopy (125) and to date the highest resolution structural data of AQP0 are from 2D crystals of AQP0 imaged at 20Å resolution by cryo-electron microscopy (126). Cryo-electron microscopy and X-ray crystallography have been used to probe the structures of human AQP1 to 3.8Å (1H6I.pdb) (127), bovine AQP1 to 2.2Å (1J4N.pdb) (128), and the *E. coli* Glpf a glycerol facilitator to 2.7Å (1LD1.pdb) resolution. Since the most highly resolved aquaporin structures available are of AQP1, the details of the AQP1 structure will be discussed.

The structure of the AQP1 monomer, resolved by cryo-electron microscopy to 7Å resolution, demonstrated six transmembrane α-helices arranged in a right-handed helical bundle tilted about 30° with respect to the membrane (129) (Fig. 1.9). Site-directed mutagenesis of AQP1 residues near and within the NPA repeats, residues 76-78 in loop B and 192-194 in loop E, led to the proposal of the hourglass model. This model suggested that the loops containing the NPA repeats dipped into the membrane from either side forming the pore of the channel (Fig. 1.9) (130). In these studies the mercury sensitivity, eliminated by substitution of Cys^{189} with a Ser, was rescued in the double mutant C189S/A73C (130). The hourglass model was further supported by resolution of the two NPA repeats juxtaposed in the center of the membrane by recent electron microscopy. The 4.5 Å resolution structure revealed that loops B and E contained short α-helices (HB, HE) that align the NPA repeats near the center of the monomer (131).

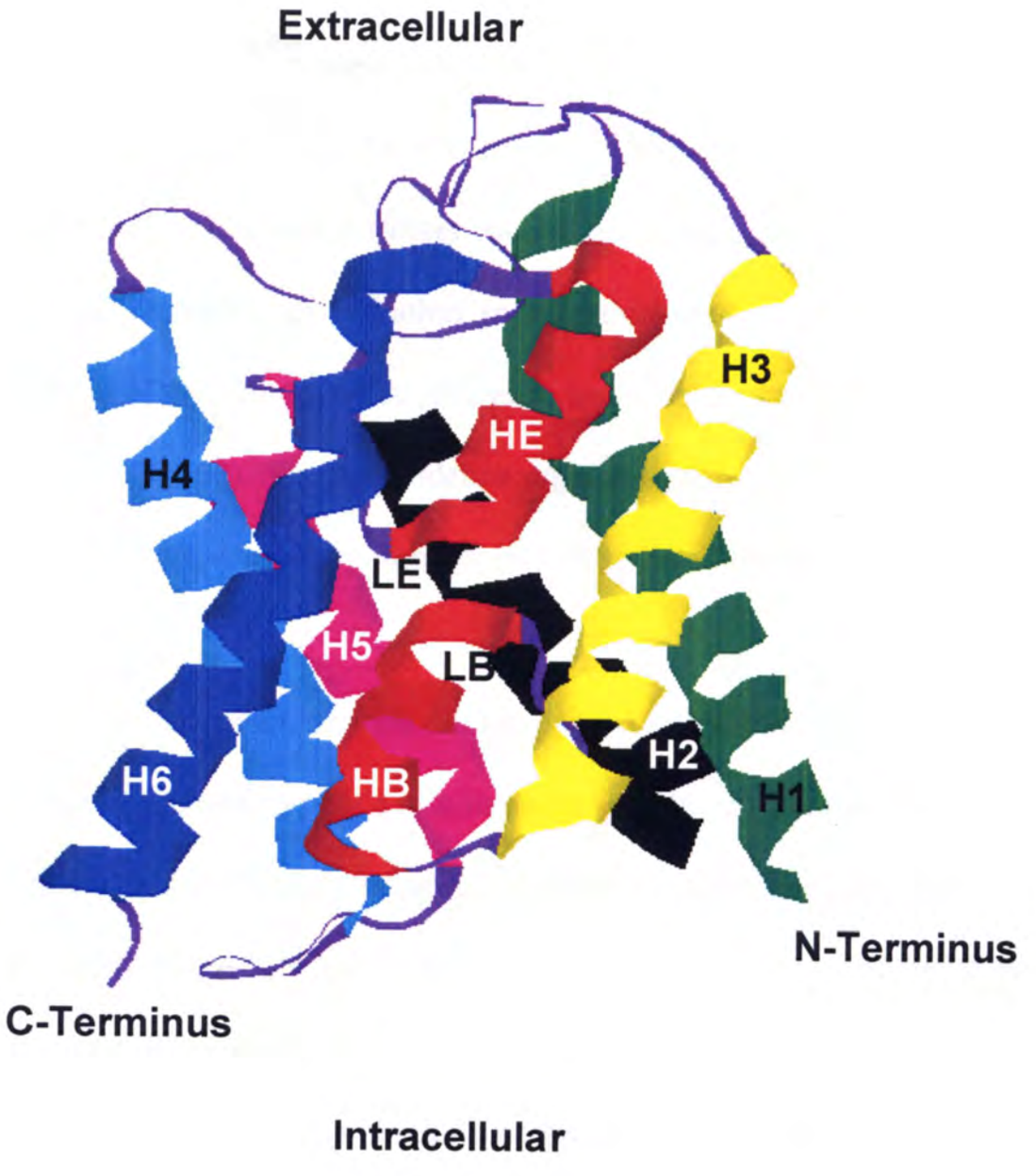

Figure 1.9. The monomeric structure of AQP1. The aquaporins have six transmembrane domains with two short helices (HB and HE) that enter the membrane from either side. The two loops containing the highly conserved Asn-Pro-Ala repeats (LB and LE) are juxtaposed in the center of the membrane and are directly involved in the movement of water through the channel. The helix assignments are shown (1H6I.pdb).

The 2 short α-helices form a pseudo-transmembrane helix that lines the pore of the channel.

Hydrodynamic studies and electron microscopy have shown that the aquaporins, including AQP0 (132) (133), are assembled as tetramers in the membrane (134). The sites of interaction among helices in different monomers have been elucidated in the AQP1 monomer (135). Based on radiation inactivation studies and site directed mutagenesis of tandem cDNA dimers of AQP1, each monomer is thought to serve as a water permeable pore (136-138). Further evidence suggesting that each monomer serves as a channel is the inhibition by mercury through an interaction with Cys^{189} located in the pore of the monomer (130).

The C-termini of the aquaporins are the most structurally diverse regions of the proteins and have been proposed to play a role in tissue specific regulation of aquaporin function. While unresolved by electron microscopy, atomic force microscopy placed the C-termini of the AQP0 and AQP1 monomers intracellularly at the interface of two monomers and the central cavity of the tetrameric structure (125, 139). Site directed mutagenesis and naturally occurring mutations of AQP0, AQP1, and AQP2 provide evidence for the involvement of the C-termini in routing newly synthesized protein to the target membrane (140-142) and in regulating protein function (139, 143, 144).

4. Pore of the Channel

The water permeability of AQP1 is estimated at 10^9-10^{10} molecules per second per monomer (145). For comparison, the maximum rate of an ion pump is 300 sec^{-1} and an

ion channel is 10^8 sec^{-1} (146). This high rate of water flux suggests that AQP1 forms a passive channel for water transport across the membrane (146).

Comparison of the recent three dimensional structural analysis of AQP1 and AQP3 has facilitated the postulation of the mechanism of transport and transport specificity of the aquaporins and the aquaglyceroporins (147). One question that is being addressed through the use of atomic resolution structures and molecular dynamic simulations is how the aquaporins maintain selectivity for water transport without ions or protons. The pore of the aquaporin channel is hydrophobic and narrows in two places within the channel to 2Å and 3Å wide (135). In AQP1, as water moves into the channel from the intracellular side of the membrane it interacts with the backbone carbonyl groups of Gly^{72}, Ala^{73}, and the side chain of His^{74} (147). Further into the channel, where it narrows to 3Å in width, water strongly interacts with the asparagine residues of the NPA repeats on one side of the pore and Phe^{24}, Val^{176}, and Ile^{191} on the other side of the pore (147). On the extracellular side of the NPA repeats water interacts with Ile^{191}, Gly^{190}, and Cys^{189} before it reaches the most narrow constriction of the channel. Within the 2Å wide region of the channel, water is oriented by the aromatic side chain of Phe^{56} for hydrogen bonding to His^{180} and Arg^{195} (147). As water moves through the channel, the orientation of the dipole moment of the water molecule rotates. This has been postulated to provide the channel's selectivity by facilitating hydrogen bonding to residues within the channel thereby disrupting the water-water hydrogen bonds (147). By breaking the hydrogen bonding between water molecules as they traverse the channel, protons cannot travel along the column of water (148). Therefore the two narrow regions in the channel, where water strongly interacts with the protein, represent the selectivity

filters of the pore (147). Ions are thought to be excluded since the diameter of hydrated ions would be too large to pass through the channel and AQP1 does not have charged residues lining the channel to strip water from the ions as is seen for other ion channels (149).

The three dimensional characterization of the residues lining the pore of AQP1 discussed above (147) are fairly conserved in AQP0. There are differences in the constriction at the NPA box, where rather than Phe^{24} as in AQP1 there is a Tyr^{23} in AQP0 and on the extracellular side of the NPA box in the AQP1 residues Cys^{189} and Ile^{191} correspond to AQP0 residues Ala^{181} and Met^{183}. These differences are highlighted in the sequence alignment in Fig 1.7.

5. Regulation of Aquaporin Water Permeability

Water transport through the AQP's 0-5 is passive, bi-directional, and occurs in response to osmotic pressure (150). The tight control of osmotic balance in cells and tissue suggests that the appropriate membrane water permeability is maintained by the regulation of water channels. Avenues of regulation that have been addressed are at the level of transcription, subcellular localization, posttranslational modification, protein-protein interactions, and protein turnover. In response to osmotic stress, the level of aquaporin protein expression can be altered by ubiquitin dependent protein turnover (151) or by acting through newly described hypertonic response elements in the promoter region of AQP1 (152).

The role of kinase stimulation and phosphorylation of aquaporins in regulating membrane water permeability has been addressed with respect to protein expression (153,

154), subcellular localization (155), and water channel gating (156). The most widely studied regulatory mechanism is the vasopressin stimulated shuttling of AQP2 to the apical membrane in the renal collecting duct principal cells. In response to vasopressin (anti-diuretic hormone), cAMP levels increase and the C-terminus of AQP2 is phosphorylated (Ser^{256}) and redistributed from intracellular vesicles to the apical membrane for the reabsorption of water (155). The PKA induced shuttling is reversed by PKC mediated endocytosis that is independent of direct phosphorylation of AQP2 (155). PKA mediated redistribution of AQP8 from intracellular vesicles to the plasma membrane has been observed in rat hepatocytes (157).

Recently, for the first time, gating of an aquaporin by phosphorylation was proposed (156). *In vitro* studies in LLC-PK1 cells showed a decreased water permeability of AQP4 following PKC stimulation. The membrane distribution of the protein was not altered and the effect was abolished by mutation of Ser^{180}. This serine, located in an intracellular loop, may sterically block the water channel when phosphorylated (156). Interestingly, AQP0 has an aspartic acid residue at this position.

The relevance of studies addressing the effect of kinase stimulation of the water permeability of AQP's 0-5 (40), AQP1 (158), and AQP4 (158) expressed in *Xenopus* oocytes has been called into question since the observed responses may be due to general changes in endocytosis and exocytosis. Treatment of oocytes, heterologously expressing a variety of transporters and ion channels, with stimulators of PKC and PKA has been shown to increase endocytosis or exocytosis, respectively (159). This process seems to be irrespective of phosphorylation sites in the expressed transporters (159).

The role of calcium in regulating membrane water permeability has been addressed with respect to AQP1, AQP2, and AQP0. Based on sequences motifs for EF hands in the C-terminus of AQP1, the regulation of AQP1 has been predicted to be regulated by calcium (139). However, the effect of calcium on AQP1 mediated permeability has not yet been addressed experimentally. The vasopressin induced trafficking of AQP2 in isolated inner medullary collecting ducts has been shown to be regulated by calcium and calmodulin inhibitors (160). Pretreatment with the calcium chelator, BAPTA, or calmodulin inhibitors abolished vesicular shuttling of AQP2 in response to vasopressin (160). Hall *et al.* showed that the water permeability of bovine AQP0 expressed in oocytes is also modulated by calcium and calmodulin (161). Lowering extracellular calcium increased bovine AQP0 permeability by 4 fold. Treatment with calmodulin inhibitors also decreased AQP0 permeability which, based on other studies, may be mediated through a direct interaction of calmodulin with the C-terminus (143, 162).

Zeuthen *et al* measured the effects of changes in extracellular pH on the permeability of AQP0, AQP1, AQP2, AQP3, AQP4, and AQP5 (163). In this study using *Xenopus* oocytes, AQP3 was the only aquaporin shown to be sensitive to pH (163). Other studies however have shown that AQP0 is sensitive to changes in extracellular pH. Thus far three reports, addressing the pH sensitivity of bovine AQP0 expressed in oocytes, have yielded conflicting results. These results vary from no effect of pH (163), to a 3 fold increase in permeability by decreasing the pH from 7.4 to 6.5 (161), to a 10 fold increase in permeability at pH 10 and no change at pH 6.5 as compared to pH 7.4 (164). Virkki *et al* also looked at the effect of pH on a fish AQP0 and found a 20%

decrease in water permeability at pH 6.5. Intracellular pH measurements within the lens indicate that peripheral fiber cell cytoplasm has a pH of 7.02, whereas deeper into the lens the fiber cells have an intracellular pH of 6.81 (165). The decrease in pH is a result of lactic acid build up due to the utilization of the glycolytic pathway in the lens interior. A decrease in pH has been shown to result in decreased gap junctional activity (165), inhibition of α-1 Na/K ATPase (43) and an effect of pH on the water channel activity of AQP0 may affect normal lens physiology.

IV. AQP0

A. General introduction

The major intrinsic protein of the ocular lens, MIP, now referred to as aquaporin 0 (AQP0) is found in lens fiber cells where it constitutes over 50% of the total membrane protein (42). Once thought to be expressed exclusively in the lens fiber cells, AQP0 has recently been found localized in the membranes of intracellular vesicles in hepatocytes (119). Within the mouse lens, AQP0 is expressed in primary fiber cells at embryonic day 11.5 and expression of AQP0 continues throughout lens development and in secondary, differentiating fiber cells for the lifetime of the animal (166). Mutations in the gene for AQP0 suggest that AQP0 is crucial for lens development and for establishing (2, 121) and preserving transparency (167). First cloned in 1984 (3), AQP0 has been speculated to play a number of roles within the lens, such as a structural protein, a gap junctional protein, an ion channel, and transporter. With the discovery in 1992 that proteins in the Major Intrinsic Protein /Aquaporin family permit the passive transport of water (4) across lipid bilayers and the demonstration that the presence of AQP0 increases membrane water permeability (40, 112, 168, 169), AQP0 has been proposed to serve as a water channel in the lens. As a water permeable channel, AQP0 may play a crucial role in maintaining lens clarity by regulating the water homeostasis within the lens (5).

As we age, AQP0 is subject to age-related posttranslational modifications, such as, deamidation and extensive backbone cleavage (8). The posttranslational modifications of AQP0 will be discussed below. The extent of posttranslational modifications increases with fiber cell age resulting in a heterogeneous distribution of newly synthesized AQP0 protein in the lens periphery and increasingly modified protein

in the lens nucleus. The modifications observed are concentrated within the C-terminus of AQP0, a putative regulatory domain that is phosphorylated (8) and possibly interacts with calmodulin (162). While, the accumulation of age-related modifications of AQP0 correlates with a decrease in fiber cell membrane water permeability (7), their impact on the water permeability, regulation of function, and the proposed role of AQP0 in the movement of water through the lens have not been determined.

B. Cataractogenic Mutations Linked to Mouse and Human AQP0

Congenital cataracts in mice have been linked to three mutations in the AQP0 gene. Cataractogenic mutations in mouse AQP0 include an amino acid substitution of A51P (Lens opacity cataract, Cat^{LOP}), the replacement of the C-terminus with a long terminal repeat sequence (Frazer cataract, Cat^{Fr}) (170), and a 76 nucleotide deletion (Hydropic fiber cataract, Hfi) (171). All three of these mutations result in impaired protein trafficking to the fiber cell membrane and the retention of the mutant AQP0 protein within intracellular organelles. Homozygous mutant mice develop bilateral opacities within the first several weeks after birth and exhibit gross disorganization of the fiber cells (2, 140, 171). The phenotypic characteristics of the heterozygous mice are much less severe and in some cases these mice develop opacities later than the homozygous mutant animals. In the recently described Hfi (hydropic fiber) mutant mouse, exon 2 of the AQP0 gene, which encodes residues 121-175, is missing (171). The lens fiber cells of the homozygous Hfi mice were disorganized and liquifaction of the center of the lens resulted in total lens opacity by three weeks of age. Heterozygous Hfi

mice presented a less severe cataract with swollen cortical fiber cells at the anterior pole of the lens (171).

Recently a transgenic mouse was engineered with a deficiency in the AQP0 protein. The homozygous AQP0 knock out animal developed cataract by post-natal day 14, whereas the heterozygous animal did not develop opacities until ~6 months of age. The opacities extended from the nucleus to the cortex and were comprised of dense opacities "surrounded by vacuolated and translucent regions" (121). Morphologically, the fiber cells of the heterozygous animals were nonuniform in shape particularly at the anterior and posterior segments and the lateral interdigitations were small and irregular (172). In the homozygous knockout, these interdigitations were absent and the cells were completely nonuniform in shape (172). The water permeability of vesicles prepared from fiber cells from the wild type, +/-, and -/- mice decreased significantly with partial and complete loss of AQP0 protein (121). Measurements of the optical quality of heterozygous knock out lenses demonstrate a loss in the ability to focus (121). These studies indicate that a threshold level of AQP0 is required for lens development and to preserve transparency, that AQP0 contributes to cellular morphology and the cellular architecture of the lens, and that AQP0 imparts water permeability to the fiber cell membranes.

Mutations in AQP0 found in two English families (48) and one American family (103) are linked to the development of congenital, dominant cataracts. A single amino acid substitution in AQP0, T138R, in one of the English families resulted in the development of progressive punctate opacities distributed throughout the lens. In the second English family, the substitution of E134G in AQP0, resulted in a nonprogressive,

uni-lamellar, Y-shaped cataract along the suture (1). The effects of these mutations on AQP0 water permeability were addressed in a *Xenopus* oocyte expression system, however since neither one of the proteins was properly trafficked to the oocyte plasma membrane a permeability measurement was not obtained (48). It is not known whether or not these mutations affect AQP0 protein trafficking in human lens fiber cells. The AQP0 gene was also linked to congenital cataracts found in an American family. The molecular defect in AQP0 is a nucleotide deletion at G214 resulting in a frameshift and an altered C-terminus (173). Interestingly, members of this family demonstrated a wide variety of phenotypes including the two phenotypes mentioned above. Two family members had punctate white opacities in the posterior cortex and to a lesser extent the anterior cortex and a Y-shaped cataract along the posterior suture (103). The phenotypes of three generations of family members were also described. A one month old had vacuoles located in the embryonic nucleus, the 38 year old father exhibited a peripheral star-shaped opacity, and a 60 year old aunt had a dense embryonic nuclear cataract (103). These observations indicate that AQP0 plays a crucial role in maintaining lens clarity of the human lens.

The phenotypic characteristics of cataracts resulting from mutations in AQP0 vary between mice and humans and among family members. Discrepancies between the phenotypes observed in mice and humans with identical cataractogenic mutations have been observed in other lens proteins (46). These variations could be due to a loss of AQP0 function, gain of mutant AQP0 function, impaired trafficking of the AQP tetramer or other proteins through the co- and post-translational machinery, to differences in the genetic background of the individual, or to the age of the individual and the

developmental stage of the cataract. Although the phenotypic characteristics vary, the formation of cataracts, as a result of mutations in the AQP0 gene, provides evidence that AQP0 is critical to establishing the ordered architecture of the lens and preserving lens transparency.

C. Postulated Roles of AQP0 in the Lens

Although AQP0 has been demonstrated to impart water permeability to lens fiber cell membranes, the role of AQP0 in the lens remains controversial. Based on the high levels of AQP0 expressed in the lens, the comparatively low water permeability of AQP0, the location of AQP0 in the fiber cell membrane, and the defects observed in the knock out and mutant AQP0 animals, many investigators in the field believe that AQP0 may serve dual or multiple functions in the lens. Therefore experimental evidence for the ability of AQP0 to function as a water channel, a structural protein, in cell-cell adhesion, an ion channel, and a transporter will be evaluated.

1. Water Transporting Properties of AQP0

The water channel activity of AQP0 has been demonstrated by a number of laboratories in an oocyte swelling assay (1, 40, 112, 150, 164, 168, 169) or in vesicles prepared from lens fiber cell membranes (7, 121). Vesicles generated from fiber cell membranes of mice with the Cat^{FR} mutation or a deficiency in AQP0 have a significantly reduced membrane water permeability as compared to the permeability of vesicles prepared from wild type animals (7, 121). In both cases, the permeability of vesicles prepared from fiber cells of the heterozygous was intermediate between that of the wild

type and homozygous mutant. These studies suggest that AQP0 specifically contributes to the water permeability of lens fiber cell membranes.

In oocytes, the rate of water transport into oocytes heterologously expressing AQP0 is dependent on the magnitude of osmotic gradient (150) and the amount of protein expressed at the oocyte membrane (168). To establish that AQP0 is involved in increasing membrane water permeability, the activation energy of water transport across the oocyte membrane in response to a hypotonic challenge was measured in the presence and absence of AQP0. The activation energy of AQP0 mediated water transport, determined from the permeability as a function of temperature, measured by two groups was 5 kcal/mol (112) and 6.9 ± 2.5 kcal/mol (168). These values were significantly lower than the activation energy for the transport of water across the oocyte membrane in the absence of AQP0 (20.6 ± 4.9 kcal/mol) and were approaching that of the self diffusion of water (4 kcal/mol), suggesting that AQP0 lowers the energy barrier to water transport across the membrane (168).

Based on the oocyte membrane surface area, the density of AQP0 tetramer in the membrane, and the rate of oocyte swelling, Chandy *et al.* estimated the single molecule permeability of bovine AQP0. With an osmotic gradient of 100 mOsmol, AQP1 and AQP0 monomers were estimated to permit transport of 7.2×10^5 and 1.7×10^4 molecules per second, respectively (168). Single molecule water permeabilities determined for AQP0 and AQP1 expressed in oocytes were 1.5×10^{-16} cm^3/sec and 1.4×10^{-14} cm^3/sec (174).

The permeability of AQP0 is lower than the other aquaporins and limited site-directed mutagenesis studies in oocytes have been performed to determine why AQP0

has a lower water permeability. These studies, based on differences in the sequence alignments of the aquaporins and aquaglyceroporins, were performed prior to resolving the AQP structure and have yielded limited information. Of the experiments in which one amino acid was substituted, only one point mutation has been shown to affect AQP0 water permeability. The permeability of bovine AQP0 was increased by ~50% with the mutation of Val160Pro in the fifth membrane spanning domain (112). Chimeric proteins have been constructed and the domains of AQP0 swapped with domains of AQP1, AQP2, and AQP3 (112, 175, 176). Now that the structure of AQP1 has been resolved, more directed predictions of the molecular determinants of AQP0 water permeability can be probed.

Site-directed mutagenesis has been employed in an attempt to impart mercury sensitivity to AQP0. Many aquaporins are inhibited by the interaction of mercury with the sulfhydryl of a cysteine residue near the pore of the channel. AQP0 and AQP4 have an alanine at this position and substitution with cysteine did not confer mercury sensitivity to either AQP0 or AQP4 (112).

Site directed mutagenesis of AQP0 has also been used to determine residues involved in the regulation of AQP0 water permeability by pH and calmodulin. Studies performed in oocytes, demonstrated that substitution of histidine 40 abolished the 4-fold increase in permeability observed when the extracellular pH was shifted from 7.4 to 6.5 (161). (Regulation of aquaporin permeability was also addressed in a previous section). Substitution of the positively charged lysine residues, 228 and 238, in the region of the C-terminus expected to bind calmodulin, residues 225-241 (162), resulted in a decrease in calmodulin binding to AQP0 (143).

2. Structural Role of AQP0

Based on the distribution of AQP0 in the membrane and the phenotypic characteristics of the AQP0 knockout mouse, AQP0 has been proposed to play a role in maintaining the structural integrity of the fiber cell architecture either by interactions with the cytoskeleton or with adjacent cells. Since many of the functions attributed to AQP0 were based on the localization of AQP0 in the fiber cell membranes, a description of the distribution of AQP0 in the membrane is provided. In the cortex, AQP0 is found in the lateral edges of the hexagonal fiber cells. As the fiber cells age and migrate toward the lens nucleus, they lose their hexagonal shape and the lateral edges become less defined (32). In older cells the lateral edges correspond to the wavy junctions that can be observed in these cells (32). Early reports of the association of AQP0 with junctional plaques seemed to be contradictory since they placed the protein in junctional plaques associated with gap junctions or dispersed in single membranes (169). A recent systematic characterization demonstrates that the association of AQP0 with junctional plaques changes with fiber cell age and thus with location in the lens (32). In young, newly differentiated fiber cells, AQP0 is found in single membranes distributed throughout the lateral membranes. In older fiber cells, AQP0 is arranged in patches of square arrays and is associated with junctional plaques (177, 32). The age-related changes, possibly in the structure of AQP0 or cytoskeletal proteins, responsible for the altered distribution of AQP0 in the fiber cell membranes are not known.

The changes in cell morphology and the loss of lateral membrane interdigitations of fiber cells in the AQP0 knock out animal are consistent with the idea that AQP0 may play a structural role in the lens (172). Age-related changes in the location of AQP0

within or lining the periphery of gap junctional plaques led Dunia *et al* to the suggestion that AQP0 may play a role in organizing the junctions (178). Interestingly in support of this idea, alterations in the size and frequency of gap junctional plaques observed in fiber cell membranes of the AQP0 knockout mouse were different than that of the wild type animal (172). In the heterozygous knock out mouse, the gap junctional area in the fiber cells decreased while the number of gap junctional plaques increased as compared to the wild type animal (172). These trends were drastically reversed in the homozygous knock out lenses (172).

Adherent cell-to-cell junctions are a fundamental component in the tightly packed nature of the fiber cell architecture. AQP0 has been suggested to adhere apposing cells based on immunohistochemistry studies of the localization of AQP0 in freeze fractured membranes (178), atomic force microscopy (AFM) of purified AQP0 in crystallized lipid sheets (125), and the aggregation of vesicles prepared with AQP0 (179). The suggestion that adhesion occurs through interactions of the extracellular loops of AQP0 in adjacent cells (178) was supported by AFM studies illustrating AQP0 in apposing lipid bilayers stacked in register with the extracellular loops of AQP0 aligned in a tongue-and-groove manner (125). In contrast, freeze-fracture analyses indicate that AQP0 tetramers found in junctional plaques in older fibers are not stacked in register in apposing fiber cells (177). It is conceivable that the preparation and crystallization of AQP0 in lipid bilayers may have artificially induced the stacking of AQP0 in adjacent bilayers observed by AFM.

Cell-to-cell adhesion by AQP0 has also been proposed to occur through protein-lipid interactions (179). AQP0 reconstituted into liposomes has been shown to promote the aggregation of proteoliposome vesicles (179). The aggregation was proposed to

result from the interaction of four positively charged amino acids in the extracellular loops of AQP0 with negatively charged phospholipids in the adjacent fiber cell membranes (177, 179). Based on sequence alignments and the current understanding of the topology of the homologous AQP1 in the membrane, there would be two, rather than four, positively charged extracellular residues per AQP0 monomer.

3. Ion channel

Phosphorylation dependent, voltage dependent, nonselective ion channel activity has been observed in lipid bilayers reconstituted with AQP0 (180, 181). While these properties were repeatedly observed in lipid bilayers, the results could not be reproduced following heterologous expression of AQP0 in *Xenopus* oocytes (112, 169) nor were they observed in lens fiber cell membranes (165, 182). The wide variety of AQP0 solute selectivity observed (180, 181, 183, 184) may have been a result of minimal purification of AQP0 prior to reconstitution into lipid bilayers and liposomes. Recently, however, whole cell patch clamp studies performed on Sf21 and mouse erythroid leukemia cells heterologously expressing AQP0, showed a weak voltage dependent ion permeability (185). This channel activity was only observed at pH 6.3 not at pH 7. The physiological relevance of these findings within the lens is not known.

4. Transport of Small Neutral Molecules

AQP0 mediated transport of radio-labeled glycerol, inositol, sorbitol, glutathione, deoxyglucose and urea has been tested in a *Xenopus* oocyte heterologous expression system (169). Bovine AQP0 increased oocyte membrane permeability to glycerol by 2

fold (169). Although glycerol transport has been demonstrated in homologous proteins in the major intrinsic protein family, this activity could not be reproduced in oocytes expressing fish AQP0 (164) or in proteoliposome vesicles derived from lens fiber cell membranes (7). Early speculations that AQP0 serves as a gap junction, permitting the communication between cells (186), have since been dismissed since AQP0 and the connexins share little sequence similarity (3) and, when heterologously expressed, AQP0 has not been shown to function as a gap junction (182).

D. Posttranslational Modifications of AQP0

1. Phosphorylation

Previous investigation of the phosphorylation state of AQP0 has shown that activators of protein kinase C (PKC), calcium and TPA (187), and activators of protein kinase A (PKA), cAMP and forskolin (188-190), stimulate phosphorylation of the C-terminus of AQP0. Previous studies, based on comparisons of the HPLC retention time of tryptic peptides of bovine AQP0 with synthetic peptide standards, reported that bovine AQP0 was phosphorylated at Ser 243 and Ser 245 (191). The water permeability of bovine AQP0 was slightly decreased by substitution of Ser 245 and Ser 243 for alanine but this appeared to be due to less efficient incorporation of the mutant protein in *Xenopus* oocyte membrane (112). Subsequent analysis of bovine and human AQP0 by tandem mass spectrometry demonstrated that the most abundant phosphorylation site was at Ser 235 (8, 192). In addition, phosphorylation at serine residues 243 and 245 in bovine AQP0, which are not conserved in the human AQP0, was not detected by mass spectrometry (8, 192) (Fig. 1.10). The phosphorylation of other aquaporins has been

shown to affect membrane water permeability by gating and trafficking mechanisms, as discussed previously, however the functional consequences of C-terminal phosphorylation of human AQP0 are not known.

2. Age-Related Deamidation of AQP0

AQP0 has been shown to be deamidated at asparagine residues 246 and 259 (8, 193) (Fig. 1.10). Deamidation of AQP0 was detected by Edman sequencing and tandem mass spectrometry following chemical derivatization (8). Deamidation of AQP0 isolated from human lenses was detected in a 7 year old lens, the youngest lens examined (8). While secondary, tertiary, and quaternary structure are known to influence the rate of deamidation, the effect of residues adjacent to the site of deamidation on the rate of deamidation can be predicted. Based on studies of the rate of deamidation of pentapeptides at pH 7.4, 37°C, in 0.15M Tris HCl, the half-time of deamidation of the Asn residues at 246 (SNG) and 259 (LNT) would be 0.96 and 46.1 days, respectively (75). The effects of deamidation and the incorporation of two negative charges into the C-terminus of AQP0 have not yet been addressed.

3. Age-Related Truncation of AQP0

AQP0 undergoes extensive backbone cleavage in normal human lenses of all ages (93, 97, 194) and an accelerated rate of truncation has been observed in cataractous lenses (95, 96, 98). SDS-PAGE and immunoblot analysis indicate that with age, AQP0, a 28 kDa protein that migrates to ~ 26 kDa, is cleaved to a 22 kDa product (93, 94, 195-197).

Human AQP0

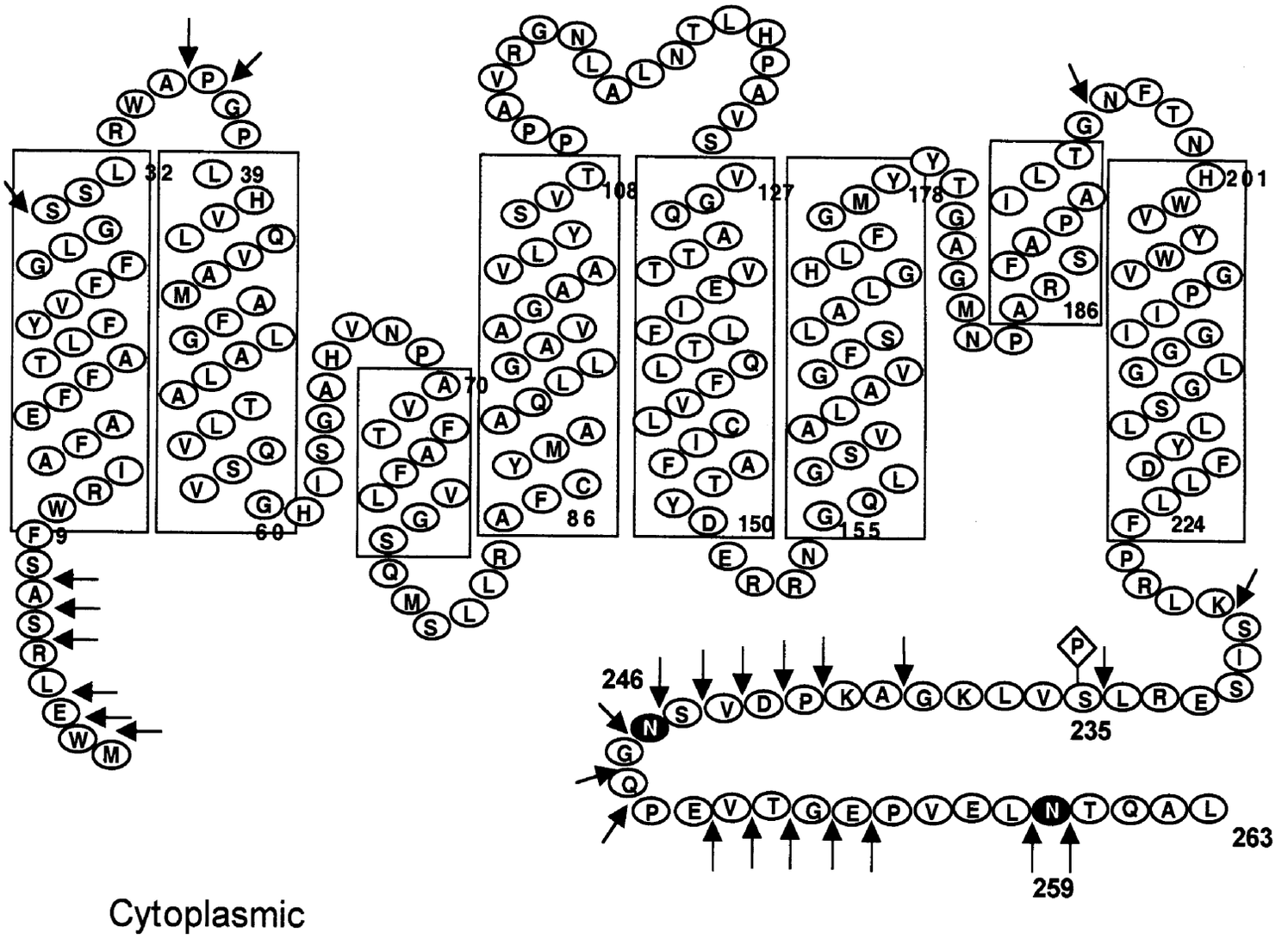

Figure 1.10. Sequence and previously identified posttranslational modifications of human AQP0. The arrows indicate sites of posttranslational truncation. The asparagine residues at positions 246 and 259 are deamidated and serine 235 is phosphorylated. Based on data presented in reference #8.

N- and C-terminal truncation was confirmed using antibodies generated against these regions of the protein (57, 97), however the exact sites of truncation were not identified. While there are a number of publications demonstrating that AQP0 is truncated with age and in cataract, mass spectrometric analysis permitted the identification of the exact sites of truncation. This information is not only useful in defining the structures of AQP0 that are present in the human lens but also in the identifying proteases that may be involved in the proteolytic processing of AQP0.

Mass spectrometric analysis of human AQP0 isolated from whole lens homogenates from patients ranging in age from 7 to 81 years revealed multiple sites of protein truncation (8). In these studies the membrane protein, containing over 50% AQP0, was isolated from whole lens homogenates and cleaved with cyanogen bromide. Cyanogen bromide cleavage at methionine residues resulted in large peptide fragments that were subsequently separated by reversed phase HPLC and mass analyzed by ESI-MS/MS. Peptides covering the entire AQP0 sequence were observed and sites of truncation were detected on the C-terminal side of residues 1, 2, 3, 5, 6, 7, 29, 35, 37, 196, 211, 228, 234, 239, 241, 242, 243, 244, 245, 246, 247, 248, 250, 251, 252, 253, 254, 258, and 259 (Fig. 1.10) (8). The exact sites of truncation were deduced from the measured and predicted masses of the truncated products. Quantitative analysis indicated that the amount of the intact N-terminal cyanogen bromide fragment, residues 1-46 and 2-46, and the amount of the intact C-terminal cyanogen bromide fragment, residues 184-263 decreased with the age of the patient. By age 86, the amount of intact N-terminal cyanogen bromide peptide was very low, whereas the intact C-terminal cyanogen bromide peptide could not be detected. Chromatographically separated fractions

containing the C-terminal peptide, 184-163, and truncation products of this peptide, 184-x, were further analyzed by MALDI-MS (Fig. 1.11). These mass spectra demonstrate a similar pattern of truncation observed in each lens and an increase in truncation with age. Mass spectrometric analysis of AQP0 isolated from noncataractous human lenses, ages 7 to 86, demonstrates that truncation of AQP0 begins as early as age 7 and continues with age (8).

An increase in the level of C-terminal truncation of AQP0 was also observed as a function of fiber cell age in a lens from a 27 year old patient. The membrane protein was isolated from six concentrically dissected layers of the lens and was mass analyzed following cyanogen bromide cleavage as described above. The outer cortical layer contained the newly differentiated, young fiber cells, whereas the inner nuclear layer was composed of the aged fiber cells of the fetal and embryonic nucleus. The pattern of AQP0 truncation as the fiber cells age is shown in Fig. 1.12. In the outer cortex, the predicted C-terminal cyanogen bromide fragment, residues 184-263 m/z 8636, was the predominant signal observed. However, in the older fiber cells the signal intensity of the intact C-terminal peptide decreased relative to truncated forms of the protein represented by peptides, residue 184 through residues 228, 234, 238, 239, 241, 243, 245, 246, 247, 248, and 259. The signals in the mass spectra were assigned by comparing the observed masses with the predicted masses of the intact and truncated C-terminal peptides. While analysis by MALDI-TOF mass spectrometry is not quantitative, the major sites of truncation appear to be after residues 243, 246, and 259. The effect of C-terminal truncation of AQP0 on the water channel activity of the protein has not been determined.

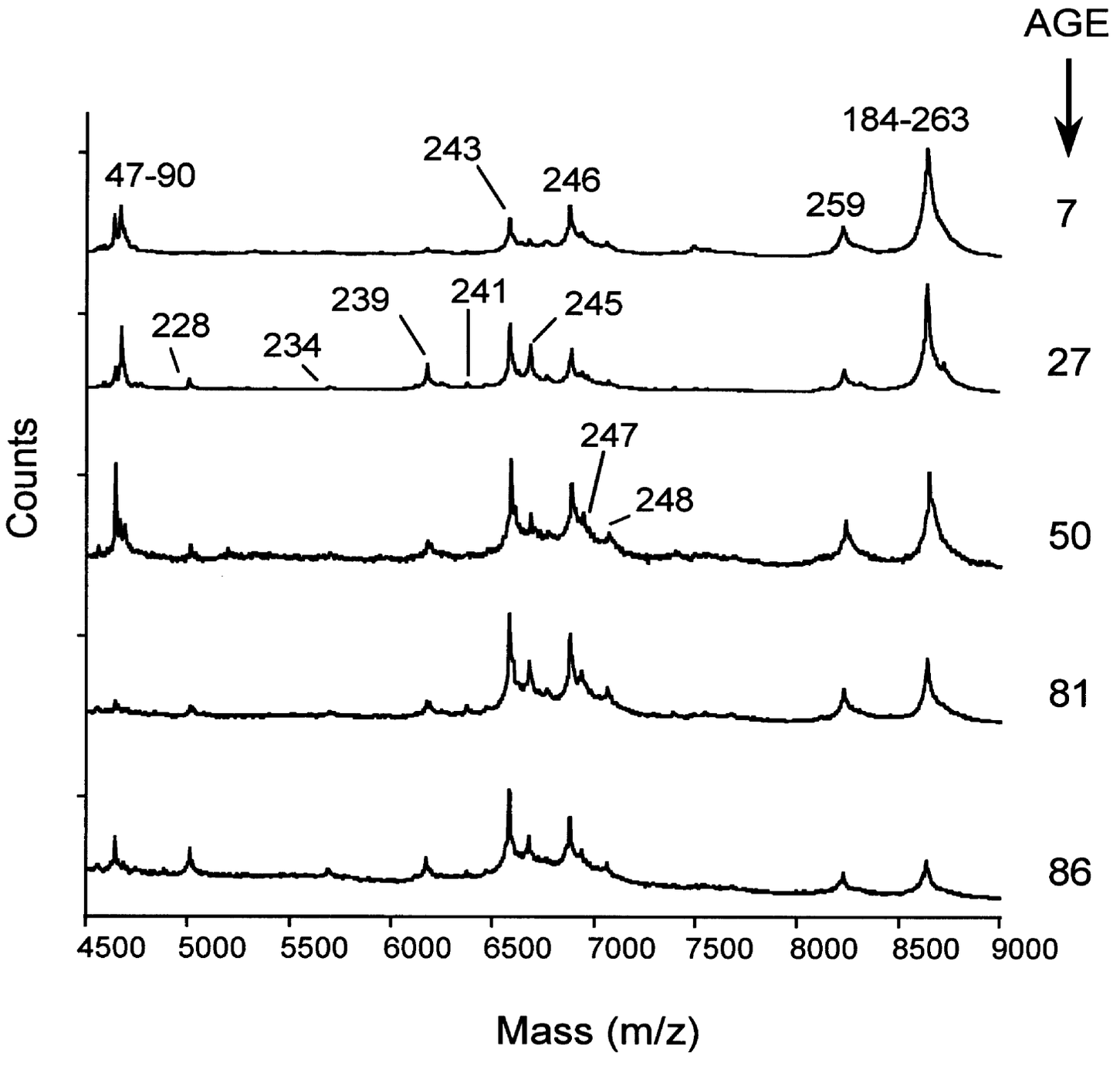

Figure 1.11. MALDI-mass spectra of an HPLC fraction containing C-terminal peptides of AQP0 from human lenses ranging in age from 7 to 86. Membrane protein isolated from whole lens homogenates was cleaved with cyanogen bromide, the peptides were separated by RP-HPLC and the fractions analyzed by MALDI-MS. The expected C-terminal peptide of AQP0, generated by cyanogen bromide cleavage, contains residues 184-263. Signals from peptides corresponding to *in vivo* truncation within the C-terminus are labeled with the C-terminal residue, 184-x. An additional cyanogen bromide cleaved peptide, residues 47-90, also eluted with the C-terminal peptides. Data presented in reference 8.

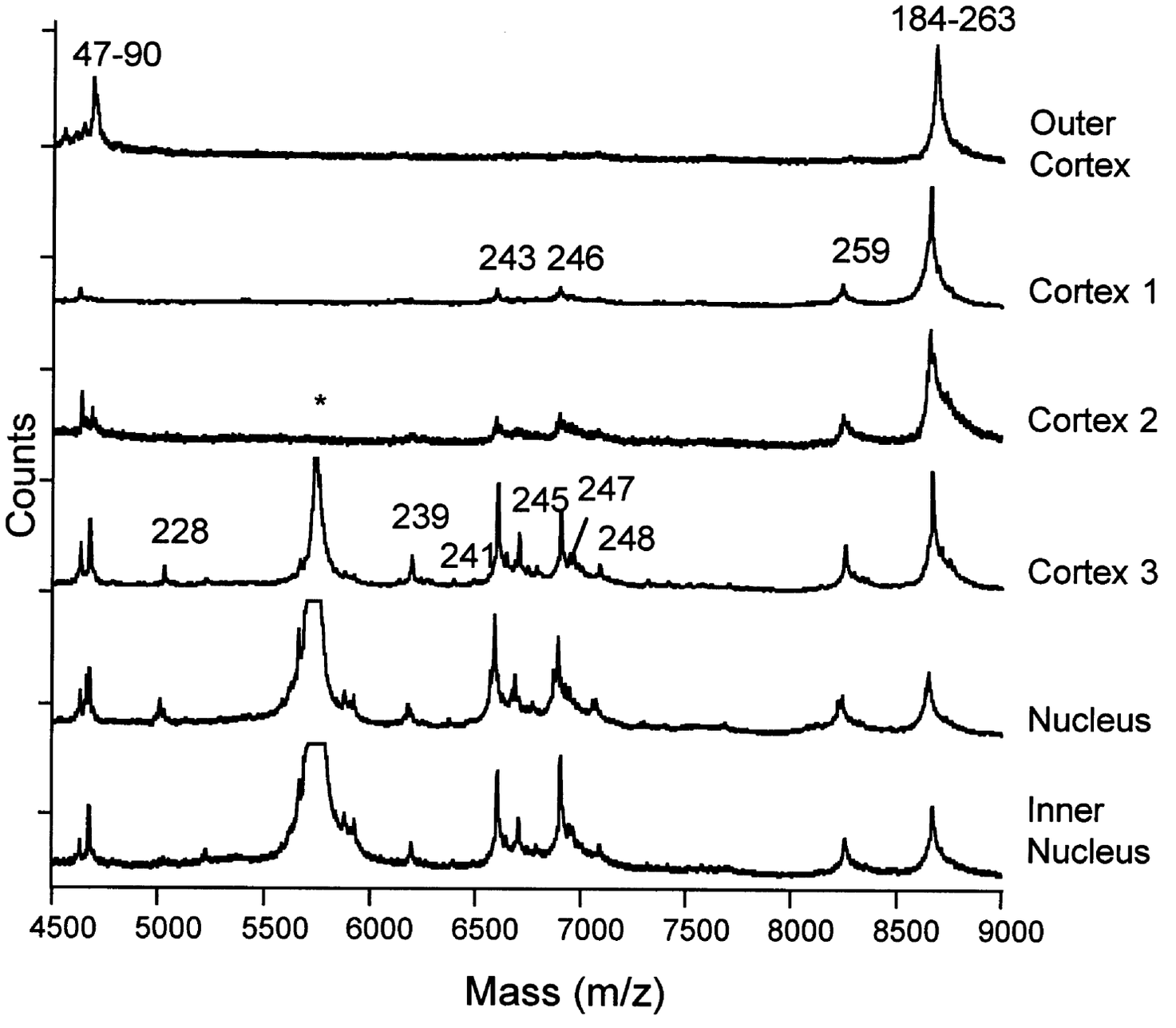

Figure 1.12. MALDI-mass spectra of C-terminal peptides of AQP0 from a 27 year old lens. The expected C-terminal peptide of AQP0, generated by cyanogen bromide cleavage, contains residues 184-263. Signals from peptides corresponding to *in vivo* truncation within the C-terminus are labeled with the C-terminal residue, 184-x. An additional cyanogen bromide cleaved peptide, residues 47-90, also eluted with the C-terminal peptides. The internal standard used for mass calibration, indicated by an asterisk, is not shown for the outer layers since it supressed the signals observed for low intensity peaks.

4. Truncation of AQP0 in Animal Models of Cataract and in Opaque Regions of Human Lenses

Covalent changes in the structure of AQP0 isolated from opaque regions of the lens have been probed by anti-sera binding. Using anti-sera generated against peptides of AQP0, immunoblotting analysis has been performed on AQP0 isolated from whole lenses or opaque tissue from cataractous lenses. The most consistent result obtained was the variability of an anti-AQP0 229-237 antibody binding to AQP0. Antibody binding to these residues increased in AQP0 isolated from human maturity-onset cortical cataract, an aged Hannover Wistar rat model of spontaneous cortical and posterior subcapsular cataract, and a streptozotocin-induced cataract rat model of diabetic cataract (98, 198, 199). The anti-AQP0 229-237 binding to AQP0 isolated from maturity-onset nuclear and cortical human cataracts increased compared to antibody binding to AQP0 in the normal lens, while anti-AQP0 252-259 and anti-AQP0 256-263 binding remained the same in cataractous and normal lenses (98, 200). There is a possibility that the presence of phosphorylation at serine 235 (8, 71) may be involved in these results of these studies.

Truncation of AQP0 has also been observed in a Guinea pig model of maturity-onset nuclear cataract. Animals subject to hyperbaric oxygen, to simulate oxidative stress, develop nuclear opacities and AQP0, actin, vimentin, ankyrin, alpha-actinin and tubulin are prematurely degraded (201). Interestingly, the cytoskeletal proteins were degraded in young treated animals, whereas AQP0 was only degraded in aged animals treated. As determined by SDS-PAGE analysis, the levels of intact AQP0 were the same in the cortex of the control and experimental animals but dramatically decreased in the

lens nucleus of the aged oxygen-treated animals (201). These studies suggest that oxidative stress may be a precursor to the formation of maturity-onset cataracts (201).

Sites of C-terminal truncation of AQP0 in the selenite-induced cataract rat model of nuclear cataract, detected by mass spectrometry, suggest that in the rat lens m-calpain may be involved in proteolysis of AQP0. AQP0 truncation unique to the selenite-induced cataract occurred after residues 231, 235, 237, 253, and 260 while truncation after residues 234, 238, and 239 were present in the selenite-treated and control animal lenses (71). A sequence alignment of AQP0 from different species is shown in Figure 1. 13. The most abundant truncation sites of AQP0 in the selenite treated animals were after residues 238 and 253 (71). Lys 238 was also a major site of truncation following *in vitro* cleavage of rat AQP0 with m-calpain (71). These data suggest that m-calpain, in addition to other proteases, may be involved in the cleavage of AQP0 in normal and cataractous rat lenses. However, since there are more isoforms of calpain and a higher level of m-calpain activity found in rat lenses than human lenses (70), the relevance of the selenite-induced cataract rat model, in which high levels of calcium activate calpains (202), to cataract formation the human lens is not known.

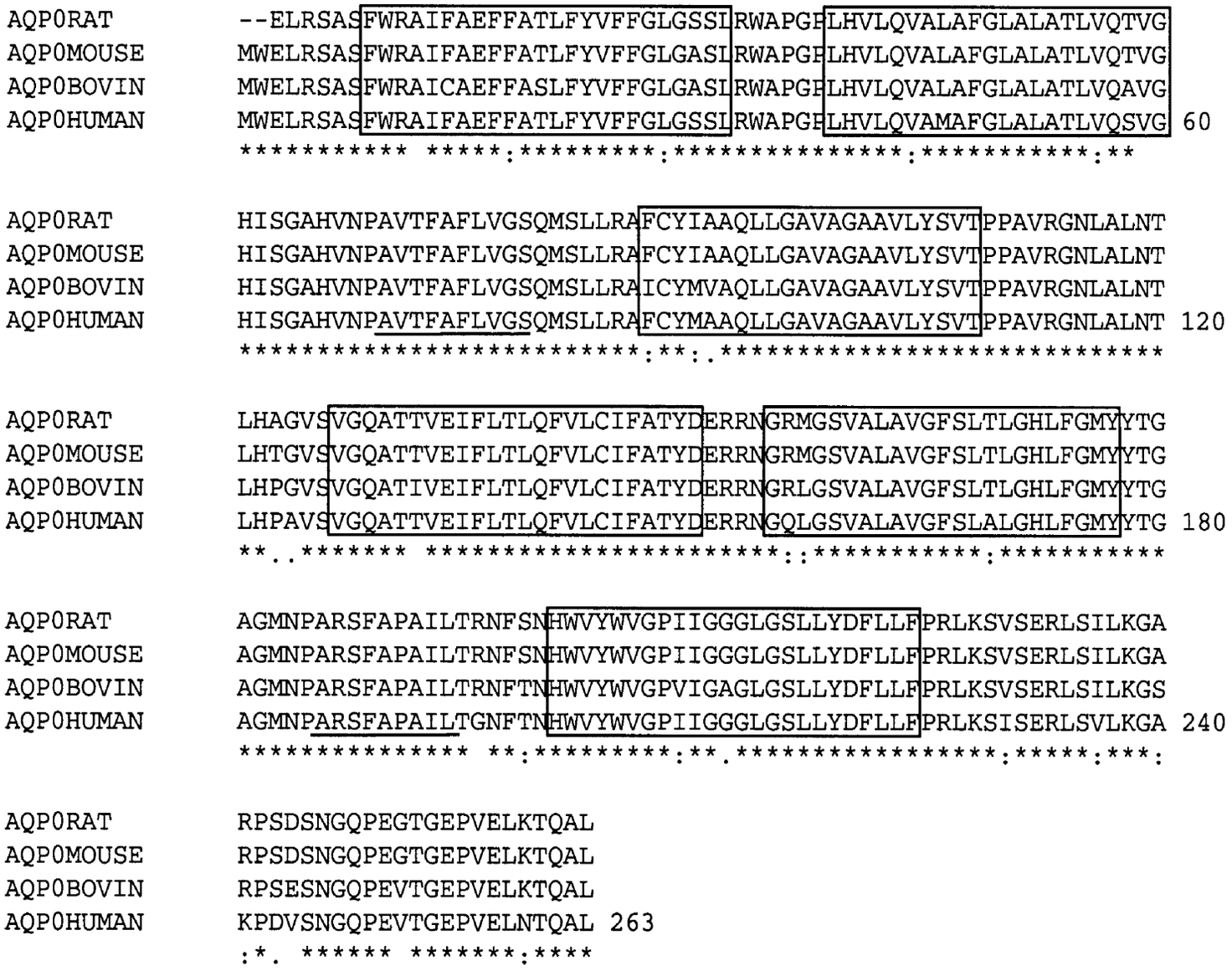

Figure 1.13. Sequence alignment of Aquaporin 0 from different species. Predicted transmembrane domains are boxed. The two short helices that do not span the membrane are underlined. Predicted topology is based on sequence alignments of mammalian aquaporins and the helices observed in the electron microscopy resolved structure of human AQP1.

CHAPTER 2

RATIONALE AND SPECIFIC AIMS

The loss of lens transparency is the leading cause of blindness worldwide. In the United States cataract surgery is the most frequently performed surgical procedure among Medicare beneficiaries costing approximately $3.5 billion per year (203). Presently, there are no universally accepted pharmacological interventions to halt or reverse the formation of cataract. While surgical replacement of diseased lenses restores vision to an estimated 1.5 million Americans per year there are risks and complications associated with the surgery. An understanding of the molecular mechanisms responsible for the onset and formation of opacities will permit the development of a means for pharmacological intervention. However, before this can be achieved, a basic understanding of normal lens physiology and the effects of age on lens physiology must be attained.

The focus of our research has been to identify age-related changes in the structure of Aquaporin 0 (AQP0) also known as the major intrinsic protein (MIP) of the lens. The most abundant membrane protein in the lens, AQP0, comprises over 50% of the total membrane protein in lens fiber cells (42). As a member of the Aquaporin family of integral membrane transporters, AQP0 has been proposed to serve as a water channel contributing to the internal circulatory system within the lens (5). Mass spectrometric analysis of AQP0 isolated from human lenses of varying ages illustrates an increase in posttranslational modifications with age (8). Preliminary data show that the age-related accumulation of modifications is reflected spatially within single human lenses yielding highly modified AQP0 in the oldest nuclear region of the lens. Correlated with the increase in posttranslational modifications of AQP0 with fiber cell age is the decrease in membrane water permeability of aged fiber cells. The effects of age-related

posttranslational modifications in the C-terminus, a putative regulatory domain of AQP0, on protein function have not been investigated. The goals of the present study are to determine the distribution of posttranslationally modified forms of AQP0 within the normal human lens by mass spectrometry and to determine how the observed modifications influence the water channel activity of the protein. The hypothesis proposed in this research project is that **age-related changes in the primary structure of AQP0 decrease the water channel activity of the protein**. To examine the structure and functional effects of age-related posttranslational modifications of human AQP0 the specific aims of this research are:

1. To determine the pattern of distribution of posttranslationally modified products of AQP0 within the normal human lens.

2. To determine the water permeability of human AQP0.

3. To construct mutants of AQP0 reflecting the posttranslationally modified forms of the protein observed in the human lens and to assay the water channel activity of the recombinant mutant proteins.

CHAPTER 3

DISTRIBUTION OF AGE-RELATED MODIFICATIONS OF AQP0 IN THE NORMAL HUMAN LENS

INTRODUCTION

The ocular lens, which transmits and focuses light onto the retina, retains aged cells and proteins throughout one's lifetime while maintaining the transparent nature of the lens for decades. As the lens grows, newly differentiating cells in the lens periphery compress the older fiber cells toward the center of the lens resulting in concentric layers of fiber cells that vary in age (14, 25). Due to the lack of cellular and protein turnover in mature fiber cells (204), proteins in the lens range in age from newly synthesized at the lens surface to proteins that are as old as the individual in the lens nucleus. The lens, therefore, provides a unique system for investigating the effects of age on protein structure. During the normal course of aging, lens proteins are subject to age-related posttranslational modifications including backbone cleavage, deamidation, isomerization, and racemization (56, 80). Backbone cleavage of aged lens proteins has been shown to occur through the proteolytic activity of enzymes (61, 65) or through spontaneous, nonenzymatic truncation events (86). The spontaneous formation of a succinimide ring at susceptible asparagine and aspartic acid residues is a common intermediate that results in deamidation, isomerization, racemization, and backbone truncation (74). Within the lens, these events are not random events but occur reproducibly with protein age (24).

Aquaporin 0 (AQP0, MIP), the most abundant membrane protein in the lens, is expressed in newly differentiating fiber cells and is present in all of the fiber cells throughout the lens. A member of the Major Intrinsic Protein/ Aquaporin family of water channels, AQP0 is a 28 kD protein with six transmembrane domains and intracellularly localized N- and C-termini. Although several different roles have been attributed to AQP0 (7), the ability of the protein to transport water has been demonstrated

reproducibly in a number of laboratories (1, 168, 169). This raises the possibility that AQP0 is a component of the internal circulatory system in the avascular lens (12) contributing to lens transparency by maintaining osmotic balance. While the precise function of AQP0 in the lens is not entirely clear, its role in maintaining transparency is evidenced by the formation of cataract in humans (1) and animals (2, 171, 205, 206) with mutations in the AQP0 gene. Studies have also shown that a deficiency in AQP0 not only results in the formation of cataract but an impaired focusing ability of the lens, a decrease in fiber cell membrane water permeability, and a non-uniform cell shape (121). The C-terminus of human AQP0, a putative regulatory domain, is phosphorylated (8) and undergoes age-related deamidation (8) and extensive backbone cleavage (8, 93, 97, 194). These age-related modifications are more prevalent in aged fiber cells within the center or nucleus of the lens resulting in a heterogeneous distribution of posttranslationally modified products of AQP0 spatially within the lens potentially impacting the movement of water through the lens. Decreased fiber cell membrane water permeability (7) and a change in membrane localization of AQP0 (32) both correlate with the accrual of posttranslational modifications of AQP0 in aging fiber cells. However, the exact age-related molecular alterations responsible for these effects are not known.

The purpose of this study was to further characterize the age-related posttranslational modifications in the C-terminus of AQP0 in order to elucidate the major products of AQP0 and their distribution in the normal aging lens. Previous mass spectrometric analysis of human AQP0 permitted the identification of many sites of C-terminal truncation, deamidation at Asn 246 and Asn 259, and phosphorylation at Ser 235 (8). The approach presented here revealed additional sites of truncation and

phosphorylation, age-related racemization/isomerization of aspartic acid, and permitted relative quantitation of these modifications with fiber cell age. Three lenses, ages 34, 35, and 38 were concentrically dissected into 3-4 layers and AQP0 was isolated from each lens section. The C-terminus and the posttranslationally modified forms of the C-terminus were released from AQP0 by trypsin cleavage and analyzed by mass spectrometry. Identification of the sites of age-related posttranslational modification and where they occur within the lens may provide insight into the mechanisms responsible for these modifications. In addition, knowledge of the spatial distribution of posttranslationally modified products of AQP0 will aid in the understanding of AQP0 function throughout the lens and its potential contribution to the circulation of water and nutrients through the lens. Finally, this approach will permit quantitative comparisons of age-related changes of AQP0 in normal human lenses as they occur with fiber cell age with those that occur in age-related cataract.

EXPERIMENTAL PROCEDURES

Dissection of Human lens and Preparation of AQP0- Human eyes were obtained from National Disease Research Interchange (Philadelphia, PA). Lenses were removed and the Tenets of the Declaration of Helsinki for dealing with human samples were strictly followed. Lenses ages 34, 35, and 38 were dissected into 3 to 4 concentric layers consisting of the outer cortex, inner cortex, outer nucleus, and the nucleus in collaboration with Dr. Donita Garland (National Eye Institute) (24). The lens sections were frozen and shipped on dry ice. Each lens section was homogenized with a hand held teflon pestle in an eppendorf tube with 10 mM NaF, 10 mM $NaHCO_3$, 5 mM EDTA pH 8.0 (300 μl) and centrifuged at 88,000 x g for 20 min at 4°C. Sodium fluoride was included in the homogenization buffer to inhibit endogenous phosphatases. To remove soluble and extrinsic membrane proteins, the pellet was washed sequentially with Tris buffer (1 mM $CaCl_2$, 1 mM EDTA, 10 mM Tris base, pH 9.1), freshly made 4 M and 7 M urea in Tris buffer, dH_20, 0.1 M NaOH, and finally dH_20. The membrane pellet was resuspended in dH_20 (200 μl) and the total protein concentration was determined by Bradford assay using bovine serum albumin as a standard (207).

MALDI-MS of intact membrane protein- The membrane protein from each lens section was analyzed by MALDI-MS using sinapinic acid matrix with formic acid and hexafluoroisopropanol (208). Peptide/matrix solutions (0.5 μl) were spotted and dried on a MALDI sample plate and were mass analyzed with a Voyager DE or Voyager DE-STR TOF mass spectrometer (Applied Biosystems) following desorption with a 337 nm nitrogen laser. Thioredoxin (11673.5 Da) and apomyoglobin (16951.6 Da) were used as

internal standards for mass calibration. The average masses of full length and truncated forms of AQP0 protein were calculated using Sherpa Lite software.

RP-HPLC-ESI-MS analysis of the C-terminus of AQP0- The membrane protein (30 μg) from each lens section was digested with trypsin at a ratio of 1:50 in 10 mM ammonium bicarbonate pH 8.8 (total volume 200μl) at 37°C for 18 h. The digestion reaction was diluted with water (0.5 ml) and centrifuged at the above conditions for 20 min to pellet the membranes. The peptides released from the membrane protein were collected, dried down under vacuum, and resuspended in water (20 μl). In order to load approximately the same amount of sample in each LC-MS analysis, the peptide concentration was assessed by spectrophotometry using the extinction coefficient of a synthetic peptide of AQP0, Ac239-263, as a standard (Ac refers to acetylation). The amount injected was typically equivalent to the peptides released from 7-10 μg of total membrane protein. The peptides were separated on a 1 x 150 mm C18 Vydac column with a flow rate of 20 μl/min in-line (Agilent 1100 Series HPLC) with an ion-trap mass spectrometer (Finnigan LCQ Classic). The HPLC gradient was 2-60% B in 120 minutes, 60-98% B in 30 minutes, and 98% B for 10 minutes and consisted of 0.02% heptafluorobutyric acid (HFBA) in water (A) and 0.02% HFBA in 60% acetonitrile (B). Mass spectra were acquired using a mass range of 300-2000 m/z and tandem mass spectrometric data were automatically collected with the dynamic exclusion feature enabled. The identity of the peptides and sites of posttranslational modifications were confirmed by tandem mass spectrometry.

Quantitative analyses of truncation between residues 239-263 and phosphorylation of tryptic peptides, 234-238 and 229-233, were based on the intensity of

the signals for peptides detected in the ion trap mass spectrometer during LC-MS. By specifying the mass to charge ratio (m/z) of a predicted peptide, the selected (or extracted) ion chromatogram was generated and the area of the peak was calculated by the Xcalibur software (Finnigan). The percent of phosphorylation was calculated from the peak area of the phosphorylated peptide compared to the sum of the peak areas for the unphosphorylated and phosphorylated peptide.

The percent of truncation observed within the tryptic peptide 239-263 was calculated from the peak area of the truncated peptide, 239-x, compared to the sum of total peak areas for the intact and all truncated forms of the peptide, 239-263. For higher molecular weight peptides, the sum of the peak areas for each charge state within the mass range 300-2000 was included in the determination of relative abundance. Multiple analyses were performed on the three sections of the 34 year old lens, these data are presented as the mean percent of modification ± the SE (n= the number of LC-MS analyses).

Identification of isomerized and racemized aspartic acid- Four versions of the peptide GAKPDV, AQP0 residues 239-244, were synthesized by solid phase peptide synthesis at the Medical University of South Carolina Biotechnology Core Facility with the aspartic acid substitutions of L-aspartic acid, L-iso-aspartic acid, D-aspartic acid, or D-iso-aspartic acid. The elution profile of the four peptides was determined using the same conditions for LC-ESI-MS as stated above.

In vitro truncation of a C-terminal synthetic peptide mimetic- An N-terminally acetylated peptide of AQP0, Ac239-263, was synthesized as above and purified. To test for the possibility of *in vitro* truncation of the C-terminus of AQP0 in the absence of proteolytic enzymes, the synthetic peptide was incubated at 37°C in ammonium bicarbonate buffer pH 8.8 for 0-96 hours. The incubation mixture was dried down and analyzed by LC-ESI-MS as described above.

This peptide, AQP0 Ac239-263, was also used as a standard for determination of the amount of lens peptide digest to use for LC-ESI-MS analysis. Following purification, the peptide concentration was determined by amino acid analysis and the extinction coefficient was calculated.

RESULTS

Three human lenses of similar age were dissected concentrically and fiber cell membranes were isolated from each lens section. Mass spectrometric analysis was utilized to measure the mass of AQP0 prior to trypsin digestion and the tryptic peptides that were released from AQP0 following trypsin digestion from each lens section. The sites of posttranslational truncation, phosphorylation, isomerization, and racemization of the C-terminus of AQP0 were identified by tandem mass spectrometry. Furthermore, the relative abundance of phosphorylation and backbone cleavage of the C-terminus of AQP0 within different regions of the lens was determined.

Dissection of human lenses and preparation of AQP0

Lens membranes containing human AQP0 were isolated from concentrically dissected regions of 34, 35, and 38 year old lenses. Concentric dissection yields young fiber cells with newly synthesized proteins in the lens cortex and fiber cells as old as the individual in the lens nucleus. The 34 year old lens was dissected into 3 sections; outer cortex, inner cortex, and the nucleus; whereas the 35 and 38 year old lenses were dissected into 4 sections; outer cortex, inner cortex, nucleus, and inner nucleus. The total amount of membrane protein per lens section in the 34 year old lens as determined by Bradford analysis, starting with the most central, nuclear layer, was 39 μg, 100 μg, and 65 μg. In the 35 year old lens the total amount of membrane protein per lens section, starting with the most central layer, was 93.6 μg, 84.8 μg, 40.2 μg, and an estimated 4.5 μg. In the 38 year old lens, starting with the central layer, the total membrane protein

was 109 μg, 110.2 μg, 34.6 μg and an estimated 7.5 μg in the outer cortical layer. Due to the small sample size of the outer cortical layers, the protein concentration was estimated from the absorption of the tryptic peptides rather than the Bradford assay.

MALDI-MS analysis of AQP0 isolated from different regions of the lens

The membrane protein from each lens section was analyzed by MALDI-TOF mass spectrometry. Figure 3.1 shows the molecular weight of AQP0 and lower molecular weight products resulting from backbone cleavage of AQP0 that occur with fiber cell age in the 35 year old lens. The signals attributed to truncation are consistent with those observed for the 38 and 34 year old lenses (Figs. 3.2, 3.3). In the newly differentiated fiber cells of the outer cortex, the most abundant signal in the mass spectrum was intact AQP0, residues 1-263. The measured and calculated masses of intact AQP0 $[M+H]^{1+}$ ions were 28,129 and 28,121 Da, respectively. Most noticeable is the increase in lower molecular weight species with fiber cell age. These signals correspond to the calculated masses of C-terminally truncated AQP0, 1-259, 1-246, and 1-243 ($[M+H]^{1+}$ ions = 27,708, 26,357, and 26,060 Da respectively). A summary of the calculated and measured masses is shown in Table 3.1. MALDI-MS analyses of the membrane protein isolated from each lens section of the 34, 35, and 38 year old are consistent with previous observations that the most abundant sites of C terminal truncation in human AQP0 are after residues 246 and 259 (8) and that the extent of backbone cleavage increases with fiber cell age (97).

In addition to the predicted truncation products of AQP0 observed in the MALDI-MS spectra, a signal was also detected that was higher than the calculated molecular weight of AQP0. In mass measurements of lens membrane protein from all of the lens sections, signals corresponding to AQP0 shifted in molecular weight by 202.7 ± 4 Da (mean ± SE, n=14) were detected. The identity of this species is unknown. However, a similar shift in mass was also detected in the internal standards for mass calibration, apomyoglobin and thioredoxin. This raises the possibility that the unknown signals observed in Figures 3.1-3.3 (28,371, 28,338, and 28,352 m/z) are a result of formation of adducts with the matrix used in the sample preparation for MALDI-MS. The sinapinic acid matrix used has a molecular weight of 224 Da.

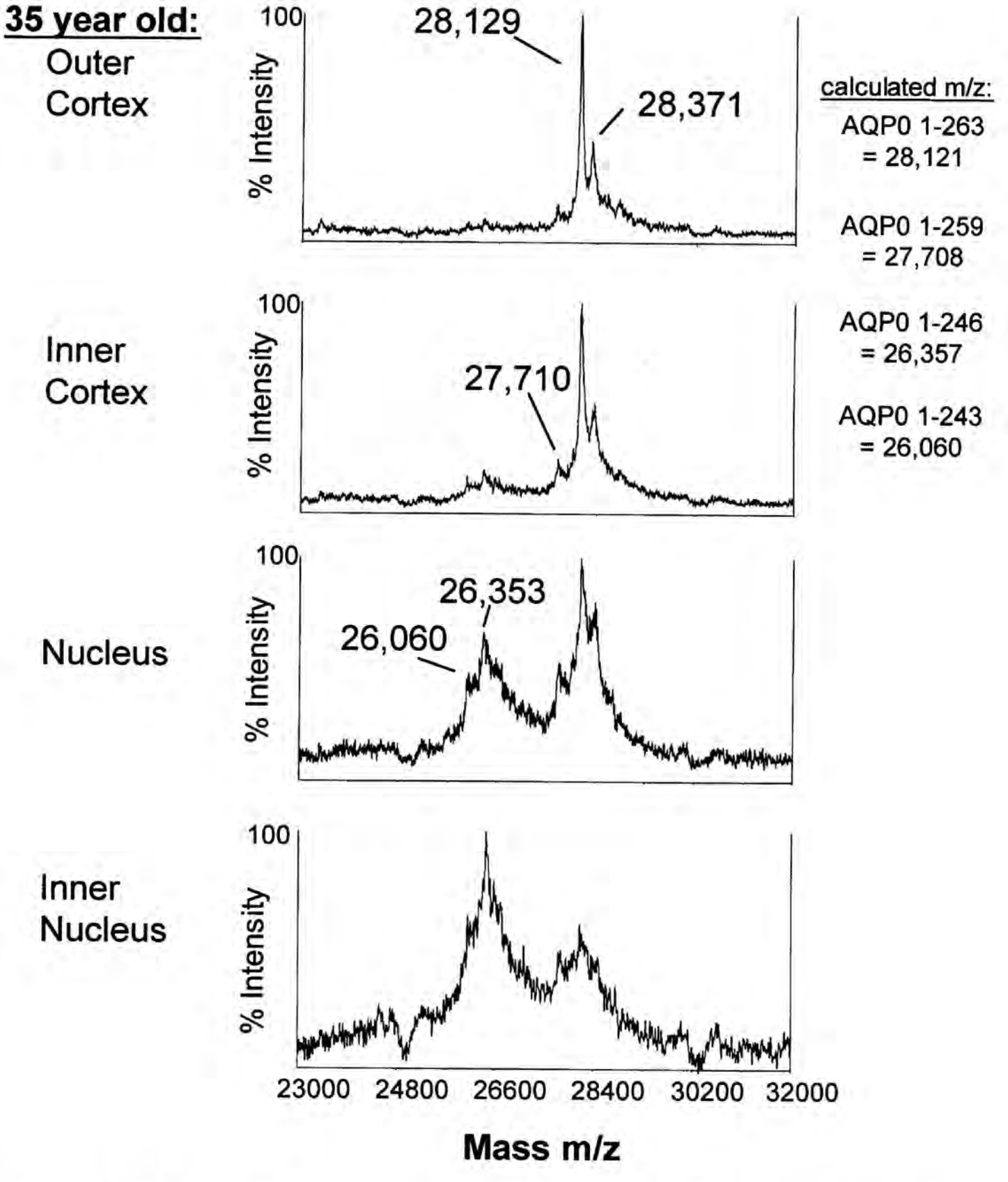

Figure 3.1. MALDI-MS of membrane protein isolated from four concentric sections of a 35 year old lens. The average expected molecular weight of AQP0 is 28,121 kD. The expected molecular weights of the truncation products of AQP0, 1-259, 1-246, and 1-243 are 27,708, 26,357, and 26,060 Da, respectively. An internal standard, apomyogobin, was used for mass calibration.

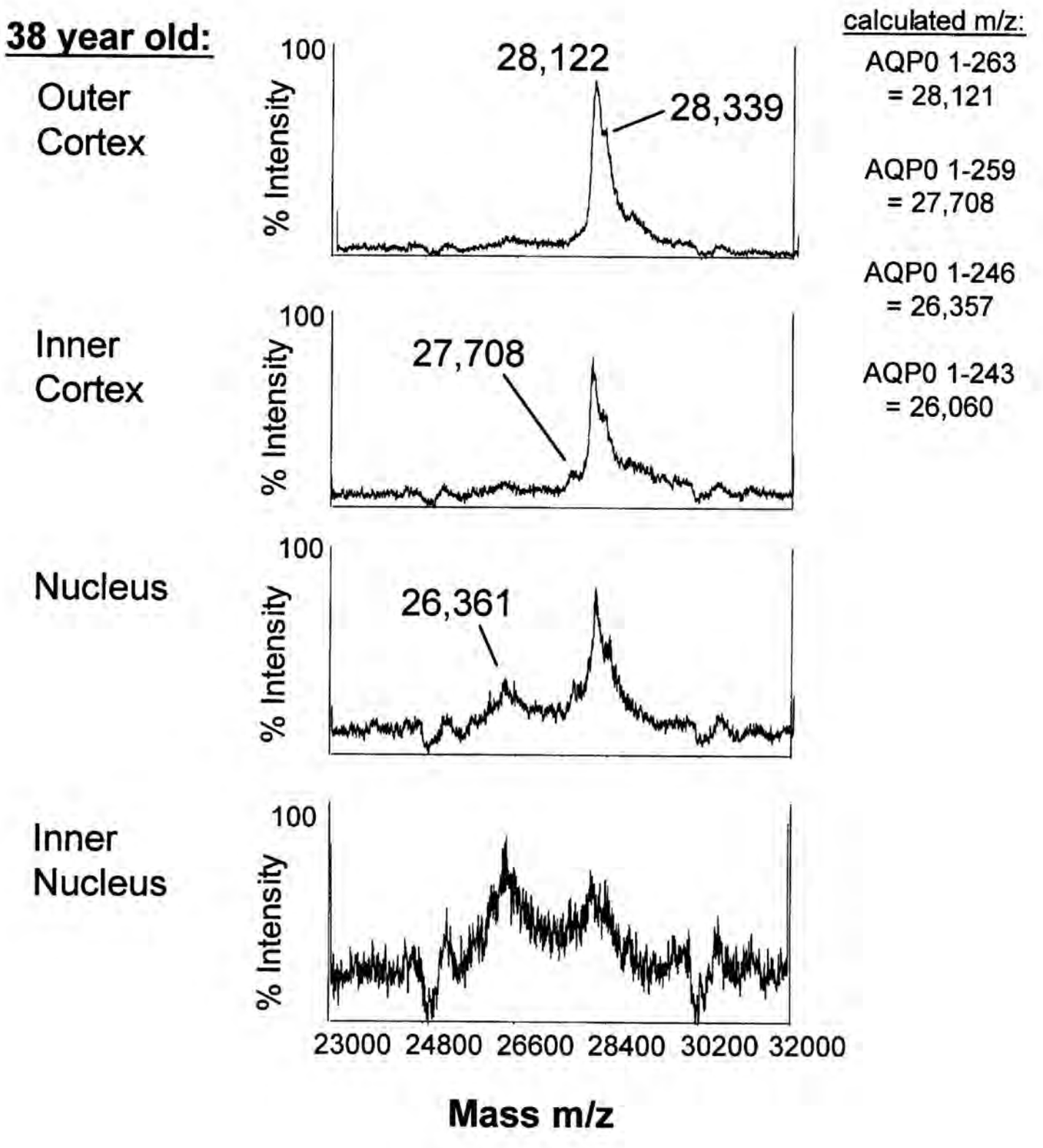

Figure 3.2. MALDI-MS of membrane protein isolated from four concentric sections of a 38 year old lens. The average expected molecular weight of AQP0 is 28,121 kD. The expected molecular weights of the truncation products of AQP0, 1-259, 1-246, and 1-243 are 27,708, 26,357, and 26,060 Da, respectively. An internal standard, apomyoglobin, was used for mass calibration.

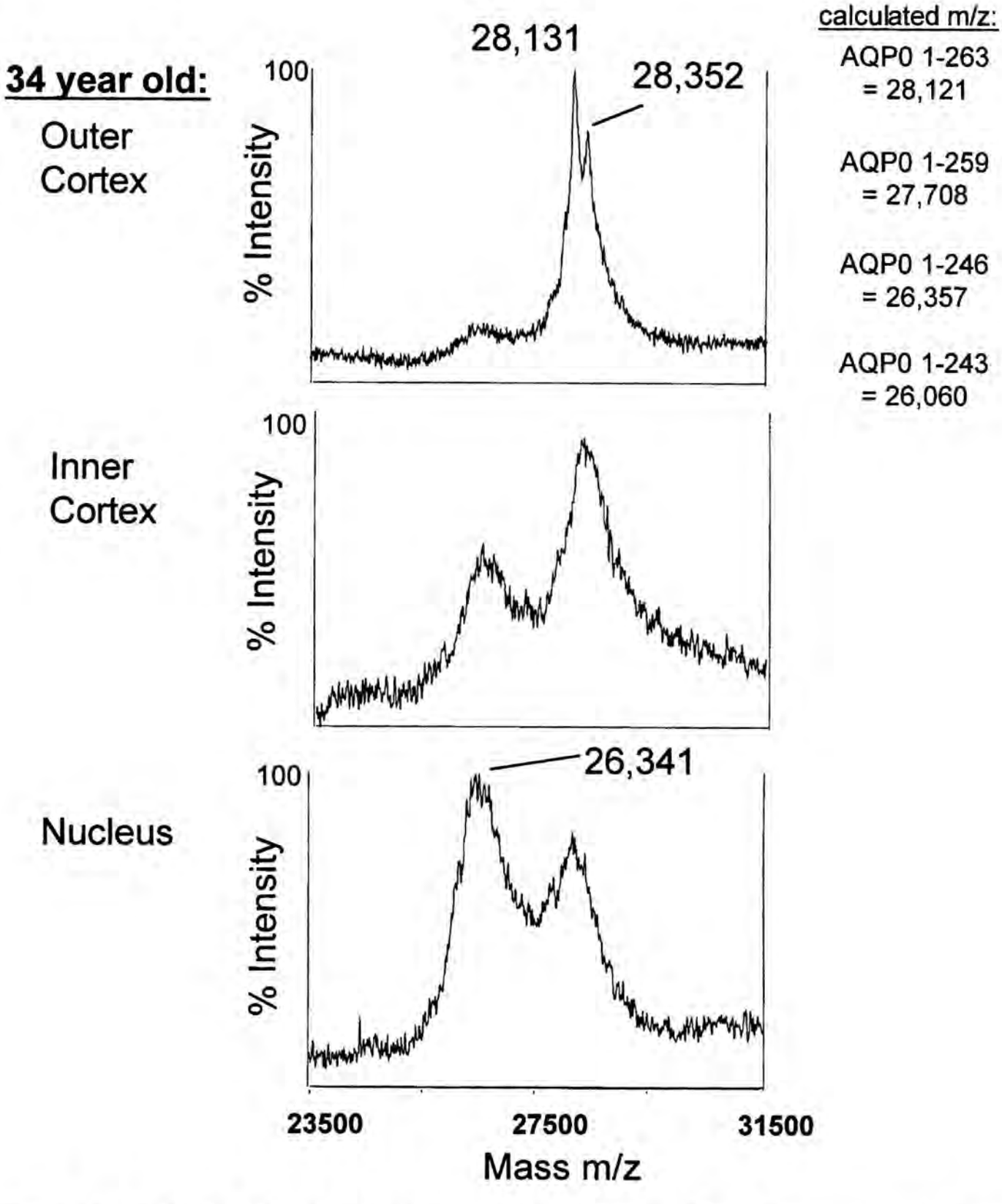

Figure 3.3. MALDI-MS of membrane protein isolated from three concentric sections of a 34 year old lens. The average expected molecular weight of AQP0 is 28,121 kD. The expected molecular weights of the truncation products of AQP0, 1-259, 1-246, and 1-243 are 27,708, 26,357, and 26,060 Da, respectively. An internal standard, apomyoglobin, was used for mass calibration.

34 year old lens*		
AQP0 Residue Numbers	**Calculated $[M+H]^{1+}$**	**Measured $[M+H]^{1+}$**
1-263	28121	28141 ± 23 (n=4)
1-259	27708	ND
1-246	26357	26374± 17 (n=3)
1-243	26060	ND

35 year old lens		
AQP0 Residue Numbers	**Calculated $[M+H]^{1+}$**	**Measured $[M+H]^{1+}$**
1-263	28121	28118 ± 7 (n=5)
1-259	27708	27706 ± 5 (n=5)
1-246	26357	26355± 15 (n=4)
1-243	26060	26058 ± 8 (n=3)

38 year old lens		
AQP0 Residue Numbers	**Calculated $[M+H]^{1+}$**	**Measured $[M+H]^{1+}$**
1-263	28121	28122 ± 6 (n=6)
1-259	27708	27709 ± 6 (n=2)
1-246	26357	26364 ± 7 (n=3)
1-243	26060	26061 ± 16 (n=2)

Table 3.1. Mass measurements of the intact and truncated forms of AQP0 by MALDI-MS. The masses of intact (1-263) and truncated forms of AQP0 were obtained from MALDI-MS data of lens sections from the 34, 35, and 38 year old lenses. The average measured mass ± SE is shown (n= the number of protein samples measured to obtain the molecular weight). *Measurements were acquired on the Voyager DE MALDI (34 year old lens samples) and the Voyager DE-STR MALDI (35 and 38 year old lens samples).

Trypsin digestion of lens membrane protein

Lens membrane proteins, while still embedded in the membrane, were digested with trypsin in an aqueous solution resulting in the cleavage and release of accessible parts of the protein (Fig. 3.4). To ensure that the C-terminus of AQP0 was completely cleaved by trypsin, the membranes from each section of the 34, 35, and 38 year old lenses were analyzed by mass spectrometry before and after digestion. Following trypsin digestion, MALDI-MS analysis of the membrane protein isolated from the 34 year old lens sections, revealed a 4,356 Da shift in mass from 28,131 Da to 23,775 Da (Fig. 3.5). This corresponds to digestion of the accessible N-and C-termini to residues 6-228 which would result in a calculated loss of 4361 Da. The $[M+H]^{1+}$ ion of full length AQP0, residues 1-263, has a calculated mass of 28,121 Da. The expected $[M+H]^{1+}$ ion of AQP0, residues 6-228, has an expected mass of 23,760 Da. These data indicate that trypsin cleaves the membrane embedded protein completely, releasing N-terminal residues 1-5 and C-terminal residues 229-263. The lack of cleavage after arginine 226 suggests that this residue may be inaccessible to trypsin. Analysis of the membrane protein from the 35 and 38 year old lens sections demonstrated complete cleavage at residue 239 and only partial cleavage at residue 233 (data not shown). This impeded the use of the data obtained from the 35 and 38 year old lens sections for the quantitative assessment of the abundance of peptides 229-233 and 234-238. Since trypsin cleavage obscures *in vivo* truncation that may occur on the C-terminal side of lysine and arginine residues, this approach was also employed to assess the possibility of using Glu-C or Lys-C for C-terminal cleavage. However, the efficiency of digestion with these enzymes was not sufficient for the quantitative analysis desired.

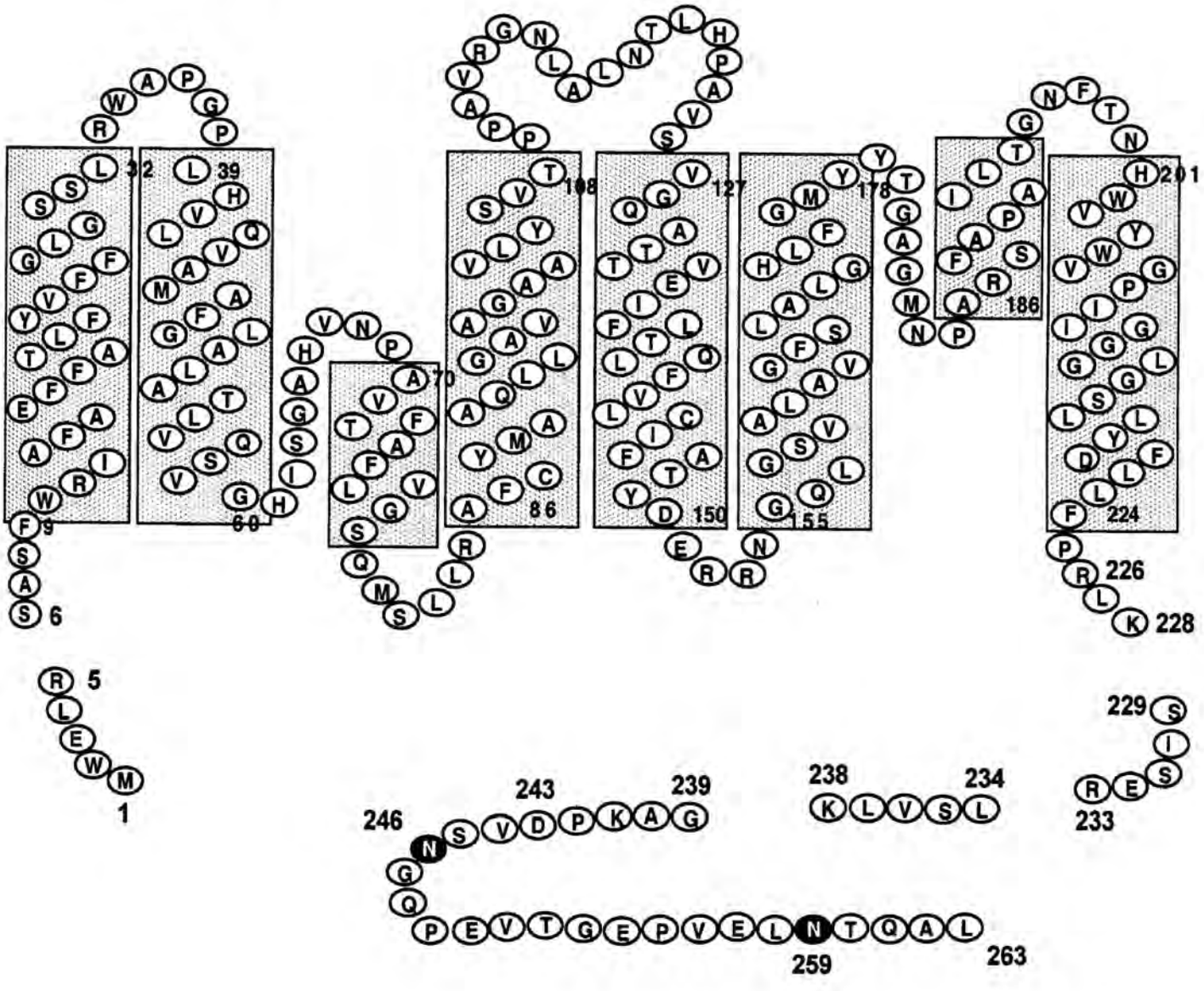

Figure 3.4. Expected Tryptic Peptides Released from Membrane Embedded AQP0. The observed tryptic peptides are residues 1-5, 229-233, 234-238, and 239-263. Trypsin cleaves on the C-terminal side of lysine and arginine residues with the exception of at lysine-proline and arginine-proline bonds.

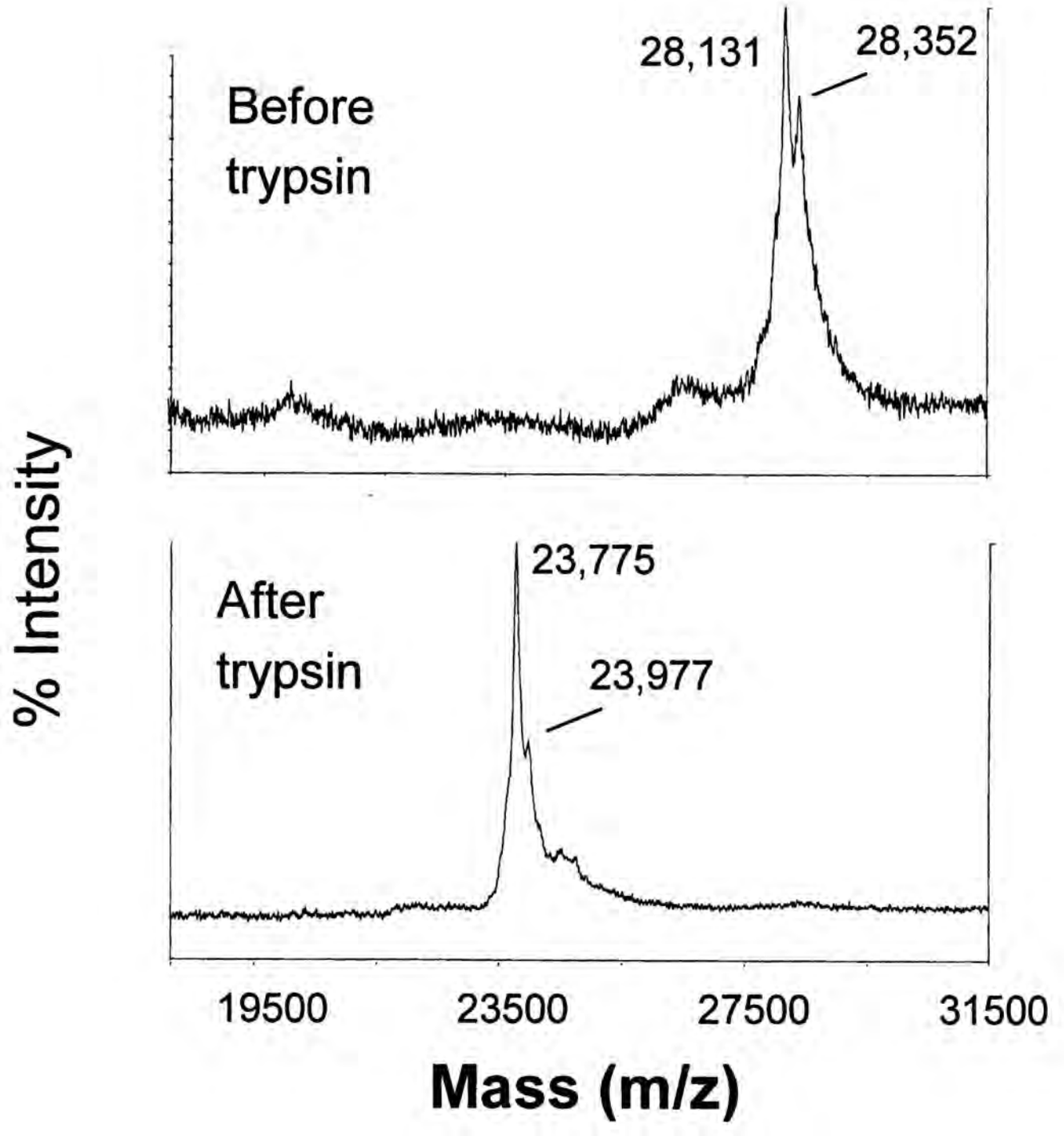

Figure 3.5. MALDI-MS of membrane protein isolated from the outer cortical section of a 34 year old lens before and after trypsin digestion. The average expected molecular weight of AQP0 is 28,121 Da. The expected molecular weight of AQP0 following tryptic cleavage of the N- and C-termini to residues 6-228 is 23,760 Da. An internal standard, apomyoglobin, was used for mass calibration.

Posttranslational modifications in the C-terminus of AQP0 identified by LC-ESI-MS

The C-terminal peptides, cleaved from AQP0 by trypsin, were isolated from lens membrane components by centrifugation. Since AQP0 is the most abundant protein in the lens, tryptic peptides of the C-terminus, 229-233, 234-238, 239-263 and posttranslationally modified forms of these peptides, were enriched in the supernatant. The soluble tryptic peptides were separated by reversed phase HPLC and the effluent was sent directly into the ion trap mass spectrometer for analysis. Figure 3.6 shows the elution profile of the C-terminal peptides, 229-233, 234-238, 239-263, and the phosphorylated forms of 229-233 and 234-235, isolated from the nuclear section of the 34 year old lens. The extracted (selected) ion chromatogram for each peptide is shown. The multiple peaks observed for peptide 239-263 indicate chromatographic separation of putative deamidated, racemized, or isomerized peptides that have the same mass ± 0.5 Da. Similar complex peak shapes were also observed for the truncated forms of 239-263 and the multiplicity of peaks increased with fiber cell age (data not shown).

Phosphorylation

Phosphorylation at Ser 235 observed previously was confirmed and new sites of phosphorylation were identified at Ser 231 and Ser 229 by tandem mass spectrometry. The phosphopeptides, 229-234 and 235-238, eluted about 20 minutes earlier than their unphosphorylated counterparts (Fig. 3.6). The mass spectrum of phosphopeptide, 229-233, indicates an 80 Da shift from 591.4 to 671.2 consistent with phosphorylation (Fig. 3.7A). Tandem mass spectrometry revealed that this peptide, SISER, was phosphorylated at Ser 231 and to a much lower extent at Ser 229 (Fig. 3.7B).

Fragmentation in the ion trap, resulting in the loss of phosphoric acid (98 Da) from the precursor and product ions that contained the site of phosphorylation, was consistent with phosphorylation at Ser 231. However, based on the observation of fragment ions at m/z 504.3 and 391.2, it appears that Ser 229 is also phosphorylated and that these two monophosphorylated forms of peptide 229-234 coelute. The doubly phosphorylated peptide, SISER, was not observed.

The level of phosphorylation at Ser 235 within different lens sections was assessed for the 34 year old lens. The percent phosphorylated peptide to the total signal for the peptide was determined. The mean percent of Ser 235 phosphorylation ± the SE in each section of the 34 year old lens was 6.4 ± 1.4 % (n=2) in the outer cortex, 15.1 ± 1.8 % (n=3) in the inner cortex, and 7.0 ± 1.1% (n=3) in the nucleus where n= the number of LC-MS analyses (Table 3.2). The level of Ser 235 phosphorylation in the inner cortex was significantly higher than in the nucleus as determined by the t-test, where $p<0.05$. Of the four lens sections in the 35 and 38 year old lenses, the same trend was observed with, the highest level of Ser 235 phosphorylation detected in the outer nuclear layer.

Since the monophosphorylated peptides of 229-233, phosphorylated either at Ser 229 or Ser 231, coeluted, the level of phosphorylation at each site was not distinguished from one another. Therefore, the percent of phosphorylation of peptide 229-233 is given. In the 34 year old lens, the mean percent of phosphorylation of peptide 229-233 was 1 ± 0.0 % (n=2) in the outer cortex, 8.9 ± 1.7 % (n=3) in the inner cortex, and 8.0 ± 3.5 % (n=3) in the nucleus (Table 3.2). The levels of phosphorylation reported are estimates and could be influenced by a number of factors including base hydrolysis of phosphoric

acid and decreased susceptibility of trypsin cleavage near phosphorylated residues. To address these concerns, the data were searched for the formation of dehydroalanine following base hydrolysis of phosphoric acid and products of incomplete trypsin cleavage and when observed were included in the quantitative analysis. These signals when observed accounted for less than 1% of the signal. In addition, the estimates of percent phosphorylation may be lower than present *in vivo* since the ionization efficiency of phosphopeptides is generally slightly lower that their unphosphorylated counterparts.

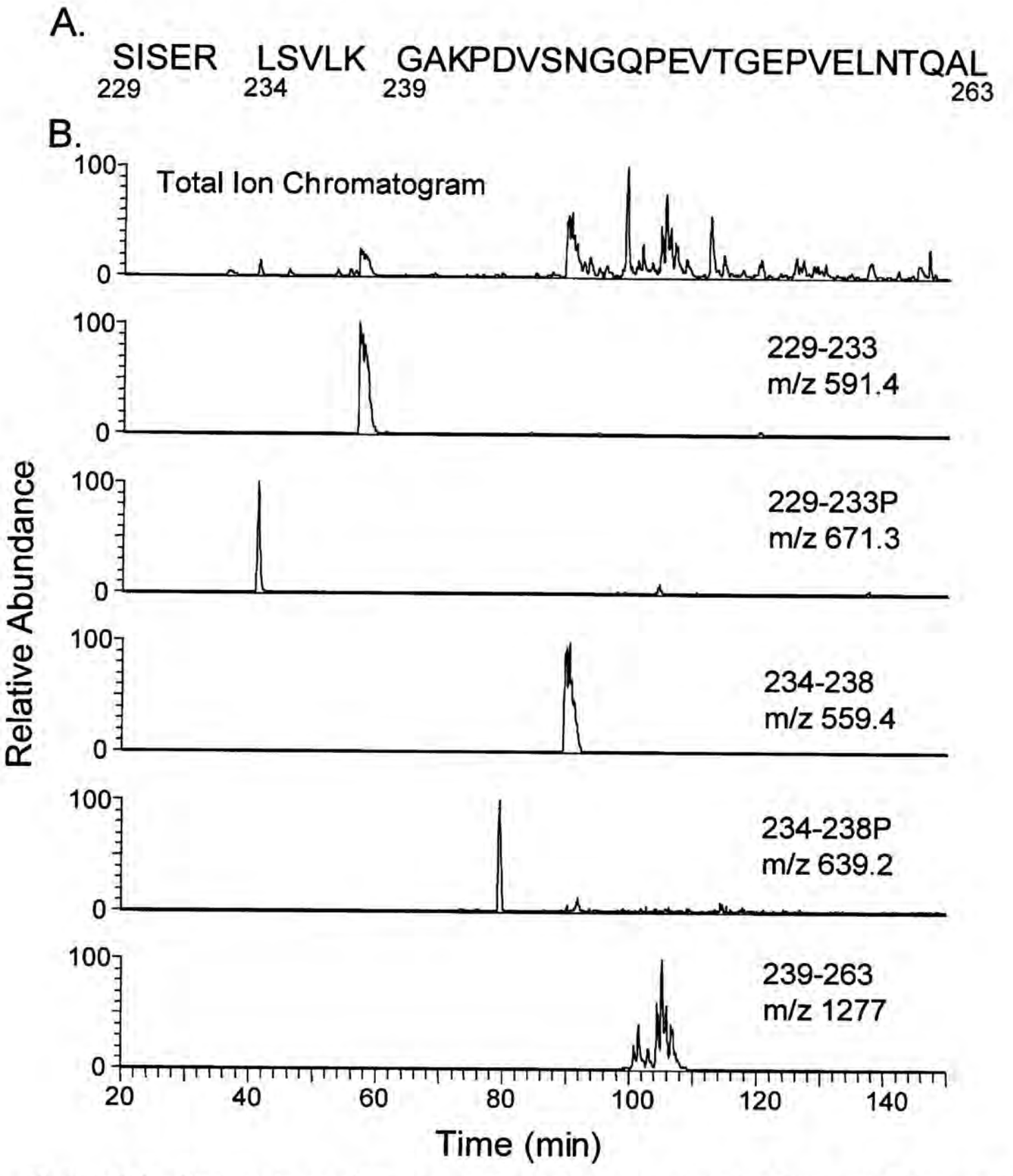

Figure 3.6. Chromatographic separation of tryptic peptides from the C-terminus of AQP0 from the nucleus of a 34 year old lens. A. Expected tryptic peptides from the C-terminus of AQP0. B. The total ion chromatogram (top panel) shows the separation of all the tryptic peptides in the mixture. The selected ion chromatograms (lower panels) show the elution profile of the expected tryptic peptides of AQP0, 229-233, 234-238, and 239-263, and the phosphorylated peptides 229-233 and 234-238 (indicated by a P). The mass to charge ratio (m/z) for each peptide is shown.

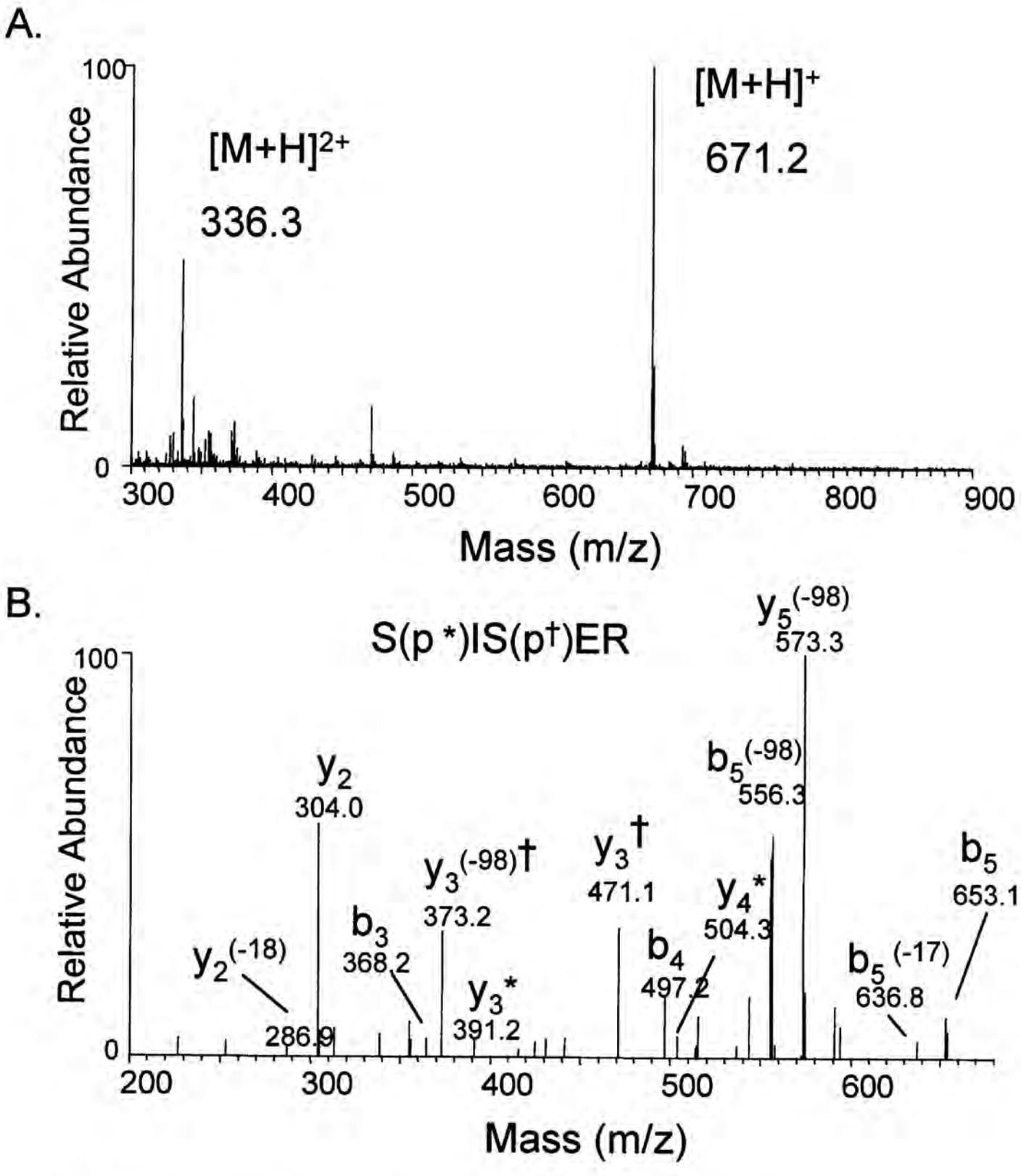

Figure 3.7. Mass spectrum and tandem mass spectrum of the phosphorylated peptide 229-233. A. The mass spectrum of phosphopeptide 229-233, with an expected m/z of 671.3, is shown. B. The tandem mass spectrum is labeled with the predicted b and y ions. B and y ions consistent with phosphorylation at Ser 231 are shown with a cross and ions consistent with phosphorylation at Ser 229 are labeled with an asterisk. Loss of 98 Da is a result of the loss of phosphoric acid upon fragmentation. The sequence of the peptide 229-233, SISER, is shown for clarity.

34 year old lens					
			Percent Phosphorylation in Each Lens Section		
AQP0 Residue Numbers:	**Calculated m/z**	**Observed m/z**	**Outer Cortex**	**Cortex**	**Nucleus**
234-238P LSVLK	639.3	639.2	6.4 ± 1.4 (n=2)	15.1± 1.8 (n=3)	7.0 ± 1.1 (n=3)
229-233P SISER	.671.3	671.3	1.0 ± 0.0 (n=2)	8.9 ± 1.7 (n=3)	8.0 ± 3.5 (n=3)

Table 3.2. Changes in the percent phosphorylation of serine residues 235, 229, and 231 with fiber cell age in sections of a 34 year old lens. The percent phosphorylation was calculated from the peak area of the phosphorylated peptide compared to the sum of the peak areas for the phosphorylated and unphosphorylated peptide. The percent of phosphorylation of peptide 229-233 is monophosphorylated at serine residue 229 or 231. The average percentage of phosphorylation at each site is shown ± SE (n=the number of measurements made). The doubly phosphorylated peptide 229-231 was not observed.

C-Terminal truncation

Based on the predicted masses of the tryptic peptide 239-263 and truncation products of this peptide, data obtained during LC-MS analyses were searched for possible truncation after each residue. Peptides truncated after residues 242, 243, 244, 245, 246, 247, 248, 249, 251, 252, 253, 254, 257, 258, 259, 260, 261, and 262 were observed and their sequences were confirmed by tandem mass spectrometry. Further truncation of the tryptic peptide 239-263 N-terminal to residue 242 and truncation of tryptic peptides, 229-233 and 234-238, were not observed since the masses of these products were not within the mass range detected.

The level of truncation at each site within the C-terminus increased with fiber cell age. In an attempt to quantitate the amount of C-terminally intact and truncated forms of AQP0, a synthetic peptide mimicking the intact C-terminal peptide, N-terminally acetylated 239-263, was spiked into the mixture of peptides released from the lens membranes by trypsin. The amount of peptide standard spiked into the sample was based on the total peptide concentration of the sample. However, the low amount of peptide sample prohibited rigorous determination of the peptide concentration. To circumvent this problem, the relative levels of truncation were determined based on the peak areas of the intact and each C-terminally truncated product of the tryptic peptide 239-263. Determination of the relative abundance of each truncated form of the peptide 239-263 permits comparisons of the level of truncation occurring at particular sites among different sections of the lens.

In order to determine if the extent of backbone cleavage of AQP0 was consistent within different regions of a normal human lens in multiple lenses of similar age, the

relative levels of truncation at each site were assessed by LC-ESI-MS analysis. For simplicity, the elution profiles of all of the truncated forms of peptide 239-263 are not shown. Figure 3.8 shows the relative level of truncation at each site in each section of the 34, 35, and 38 year old lenses. These data are also shown in table format in Tables 3.3, 3.4, and 3.5. The level of truncation after residues 242, 249, and 257 was too low for quantitative assessment. Multiple analyses were performed on each section of the 34 year old lens and the mean percent of truncation at each site is shown ± SE (Fig. 3.8A). Although there was an additional lens section in the 35 and 38 year old lenses, the pattern of C-terminal truncation was remarkably similar in each lens tested (Fig. 3.8B,C). Consistent with previous studies (8) and the MALDI-MS analysis of the membranes (Fig. 3.1), peptides truncated after Asn 246 and Asn 259 were the predominate signals observed. These data indicate that in different human lenses of similar age and, based on gross concentric dissection, that the spatial distribution of these truncation products within the lens is fairly constant from lens to lens.

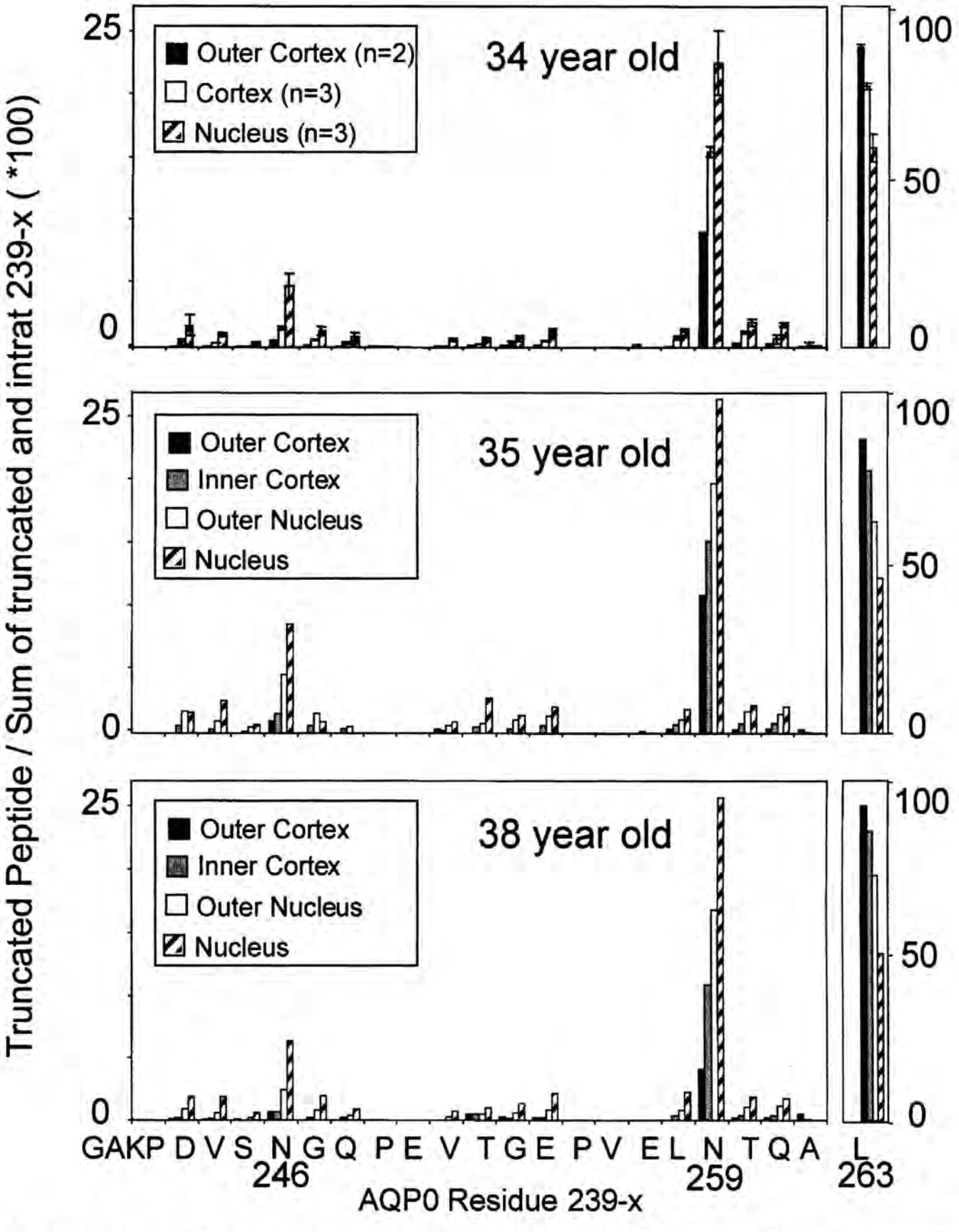

Figure 3.8. Changes in the relative abundance of truncated forms of the C-terminal peptide 239-263 with fiber cell age in 34, 35, and 38 year old lens sections. The mean percent truncation ± SE, (n = 2 or 3 separate analyses) is shown. Multiple analyses were performed on the 34 year old lens sections (top panel). In the 34 year old lens, the sections are labeled outer cortex (black), cortex (white), nucleus (hatched). In the 35 and 38 year old lenses, the sections are labeled outer cortex (black), inner cortex (grey), outer nucleus (white), and nucleus (hatched).

34 Year old lens sections

Peptide	Expected m/z	Observed m/z	Outer Cortex	Cortex	Nucleus
239-242	372.2	371.1	0.0	0.0	0.0
239-243	487.2	487.3	0.1 ± 0.0	0.4 ± 0.2	1.7 ± 0.8
239-244	586.3	586.3	0.1 ± 0.0	0.3 ± 0.0	1.0 ± 0.2
239-245	673.3	673.3	0.0	0.0	0.3 ± 0.1
239-246	787.4	788.3	0.6 ± 0.1	1.5 ± 0.1	4.8 ± 1.0
239-247	844.4	845.1	0.2 ± 0.1	0.6 ± 0.1	1.3 ± 0.3
239-248	972.5	973.4	0.1± 0.0	0.3 ± 0.1	0.8 ± 0.3
239-249	1069.5	1070.6	0.1± 0.0	0.1 ± 0.0	0.0
239-250	1198.6	ND	ND	ND	ND
239-251	1297.6	1298.6	0.1± 0.0	0.1 ± 0.1	0.6 ± 0.1
239-252	1398.7	1399.6	0.1± 0.1	0.2 ± 0.0	0.6 ± 0.1
239-253	1455.7	1456.7	0.1± 0.0	0.3 ± 0.1	0.7 ± 0.2
239-254	1584.7	1585.7	0.1± 0.1	0.5 ± 0.0	1.2 ± 0.2
239-255	1681.8	ND	ND	ND	ND
239-256	1780.9	ND	ND	ND	ND
239-257	1909.9	1911.0	0.0	0.0	0.0
239-258	2023.0/1012.0	1012.7	0.1± 0.1	0.8 ± 0.1	1.3 ± 0.1
239-259	2137.0/1069.0	1070.0	8.9± 0.2	15.5 ± 0.4	22.5 ± 2.5
239-260	2238.1/1119.6	1120.7	0.3± 0.0	1.2 ± 0.1	2.0 ± 0.3
239-261	2366.1/1183.6	1185.5	0.3± 0.0	0.7 ± 0.3	1.8 ± 0.2
239-262	2437.2/1219.1	1220.4	0.1± 0.1	0.2 ± 0.2	0.1 ± 0.1
239-263	2550.3/1275.6	1277.0	87.9± 0.1	76.5 ± 1.1	58.5 ± 4.0

Table 3.3. Changes in the relative abundance of truncated forms of the C-terminal peptide 239-263 with fiber cell age in sections of a 34 year old lens. The percentage of truncation at each site is shown. ND indicates peptides that were not detected. Peak areas that were too low to determine are denoted by 0.0%. The identity of each peptide was confirmed by tandem mass spectrometry.

35 Year old lens sections

Peptide	Expected m/z	Observed m/z	Outer Cortex	Cortex	Nucleus	Inner Nucleus
239-242	372.2		0.0	0.0	0.0	0.0
239-243	487.2	487.3	0.0	0.6	1.7	1.7
239-244	586.3	586.3	0.0	0.3	1.0	2.5
239-245	673.3	673.3	0.0	0.1	0.5	0.7
239-246	787.4	788.3	1.0	1.6	4.7	8.7
239-247	844.4	845.1	0.0	0.6	1.6	0.9
239-248	972.5	973.4	0.0	0.4	0.5	0.0
239-249	1069.5		0.0	0.0	0.0	0.0
239-250	1198.6	ND	ND	ND	ND	ND
239-251	1297.6	1298.6	0.4	0.2	0.6	0.9
239-252	1398.7	1399.6	0.0	0.5	0.8	2.8
239-253	1455.7	1456.7	0.0	0.4	1.1	1.4
239-254	1584.7	1585.7	0.0	0.6	1.4	2.1
239-255	1681.8	ND	ND	ND	ND	ND
239-256	1780.9	ND	ND	ND	ND	ND
239-257	1909.9		0.0	0.1	0.0	0.0
239-258	2023.0/ 1012.0	1012.6	0.4	0.7	1.1	1.9
239-259	2137.0/ 1069.0	1070.0	10.9	15.2	19.8	26.5
239-260	2238.1/ 1119.6	1120.7	0.3	0.8	1.8	2.2
239-261	2366.1/ 1183.6	1185.5	0.4	0.9	1.5	2.2
239-262	2437.2/ 1219.1		0.3	0.1	0.0	0.0
239-263	2550.3/ 1275.6	1277	86.2	76.9	62.1	45.6

Table 3.4. Changes in the relative abundance of truncated forms of the C-terminal peptide 239-263 with fiber cell age in sections of a 35 year old lens. The percentage of truncation at each site is shown. Masses were observed in the inner nuclear lens section. ND indicates peptides that were not detected. Peak areas that were too low to determine are denoted by 0.0%. The identity of each peptide was confirmed by tandem mass spectrometry.

38 year old lens

Peptide	Expected m/z	Observed m/z	Outer Cortex	Cortex	Nucleus	Inner Nucleus
239-242	372.2		0.0	0.0	0.0	0.0
239-243	487.2	487.2	0.1	0.2	0.9	1.9
239-244	586.3	586.3	0.1	0.1	0.6	1.9
239-245	673.3	673.3	0.1	0.0	0.2	0.6
239-246	787.4	788.4	0.7	0.7	2.5	6.3
239-247	844.4	845.4	0.0	0.2	0.8	2.0
239-248	972.5	973.5	0.0	0.2	0.4	0.9
239-249	1069.5		0.0	0.0	0.0	0.0
239-250	1198.6	ND	ND	ND	ND	ND
239-251	1297.6	1298.6	0.0	0.0	0.3	0.8
239-252	1398.7	1399.7	0.5	0.5	0.6	1.0
239-253	1455.7	1456.7	0.3	0.2	0.6	1.4
239-254	1584.7	1585.8	0.2	0.2	0.8	2.1
239-255	1681.8	ND	ND	ND	ND	ND
239-256	1780.9	ND	ND	ND	ND	ND
239-257	1909.9/ 956.0	956.2	0.0	0.0	0.0	0.0
239-258	2023.0/ 1012.0	1012.7	0.0	0.4	0.9	2.3
239-259	2137.0/ 1069.0	1070.0	4.1	10.9	16.8	25.7
239-260	2238.1/ 1119.6	1120.8	0.2	0.4	1.1	1.9
239-261	2366.1/ 1183.6	1185.5	0.3	0.4	1.1	1.8
239-262	2437.2/ 1219.1		0.5	0.1	0.0	0.0
239-263	2550.3/ 1275.6	1277.0	92.9	85.4	72.4	49.5

Table 3.5. Changes in the relative abundance of truncated forms of the C-terminal peptide 239-263 with fiber cell age in sections of a 38 year old lens. The percentage of truncation at each site is shown. Masses were observed in the inner nuclear lens section. ND indicates peptides that were not detected. Peak areas that were too low to determine are denoted by 0.0%. The identity of each peptide was confirmed by tandem mass spectrometry.

Spontaneous backbone cleavage at Asn 246 and Asn 259

Since the prevalent sites of truncation were also known sites of deamidation, the possibility of spontaneous backbone cleavage of a synthetic peptide of the C-terminus of AQP0 was assessed. An N-terminally acetylated synthetic peptide of AQP0, Ac239-263, was purified and incubated at 37°C in 10 mM ammonium bicarbonate buffer pH 8.8. After 96 hours of incubation, a low level of truncation was observed on the C-terminal side of asparagine residues that correspond to Asn 259 and Asn 246 (Fig. 3.9). In addition following the incubation, a single peak at time zero was transformed into two chromatographically separated peaks for the intact and truncated forms of the peptide. These peaks could result from deamidation of asparagine to aspartic acid in the intact peptide and the formation of a C-terminal asparagine and to a lesser extent aspartic acid amide in the truncated peptides (Fig. 1.6) (86). The mass spectrometer settings used in this study do not easily distinguish a 1 Da shift due to deamidation in full scan mode. Compared to the signal intensity of the intact peptide, after a 96 hour incubation ~1% of the peptide was truncated to Ac239-259 and less than 1% was truncated to Ac239-246. These data indicate that spontaneous nonenzymatic truncation at Asn 246 and Asn 259 occurs *in vitro* and raise the possibility that spontaneous backbone cleavage may be the mechanism by which AQP0 is truncated, at residues Asn 246 and Asn 259, in the human lens. The slow rate of *in vitro* truncation that occurs under these incubation conditions which mimic the conditions used during cleavage of the protein with trypsin also suggests that minimal spontaneous truncation occurred at these sites during the 20 hour trypsin digestion.

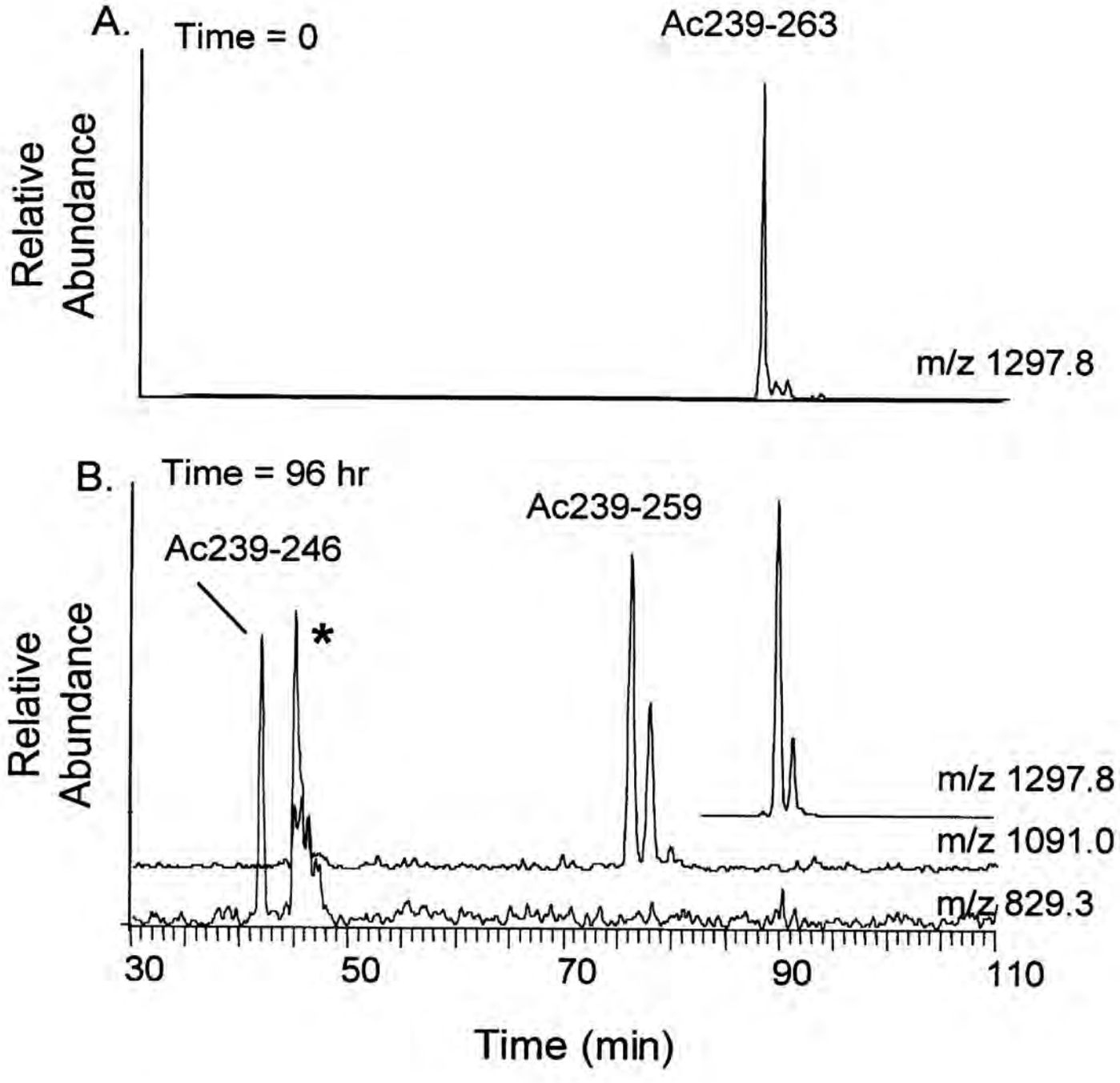

Figure 3.9 *In vitro* spontaneous truncation of a synthetic peptide of AQP0 239-263 on the C-terminal sides of Asn 246 and Asn 259. A. The top panel illustrates the selected ion chromatogram of the synthetic peptide Ac-239-263 (m/z= 1297.8) at time zero. B. After a 96 hour incubation at 37°C the peptides, Ac 239-246 (m/z= 829.3), Ac 239-259 (m/z =1091.0) were observed indicating the formation of truncated products *in vitro* in the absence of proteolytic enzymes. The peptide sequences were confirmed by tandem mass spectrometry. The asterisk indicates a contaminant.

Isomerization of aspartic acid

The complex peak shape of the chromatographically separated truncated peptides of the C-terminus led to the hypothesis that deamidation and/or isomerization/racemization of asparagine or aspartic acid occurred. Age-related isomerization and racemization of aspartic acid residue 243, was observed in the truncated peptide 239-244, GAKPDV. In the inner cortical and nuclear sections of all three lenses tested, a new peak appeared that was chromatographically separated but had the same mass and fragmentation pattern as peptide 239-244. Figure 3.10A shows the elution profile of the truncated peptide 239-244, $[M+H]^{1+}$ ion 586.3 Da, in the three sections of a 34 year old lens. Two major peaks and an earlier eluting minor peak were observed in the nuclear fiber cells of the 34, 35, and 38 year old lenses examined (Fig. 3.11).

The tandem mass spectra of these peptides were searched for fragment ions which have been shown to be specific for iso-Asp containing peptides (91). Fragmentation on the N-terminal side of an iso-Asp results in the formation of a b ion that has an additional 18Da (b_4+H2O) and a y ion that has lost 46Da (y_2-46) (91). The tandem mass spectrum of the first peptide that eluted with a mass of 586.3 (55.01 min) contained y_2 and b_4 fragment ions, with $[M+H]^{1+}$ of 187.2 and 372.3 Da, consistent with the presence of an GAKPiso-DV (Fig. 3.11A). These fragment ions were absent from the tandem mass spectrum of the later eluting peptide with a mass of 586.3 (57.76 min) (Fig. 3.11B).

Since the fragmentation pattern obtained in the tandem mass spectrum does not indicate the presence of L or D stereoisomers of the aspartic acid (91), peptides were synthesized incorporating L-Asp, L-iso-Asp, D-Asp, or D-iso-Asp into the peptide GAKPDV in order to determine if isomerization of aspartate (α-Asp) to isoaspartate (β-

Asp) and/or racemization of L-Asp to D-Asp had occurred at position 243. The peptide containing the L-iso-Asp eluted first, followed 2 minutes later by peptide containing D-Asp, then after 1 minute D-iso-Asp, and 2.6 minutes later the L-Asp containing peptide eluted (Fig. 3.12B.). The elution profile and the time between the elution of the peptides permitted the identification of the age-related change in Asp 243 as racemization and isomerization from L-Asp to D-iso-Asp, the major product, and D-Asp, a minor product. Due to the use of a precolumn flow splitter, the retention times were not reproducible. The changes in relative abundance of the racemized and isomerized aspartic acid 243 with fiber cell age in the 34, 35, and 38 year old lenses is shown in Table 3.6.

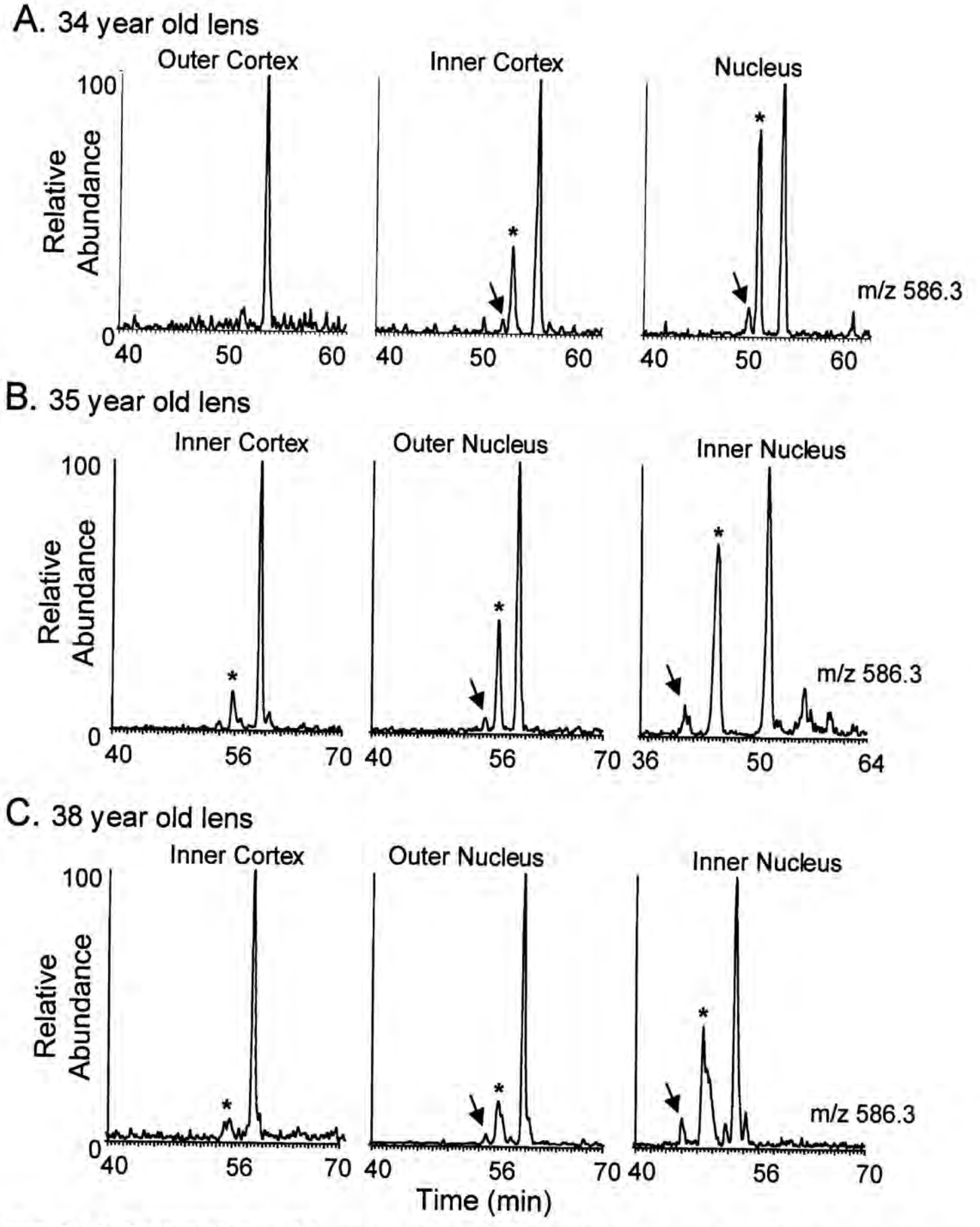

Figure 3.10. Chromatographic separation of isomerized and racemized aspartic acid 243 with fiber cell age in the 34, 35, and 38 year old lens sections. Selected ion chromatograms for the truncated peptide GAKPDV, residues 239-244 (m/z 586.3). Asterisks indicate the D-iso-Asp containing peptide. Arrows indicate D-Asp containing peptide. The unlabeled peak contains L-Asp. A. 34 year old lens sections. B. 35 year old lens sections. C. 38 year old lens sections. This peptide was not detected in the outer lens sections of the 35 and 38 year old lenses.

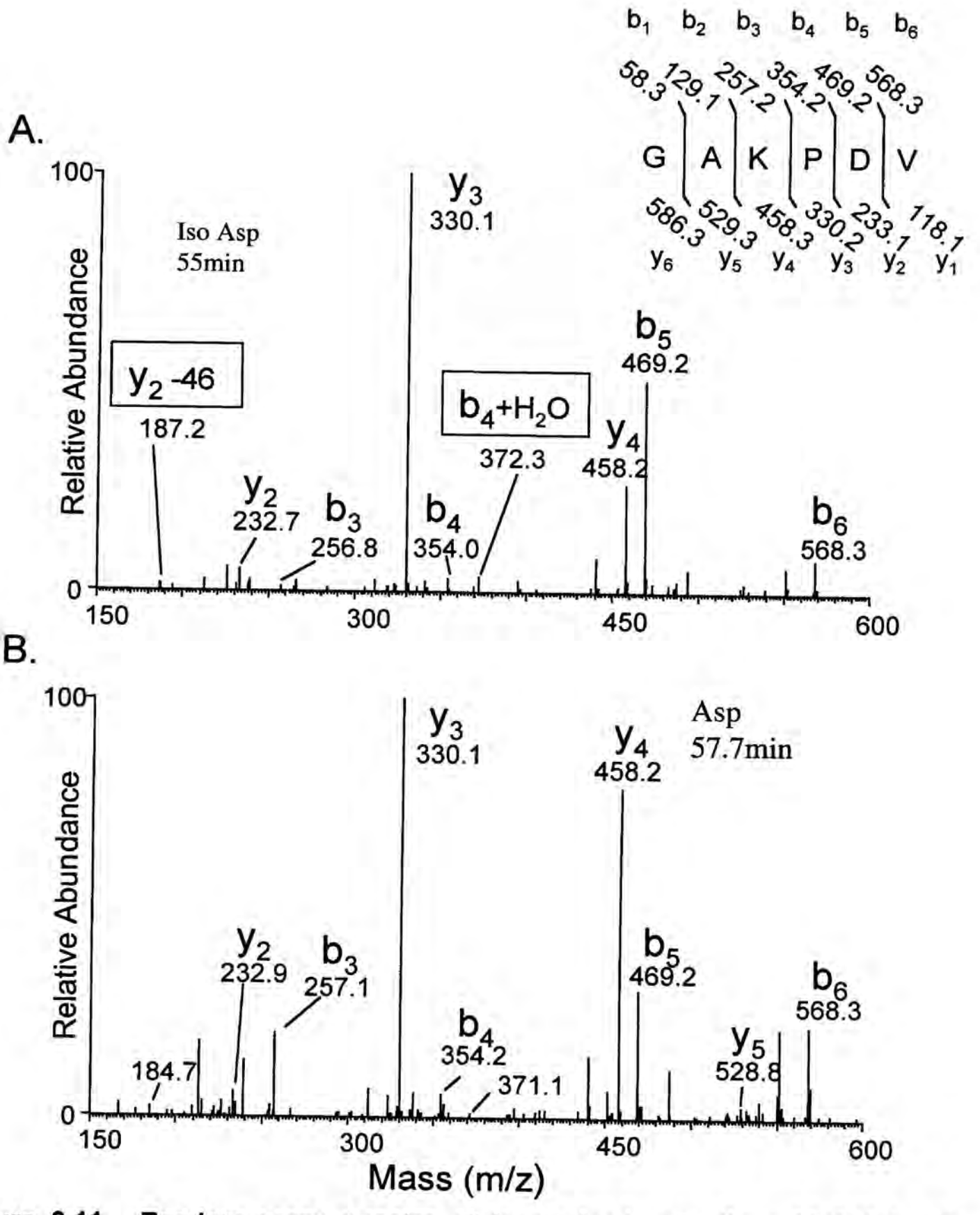

Figure 3.11. Tandem mass spectra of isomerized aspartic acid 243 in the truncated peptide 239-244 m/z 586.3. A. Tandem mass spectrum of the peptide GAKPDV , residues 239-244, eluting at 55 minutes. This peptide corresponds to the peaks labeled with an asterisk in Fig. 3.15. Predicted fragments indicating the presence of iso-aspartic acid are boxed. B. Tandem mass spectrum of the peptide GAKPDV , residues 239-244, eluting at 57.7 minutes. This peptide corresponds to the unlabeled peaks in Fig. 3.15. B and y ions are labeled and the predicted fragmentation of the peptide is shown.

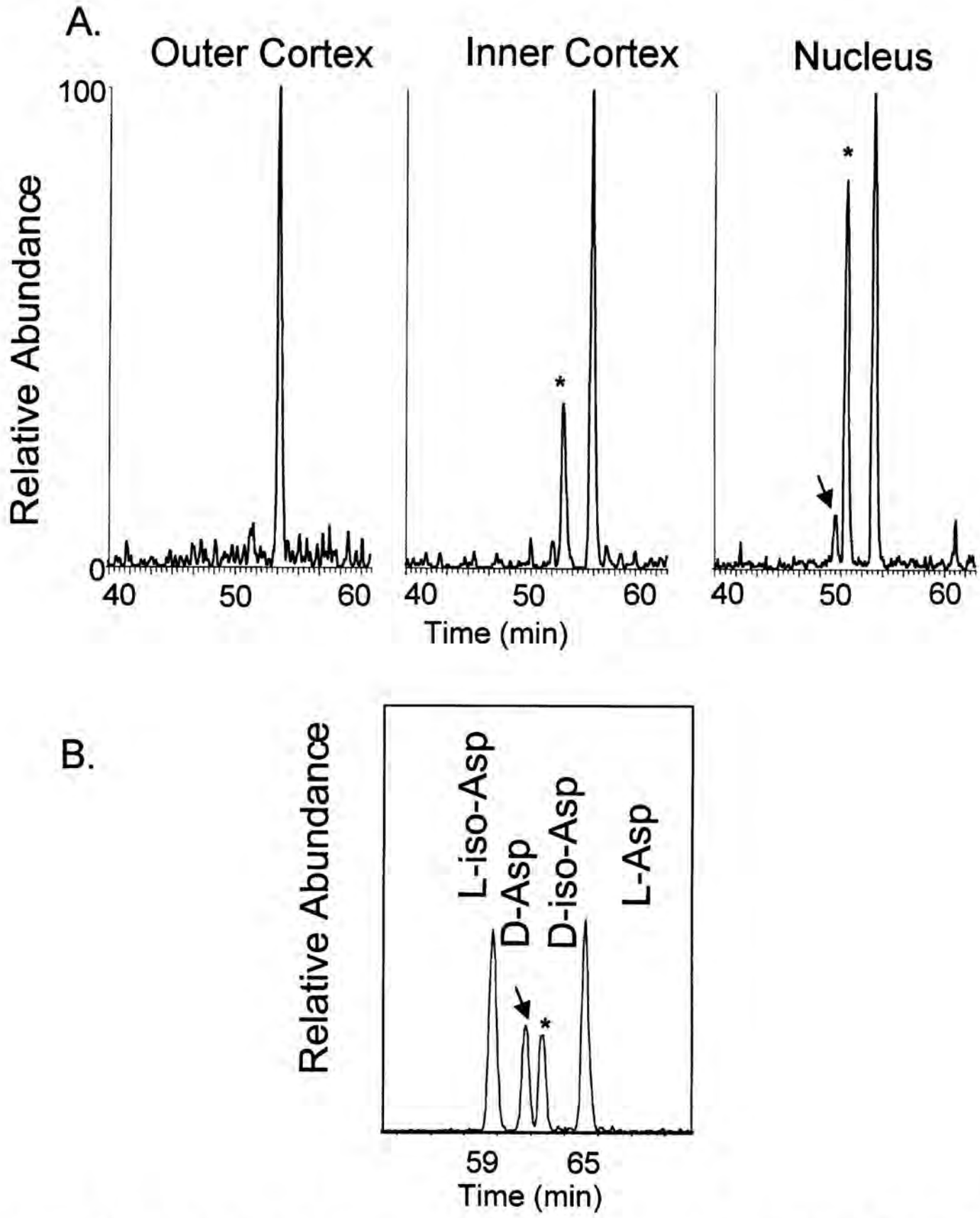

Figure 3.12. Age-related isomerization and racemization of aspartic acid 243 in the 34 year old lens and chromatographic separation of isomerized and racemized synthetic peptide 239-243. A. Selected ion chromatograms for the truncated peptide GAKPDV, residues 239-244 (m/z 586.3). B. The effect of aspartic acid racemization and isomerization on the elution profile of synthetic peptide standards, GAKPDV. Asterisks indicate the D-iso-aspartic acid containing peptide, arrows indicate the D-asp containing peptide.

34 year old lens			
Lens Section	**Peak 1 (D-Asp)**	**Peak 2 (D-Iso-Asp)**	**Peak 3 (L-Asp)**
Outer Cortex	ND	ND	100 (n=2)
Cortex	2.7 (n=1)	26.4 ± 1.5 (n=3)	73.6 ± 2.3 (n=3)
Nucleus	7.5 ± .3 (n=3)	41.3 ± 1.7 (n=3)	51.2 ± 1.9 (n=3)

35 year old lens			
Lens Section	**Peak 1 (D-Asp)**	**Peak 2 (D-Iso-Asp)**	**Peak 3 (L-Asp)**
Outer Cortex	ND	ND	ND
Cortex 1	ND	18.4	81.6
Outer Nucleus	4.5	30.0	65.5
Nucleus	6.7	42.6	50.7

38 year old lens			
Lens Section	**Peak 1 (D-Asp)**	**Peak 2 (D-Iso-Asp)**	**Peak 3 (L-Asp)**
Outer Cortex	ND	ND	ND
Cortex 1	ND	17.0	83.0
Outer Nucleus	3.1	23.2	73.7
Nucleus	5.3	42.8	51.9

Table 3.6. Changes in the relative abundance of isomerized and racemized Asp 243 in the truncated peptide 239-244 with fiber cell age in concentric sections of the 34, 35, and 38 year old lenses. The signal intensity of the peptides 239-244 m/z 586.3 were determined from LC-ESI-MS analysis. The percent of the total signal for each peak ± SE are shown (n= the number of measurements). Only one measurement per lens section of the 35 and 38 year old lenses was obtained. Peak 1 is indicated by an arrow, peak 2 by an asterisk, and peak 3 unlabeled in Fig. 3.10.

DISCUSSION

Previous characterization of human AQP0 utilizing western blotting techniques revealed age-related modifications and changes with fiber cell age (97). More recent mass spectrometric analysis of human AQP0, following cyanogen bromide cleavage, permitted the identification of the exact sites of truncation, phosphorylation at Ser 235, and deamidation at Asn 246 and Asn 259 in whole lens homogenates of varying age. The approach presented here provides a more detailed view of the posttranslational modifications of AQP0 as a function of fiber cell age during the normal aging process. Previously undetected posttranslational modifications identified in the analysis of C-terminal peptides released from AQP0 by trypsin, include additional sites of truncation at residues 249, 260, 261, and 262, phosphorylation at Ser 231 and to a lower extent at Ser 229, and racemization/isomerization of L-Asp 243 to D-iso-Asp. A summary of the posttranslational modifications of human AQP0 observed in this and an earlier study (8) is shown in Figure 3.13 and Table 3.7. The modified tryptic peptides, smaller in mass than the previously reported cyanogen bromide fragments, were more amenable to chromatographic separation and sequence confirmation by tandem mass spectrometry.

Examination of the phosphorylation state of AQP0 revealed alterations in the level of phosphorylation with fiber cell age. Activators of protein kinase C (PKC), calcium and TPA (187), and activators of protein kinase A (PKA), cAMP and forskolin (188-190), have been shown to stimulate phosphorylation of the C-terminus of AQP0. While the kinases responsible for *in vivo* phosphorylation of AQP0 are not known, the residues adjacent to Ser 229 and Ser 231 form consensus sequences for phosphorylation by casein kinase II and PKC, respectively. Consistent with previous observations that

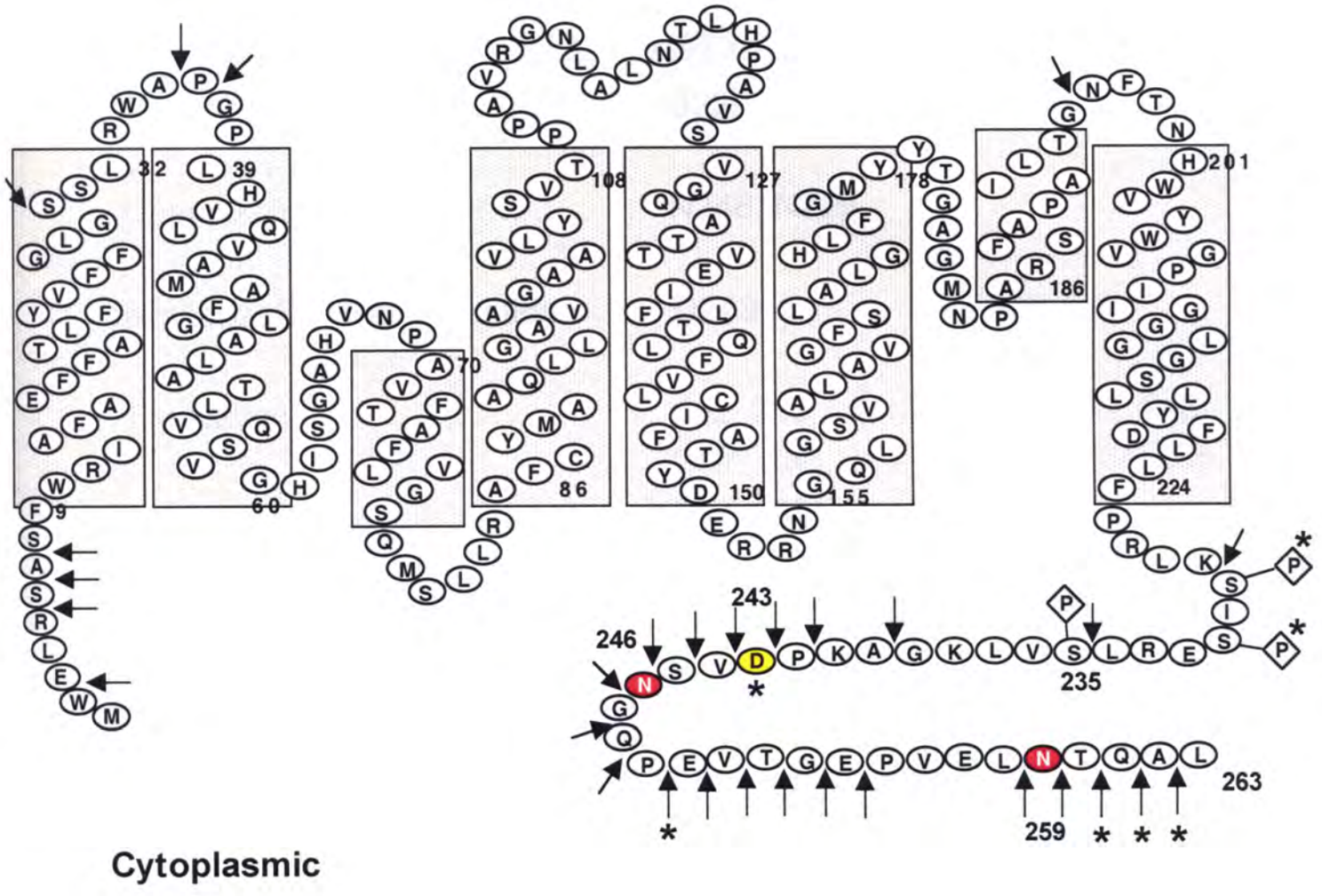

Figure 3.13. Primary sequence and newly identified sites of posttranslational modifications of human AQP0. Asparagine residues at sites 246 and 259 (filled circles) are deamidated. The aspartic acid 243 is isomerized and racemized (filled circle). Serines 229, 231, and 235 are phosphorylated. Arrows indicate sites of posttranslational truncation. The asterisks indicate the posttranslational modifications identified in this study.

C-terminal Posttranslational Modifications of Human Aquaporin 0:

Phosphorylation	S229*, S231*, S235
Deamidation	N246, N259
Isomerization/Racemization	D243*
Truncation	242, 243, 244, 245, 246, 247, 248, 249*, 250, 251, 252, 253, 254, 258, 259, 260*, 261*, 262*

Table 3.7. Summary table of previously identified and novel posttranslational modifications observed in the C-terminus of human AQP0. The asterisks indicate novel posttranslational modifications identified in this study. The presence of all of the posttranslational modifications listed above was confirmed by tandem mass spectrometry in this study.

cAMP induced phosphorylation of AQP0 was higher in the inner cortex and nucleus than the outer cortex (209, 210), the levels of phosphorylation at Ser 235 and Ser 229/Ser 231 were highest in the inner cortex and outer nucleus and lowest in the outer lens cortex. The role of C-terminal phosphorylation of AQP0 is not known (112), although it is conceivable that phosphorylation within the putative calmodulin binding domain of AQP0 (162) could affect the calcium/calmodulin mediated effects on the water permeability of AQP0 (161). Phosphorylation of other aquaporins has been shown to affect membrane water permeability through channel gating and a shuttling mechanism that redistributes that protein between intracellular vesicles and the plasma membrane (118, 156). Changes in the level of phosphorylation within different regions of the lens indicate that the activity of AQP0 may be regulated spatially within the lens.

Age-related isomerization and racemization of aspartic acid residue 243 from L-aspartate (L-α-Asp) to D-iso-aspartate (D-β-Asp) was detected in the truncated peptide 239-244 in all three lenses examined. Isomerization and racemization of aspartic acid residues is commonly observed in aged proteins of the lens, teeth, erythrocytes, and brain and has been shown to impact the function of a number of proteins (77, 81). The age-related formation D-iso-Asp has also been shown at aspartic acid residues 58 and 151 in α-A crystallin (79, 80). Isomers arise through spontaneous formation of an unstable 5-membered succinimide ring when the side chain carbonyl carbon of Asp or Asn, in the case of deamidation, is attacked by the α-amino of the carboxyl residue (Fig. 1.5) (74). Hydrolysis of the succinimide ring results in four products, L-Asp, L-iso-Asp, D-Asp, D-iso-Asp. During isomerization to iso-Asp, the peptide backbone is transferred to the side chain of the aspartic acid thereby incorporating an additional carbon in the peptide

backbone. During racemization of L-Asp to D-Asp, the configuration around the α-carbon is inverted. Even though, studies characterizing the rates of spontaneous racemization and isomerization of aspartate in peptides and proteins, demonstrate that the primary product formed *in vitro* is L-iso-Asp (74), in the analyses of aged proteins taken directly from cells or tissues, the D-iso-Asp isomer was the primary product observed (79, 81). The prevalence of the D-iso-Asp may result from the influence of the local environment and conformation (79) or alternatively, from repair of the isomerized and racemized aspartate by protein L-isoaspartate 0-methyltransferase (PIMT) (211). PIMT activity has been observed in the normal and cataractous human lenses (212). The enzymatic repair of L-iso-Asp and D-Asp residues back to the L-Asp in peptides and proteins has been demonstrated to restore protein activity (81, 213). Since D-iso-Asp is not a substrate for the enzyme (89), in aged tissues with endogenous PIMT, the predicted products are L-Asp and D-iso-Asp. These observations are consistent with the suggestion that PIMT may be involved in the repair of lens proteins in the normal aging lens (212).

Many lens proteins are subject to age-related truncation. By defining the exact sites of protein truncation, the mechanisms involved in backbone cleavage can be addressed. In normal lenses from 34-38 years of age, C-terminal truncation was observed at many sites within the tryptic peptide, 239-263, and semi-quantitative analysis indicated that truncation at all of the observed sites increased as the fiber cells aged. The pattern and distribution of truncation products spatially within the lens was very similar in the three lenses tested suggesting programmed, non-random changes that occur as the fiber cells age. Measured molecular weights of lens membrane proteins from each section of

the lens, prior to trypsin digestion, demonstrate that the major truncation products in the 34-38 year old lens are a result of cleavage on the C-terminal side of asparagine residues 246 and 259. This result was further confirmed by analysis of C-terminal peptides following trypsin digestion. In addition to the action of proteases, aging peptides (74) and proteins (86) are subject to spontaneous backbone cleavage at residues that can form a succinimide intermediate. Truncation of α-A crystallin at Asn 101 has been proposed to occur during the formation of a succinimide ring resulting in a penultimate asparagine or an aspartic acid amide in the truncated peptide (Fig. 1.6) (86). Since the prominent sites of truncation in AQP0 are also known sites of deamidation (8), the potential of the C-terminus of AQP0 to undergo spontaneous backbone cleavage was investigated. After incubating a synthetic peptide of AQP0, Ac239-263, at 37°C for 96 hr, a low level of backbone cleavage was observed at asparagine residues corresponding to Asn 259 and Asn 246. Based on the rate of deamidation of pentapeptides at pH 7.4, 37°C, in 0.15M Tris HCl, the predicted half-time of deamidation of the Asn residues at 246 (SNG) and 259 (LNT) would be 0.96 and 46.1 days, respectively (75). The higher rate of truncation observed at residue 259 is consistent with the suggestion by Geiger *et al* that a slow rate of deamidation may increase the likely hood of backbone cleavage (74). These data suggest that truncation at susceptible asparagine and aspartic acid residues in the human lens may be due to age-related succinimide formation and spontaneous backbone cleavage. The reproducibility of these timed events that occur within specific regions of the normal aging lens are consistent with the idea that these age-related modifications can serve as molecular clocks to alter function or regulation of function at a given time (75).

Since deamidation, isomerization, racemization, and truncation can be linked through the spontaneous formation and hydrolysis of a succinimide ring (74) quantitation of these modifications must be interpreted with caution. In order to compare the relative abundance of posttranslational modifications that occur as a function of fiber cell age, the sections of each lens were prepared in parallel and under the same conditions. The age-related changes seen in the older lens fiber cells and the reproducibility of the levels of truncation at each site among the different lenses suggest that the observed posttranslational modifications occurred *in vivo* and not during preparation of the sample. Additionally by focusing on the C-terminal 24 amino acid residues, truncation at the N-terminus and further into the C-terminus, both of which have been observed previously (8), was not addressed.

The approach presented here permitted the analysis of posttranslational modifications of an integral membrane protein from dissected regions of a single human lens. Isolation of peptides released from AQP0 by trypsin greatly simplified the peptide mixture as compared to previous cyanogen bromide cleavage of the entire membrane protein fraction. This digestion approach, in conjunction with a chromatographic separation aimed at resolving many small peptides with similar sequences and tandem mass spectrometry, permitted the identification of novel posttranslational modifications and sequence confirmation of all of the posttranslationally modified products reported. The method required minimal sample preparation and detailed structural data were obtained on protein isolated from about 5% of the lens. This method will enable determination of structural changes in AQP0 that may occur in the anterior and posterior

poles of the lens, the zone of differentiation, in opaque regions of a cataractous lens, and in the region of the lens in which the age-related barrier to water develops.

The age-related modifications of the C-terminal tail of AQP0 that occur in the normal human lens include removal of parts of the protein by truncation, incorporation of a negative charge following deamidation, and the insertion of an additional carbon in the peptide backbone as a result of isomerization of aspartate. The effects of these modifications, within a putative regulatory domain, on AQP0 function and regulation of function is not known. It is conceivable that phosphorylation and other posttranslational modifications affect water permeability, the calcium and calmodulin mediated regulation of permeability (161), and/or the localization of AQP0 in the fiber cell membrane (32). The molecular modifications responsible for the decrease in fiber cell membrane water permeability as a function of age have not been determined (6, 7). As the only aquaporin in the lens fiber cells, AQP0 may contribute to the internal circulation within the lens therefore the spatial distribution of posttranslationally modified products may impact this transport and regulation of transport. The effects of these modifications on the function of AQP0 and how they pertain to maintaining lens transparency in the normal aging lens or to the formation of age-related cataract remain to be elucidated.

CHAPTER 4

THE WATER PERMEABILITY OF HUMAN AQUAPORIN 0

INTRODUCTION

AQP0, the only aquaporin found in the lens fiber cells, is postulated to function as a water channel and contribute to the transport of water through the lens (5). The ability of AQP0 to increase membrane water permeability has been demonstrated when the protein is expressed in *Xenopus* oocytes (112, 168, 169) and when reconstituted into proteoliposome vesicles (7, 121). While the water permeabilities of AQP0's cloned from frog (169), calf (112), and fish (164) have been assessed, at the onset of this work, the water permeability of human AQP0 had not yet been determined. Within the human lens, the rate of water movement into the lens nucleus decreases as a function of age (6). Likewise, the permeability of fiber cell membranes, isolated from fiber cells of varying age, decreases with fiber cell age (7). Structural characterization of human AQP0 demonstrates the protein undergoes many age-related posttranslational modifications, such as backbone cleavage and deamidation (8). Although the decrease in fiber cell membrane water permeability correlates with the age-related accumulation of posttranslational modifications in AQP0, the molecular determinants responsible for the decreased permeability are not known. In addition to the potential effects of age-related posttranslational modifications on the permeability of AQP0, there is conflicting evidence in the literature pertaining to the sensitivity of AQP0 to changes in extracellular pH (161, 164). This is of particular interest within the lens since the pH ranges from 7.02 in the lens periphery to 6.82 within the lens nucleus (165) which may impact AQP0 mediated water transport within the lens. In order to characterize the permeability of human AQP0, a method was established in our laboratory to measure the aquaporin water

channel activity. This assay will permit the future characterization of the effects of age-related posttranslational modifications on the water permeability of human AQP0.

The ubiquitous nature of water and the lack of aquaporin selective inhibitors have made the transport of water through aquaporins a challenge to investigate. Several of the aquaporins are potently inhibited by mercury, however, this is not the case for AQP0 (112). Since water transport through the aquaporins is bi-directional depending on the osmotic gradient (150), approaches to study the contribution of specific aquaporins to membrane water permeability typically measure the rates of swelling or shrinking in response to an osmotic challenge. Methods developed employ light scattering; light, fluorescence, or confocal microscopy; volume sensitive dyes; and deuterated or tritiated water. General strategies for examination of the permeability of heterologously expressed wild type and mutant aquaporins and more recent advances in measuring the permeability of aquaporins in cell culture, intact tissues, and whole animals are reviewed (109, 116, 214).

The most routinely utilized methods for the comparison of wild type and mutant aquaporin permeability involve the use of *Xenopus* oocytes or proteoliposome vesicles. Heterologous expression of aquaporins in *Xenopus* oocytes, in conjunction with an osmotic swelling assay, provides a relatively simple method for determination of membrane water permeability. Briefly, this method involves the injection of aquaporin RNA into *Xenopus* oocytes and measurement of the rate of oocyte swelling following a hypotonic challenge (215). Advantages of the oocyte assay include the ease in injection and manipulation of oocytes due to their large size, multi-subunit membrane proteins can be translated, assembled, and expressed from injected RNA, and the simplicity of the

swelling assay (216). Disadvantages of this method include the transient nature of protein expression, the variability in oocyte quality and level of protein expressed, the fact that endogenous proteins may interfere with characterization of the protein of interest, the lack of sensitivity of the assay (216). *Xenopus* oocytes are routinely used for the characterization of heterologously expressed mutant and wild type aquaporins.

On the other hand, studies using proteolipsome vesicles offer the ability to measure the permeability of aquaporins from a variety of sources. For example, vesicles can be prepared from the tissue of interest with endogenously expressed aquaporins (7) or from yeast spheroplasts heterologously expressing wild type or mutant aquaporins (217). An additional advantage of using the yeast expression system is the ability to assay the permeability of aquaporins with impaired plasma membrane trafficking since the expressed protein can be obtained from intracellular spheroplasts (217). In this approach the proteoliposome vesicles, loaded with a fluorescent dye, are subject to a hypertonic challenge and the rate of fluorescence quenching, as the vesicles shrink, is monitored by stopped-flow fluorimetry (218).

Methods have also been developed for the investigation of aquaporin activity in cultured cells grown on glass coverslips, grown on transwells, and cells in solution. Techniques to measure the water permeability of cells grown on coverslips rely on the dilution of fluorescence in fluorescently labeled cells (219) or changes in cell thickness (109) following exposure to a hypotonic challenge. Changes in cell thickness have been detected indirectly by measured the height of beads layered on top of cells (220) or directly by laser scanning reflection microscopy (214). The expression of aquaporins in epithelial cells and their involvement in secretion (221), has prompted the use of

transwell supports to investigate the movement of water across cell layers. While these experiments require an apparatus equipped to measure nanoliter changes in the water level, the use of transwells will facilitate characterization of mechanisms involved in driving the net flow of water across membranes and in regulating aquaporin function (27). Recently, a very simple centrifugation method was described to measure the water permeability of cells isolated from tissue. In this case hepatocytes, incubated in hypotonic media containing tritated water, were spun through a layer of silicone into lysis buffer. The radioactivity that spins down inside the cells serves as a measure of water uptake (222). This method could be expanded to other cell types and possibly to oocytes.

In tissues that express multiple aquaporins, comparisons among wild type animals and transgenic aquaporin deficient animals are permitting the examination of the contribution of each aquaporin to osmotic homeostasis. For instance, the contribution of AQP1 and AQP4 to water movement within specific regions of the brain and spinal cord were physically mapped by comparing the water permeability of tissue slices isolated from wild type animals with those obtained from AQP1 and AQP4 knock out animals (223). In this case, the amount of light transmitted through a 100 μm tissue slice, bathed in a known concentration of absorbing chromophore was measured. As the tissue swells, in response to an osmotic gradient, the chromophore above the tissue slice is displaced and more light is transmitted (223). Another approach assayed the contribution of AQP1 and AQP5 to the movement of water across the cornea *in vivo* using scanning confocal microscopy. These studies suggest that AQP5 in epithelial cells and AQP1 in endothelial cells function together to maintain osmotic homeostasis within the cornea (41). These

types of studies will facilitate investigation of the role of individual aquaporins in maintaining osmotic balance in cells as well as intact tissues and organs.

While all of the above mentioned methods for measuring aquaporin water permeability are valuable and provide solutions for specific questions, for our purposes the *Xenopus* oocyte swelling assay was the most appropriate choice. Since a cell culture model of lens fiber cells does not exist and vesicles prepared from lens fiber cell membranes contain a mixture of posttranslationally modified products of AQP0, a heterologous expression system would permit characterization of human AQP0 and future characterization of the effects of posttranslational modifications on the permeability of AQP0. The heterologous expression of functional channels in the oocyte membrane has been successful for many membrane proteins, including aquaporins and a large body of literature exists on the permeability of aquaporins as measured in oocytes.

The purpose of this study was to establish and characterize the *Xenopus* oocyte assay in our laboratory and determine the water channel activity of human AQP0. In order to ascertain that the swelling assay performed as stated in the literature, several control experiments were performed including the measurement of the membrane water permeability of oocytes injected with human AQP1, bovine AQP0, and α7 nicotinic receptor (mock) RNA. Once the reproducibility of the assay was confirmed, human AQP0 was cloned, the water permeability measured, and the sensitivity of AQP0 to a reduced pH was assessed.

EXPERIMENTAL METHODS

Preparation of Bovine AQP0 cDNA template for in vitro transcription-To incorporate elements necessary for *in vitro* transcription, Bovine AQP0 cDNA in a pBluebac III vector, a gift from Dr. Swamy-Mruthinti (Medical College of Georgia), served as a template for the generation of a cDNA transcript by polymerase chain reaction (PCR). PCR was performed using a standard protocol supplied with the Taq PCR Core kit (Qiagen). The sense oligonucleotide encoded the T7 RNA polymerase promoter, an alfalfa mosaic virus (AMV) enhancer sequence (224), and the first 20 nucleotides of AQP0 coding sequence: 5' T AAT ACG ACT CAC TAT AGG GAG CTC CGT TTT TAT TTT TAA TTT TCT TTC AAA TAC TTC CAC ATG TGG GAA CTG CGG TCA GC 3'. The AMV enhancer sequence was included adjacent to the start codon of AQP0 to enhance the efficiency of protein translation in the oocyte (224). The antisense oligonucleotide corresponded to nucleotides in the 3' untranslated region of AQP0 followed by a polyA tail: 3' CAT CTC GAG CCC AGA AGC TTC CTA CTC CCT C poly $A_{(50)}$ 5'. The PCR product was gel purified and the sequence confirmed by automated sequencing. The 900 nucleotide PCR product served as a template for *in vitro* transcription by T7 RNA polymerase.

Cloning of Human AQP0- Human lens cDNA, kindly supplied by Kirsten Lampi (Oregon Health Sciences University), served as a template for the amplification of human AQP0 by PCR. The sense oligonucleotide primer incorporated BamHI and SacI restriction sites, an alfalfa mosaic virus enhancer sequence (AMV), and the first 24 nucleotides of the coding region of human AQP0 as determined from the gene sequence

(225): 5' GAC TGC GAG CTC GGA TCC GTT TTT ATT TTT AAT TTT CTT TCA AAT ACC TCC ACC ATG TGG GAA CTG CGA TCA GCC TCC 3'. Sac I and BamHI restriction sites were incorporated for the ligation of the final PCR product into a pBluescript vector (Stratagene) or into a mammalian expression vector, pcDNA3.1+ (Invitrogen), respectively. The antisense oligonucleotide primer was complementary to nucleotides 846-868 in the 3' untranslated region of AQP0 and incorporated an ApaI restriction site: 5'AGT CGC GGG CCC TTC TTC ATC TAG GGG GCT GGC TAA A 3'. The PCR product was digested with SacI and ApaI and cloned into a pBluescript SK+ vector (Stratagene) containing a 3' poly A tail for high levels of protein expression in *Xenopus* oocytes (224) (Fig. 4.1). The AQP0 pBS vector construct was transfected into TOP 10F' *E.coli* (Invitrogen) by electroporation and ampicillin resistant colonies were selected. Plasmid DNA, from positive colonies, was purified using Mini prep kit (Qiagen) and screened by restriction endonuclease analysis. The sequence and correct orientation of AQP0 in the vector was confirmed by automated DNA sequencing using a T7 primer and an internal primer, GCA GCC TCC TGT ACG ACT TC, to check the sequence encoding the C-terminus

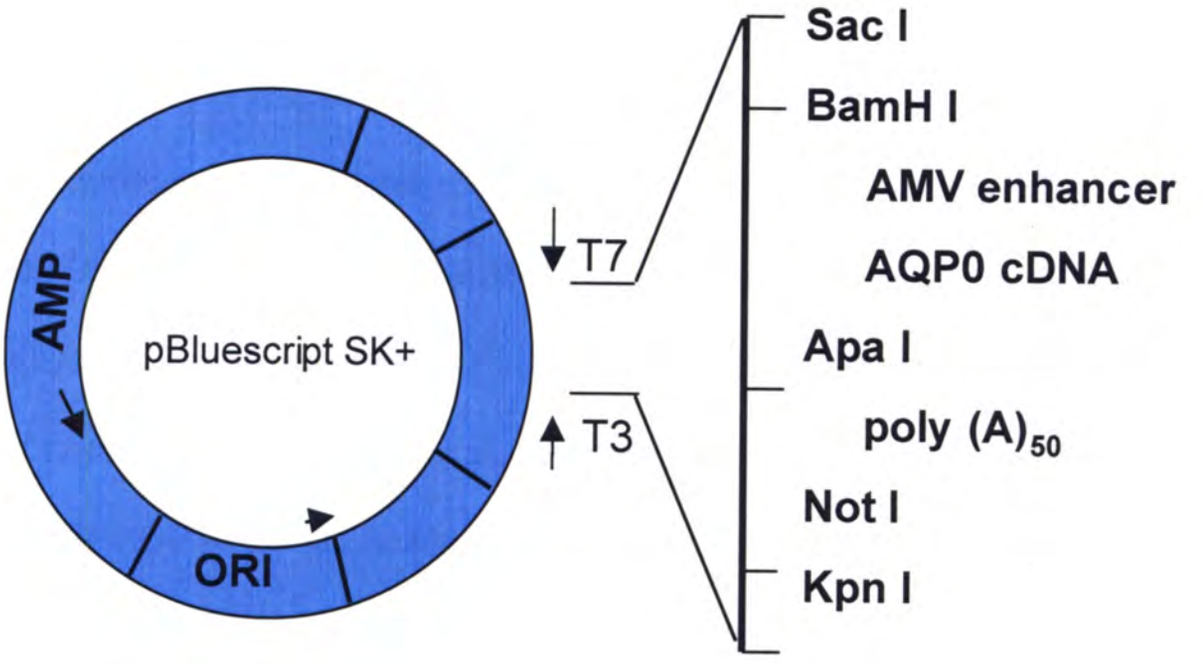

Figure 4.1. Design of human AQP0 vector construct. The vector construct contains elements necessary for *in vitro* transcription and heterologous expression in oocytes including a T7 RNA polymerase promoter, an AMV transcriptional enhancer region, and a polyA tail.

Preparation of Bovine AQP0, Human AQP0, Human AQP1, and Nicotinic receptor RNA- Human AQP1 cDNA, cloned into a pBluescript KS vector modified for protein expression in *Xenopus* oocytes, was obtained from American Type Culture Collection (4). Human AQP0 and AQP1 vector constructs were linearized with NotI and SmaI endonucleases. The linearized DNA was precipitated with 1/10 volume of 8 M ammonium acetate and 2 volumes of ethanol. The solution was chilled for at least 15 minutes at –20 °C and the precipitated DNA isolated by centrifugation for 15 minutes in a microcentrifuge. The supernatant was discarded and the pellet resuspended in nuclease free water (Ambion) water at 0.5 μg/μl. Linearized human AQP0 and AQP1 plasmids, and the bovine AQP0 PCR product served as templates for *in vitro* transcription. *In vitro* transcription was performed using Ambion's mMessage mMachine kit according to the manufacturer's instructions. Capped RNAs, encoding bovine and human AQP0, were synthesized by T7 RNA polymerase whereas, the AQP1 RNA was transcribed by T3 RNA polymerase. Following a 2 hour incubation with RNA polymerase, the template DNA was digested and the RNA precipitated. The RNA concentration was determined by measuring the optical density at 260 nm (1U OD_{260} = 40 μg/ml ssRNA; OD_{260}/OD_{280} ~2 for pure ssRNA). RNA was diluted to 1 mg/ml with nuclease free water and aliquots (5 μl) were stored at –80°C. Due to the labile nature of RNA repeated freeze-thaw cycles were avoided. The α7 nicotinic receptor RNA, prepared in a similar manner, was a gift from Dr. Jim McLaughlin (University of North Carolina). Prior to injection into *Xenopus* oocytes, the quality of the RNA was assessed by ethidium bromide staining following electrophoresis on a 1 % agarose gel. RNA of the incorrect size or which appeared as a smear after ethidium bromide staining was not used for injection.

Establishment and maintenance of Xenopus leavis colony- Female oocyte positive frogs were purchased from *Xenopus* Express (Homosassa, FL), *Xenopus* One (Dexter, MI), or Nasco (Fort Atkinson, WI). Generally the health of the frogs varied greatly irrespective of the provider, however the best results were obtained with frogs from *Xenopus* Express. To increase the quantity of oocytes for harvesting, oocyte development was induced by treatment with human chorionic gonadotropin (HCG) prior to shipment of the animals. Upon arrival, frogs were housed in a translucent plastic tank (18 x 12 x 12 inches) with a tight fitting lid containing air holes. The tank was filled to a height of 10 cm with water, approximately 10 gallons, and a ratio of 4 frogs per 10 gallons of water was maintained. The frogs were fed 5-10 g of diced calf liver three times a week in a small separate tank filled with water from the home tank. If all the liver had been cleared within fifteen minutes additional liver was added to the tank. The water in the home tank was changed completely three times per week and the tank cleaned with 95% ethanol and rinsed with water. At least 24 hours prior to changing the home tank water, tap water in a thirteen gallon carboy was conditioned with 1 ml Prime (Seachem) and 5 ml Amquel (Novalek) to remove chlorine, chloramine, and ammonia. After each water change, three drops of Maroxy (Mardel) an anti-fungal and anti-bacterial treatment and 1 ml of Stress Coat (Aq. Pharm.) with aloe vera were added to the tank. Neutral pH was maintained by the addition of a teaspoon of alkaline buffer (Seachem) to the tank water. An external filtration system (Fluval canister filter 204), including carbon, ammonia remover, biomax, and mechanical filters, was incorporated to continually filter the tank water. The

ammonia remover was replaced every week, the carbon every two weeks, the biomax every six months and the mechanical filters cleaned with each change of the tank water.

The quantity and quality of oocytes has been reported to decrease during the summer months (216) and this was observed in our facility with the best data being obtained between the months of January and April. In an attempt to minimize the seasonal variation, the water temperature was held between 16-20°C by a closed loop refrigeration system. While the reported ideal air temperature for maintaining a healthy colony is 19-21°C, the room in which the frogs were housed fluctuated in temperature from 22-24°C. Frogs were maintained in 12/12 hour light/dark cycles using a fluorescent bulb and were not exposed to natural light.

Preparation of oocytes- Female *Xenopus* laevis were anesthetized by immersion in 750 ml of cold 0.2% (w/v) tricaine: 3-aminobenzoic acid ethyl ester, methane sulfonate salt (Sigma) in dechlorinated water in a plastic container placed in the refrigerator for 20-30 minutes. Surgical instruments, including two pair of No. 3 forceps, a pair of sharp scissors, and a hemostat were sterilized in 70% ethanol for 20 minutes and dried prior to the surgery. Once anesthetized, the frog was placed on its back on top of an ice filled tray covered with aluminum foil. To prevent the skin from drying out about 50 ml of dechlorinated water was poured over the frog. A few centimeters to the left or right of the midline in the lower abdominal area, the skin was pinched and pulled up using the forceps. While holding the skin up, a small incision was made by cutting the skin with the scissors. Careful not to cut more deeply than the layer of skin, the incision was enlarged to less than one centimeter in length. Next, the muscle layer was gently pulled

up using the forceps and an incision about 0.5 cm in length was made through the muscle wall with the scissors. The ovarian lobes containing hundreds of oocytes were gently pulled through the incision with forceps. Lobes of the ovary were cut away and placed directed into a dish of OR2-Mg buffer (82.5 mM NaCl, 2.5 mM KCl, 20 mM $MgCl_2$, 5 mM HEPES, pH 7.4) *(216)*. To suture the skin and muscle together, a curved needle pierced the skin and muscle on one side of the incision followed by the muscle and skin on the other side. Typically one stitch using absorbable sutures (Roboz cat no. SUT-570-31) was sufficient. Following surgery the frog recovered from the anesthetic in a plastic container with less than 1 cm height of dechlorinated water ensuring that the frog would not drown. Once the frog regained consciousness, after about two hours, it was returned to the home tank. Generally surgery was performed up to three times on a particular frog and then it was euthanized in 2% tricaine in sodium bicarbonate buffer pH 7 for 1 hour. Procedures were in compliance with the Medical University of South Carolina animal guidelines.

The ovarian lobes were teased apart with forceps into small clumps containing 10-15 oocytes and were placed into a 15 ml conical tubes up to the 3 ml demarcation. The follicular layer was removed from the oocytes by gentle rocking in 1.5 mg/ml collagenase A (Sigma) in OR2-Mg buffer (8 ml) for 1.5- 2 hours at room temperature. Due to the batch to batch variability in the efficiency of collagenase, the incubation time was adjusted accordingly. Prolonged collagenase treatment disturbs the oocyte membrane integrity resulting oocytes that were no longer spherical. To remove the excess collagenase, oocytes were washed at least three times with fresh OR2-Mg buffer and placed in a petri dish for sorting. Coated tissue cultures dishes were avoided to prevent

oocytes from sticking to the bottom of the dish. Healthy stage V and VI oocytes with uniformly pigmented animal (brown) and vegetal (yellow) hemispheres were selected based their appearance under a dissecting scope (216). Oocytes that were mottled in color, had a gray spot on the animal pole, or were not spherical in shape were discarded. Any remaining folliculated oocytes, which were detected under a dissecting scope by a glassy sheen on the oocyte surface that contains blood vessels, were also discarded. A mechanical 3 ml pipette pump with a cut and fire polished pasteur pipet was used to manipulate the oocytes. Typically about 25-50 percent of the oocytes were discarded at this step. Following selection, healthy appearing oocytes were stored at 18°C in ND96 storage buffer (96 mM NaCl, 2 mM KCl, 1 mM $MgCl_2$, 1.8 mM $CaCl_2$, 5 mM HEPES pH 7.4) supplemented with gentamicin (40 μg/ml), 2.5 mM Na-pyruvate, and 3% (v/v) horse serum (GibcoBrl). ND96 and OR2-Mg media were made fresh and filter sterilized (0.22 μm cutoff) prior to each use. The media was changed daily and unhealthy oocytes were discarded. Typically about 25-50 percent of the oocytes died after the first night in culture.

It became immediately apparent that there was a large variability in the quality of the oocytes. Unlike studies of heterologously expressed ion channels when the resting membrane potential can indicate oocyte health, this would not be compatible with the swelling assay for obvious reasons. As a result, oocytes used in the assay are selected based on their appearance under a dissecting scope. Since the health of the oocyte directly impacts the experimental results, great lengths were taken to obtain and maintain healthy frogs.

Oocyte injection- Twenty-four hours after harvesting, oocytes were injected with variable amounts (0.1- 50 ng) of bovine and human AQP0, human AQP1, or α7 nicotinic receptor RNA in 50 nl of water. Injections were performed with a positive displacement 10 μl pipet (Nanoject, Drummond) with a pulled glass capillary needle. Pipet tips were pulled from glass tubes 8 inches in length (Drummond 3-000-210-G8) using a Flaming/Brown P-97 micropipet puller (Sutter Instruments). The tips of the pipet tips were broken off with a scalpel blade with the aid of a dissecting scope. Tips that were too narrow could not be loaded with mineral oil and tips that were too large either smashed the oocyte during injection or resulted in a large oozing wound. The glass pipet tips were loaded from the base with about 2 cm of white paraffin oil (VWR) using a syringe and 21 gauge needle. The pipet tip was then inserted onto the steel shaft of the pipet and the pipet was placed into a 3-axis micromanipulator. The following steps were performed with the aid of a dissecting scope. While excluding air bubbles, five μl of RNA, deposited on a petri dish, were back loaded into the pipet tip by dialing up the pipet. To facilitate the injection process, oocytes were lined up in grooves cut into a plexiglass plate that fit into a 35 x 10 mm petri dish filled with ND96. The pipet was positioned about 45° from vertical and the tip inserted at the junction of the animal and vegetal hemispheres. Due to the variability in the translation efficiency of oocytes at different levels of maturation, oocytes selected for injection were similar in size and color. Oocytes were injected with RNA (0.1-50 ng) in 50 nl of water and control oocytes were left uninjected or injected with 50 nl of water. Following injection oocytes were incubated in ND96 buffer plus supplements at 18°C for 48 hours prior to the osmotic swelling assay.

Water Permeability Assay - Forty-eight hours after RNA injection, prior to the osmotic swelling assay, oocytes were equilibrated at room temperature in fresh ND96 buffer (190 mosmol) without pyruvate, gentamicin, or horse serum. The swelling assay was performed at room temperature and involved the transfer of oocytes to a chamber containing 30% ND96 in water (70 mosmol). The dilution of ND96 was made by adding one volume of ND96 to two volumes of deionized water and the osmolarity was measured using a vapor pressure osmometer (Wescor-5500) *(168)*. The oocytes were dropped into a hypotonic solution and the inwardly directed osmotic gradient resulted in oocyte swelling. Images of 5-8 oocyte silhouettes were recorded every 5 seconds for up to 2 minutes using a Zeiss IM 35 microscope equipped with computer interfaced camera.

Data processing using Adobe Photoshop or Labview- Data were collected in jpeg files that contained images of 5-8 oocytes per file. If images were recorded every five seconds for 60 seconds there would be 13 files per assay. Typically for each experimental condition tested (e.g. amount of RNA injected), 3 assays were performed. Two approaches were taken to retrieve data from the images. First the pixel count of the oocytes was determined in Adobe Photoshop 3.0. In Photoshop, images were adjusted to define the edge of the oocyte by changing the brightness to 10 and the contrast to 100 and displaying the actual pixels. Each oocyte was selected using the magic wand feature and the pixel count of each oocyte was recorded into a spreadsheet. This tedious and time-consuming process was replaced by the development of data processing software. The second approach utilized Labview software (National Instruments). Labview was programmed to extract data from the images and download the pixel count for each

oocyte into columns of a spreadsheet. Details of the Labview program are provided in the Appendix. Data from files of subsequent time points were entered into subsequent rows. The software maintained the oocyte position in consecutive images resulting in a column of pixel counts for each oocyte as it increased in area with time. The raw data were then downloaded into an Excel spreadsheet and the relative volume and permeability calculations made automatically.

Calculation of oocyte volume- The relative oocyte volumes were calculated from the oocyte cross sectional area, in pixels, by the equation: $(A/A_0)^{3/2} = V/V_0$ where A is the cross sectional area at time 0 and V is the volume as a function of time. This assumes that the oocytes are spherical. Since the volume would often decrease during the first 10 seconds of the assay, possibly due to an endogenous regulatory volume decrease mechanism, the initial rate of oocyte swelling was determined from the slope of relative volume change with time from 10-60 seconds. Analysis of the rate of oocyte swelling indicated that the rate of oocyte swelling was linear and consistent permeability measurements were obtained from images recorded every five seconds, from 10 to 60 seconds into the assay. The permeability coefficient (Pf) was calculated from the initial oocyte volume (9×10^{-4} cm^3), initial oocyte surface area ($S = 0.045$ cm^2), the molar ratio of water ($V_w = 18$ ml/mol), the osmotic gradient, and the initial rate of oocyte swelling using the formula: $Pf = ((1000 \times V_0) / (S \times V_w \times osm_{in} - osm_{out})) \times (d(V_t / V_0)/dt)$ *(215, 217)*. The mean permeabilities ± SE are shown. The significance of difference between mean permeabilities was determined by the two-tailed paired Student's t-test. $P<0.05$

was considered significant. The data presented are representative of multiple assays performed in batches of oocytes from multiple frogs using multiple batches of RNA.

Effect of pH on AQP0 water channel activity- To measure the effects of pH on AQP0 water channel activity, oocytes injected with varying amounts of human AQP0 RNA were incubated in 100% ND96 at pH 6.5 (190 mosmol) for 5 minutes prior to the swelling assay. The rate of oocyte swelling was measured after subjecting the oocytes to 30% ND96 pH 6.5 (70 mosmol). The pH of the 100% ND96 was adjusted to 6.5 rather than 7.6 by using MES (2-(N-morpholino) ethanesulfonic acid) to buffer the solution instead of HEPES *(161)*.

Production of Antibodies to Full-length AQP0, the Amino-Terminus of AQP0, and the C-terminus of AQP0- Antibodies were raised in New Zealand white rabbits by the MUSC Antibody Production Facility. The rabbits were inoculated subcutaneously with the antigen mixed with complete Freund's adjuvant. Three weeks later the rabbits were boosted intramuscularly with antigen in incomplete Freund's adjuvant. Antibody specificity and titer were assessed following separation by SDS-PAGE and immunoblotting of bovine lens membrane protein with each of the sera described below (Fig. 4.2).

Antibodies were generated against purified bovine AQP0. AQP0 was purified from bovine lens membrane proteins by anion exchange chromatography in 1% octyl glucoside (226) and used to generate polyclonal anti-AQP0 antibodies. This antibody worked well for immunoblotting and immunocytochemistry. Antibodies were generated

against the N-terminus of human AQP0, residues 1-9, MWELRSASFC and the C-terminus of human AQP0, residues 250-263, CEVTGEPVELKTQAL. These peptides were synthesized with cysteine residues for conjugation to the carrier protein keyhole limpet hemocyanin.

Immunoblotting- Following the swelling assay, oocytes expressing wild type and mutant AQP0 were homogenized and total membranes were isolated by centrifugation and washed with aqueous buffer. Samples were suspended in buffer containing 0.25 M Tris-HCl, pH 6.8, 5% (w/v) SDS, 0.05% bromophenol blue, 10% (v/v) glycerol, and 2.5% ß-mercaptoethanol and incubated at room temperature for 30 minutes. Oocyte membranes (5 μl) were loaded onto a 14% Tris-glycine gel and electrophoresis was performed at 125V for 2 h. Protein was electroblotted onto 0.2 μm nitrocellulose membrane and incubated with anti-N-terminal AQP0 antibody (1:1000) overnight at 4°C. Protein was detected by enhanced chemiluminescence.

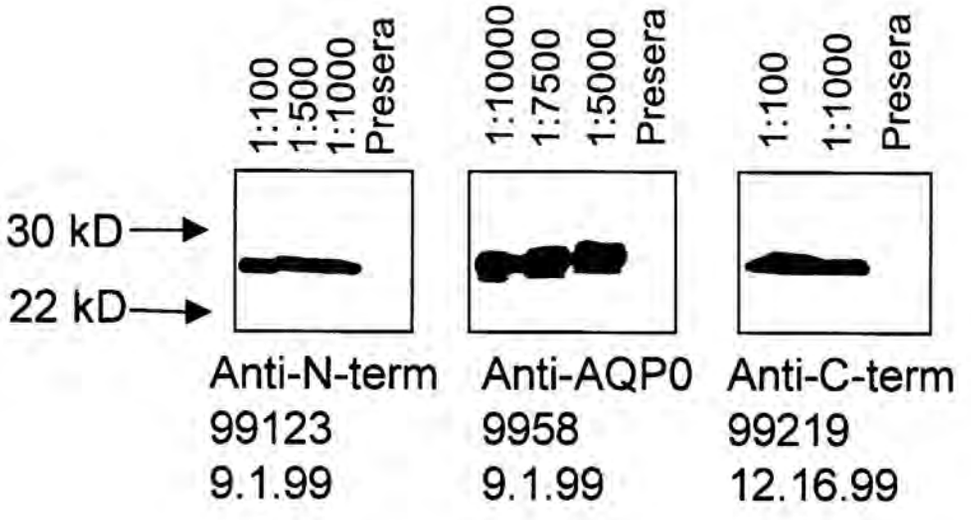

Figure 4.2. Anti-AQP0 polyclonal antibody generation. The activities of the anti-AQP0 N-terminal antisera, anti-AQP0 antisera, and anti-AQP0 C-terminal antisera were tested. Western blot analysis was performed on bovine lens membrane protein (0.5mg) that had been separated by SDS-PAGE and electroblotted onto nitrocellulose. The serial numbers of the immunized rabbit and date tested are provided.

RESULTS

Bovine AQP0 water permeability

Forty-eight hours after injection with 25 or 50 ng of bovine AQP0 RNA, oocytes were subject to the osmotic swelling assay. Images of the oocytes, injected with water as a negative control or bovine AQP0 RNA, were collected every 10 seconds following a hypotonic challenge. An example of the raw data is shown in Figure 4.3. As anticipated, oocytes expressing the aquaporin swell and burst more rapidly than control oocytes. The relative oocyte volume was calculated from the cross sectional area of the oocyte image, in pixels, and the relative increase in oocyte volume with time is shown in Figure 4.4A. The rate of oocyte swelling was, in turn, used to calculate the osmotic membrane permeability (P*f*). The mean P*f* of oocytes injected with 25 or 50 ng of bovine AQP0 RNA was 4.4 ± 0.6 x 10^{-3} cm/s (n=6) and 6.5 ± 0.7 x 10^{-3} cm/s (n=7) respectively (Fig. 4.4B). Due to the diffusion of water across the oocyte membrane in the presence of an osmotic gradient, control oocytes also increased in volume but much more slowly than aquaporin expressing oocytes, P*f* = 1.8 ± 0.2 x 10^{-3} cm/s (n=3). The P*f* measurements of bovine AQP0 are consistent with values reported in the literature, P*f* = 4.5 ± 0.8 x 10^{-3} cm/s (n=8) (112), suggesting that the osmotic permeability assay functions as anticipated.

α7 Nicotinic receptor water permeability

As an additional negative control, and to ensure that the injection of RNA and subsequent heterologous expression of membrane protein does not affect the oocyte membrane permeability to water, oocytes were injected with RNA encoding the α7 nicotinic receptor. The nicotinic receptor has not been shown to transport water and, as

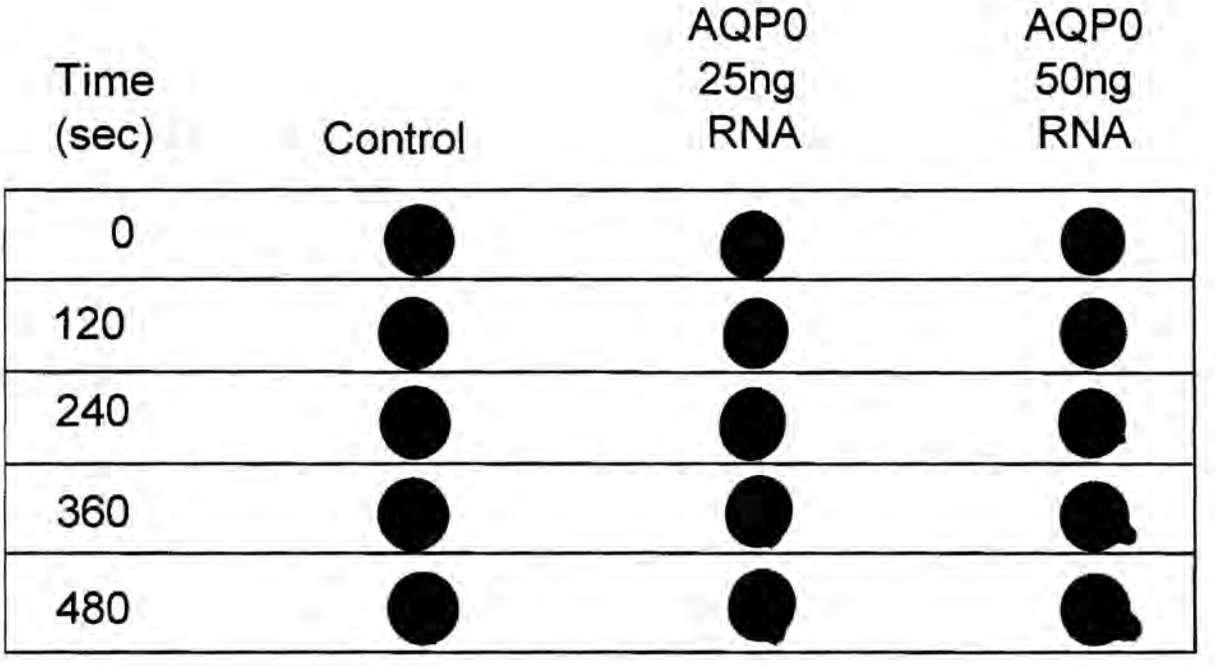

Figure 4.3. Permeability of bovine AQP0 as measured in the *Xenopus* oocyte swelling assay. Time course of bovine AQP0 injected oocyte swelling following exposure to hypotonic media. *Xenopus* oocytes injected with water or bovine AQP0 RNA (25 or 50 ng) were subjected to an inwardly directed osmotic gradient. Images were recorded every ten seconds. One representative oocyte from each experiment every two minutes is shown. Note that after several minutes the oocytes begin to burst.

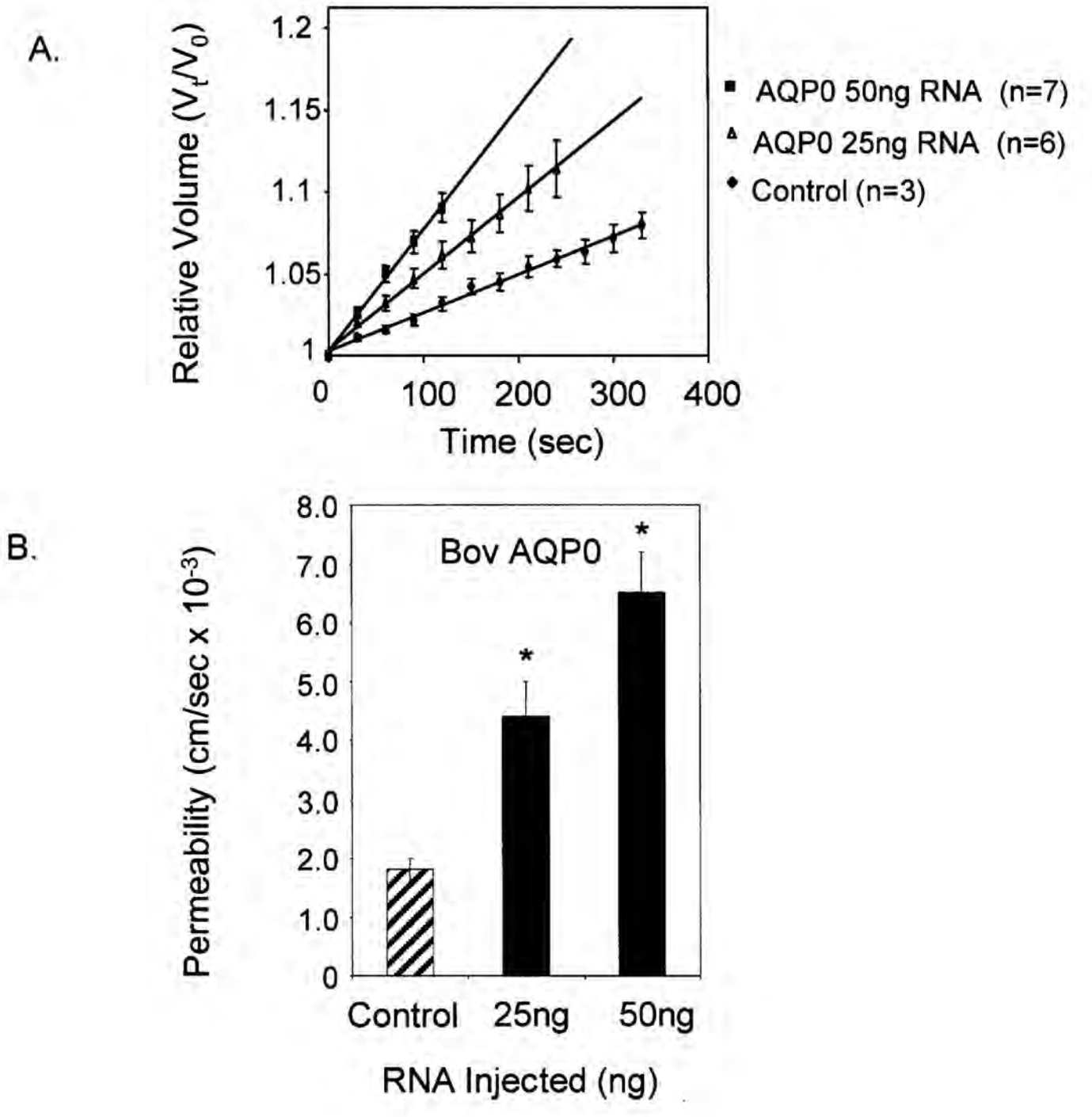

Figure 4.4. Relative increase in oocyte volume and osmotic membrane permeability of oocytes expressing bovine AQP0. A. Oocyte volume was calculated from the pixel count of images recorded during the swelling assay (see Fig. 4.1) and the increase in oocyte volume with time is shown (n= number of oocytes). B. The osmotic membrane permeability (P*f*) was determined from the initial rate of oocyte swelling in response to an osmotic gradient.

such, was not expected to contribute to the oocyte membrane water permeability. The mean permeabilities of oocytes injected with the α7 RNA or 50 nl of water were 3.2 x 10^{-3} ± 0.04 x 10^{-3} cm/sec (n=15) and 3.1 x 10^{-3} ± 1.1 x 10^{-3} cm/sec (n=6), respectively. The permeabilities of the water injected and mock RNA injected oocytes were not significantly different from one another suggesting that heterologous expression of membrane protein alone does not affect water transport across the oocyte membrane.

Cloning of human AQP0

Human AQP0 was cloned from reverse transcribed human lens mRNA into a vector modified for the heterologous expression of protein in *Xenopus* oocytes. The cDNA sequence, confirmed by automated sequencing, was consistent with the sequence predicted from the genomic clone of human AQP0 (225). The cDNA sequence results and translated protein sequence are shown in Figures 4.5, and 4.6, respectively.

Human AQP0 water permeability

The osmotic water permeability (Pf) of human AQP0 was determined using the Xenopus oocyte swelling assay. Due to the low permeability of AQP0 relative to other aquaporins, Xenopus oocytes were injected with a variable amount of human AQP0 RNA to determine the amount necessary to elicit a measurable response in the swelling assay. Figure 4.7 shows the relative increase in oocyte volume with time and the membrane water permeability of oocytes injected with 0.1, 1, 5, or 10 ng of AQP0 RNA. The permeability of oocytes injected with 5-10 ng of AQP0 RNA was 9.94 ± 0.2 x 10^{-3} cm/sec (n=15) about ~5 fold greater than uninjected control oocytes. An additional

ATGTGGGAACTGCGATCAGCCTCCTTTTGGAGGGCCATATTCGCTGA

GTTCTTTGCCACCCTCTTCTATGTCTTCTTTGGGCTGGGGTCCTCACT

GCGCTGGGCTCCTGGACCCCTGCATGTTCTGCAGGTGGCTATGGCAT

TTGGCTTGGCCCTGGCTACACTGGTGCAGTCTGTGGGCCACATCAGT

GGAGCCCACGTCAATCCTGCAGTCACTTTTGCTTTCCTTGTGGGCTCC

CAGATGTCCCTGCTCCGTGCCTTCTGCTATATGGCAGCCCAGCTCCT

GGGAGCTGTGGCTGGGGCCGCTGTGCTGTATAGCGTTACCCCACCT

GCTGTCCGAGGAAACCTAGCACTCAACACGTTGCACCCTGCGGTGAG

CGTGGGCCAGGCAACCACAGTGGAGATCTTCCTGACGCTCCAGTTCG

TGCTCTGCATCTTTGCCACATACGACGAGAGGCGGAATGGCCAACTG

GGCTCCGTGGCCCTGGCCGTTGGCTTCTCCCTTGCCCTGGGGCACCT

CTTTGGGATGTATTATACTGGTGCAGGCATGAATCCTGCCCGCTCCTT

TGCTCCTGCCATTCTCACTGGGAACTTCACTAACCACTGGGTGTACTG

GGTAGGCCCAATCATTGGAGGGGGTCTGGGCAGCCTCCTGTACGACT

TTCTTCTCTTCCCCCGGCTCAAGAGTATTTCTGAGAGACTGTCTGTCC

TCAAGGGTGCCAAACCCGATGTCTCCAATGGACAACCAGAGGTCACA

GGGGAACCTGTTGAACTGAACACCCAGGCCCTGTAG

Figure 4.5. Human AQP0 cDNA sequence results. Human AQP0 cDNA was cloned from total lens mRNA and sequenced.

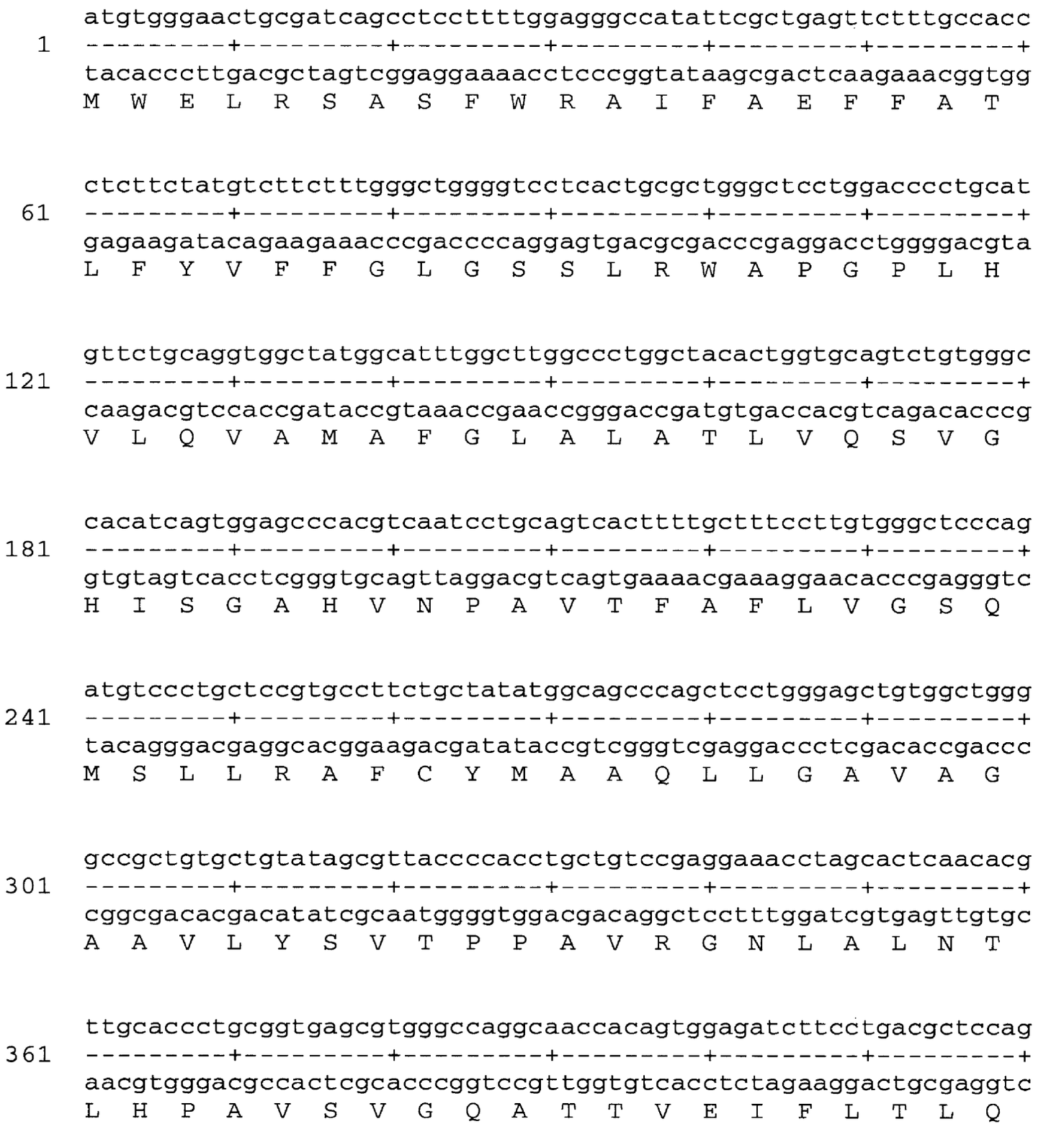

Figure 4.6. Human AQP0 cDNA and translated amino acid sequence.

```
    ttcgtgctctgcatctttgccacatacgacgagaggcggaatggccaactgggctccgtg
421 ---------+---------+---------+---------+---------+---------+
    aagcacgagacgtagaaacggtgtatgctgctctccgccttaccggttgacccgaggcac
    F  V  L  C  I  F  A  T  Y  D  E  R  R  N  G  Q  L  G  S  V

    gccctggccgttggcttctcccttgccctggggcacctctttgggatgtattatactggt
481 ---------+---------+---------+---------+---------+---------+
    cgggaccggcaaccgaagagggaacgggaccccgtggagaaaccctacataatatgacca
    A  L  A  V  G  F  S  L  A  L  G  H  L  F  G  M  Y  Y  T  G

    gcaggcatgaatcctgcccgctcctttgctcctgccattctcactgggaacttcactaac
541 ---------+---------+---------+---------+---------+---------+
    cgtccgtacttaggacgggcgaggaaacgaggacggtaagagtgacccttgaagtgattg
    A  G  M  N  P  A  R  S  F  A  P  A  I  L  T  G  N  F  T  N

    cactgggtgtactgggtaggcccaatcattggaggggtctgggcagcctcctgtacgac
601 ---------+---------+---------+---------+---------+---------+
    gtgacccacatgacccatccgggttagtaacctcccccagacccgtcggaggacatgctg
    H  W  V  Y  W  V  G  P  I  I  G  G  G  L  G  S  L  L  Y  D

    tttcttctcttcccccggctcaagagtatttctgagagactgtctgtcctcaagggtgcc
661 ---------+---------+---------+---------+---------+---------+
    aaagaagagaaggggccgagttctcataaagactctctgacagacaggagttcccacgg
    F  L  L  F  P  R  L  K  S  I  S  E  R  L  S  V  L  K  G  A

    aaacccgatgtctccaatggacaaccagaggtcacaggggaacctgttgaactgaacacc
721 ---------+---------+---------+---------+---------+---------+
    tttgggctacagaggttacctgttggtctccagtgtcccttggacaacttgacttgtgg
    K  P  D  V  S  N  G  Q  P  E  V  T  G  E  P  V  E  L  N  T

    caggccctgtag
781 ---------+--
    gtccgggacatc
    Q  A  L  *
```

Figure 4.6. Human AQP0 cDNA and translated amino acid sequence.

example, shown in Figure 4.8, illustrates the membrane water permeability and the total AQP0 protein expression in oocytes injected with 0.1, 0.5, 1, 5, or 10 ng of AQP0 RNA. As the amount of AQP0 RNA injected into the oocyte increased, the level of total protein expression and the membrane water permeability increased in a dose dependent manner (Fig. 4.8). At the 10 ng amount of RNA injected, the oocyte membrane permeability was $6.8 \pm 0.2 \times 10^{-3}$ cm/sec (n=15) about 3 fold higher than uninjected controls. These two examples demonstrate that human AQP0 confers water permeability to the oocyte membrane and that the permeability measurements are dependent on the amount of AQP0 protein expressed. In addition, the permeability of human AQP0 is similar to the permeability measurements of AQP0's from other species (112, 168, 169).

These examples also demonstrate one of the drawbacks of the oocyte assay, which is the variability in permeability measurements made in different batches of oocytes injected with the same amount of AQP0 RNA. Attempts to use the maximum permeability for comparisons were not valid since at higher levels of RNA injected (>20 ng) the results were unpredictable with the permeability increasing, decreasing, or remaining the same. These observations suggest that in order to directly compare the permeabilities of different aquaporins, or wild type and mutant aquaporins, the amount of aquaporin expressed at the surface of the oocyte must be determined.

Human AQP1 water permeability

To further test the performance and dynamic range of the assay, the permeability of AQP1 was measured. AQP1, which is found in many tissues including the lens epithelial cells, has a higher water permeability than AQP0. The membrane water

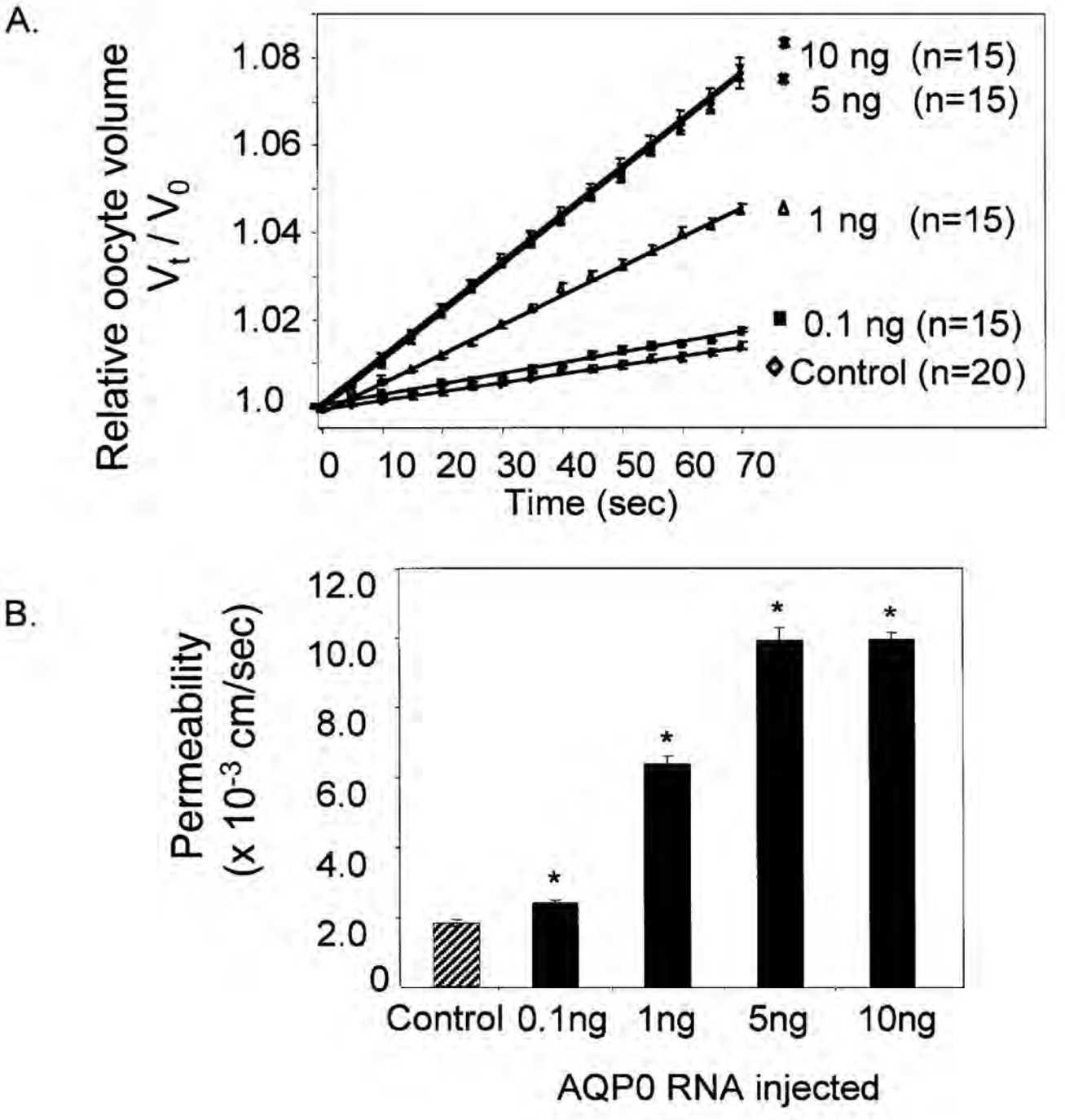

Figure 4.7. Relative increase in oocyte volume and osmotic membrane permeability of oocytes expressing human AQP0. Oocytes were injected with varying amounts of human AQP0 RNA. Control oocytes were uninjected. A. The mean relative oocyte volume ± SE is shown. B. The mean permeability ± SE is shown (n=number of oocytes). Asterisks indicate permeabilities that are significantly different than control as determined by the t-test, $p \geq 0.05$.

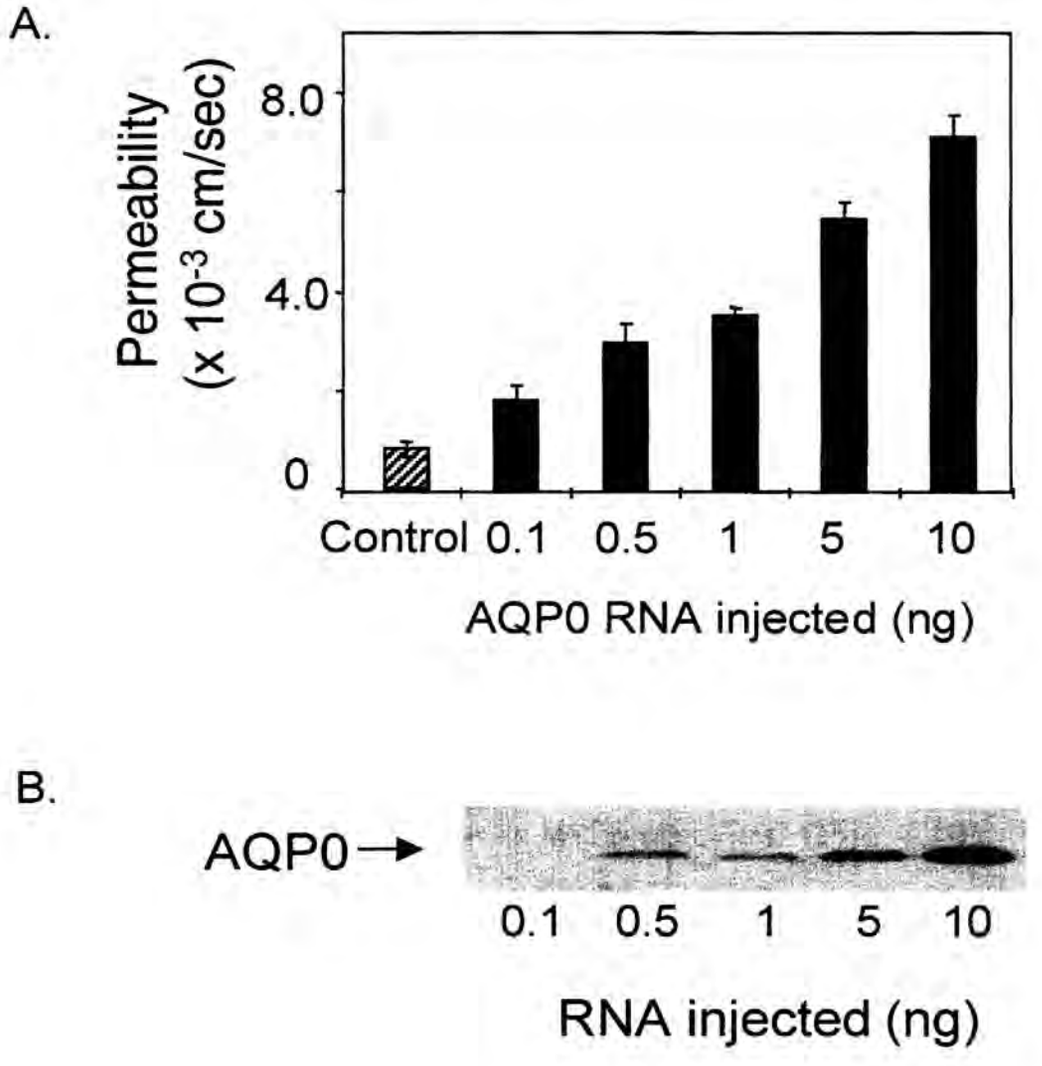

Figure 4.8. Effect of the amount of human AQP0 RNA injected on osmotic membrane permeability and protein expression. Oocytes were injected with varying amounts of human AQP0 RNA. Control oocytes were uninjected. A. The mean permeability of three swelling assays with 5 oocytes per assay ± SE is shown. B. Following the permeability assay, the total membrane protein was prepared from 5 oocytes. Protein from one third of the membrane preparation was separated by SDS-PAGE. Immunoblot analysis was performed with an anti-AQP0 1-9 antibody and the protein detected by enhanced chemiluminscence.

permeability of oocytes injected with 0.6 or 2.5 ng of AQP1 RNA was 11.6 ± 1.1 x 10^{-3} cm/sec (n=5) or 19.5 ± 1.4 x 10^{-3} cm/sec (n=3) (Fig. 4.9). The P*f* measurements of oocytes injected with AQP1 RNA are consistent with measurements reported in the literature of 25 ± 1.9 x 10^{-3} cm/sec (n=6) (169) and 19 ± 2 x 10^{-3} cm/sec (n=10) (40) further suggesting that the swelling assay is working properly.

pH Effects

To investigate the effect of extracellular pH on the permeability of human AQP0, the osmotic swelling assay was performed at pH 6.5 rather than 7.6. The permeability of oocytes expressing AQP0 was not affected by reducing the pH. This result was further supported by examining the effect of pH on oocytes injected with varying amounts of AQP0 RNA where again no differences were observed (Fig. 4.10). This experiment, performed several times with different batches of oocytes, consistently showed no significant differences in the permeability of human AQP0 expressing oocytes at pH 6.5 or 7.6.

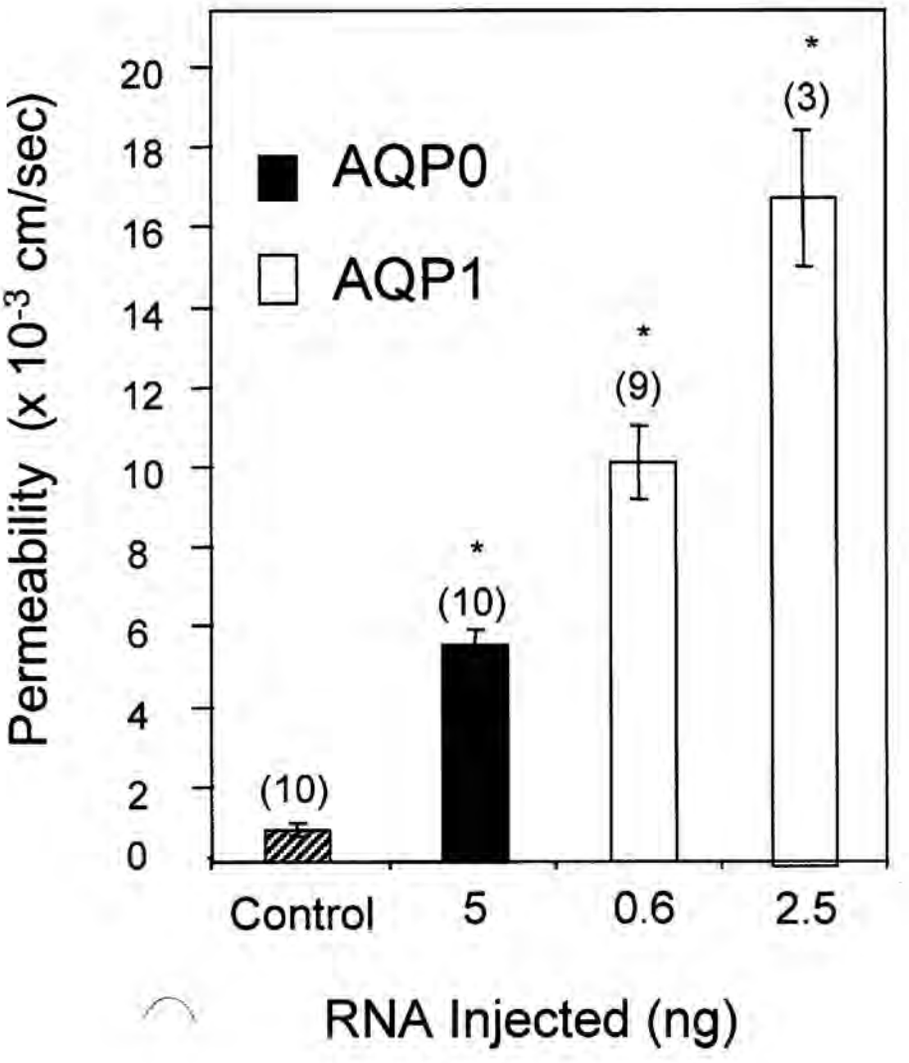

Figure 4.9. Permeability of Human AQP0 and Human AQP1. Oocytes were injected with 5 ng of human AQP0 RNA (black bars) or 0.6 or 2.5 ng human AQP1 RNA (gray bars). Control oocytes (hatched bar) were uninjected. The mean permeability ± SE is shown, (n) is the number of oocytes. AQP1 RNA injected oocytes burst within 1 minute.

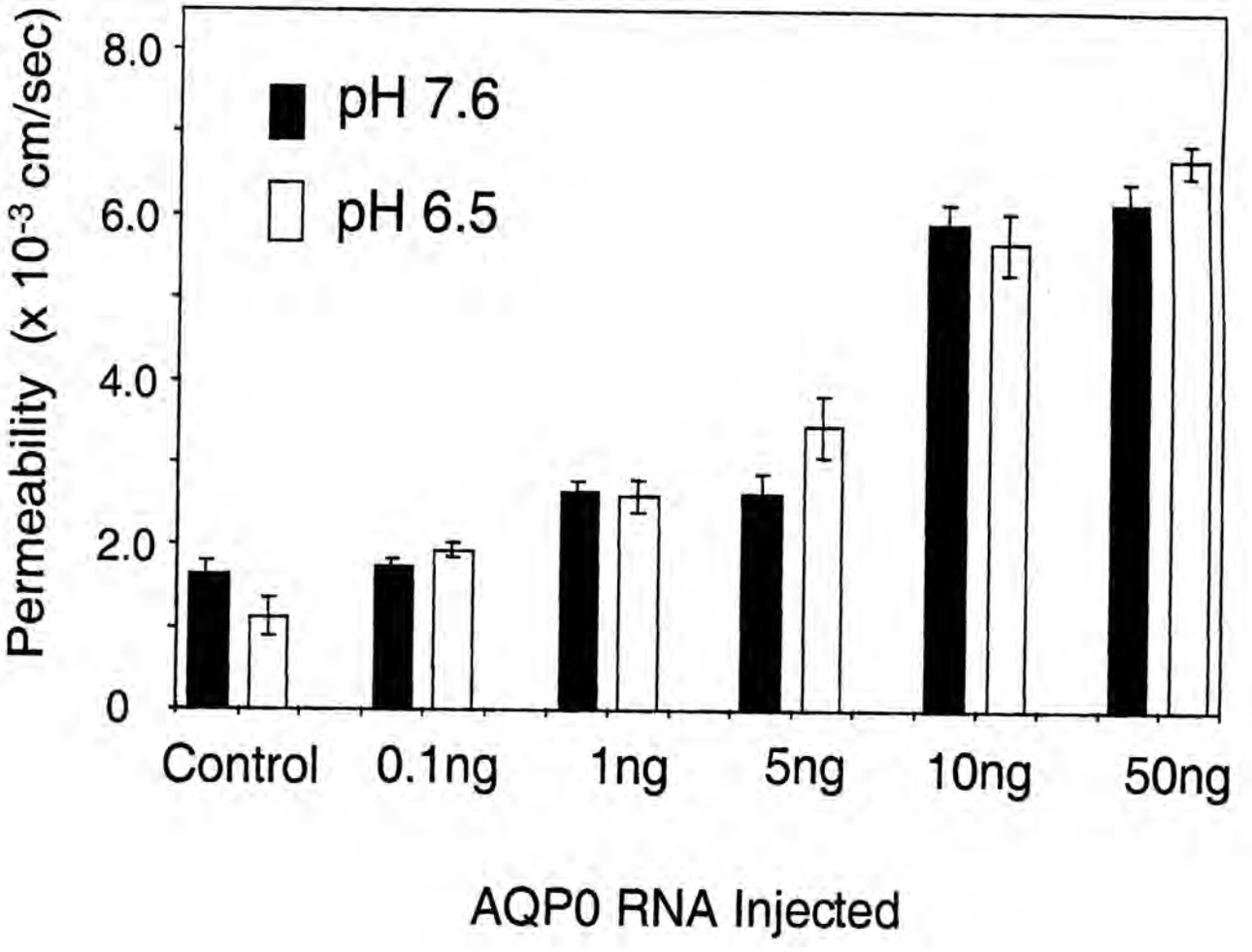

Figure 4.10. Effect of a reduced pH on the permeability of human AQP0. Oocytes were injected with varying amounts of human AQP0 RNA and the swelling assay was performed at pH 6.5 or pH 7.6. Control oocytes were uninjected. The mean relative oocyte volume ± SE is shown (n=15). The assay was performed at 22°C.

DISCUSSION

The *Xenopus* oocyte osmotic swelling assay has been established in our laboratory to measure the water permeability of human AQP0. The oocyte swelling assay was chosen since it provides a simple method for expressing and measuring the water permeability of wild type and mutant forms of aquaporins and will be amenable to the future investigation of the effects of age-related posttranslational modifications on AQP0 permeability. Although there are limitations in using the oocyte assay, there is not a fiber cell culture model available and proteoliposome vesicles generated from lens fiber cells contain a mixture of posttranslationally modified forms of AQP0. In order to characterize the assay, the membrane water permeabilities of oocytes injected with RNA encoding bovine AQP0, human AQP1, or mock RNA were examined and compared to values reported in the literature. A summary of the permeability measurements is shown in Table 4.1. The measured values of permeability are consistent with the literature values, evidence that the assay was working properly. Once the assay was established the permeability and pH sensitivity of human AQP0 were measured.

Human AQP0 increased the oocyte membrane water permeability to water 3-5 fold over control oocytes. This was similar to the permeabilties of AQP0's from other species. At the onset of this work, human AQP0 had not yet been cloned nor had the water permeability been measured. However, in light of the finding that two mutations in human AQP0, E134G and T138R, result in congenital cataracts (48), the permeability of human AQP0 was recently assessed in the oocyte system (1). These findings were consistent with the results presented in this study (Table 4.1). In addition, one of the potential drawbacks of using the oocyte system was illuminated by this study. The

Aquuaporin RNA injected	AQP Permeability (n)	(cm/sec x 10^{-3}) ± SE	Permeability of control oocytes (n)	(cm/sec x 10^{-3}) ± SE
Frog AQP0 (10 ng) Kushmerick, *et al.* 1995	(4)	2.4 ± 0.6	(4)	1.2 ± 0.15
Rat AQP0 (5 ng) Yang, *et al.* 1997	(10)	1.3 ± 0.2	(8)	0.67 ± 0.06
Killifish AQP0 (ng) Virkki, *et al.* 2001	(3-6)	2-5‡	(3-6)	0.5
Bovine AQP0 (10 ng) Mulders, *et al.* 1995	(8)	4.5 ± 0.8	(8)	1 ± 0.3
* Bovine AQP0 (25 ng)	(6)	4.4 ± 0.6*	(3)	1.8 ± 0.2
* Bovine AQP0 (50)ng	(7)	6.5 ± 0.7*	(3)	1.8 ± 0.2
Human AQP0 (5 ng) Francis, *et al.* 2000	3 fold increase over control oocytes (10-15)			
*Human AQP0 (5 ng)	5 fold increase over control oocytes (15) *			
* Human AQP1	(3)	19.5 ± 1.4 *		
Human AQP1 Kushmerick, *et al.* 1995	(6)	25 ± 1.9		
Human AQP1 Yang, *et al.* 1997	(10)	19 ± 2.0		
* α7 RNA	(15)	3.2 ± 0.04 *	(6)	3.1 ± 1.1

‡ Range due to day of measurement
* Indicates permeabilities measured in this study.

Table 4.1. Comparison of osmotic membrane water permeabiltiy measurements with literature values.

mutant AQP0 proteins, E134G and T138R, were not trafficked to the oocyte membrane and, therefore, the effect of the mutations on water permeability could not be assessed (1). It is not known whether these mutant AQP0 proteins are trafficked to the fiber cell membrane in the cataractous human lens.

In using the *Xenopus* oocyte assay to measure the permeabilities of AQP0 and AQP1, limitations of the assay including limited dynamic range of permeability measurements, low sensitivity, and the variability in measurements among different batches of oocytes became apparent. The dynamic range of the measurements was limited by the rate of simple diffusion of water across the oocyte membrane and the loss in the linearity of the rate of swelling as the oocyte reached 110% of its original volume. Practically, this requires that enough RNA be injected to elicit a measurable response while maintaining the linear rate of initial oocyte swelling. With the low permeability of AQP0, the former limitation is more of a concern and with the higher permeability of AQP1 the latter was a concern. In order to address these concerns, several investigators have performed the assay at 10°C (161). Lowering the temperature slows the rate of simple diffusion of water across the oocyte membrane thereby lowering limit of detection and expanding the dynamic range of the measurements. Other modifications to increase the sensitivity of the oocyte assay have been attempted by a number of investigators (150, 227, 228), however these methods have had limited success or prohibitively complicate the acquisition of the data.

Another limitation of the swelling assay, revealed following the injection of varying levels of AQP0 RNA, is that a direct comparison of the water permeability among aquaporins cannot be made without measuring the amount of aquaporin expressed

at the oocyte surface. Typically, the total protein expression is shown by western blot analysis as a measure of the amount of protein expressed in the oocyte (1) although this includes protein expressed and localized in intracellular stores. While many methods have been attempted to normalize the permeability by the amount of protein expressed at the oocyte membrane (40, 174, 229, 230), they are usually labor intensive and still simply provide an estimate. This aspect of the swelling assay will be addressed and discussed in more detail in the next chapter.

Other concerns to note in using the oocyte as a model system include the fact that the plasma membrane lipid profiles and protein complement are much different in the oocyte than the lens fiber cell. Fiber cell membranes are composed of 40-50% sphingomyelin and 10-20% phosphotidylethanolamine with very high levels of cholesterol (50), whereas the most abundant lipid in oocyte membranes is phosphotidylcholine (231). Lipid-protein interactions have been shown to affect the structure and function of integral membrane channels (232) and it is not known if these changes in lipid composition affect AQP0 water permeability. In addition to differences in the lipid profile between oocytes and lens fiber cells, a different complement of proteins in the oocyte may affect aquaporin function and the regulation of aquaporin function. Despite these concerns, the *Xenopus* oocyte swelling assay provides a valuable approach to investigating the effects of structural changes on aquaporin water channel activity.

Since studies showing an affect of extracellular pH on the permeability of aquaporins have been inconsistent and the sensitivity of human AQP0 to pH had not yet been assessed, the effect of pH on human AQP0 was measured. It has been proposed that

the decrease in pH from the lens periphery toward the center of the lens could affect AQP0 mediated water transport within the lens (161). The permeability of human AQP0 as measured in the oocyte assay was not affected by a decrease in extracellular pH. With respect to the conflicting reports in the literature, it is a possibility that the effect of pH on bovine AQP0 was an artifact of the system since heterologous protein expression in oocytes results in a large pool of intracellular protein and pH and temperature have both been shown to affect exocytosis (233). With regard to human AQP0, there is no evidence that a reduction in pH from 7.6 to 6.5 affects the water permeability.

Of the mammalian aquaporins, AQP0 exhibits the lowest membrane water permeability (40) and this has raised the question of whether AQP0 functions exclusively as a water channel in the lens. While many other functions of AQP0 have been proposed, the ability of bovine and human AQP0 to increase membrane water permeability has clearly been demonstrated. The sheer density of AQP0 in the fiber cell membrane suggests that the total contribution of AQP0 to water movement within the lens could be significant (168). A trans-lens flux of water which included AQP1 in the layer of epithelial cells and AQP0 in the lens fiber cells has been estimated to exchange fluid within the lens once every two hours (27). While there are limitations of the oocyte assay, the assay established in this study can be used to address whether posttranslationally modified forms of AQP0 observed in the normal human lens contribute to fiber cell membrane water permeability.

CHAPTER 5

THE EFFECTS OF POSTTRANSLATIONAL MODIFICATIONS ON THE WATER PERMEABILITY OF AQUAPORIN 0

INTRODUCTION

Aquaporin 0 (AQP0), also known as the major intrinsic protein (MIP), is a water permeable channel abundant in the ocular lens. The first sequenced member of the Aquaporin family (3), AQP0 shares the highest sequence similarity (~80%) with the vasopressin regulated AQP2 of the kidney collecting duct. The aquaporins are ubiquitously distributed transmembrane water channels responsible for maintaining water homeostasis of entire organisms as well as individual tissues (221). Impairment of aquaporin function results in a wide spectrum of pathologies including nephrogenic diabetes insipidus (118), deafness (123), Sjogren's syndrome (124), and cataract (1). Of the eleven known mammalian aquaporins six have been identified in the eye and are thought to act in a concerted manner to provide osmotic balance, a critical need for maintaining lens transparency (117). Within the lens, AQP1 is restricted to epithelial cells lining the anterior lens surface whereas AQP0 is distributed throughout the fiber cells comprising the bulk of the lens. Many functions have been attributed to AQP0, however, demonstration of the ability of AQP0 to confer membrane water permeability (112, 168, 169), raises the possibility that it may contribute to the movement of water and circulation of nutrients within the avascular lens (12). While the precise role of AQP0 *in vivo* is not entirely known, the importance of AQP0 in maintaining lens transparency is evidenced by mutations in human (1) and mouse (2, 171, 205, 206) AQP0 which result in the formation of cataracts. In addition to the development of lens opacities, phenotypic characteristics of the AQP0 knock out mouse include loss of the focusing ability of the lens, as well as, a decreased fiber cell membrane water permeability (121).

Many proteins within the human lens, including AQP0, are retained throughout the lifetime of an individual and consequently accumulate age-related posttranslational modifications. This is a result of normal lens development and aging in which mature lens fiber cells, rather than being shed or turned over, are buried under newly differentiating cells at the lens surface. Once the older fiber cells are buried to the depth of 300-500 μm, in the chick lens, they abruptly lose their nuclei and organelles (16) and concomitantly lose their capacity for protein synthesis and protein turnover. The accrual of age-related posttranslational modifications of lens proteins can impact protein function in a number of ways. Age-related modifications are implicated in the loss of Na/K ATPase activity (12), loss of pH sensitivity of gap junctional connexin 50 (59), cytoskeletal remodeling via cleavage of α-spectrin (58), and partial loss of the chaperone activity of αA-crystallin (60). AQP0, the most abundant membrane protein in the lens, undergoes deamidation and extensive backbone cleavage in normal human lenses of all ages (93, 97, 194) and an accelerated rate of truncation has been observed in cataractous lenses (95, 96, 98). Structural characterization by mass spectrometry has permitted the identification of deamidation at Asn residues 246 and 259, phosphorylation of Ser 235, and backbone cleavage at many sites within the C-terminus of human AQP0 (8). While an increase in posttranslational modifications of AQP0 with age correlates with the observed decrease in fiber cell membrane water permeability (7), the exact molecular changes responsible for the altered permeability remain undefined.

Sequence alignment of the aquaporins demonstrates that the C-termini are the most diverse regions of these proteins and as such these domains are thought to regulate aquaporin function in a tissue specific manner. Molecular models of the prototypical

aquaporin, AQP1, resolved by cryo-electron microscopy, depict a right-handed bundle of six tilted α-helices with two short helices dipping into the membrane from either side (131) allowing the juxtaposition of two Asn-Pro-Ala repeats necessary for water permeability (130). Studies have shown that the aquaporins are assembled as tetramers (132-134) with each monomer serving as a water permeable pore (136, 137). While unresolved by electron microscopy, atomic force microscopy placed the C-termini of each monomer intracellularly at the interface of two monomers and the central cavity of the tetrameric structure (125, 139). The C-terminus of AQP0 has been suggested to serve as a channel gate (184). Site directed mutagenesis and naturally occurring mutations of AQP0, AQP1, and AQP2 provide evidence for the involvement of the C-termini in routing newly synthesized protein to the target membrane (140-142) and in regulating protein function (139, 143, 144). Hall *et al.* showed that the water permeability of AQP0 is modulated by calcium and calmodulin (161) which, based on other studies, may be mediated through a direct interaction of calmodulin with the C-terminus (143, 162).

The purpose of the present study was to examine the effects age-related C-terminal modifications of AQP0 on ability of the protein to transport water. Based on truncation of AQP0 observed in previous studies (Fig. 1.13, 1.14) (8, 71), the permeability of full-length AQP0, residues 1-263, and truncated forms of AQP0, residues 1-234, 1-238, and 1-243, was measured in a *Xenopus* oocyte osmotic swelling assay. The high levels of deamidated AQP0 observed in a seven year old normal human lens (8), prompted investigation of the effect of replacing asparagines 246 and 259 with aspartic acid. The effect of substitution of a known phosphorylation site, Ser 235 (8) on membrane water permeability was also assessed. Since the level of aquaporin expression

at the surface of the oocyte directly affects the water permeability imparted to the membrane, an extracellular binding assay was developed to ascertain the efficiency of wtAQP0 and mutant AQP0 protein expression at the oocyte surface.

EXPERIMENTAL PROCEDURES

Construction of AQP0 Mutants- Human AQP0 cloned into a pBluescript SK+ vector served as a template for site directed mutagenesis. C-terminally truncated forms, and the S235A, S235D, N246D, and N259D mutants of AQP0 were constructed by PCR with complementary pairs of primers using the Quickchange site-directed mutagenesis kit (Stratagene). Truncated forms of AQP0 were synthesized by incorporating stop codons at positions 235, 239, or 244, with the following oligonucleotide primers and their complements: 5'GAG AGA CTG TCT GTC CTC TAG GGC GCC AAA CCC GAT 3', 5'ATT TCT GAG AGA CTG TAG GTC CTC AAG GGT GCC AAA 3', 5'GGT GCC AAA CCC GAC TAG TCC AAT GGA CAA CCA GAG G 3'. The resulting plasmids were termed AQP0 1-234, 1-238, and 1-243 respectively. The serine at position 235 was substituted with alanine (S235A) or with aspartic acid (S235D) with the following primer and their complements: 5'ATT TCT GAG AGA CTG GCG GTC CTC AAG GGT GCC AAA 3' or 5'ATT TCT GAG AGA CTG GAC GTC CTC AAG GGT GCC AAA 3', respectively. Deamidation of asparagine 246 and 259 was mimicked by substitution with an aspartic acid. To generate the N246D or N259D mutant AQP0 the following primers and their complements were utilized: 5' GCC AAA CCC GAC GTC TCC GAC GGA CAA CCA GAG GTC 3' or 5' GGG GAA CCT GTT GAG CTC GAC ACC CAG GCC CTG TAG 3', respectively. Incorporation of the desired mutations was confirmed by automated DNA sequencing.

Preparation of AQP RNA- Wild type and mutant plasmids were linearized with NotI endonuclease and capped RNA was synthesized by *in vitro* transcription with T7 RNA

polymerase using mMessage mMachine (Ambion). Following precipitation, drying, and resuspension of the RNA in nuclease free water, the concentration of RNA was determined by measuring the optical density at 260 nm. Prior to injection into *Xenopus* oocytes, the quality of the RNA was assessed by ethidium bromide staining following electrophoresis on a 1% agarose gel.

Preparation and Injection of Xenopus Oocytes*-See Chapter 4 for details.*

Briefly, oocytes were injected with varying amounts of mutant or wild type human AQP0 RNA (0.1 ,1, 5, 10 ng). Control oocytes were uninjected. Oocytes were incubated at 18°C in ND96 buffer. Buffer was replaced daily.

Water Permeability Assay*- See Chapter 4 for details.*

Briefly, forty-eight hours after RNA injection, prior to the osmotic swelling assay, oocytes were equilibrated at room temperature in fresh ND96 buffer (190 mosmol) without pyruvate, gentamicin, or horse serum. The swelling assay was performed at room temperature and involved the transfer of oocytes to a chamber containing 30% ND96 in water (70 mosmol). The oocytes were dropped into a hypotonic solution and the inwardly directed osmotic gradient resulted in oocyte swelling. Images of 5-8 oocyte silhouettes were recorded every 5 seconds for up to 80 seconds. The oocyte membrane permeability was calculated as described previously from the rate of oocyte swelling. Each assay of 5-8 oocytes was performed in triplicate. Experiments with each AQP0 mutant were performed in parallel with the wild type AQP0.

Immunocytochemistry- Forty-eight hours after injection with 10 ng of wild type or mutant AQP0 RNA, oocytes were fixed with calcium acetate buffered 4% para-formaldehyde for 30 minutes at room temperature. Oocytes were washed with PBS, placed into a cryomold containing OCT 4583 compound (Sakura), frozen, and 10 μm sections obtained. Oocyte sections were blocked with 1% BSA, 5% nonfat dry milk in Tris buffer (20 mM Tris-HCl pH 7.4, 137 mM NaCl) then incubated with anti-AQP0 antibody (1:100) in 0.1% BSA, 0.5% nonfat dry milk in Tris buffer overnight at 4°C. Secondary antibody incubation was performed using 1:1000 anti-rabbit IgG conjugated to TRITC (Sigma) under subdued lighting for 1 h at room temperature. The sections were washed with Tris buffer and a final rinse of water and images recorded using a fluorescence microscope (Axioplan2 Imaging, Zeiss).

Immunoblotting- Following the swelling assay, oocytes expressing wild type and mutant AQP0 were homogenized and total membranes were isolated by centrifugation and washed with aqueous buffer (217). Samples were suspended in buffer containing 0.25 M Tris-HCl, pH 6.8, 5% (w/v) SDS, 0.05% bromophenol blue, 10% (v/v) glycerol, and 2.5% ß-mercaptoethanol and incubated at room temperature for 30 minutes. Oocyte membranes (5 μl) were loaded onto a 14% Tris-glycine gel and electrophoresis was performed at 125V for 2 h. Protein was electroblotted onto 0.2 μm nitrocellulose membrane and incubated with anti-N-terminal AQP0 antibody (1:1000) overnight at 4°C. Protein was detected by enhanced chemiluminescence and quantified using a FluorS Imager (Biorad). To compare the expression of the AQP0 1-243 truncation mutant to the

full-length protein, a standard curve was generated using known concentrations of bovine lens membrane protein.

Protein expression at the oocyte membrane surface- The protocol for measuring the surface protein expression at the oocyte membrane was modified from Shih *et al.* (234). Immediately following each swelling assay, 7-8 oocytes were fixed in 4% para-formaldehyde in ND96 buffer pH 7.4 for 15 minutes at room temperature. Since oocytes expressing AQP0 burst after about 10 minutes in 30% ND96, oocytes were subject to hypotonic solution for no longer than 70 seconds prior to fixing. Following fixing, oocytes were washed three times by gentle transfer to fresh 100% ND96 buffer supplemented with 5% horse serum in a 24 well plate and any damaged oocytes were discarded. Primary antibody incubation was performed with 1:100 rabbit anti-AQP0 antibody in ND96 buffer overnight at 4°C followed by three washes. Oocytes were then incubated with 0.1 μCi of [^{125}I] goat anti-rabbit IgG (New England Nuclear, specific activity 1190 Ci/mmol) in a total volume of 0.6 ml ND96 buffer overnight at 4°C and subsequently washed as above. [^{125}I] counts per minute were measured in a gamma counter (LKB, Compu Gamma Cs 1282). The specific binding was obtained by subtracting nonspecific binding of the 1° and 2° antibody to uninjected control oocytes from the total binding of antibody to oocytes heterologously expressing AQP0. The mean specific binding ± SE is shown. The standard error of specific binding includes the errors associated with mean binding to uninjected oocytes and the mean binding to injected oocytes. For each amount of RNA injected, three measurements were made with 7-8 oocytes per measurement.

RESULTS

The permeability of AQP0 mutants

The oocyte membrane water permeability of oocytes injected with 10 ng of wtAQP0 was 6.7 ± 0.1 x 10^{-3} cm/sec (n=176), about 3 fold higher than control uninjected oocytes which had a permeability of 2.2 ± 0.2 x 10^{-3} cm/sec (n=163). The results shown in figure 5.1 were compiled from multiple assays. Statistical analyses were performed in individual experiments comparing the permeability of a mutant to the wild type permeability in each experiment and are consistent with the compiled results shown in figure 5.1.

To determine the effect of potential phosphorylation at Ser 235, an abundant site of phosphorylation observed in the human lens (8), this serine residue was replaced with either an alanine to prevent phosphorylation or an aspartic acid mimic the negative charge of a phosphate group. The permeabilities of oocytes expressing AQP0 S235A or S235D were not significantly different than oocytes expressing the wild type protein (Fig. 5.1). At the 10 ng amount of S235A RNA injected, the oocyte membrane water permeability was 5.9 ± 0.3 x 10^{-3} cm/sec (n=31). At the 10 ng amount of S235D RNA injected, the oocyte membrane water permeability was 5.8 ± 0.2 x 10^{-3} cm/sec (n=15). These data suggest that the removal of the phosphorylation site or the incorporation of a negative charge at this position within AQP0 does not directly affect the permeability of AQP0.

The effect of C-terminal deamidation of asparagine residues 246 and 259 to aspartic acid on AQP0 water permeability was also examined. Although deamidation of asparagine typically results in the formation of isomers of aspartic acid that may impact

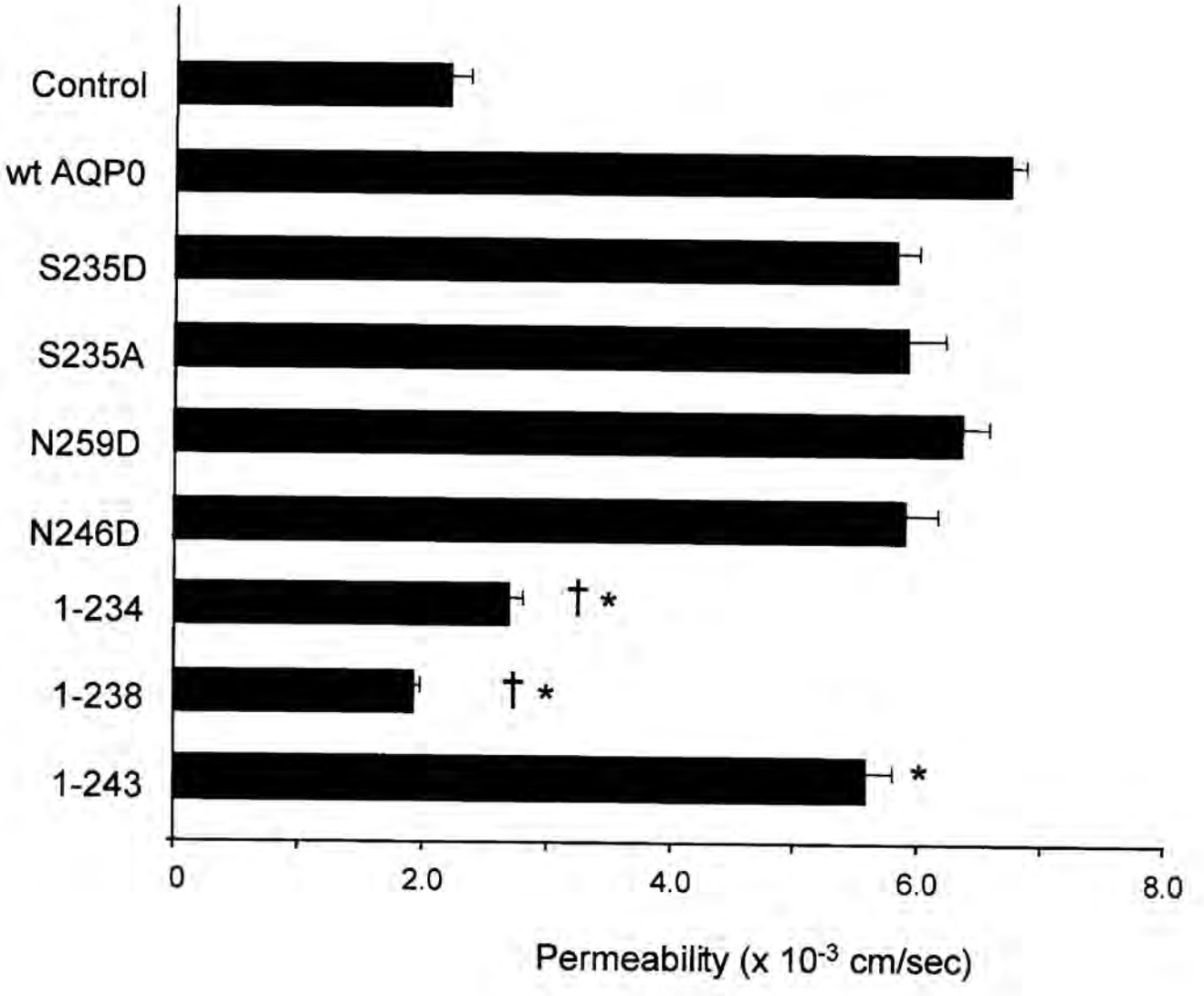

Figure 5.1. Permeability of wild type and mutant AQP0. *Xenopus* oocytes were injected with 10 ng of AQP0 or mutant AQP0 RNA. The mean permeability of multiple assays with 5-8 oocytes per assay ± SE is shown (n ≥10). Asterisks indicate permeabilities that are significantly different from the P*f* of wtAQP0 injected oocytes as determined by a paired *t*-test (* $p<0.05$). † indicates permeabilities that are not significantly different than uninjected control oocytes.

protein function in different ways (74, 81), the effect of incorporating negative charge at the sites of deamidation by substituting aspartic acid for asparagine was assessed. At the 10 ng amount of N246D RNA injected, the oocyte membrane water permeability was 5.9 ± 0.3 x 10^{-3} cm/sec (n=15), whereas the oocyte membrane water permeability of N259D injected oocytes was 6.3 ± 0.1 x 10^{-3} cm/sec (n=15) (Fig. 5.1). The permeabilities of oocytes expressing N246D or N259D were not significantly different than oocytes expressing the wild type AQP0. These data suggest that deamidation of asparagine to L-aspartic acid and the incorporation of a negative charge at position 246 or 259 does not directly affect the AQP0 water permeability.

To assess the effects of C-terminal truncation on the water permeability, stop codons were incorporated into the AQP0 cDNA to generate proteins truncated after residues 234, 238, and 243. The effect of truncation at residues 243 and 234 on AQP0 permeability was addressed since these are among the most abundant truncation products found in the human lens (Fig. 1.13, 1.14) (8). The effect of truncation at residue 238 was tested since, in addition to being observed in the human lens, it is a major calpain proteolytic product found in the rat selenite-induced cataract (71). Following heterologous expression of the full-length and truncated forms of AQP0 in oocytes, the swelling assay indicated that C-terminal truncation resulted in a decreased membrane permeability to water. Figure 5.1 shows the mean permeability of oocytes injected with 10 ng of the full-length or mutant AQP0 RNA. The permeabilities of oocytes injected with 1-234 RNA or 1-238 RNA were 2.7 ± 0.1 x 10^{-3} cm/sec (n=10) or 1.9 ± 0.1 x 10^{-3} cm/sec (n=10), respectively and were similar to that of uninjected control oocytes. The permeability of the AQP0 truncated after residue 243, 5.6 ± 0.2 x 10^{-3} cm/sec (n=54), was

only ~15% lower than the full-length AQP0 permeability. These data suggest that C-terminal truncation affects the permeability of AQP0.

Immunocytochemisty

To determine whether the decreased membrane permeability of C-terminally truncated AQP0 was a result of impaired protein trafficking to the oocyte membrane, immunocytochemistry was performed on oocyte slices. Figure 5.2 shows the immunofluorescence localization of wild type and mutant AQP0 proteins expressed in *Xenopus* oocytes. Immunostaining with a polyclonal anti-AQP0 antibody indicated that the wild type AQP0, S235A, S235D, N246D, N259D, and 1-243 proteins were incorporated into the oocyte plasma membrane. However, AQP0 protein truncated after residue 234 or 238 was retained intracellularly and therefore did not contribute to the oocyte membrane water permeability. Interestingly, AQP0 1-234 was diffusely distributed throughout the oocyte cytosol while AQP0 1-238 was concentrated just inside the oocyte membrane.

Effect of truncation on protein expression

Since the removal of 25 (AQP0 1-238) or 29 (AQP0 1-234) amino acid residues from the C-terminus impaired routing of the protein to the oocyte plasma membrane, the effect of losing 20 residues on the expression of AQP0 1-243 protein was examined. After injecting oocytes with equal amounts of full-length or 1-243 AQP0 RNA, the level of protein expression in oocyte membranes was compared by immunoblot analysis. While the permeability of AQP0 1-243 was consistently about 15% lower than that of the

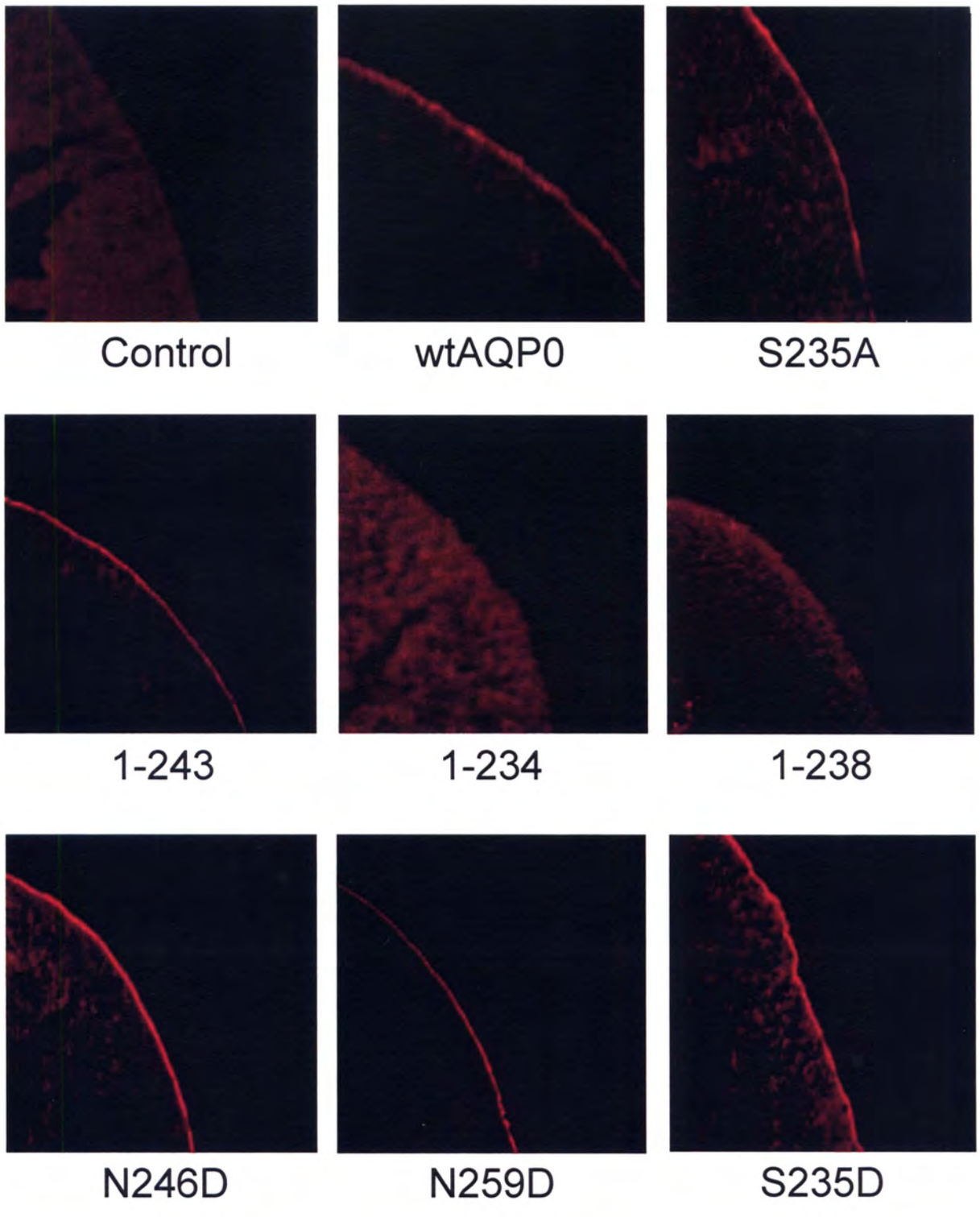

Figure 5.2. Immunofluorescent staining of *Xenopus* oocytes injected with 10 ng of wild type or mutant AQP0 RNA. Control oocytes were uninjected. Forty-eight hours after RNA injection, oocytes were fixed and sectioned. Sections were mounted and stained with a polyclonal rabbit anti-AQP0 antibody and the protein detected by an anti-rabbit IgG labeled with TRITC.

full-length protein, the amount of full-length and 1-243 protein expressed in the oocytes appeared nearly identical (Fig. 5.3). Since total oocyte membranes includes intracellular stores of overexpressed protein, this approach did not address the amount of protein at the oocyte surface contributing to the membrane water permeability. In order to determine if the truncated protein exhibited a lower permeability than the full-length AQP0 or if it was not as efficiently incorporated into the oocyte membrane, an extracellular binding assay was developed to measure the surface expression of AQP0 protein.

Effect of truncation on expression of protein at the oocyte surface

The heterologous expression of AQP0 protein at the oocyte plasma membrane was assessed by anti-AQP0 antibody binding to the surface of the oocyte. While other methods for quantitating protein expression at the oocyte surface have been described (40, 174, 229, 230), modification of the Shih *et al.* approach (234) did not require incorporation of additional mutations, surface accessible lysine or cysteine residues, or micro-dissection of oocyte membranes. Following the swelling assay, whole oocytes were fixed and incubated with a rabbit anti-AQP0 1° antibody and an anti-rabbit [^{125}I] labeled 2° antibody. The level of [^{125}I] detected was assumed to be directly related to the amount of protein expressed at the oocyte surface. As expected, as the level of AQP0 RNA injected increased so did the permeability and the amount of protein expressed on the oocyte surface (Fig. 5.4). As seen previously, for equal amounts of RNA injected into the oocytes, the osmotic membrane permeability of 1-243 was less than that of the full-length protein. However, the binding assay showed that the specific binding of antibodies to 1-243 expressing oocytes was less than oocytes expressing the full-length

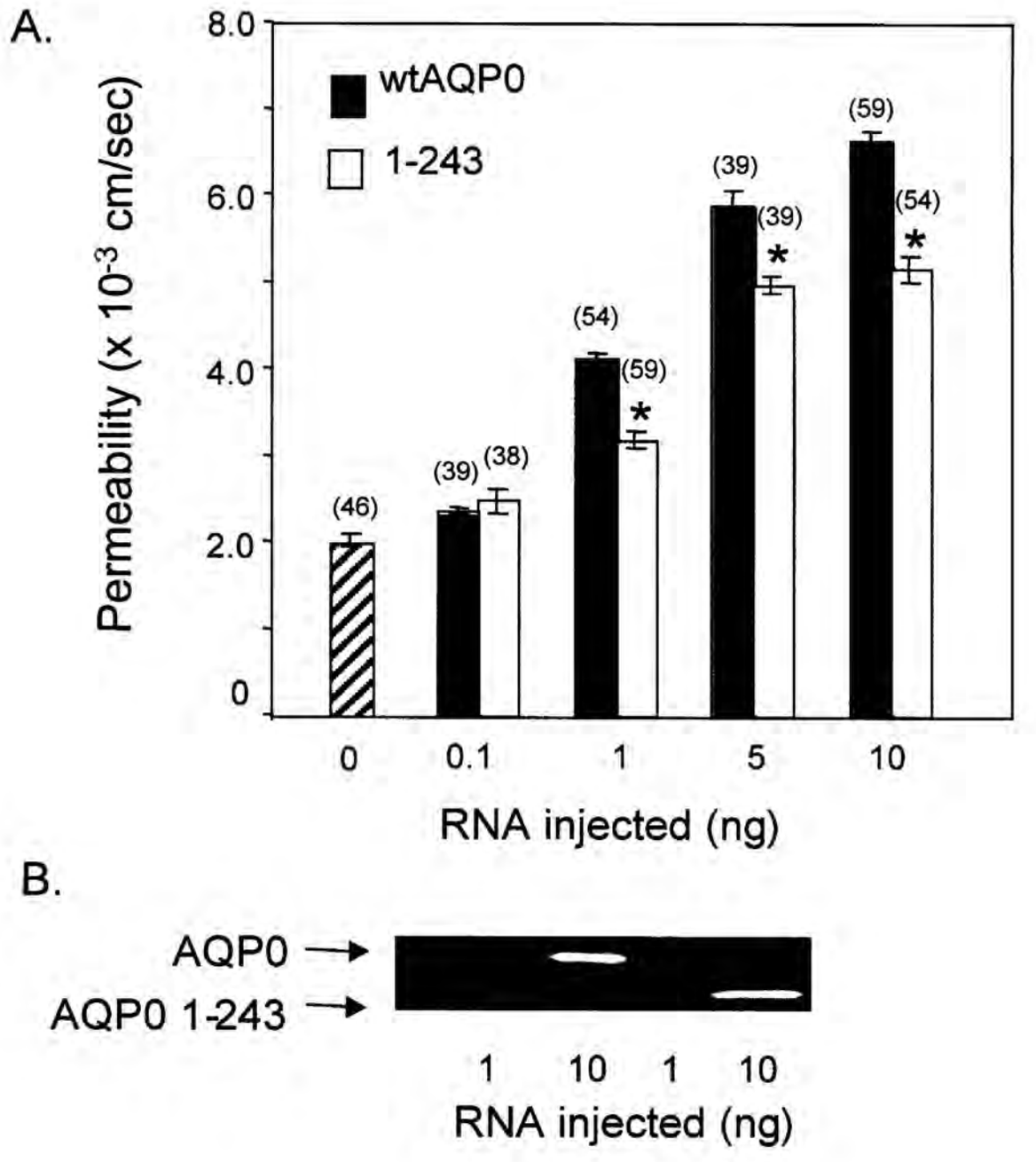

Figure 5.3. Permeability and total protein expression of wt and truncated AQP0. A. Oocytes were injected with 0.1, 1, 5, 10, or 50 ng of wtAQP0 RNA (black bars) or 1-243 AQP0 RNA (white bars). Oocytes injected with 0.1ng of RNA were not different than control oocytes. The mean permeability of multiple assays from different preparations of RNA and different batches oocytes ± SE is shown. Asterisks indicate permeabilities that are significantly different from the P*f* of wtAQP0 injected oocytes as determined by a paired *t*-test (* $p \leq 0.05$). B. Following the permeability assay, total oocyte membrane protein was prepared from 5 oocytes injected with 1 or 10 ng of wtAQP0 RNA or 1-243 AQP0 RNA and separated by SDS-PAGE. Immunoblot analysis was performed with an anti-AQP0 1-9 antibody and the protein detected by enhanced chemiluminscence.

protein. In order to examine the relationship between permeability and surface expression, the data are presented as specific permeability versus specific binding (Fig. 5.4C). These data suggest that at equal levels of protein expression, the water permeability of the full-length and truncated protein is indistinguishable. These data are consistent with the idea that removal of the C-terminal 20 amino acids results in decreased efficiency of the routing and/or incorporation of the truncated protein into the oocyte membrane. This analysis, also applied to the S235A mutant, indicated that the permeabilities of wtAQP0 and the S235A protein were indistinguishable (Figure 5.5).

With regard to the AQP0 mutants, S235D, N246D, and N259D, we were unable to determine the surface expression of these mutant proteins due to an insufficient supply of healthy frogs and oocytes between the months of August 2001 and January 2002. However the permeability data obtained are consistent with the idea that neither mimicking phosphorylation with a negatively charged aspartic acid residue nor replacing the asparagine residues with aspartic acid to mimic deamidation directly affected AQP0 water permeability.

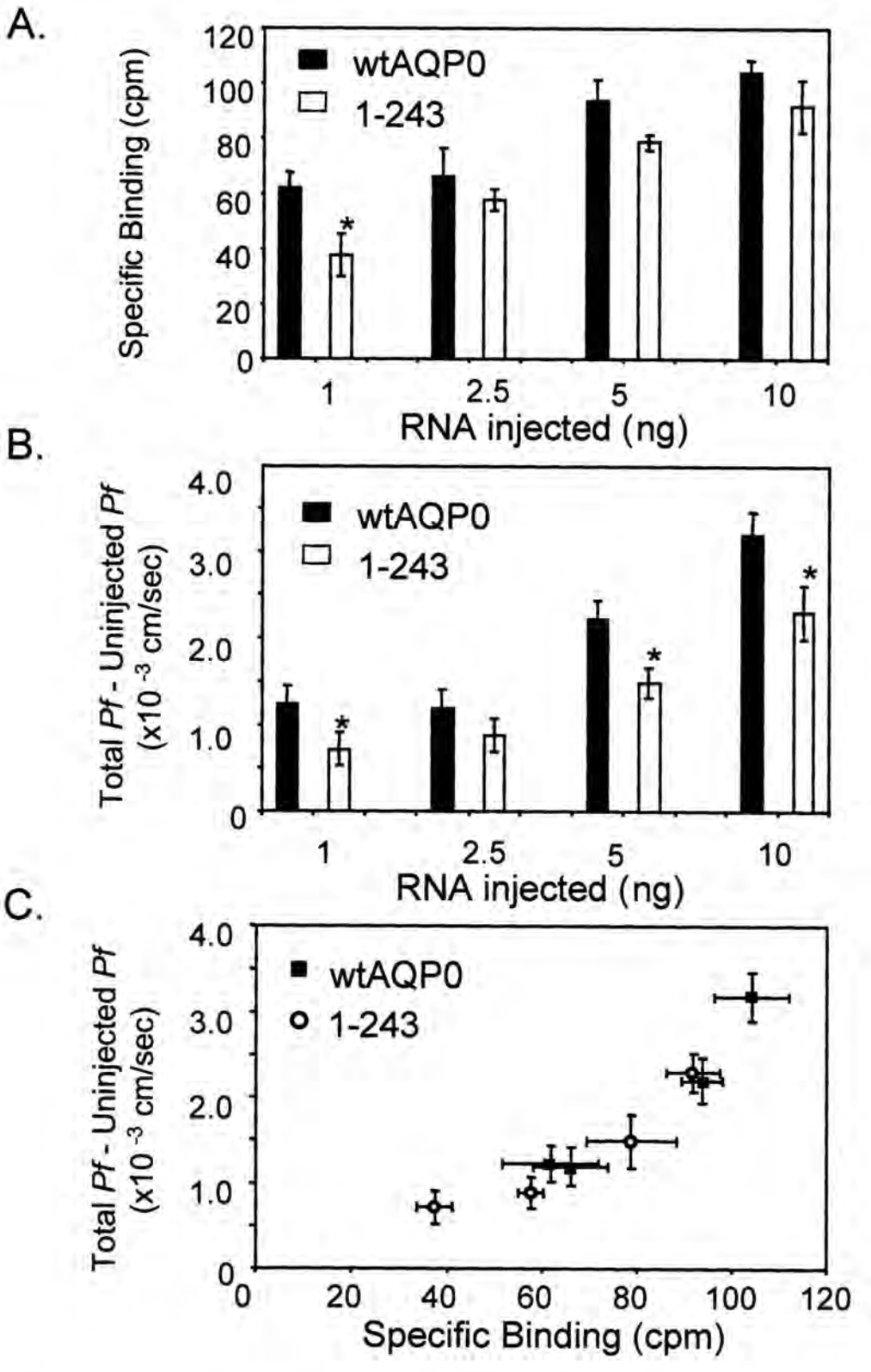

Figure 5.4. A. Expression of wtAQP0 protein (black bars) and 1-243 protein (white bars) at the oocyte surface as determined by [^{125}I] labeled antibody binding. Oocytes were incubated with a rabbit anti-AQP0 antibody followed by [^{125}I] labeled anti-rabbit IgG. The specific binding was calculated by subtracting nonspecific binding of antibody to the uninjected oocyte from the total antibody binding to AQP0 expressing oocytes. The mean binding of three assays with 8 oocytes per assay ± SE is shown (n=3). **B.** Water permeability of oocytes injected with varying levels of wtAQP0 RNA (black bars) and 1-243 RNA (white bars). The water permeability of uninjected oocytes was subtracted from that of experimental oocytes. The mean permeability of three assays with 8 oocytes per assay ± SE is shown (n=24). Asterisks indicate binding or permeability of 1-243 that is significantly different from that of the wtAQP0 injected oocytes as determined by a paired *t*-test (* $p \leq 0.05$). **C.** Full length and 1-243 AQP0 protein expression at the oocyte surface versus the membrane water permeability measured in oocytes.

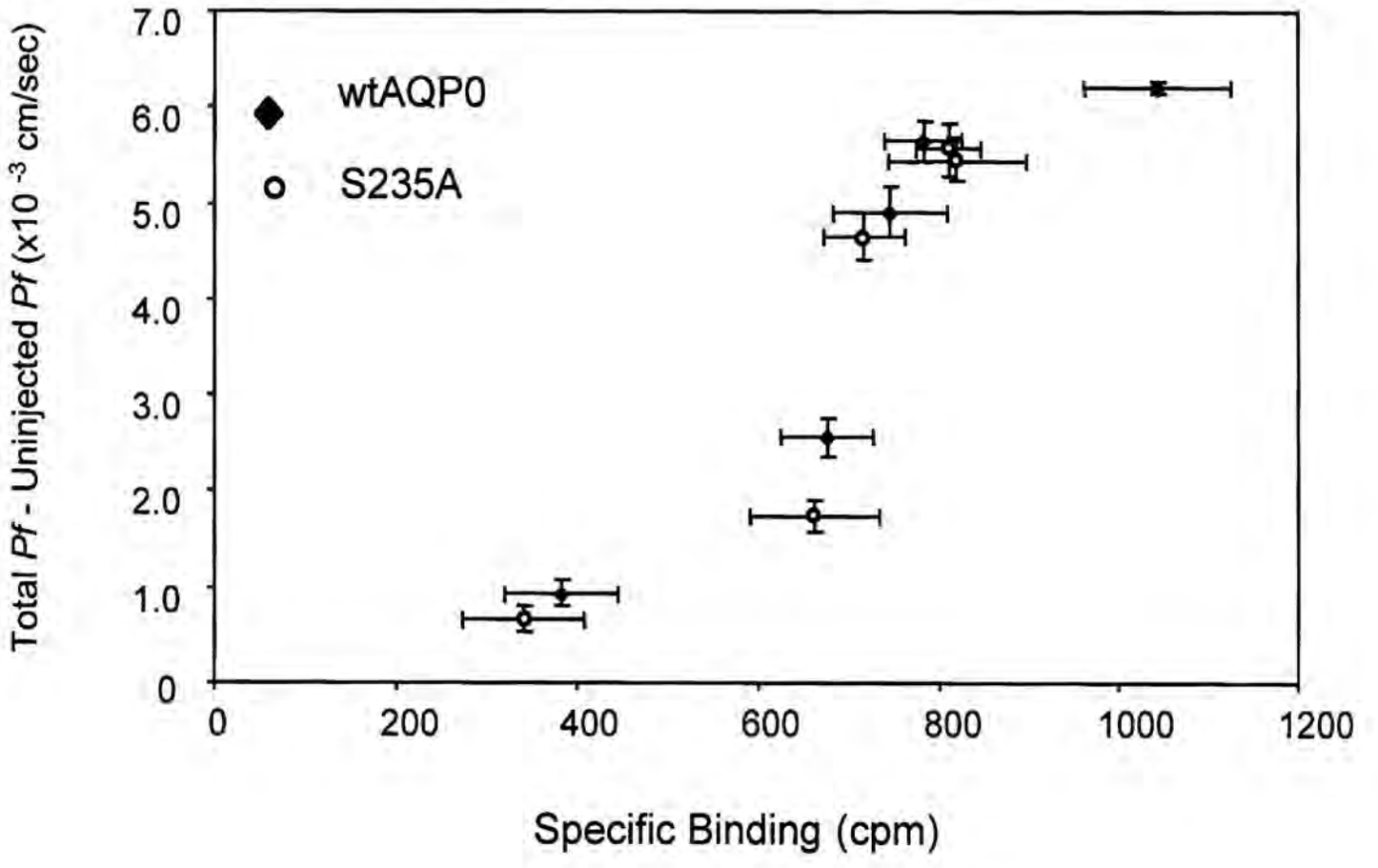

Figure 5.5. Effect of substitution of a phosphorylation site on the water permeability of AQP0. Permeability versus surface protein expression. Following injection of oocytes with varying amounts of wtAQP0 (blue) or AQP0 S235A (red) RNA, the membrane permeability to water was determined and expression of AQP0 at the oocyte surface was measured using a primary antibody against AQP0 and an I^{125} labeled secondary antibody. Averages ± S.E. are shown (n=21 for P*f*, n=3 for binding).

DISCUSSION

As the only aquaporin found in the lens fiber cells, AQP0 has been postulated to play a role in maintaining water homeostasis within the lens. The most recent model of water transport through the lens implies that water transverses the membrane into inner fiber cells through AQP0 (5). This assumes that AQP0 is functional in older lens fiber cells closer to the center of the lens. However, studies of the permeability of vesicles generated from fiber cell membranes demonstrate a decrease in water permeability with fiber cell age (7). In order to determine if aged AQP0 maintains the ability to transport water, the effects of phosphorylation and age-related posttranslational modifications on AQP0 water permeability were determined. Consistent with the proposed role of AQP0 in the model of transport, C-terminal truncation to residue 243 and deamidation at Asn 246 and Asn 249, modifications observed in the normal human lens, do not directly affect AQP0 water permeability.

The *Xenopus* oocyte swelling assay proved useful in screening for potential effects of mutations that mimicked posttranslational phosphorylation, deamidation and truncation. Substitution of the phosphorylation site with alanine or mimicking phosphorylation with a negatively charged aspartic acid residue did not alter the permeability of AQP0. Likewise the AQP0 permeability was not affected by replacing the asparagine residues with aspartic acid to mimic deamidation. C-terminal truncation of AQP0 at residue 243 consistently resulted in a 15% decrease in membrane water permeability as compared to the full-length protein. However after assessing the expression of protein at the oocyte surface, the permeabilities of the full-length protein

and AQP0 1-243 were indistinguishable. These data suggest that within the human lens one of the major truncation products, AQP 1-243, and AQP0 deamidated at Asn 246 and Asn 259 may remain functionally viable during the aging process.

Further truncation to residues 234 and 238 resulted in protein that was improperly routed to the oocyte plasma membrane precluding the measurement of water permeability. Hall *et al.* obtained similar results following the expression of bovine AQP0 1-228 in oocytes (168). These data are consistent with previous findings that the C-termini of the aquaporins are involved in routing newly synthesized protein to the target membrane (140-142). However within the lens, backbone cleavage of AQP0 is a posttranslational event. Therefore misrouting of truncated AQP0 to the fiber cell membrane would not be of consequence unless the protein was regulated by a shuttling mechanism. Other aquaporins undergo shuttling to and from the plasma membrane in response to C-terminal phosphorylation (144). However, it is appropriate to mention that redistribution of aquaporins by a shuttling mechanism observed in endogenously expressed aquaporins cannot be detected in the oocyte model system (159, 229). Although AQP0 has recently been localized to intracellular vesicles in hepatocytes (119), there is no evidence that lens AQP0 is regulated by a shuttling mechanism.

Although these modifications did not directly affect the permeability of AQP0, it remains to be determined whether these modifications may impact regulation of channel activity, localization of the protein in the membrane, or the structural properties attributed to AQP0 (125). Modulation of AQP0 water permeability by calcium/calmodulin (161) could potentially be affected by phosphorylation and truncation occurring within the proposed calmodulin binding domain, residues 225-241 (162). Since calmodulin binds

basic amphipathic helices, phosphorylation at Ser 235 could potentially inhibit calmodulin binding. In addition, the change in the distribution of AQP0 in the cell membranes as the fiber cells age (32) may be due to alterations in the interactions of AQP0 with cytoskeletal proteins. Future investigation of the proteins that interact with AQP0 will provide insight into how phosphorylation and age-related posttranslational modifications may affect protein function, regulation of protein function, and the distribution of AQP0 in the fiber cell membrane.

Many lens proteins, including AQP0, crystallins, connexins, and cytoskeletal proteins, are posttranslationally modified with age. Whether these structural changes produce a physiologically relevant effect or are the result of degradation of vestigial protein is the subject of current investigation. The fact that truncation and deamidation occur in the normal human lens by the age seven, the youngest lens analyzed (8), suggests that these modifications are normal programmed events. The data presented here are consistent with the idea that deamidated AQP0 and truncated AQP0 1-243 maintain the ability to transport water. The ability of the aged protein to retain water channel activity is significant with respect to understanding its potential contribution of AQP0 to circulation throughout the lens. The decrease in water permeability in aged fiber cells observed by Mathias *et al.* (7) may be due to other age-related modifications of AQP0 not tested in this study or to the effect of these modifications on protein-protein interactions. Furthermore, the involvement of AQP0 in the decreased rate of water diffusion into aged lenses and the formation of a physiological barrier to the movement of water into the lens nucleus observed by Moffat *et al.* (6, 15) remains to be elucidated.

CHAPTER 6

DISCUSSION

There have been many exciting developments in the field of aquaporin research since the onset of this project. Electron and X-ray crystallographic resolution of the structures of several members of the aquaporin family are affording a more detailed view of the arrangement of the aquaporin monomer in the membrane and yielding insight into the molecular determinants of channel selectivity (127, 128). Studies involving transgenic mice, generated with a deficiency in the AQP0 protein, have demonstrated the involvement of AQP0 in imparting water permeability to the fiber cell membrane, in establishing normal fiber cell morphology, in the focusing of the lens, and in maintaining lens transparency (121). With respect to human AQP0, three mutations in the AQP0 gene were linked to the development of congenital cataracts providing further evidence that AQP0 plays a role in maintaining clarity in the human lens (48, 173).

While the long term goals of this research are to understand the role of AQP0 in the normal aging lens and the development of maturity-onset cataract, the goal of this project was to begin to spatially map the distribution of posttranslationally modified forms of AQP0 in the normal human lens and to determine if these posttranslational modifications affect the water channel activity of the protein. Based on previous reports in the literature, we hypothesized that age-related changes in the structure of human AQP0, the only aquaporin expressed in the lens fiber cells, were responsible for the age-related decrease in fiber cell membrane water permeability. Efforts were concentrated on the C-terminus of AQP0 since it is a proposed regulatory domain and is the site of many typical and age-related posttranslational modifications.

Structural characterization of the C-terminus of AQP0 isolated from different regions of the human lens revealed an enormous heterogeneity in the primary sequence and differences in the extent of posttranslational modification depending on the location within the lens. Novel posttranslational modifications identified in the C-terminus of human AQP0 include, phosphorylation of Ser 229 and Ser 231, additional sites of truncation after residues 249, 260, 261, and 262, and racemization/isomerization of L-aspartic acid 243 to D-iso-aspartic acid. A summary of previously identified and novel posttranslational modifications of AQP0 are shown in Table 6.1A. C-terminal truncation and aspartic acid isomerization increased with fiber cell age, whereas phosphorylation changed with the position in the lens but not in an age-related manner (Fig. 3.9, 3.17). In a heterologous *Xenopus* oocyte expression system, the effects of phosphorylation, deamidation, and C-terminal truncation on AQP0 water permeability were assessed (Fig. 5.1). A list of recombinant AQP0 proteins used to examine the effects of truncation, deamidation, and phosphorylation is shown in Table 6.1B. None of the modifications tested directly affected AQP0 water permeability suggesting that the aged protein may remain functionally viable in the aging human lens. Truncation of the C-terminus affected protein trafficking and incorporation of newly synthesized protein into the plasma membrane (Fig. 5.2). While these results do not explain the previously observed age-related decrease in fiber cell membrane permeability, they are consistent with the role of AQP0 proposed in the model of internal circulation within the lens. Our findings have also yielded insight into potential mechanisms involved in protein truncation and protein repair in the normal aging human lens. The data generated in this study provide a

A.

C-terminal Posttranslational Modifications of Human AQP0:

Phosphorylation	S229*, S231*, S235
Deamidation	N246, N259
Isomerization/Racemization	D243*
Truncation	242, 243, 244, 245, 246, 247, 248, 249*, 250, 251, 252, 253, 254, 258, 259, 260*, 261*, 262*

B.

The Water Permeability of Recombinant Mutants of Human AQP0:

S235A	Not Distinguishable from wtAQP0
N246D	Not Distinguishable from wtAQP0
N259D	Not Distinguishable from wtAQP0
1-243	Not Distinguishable from wtAQP0
1-234	Protein not properly trafficked to membrane
1-238	Protein not properly trafficked to membrane

Table 6.1. Summary of posttranslational modifications identified in AQP0 and the effects of particular modifications on water channel activity. A. Posttranslational modifications observed in the C-terminus of human AQP0. The asterisks indicate novel posttranslational modifications identified in this study. The presence of all of the posttranslational modifications listed above was confirmed by tandem mass spectrometry in this study. B. The effect of modifications of protein sequence on the ability of AQP0 to transport water.

view of the spatial distribution of posttranslationally modified forms of AQP0 as a function of fiber cell age and, as such, establish a basis for understanding the role of AQP0 in the normal aging lens and for investigating the changes in AQP0 protein structure that may be specific to the onset or presence of cataract.

Phosphorylation of AQP0

The C-terminus of human AQP0 is phosphorylated at serine residues 229, 231, and 235. Interestingly the levels of phosphorylation varied spatially in the lens and could indicate spatial regulation of AQP0 function. In the outer cortex, cortex, and nuclear sections of the 34 year old lens, the levels of phosphorylation were 6.4, 15.1 ± 1.8, and 7.0 ± 1.1% for Ser 235, and 1.0, 8.9 ± 1.7, and 8.0 ± 3.5% (n=3) for residues 229-233, respectively. These data are consistent with previous studies showing that cAMP induced phosphorylation of AQP0 was higher in the inner cortex and nucleus than the outer cortex (209, 210). Although the kinases responsible for *in vivo* phosphorylation of AQP0 are not known, the serine residues at positions 229 and 231 are within consensus sequences for phosphorylation by casein kinase II and protein kinase C, respectively. In considering the levels of AQP0 phosphorylation, it is interesting to note that studies with a homologous aquaporin have shown that phosphorylation of one monomer of the AQP2 tetramer is sufficient for channel regulation (235).

The effect of phosphorylation on AQP0 is not known. Substitution of the serine at position 235 with an alanine did not affect AQP0 mediated water permeability and the effects of phosphorylation at Ser 229 and Ser 231 on the activity of AQP0 have not yet been addressed experimentally. Interestingly the three sites of phosphorylation lie within

the proposed calmodulin binding domain of AQP0, residues 225-241 (162). Evidence consistent with a direct interaction of calmodulin with the C-terminus of AQP0 includes fluorescence studies indicating an interaction between a synthetic peptide corresponding to AQP0 residues 225-241 (162) and calmodulin and mutagenesis studies demonstrating decreased calmodulin binding with substitution of lysine residues 228 and 238 with asparagine (143). Since calmodulin binds basic amphipathic helices, incorporation of negatively charged phosphate moieties may disrupt this interaction. Calcium and calmodulin have also been shown to regulate AQP0 mediated water permeability (161). Hall *et al* observed an increase in AQP0 water permeability in the presence of calmodulin inhibitors. One possible scenario is that calmodulin binds the C-terminus of AQP0 thereby blocking the channel and release of calmodulin from the C-terminus would increase permeability. Phosphorylation, by interrupting calmodulin binding could maintain the protein in an open state. The mechanism of calmodulin regulated AQP0 permeability and the potential effects of C-terminal phosphorylation on calmodulin binding remain to be determined.

The phosphorylation of other aquaporins, such as AQP2 and AQP8, is involved in regulating membrane water permeability by redistribution of the aquaporin protein from intracellular stores to the plasma membrane (157, 236). Although there is no evidence that AQP0 in the lens is regulated by a shuttling mechanism, AQP0 protein recently identified in hepatocytes was found in intracellular stores and was absent from the plasma membrane (119). It seems that if lens AQP0 were regulated by a trafficking mechanism this would occur in the differentiating fiber cells prior to removal of membrane bound organelles. In one study of maturity-onset cataract, AQP0 was found in intracellular

membrane vesicles in the lens. However this appeared to be due to membrane damage rather than a trafficking mechanism utilized by a normal lens (237).

Backbone Cleavage of AQP0

The occurrence of age-related backbone cleavage of many proteins within the lens has long been recognized. More recent examination of the exact sites and the extent of truncation of AQP0 by mass spectrometry has permitted us to address long standing questions in the field of lens research regarding protein truncation. These include the following: Is protein truncation a random or programmed event? What are the mechanisms and/or proteases responsible for protein truncation? Are truncated proteins nonfunctional, vestigial remnants or do truncated proteins remain functional in aged lens fiber cells?

The specificity, selectivity, and lens to lens reproducibility in terms of which proteins undergo proteolytic processing, the sites and extent of backbone cleavage, and the spatial distribution of truncation products all suggest that age-related protein truncation is a non-random, programmed event that occurs in the normal lens. For instance, not all lens proteins are truncated. As the fiber cells age, tropomodulin, tropomyosin, and F-actin, remain intact (58), band 4.1 and other cytoskeletal proteins (17) are totally degraded, while Cx50 (59), α-A crystallin (24), and AQP0 are truncated. The sites of backbone cleavage are reproducible from lens to lens. In whole lens homogenates from patients age 7 to 80 years, the sites of AQP0 C-terminal truncation remained the same while the extent of truncation at each site increased with the age of the patient (Fig. 1.12). Consistent with this observation, AQP0 from lenses of patients ages 34, 35, and 38 exhibited the same sites of truncation, whereas the level of each truncated

product of AQP0 varied depending on the age of the fiber cell and thus the location within the lens. Furthermore, analysis of concentrically dissected lens sections from the three lenses age 34-38 indicated that the spatial distribution of truncated products of AQP0 was consistent from lens to lens. While AQP0 is the only integral membrane protein that has been subject to this type of extensive analysis, observations of reproducible patterns of truncation of the cytosolic crystallin proteins are consistent with the above observations of AQP0 (24). The reproducibility of the identity of the proteins that undergo truncation, the sites at which they are truncated, and the concentric distribution of truncated products within the lens suggests that these are events that occur in a predictable manner during the normal aging process. It remains to be determined whether the development of maturity-onset cataract is a result of the progression of truncation or other age-related posttranslational modifications of AQP0 that occur in the normal aging lens.

By defining the sites of truncation and the relative level of truncation, the involvement of specific enzymes and the mechanisms responsible for backbone cleavage within different regions of the lens can be addressed. Backbone cleavage of lens proteins has been suggested to begin in the zone of denucleation where proteases are actively removing the nucleus and membrane bound organelles (58). Based on mass spectrometric analysis of AQP0 prior to trypsin digestion (Fig. 3.1-3.3) and the C-terminal fragments released after trypsin digestion (Fig. 3.10), the most abundant sites of AQP0 truncation were first detected in the outer lens cortex, the lens section containing newly differentiated fiber cells and newly synthesized AQP0. The fact that the two most abundant sites of truncation, at asparagine residues 246 and 259, are known sites of

deamidation led us to question whether or not truncation occurred spontaneously following formation and hydrolysis of a succinimide ring. This mechanism has been proposed to be responsible for backbone cleavage at susceptible asparagine residues of another lens protein, α-A crystallin. To address whether this was a possibility in AQP0, spontaneous truncation of a synthetic peptide, mimicking the C-terminal sequence of AQP0, residues 239-263, was tested. Backbone cleavage on the C-terminal sides of the Asn residues that correspond to Asn 246 and 259 was observed *in vitro*, in the absence of proteases (Fig. 3.14). The spontaneous *in vitro* truncation observed raises the possibility that this may be the mechanism responsible for backbone cleavage at these particular sites in AQP0 in the human lens.

Backbone cleavage of AQP0 may also occur through the action of proteases. Amino-peptidases, membrane associated proteases, calpains and caspases have all been found in the lens (61, 64-66). In the 34, 35, and 38 year old lenses examined and in previously analyzed noncataractous 50, 81 and 86 year old lenses (8), truncation occurred at almost every site between residues 239-263 with the exception of after residues Pro^{255} and Val^{256}. It is possible that these residues are protected from proteolytic cleavage or that they do not form a substrate for the proteases that are active. M-calpain has been shown to cleave the C-terminus of rat AQP0 at some but not all of the sites that are truncated in the selenite-induced cataract model (71). These data suggest that in the cataractous and control rat lenses multiple proteases may be acting on the C-terminus. With the exception of truncation observed at Asn 246 and 259, the backbone cleavage along the C-terminus of human AQP0 was at similar levels in each lens section of the 34-38 year old lenses suggesting the activity of a nonspecific protease or mixture of

proteases (Fig. 3.10). Although, the presence of a carboxy-peptidase in the lens has been implicated in cleavage of other lens proteins (62), a specific carboxy-peptidase has not been identified. Future characterization of the sites and extent of AQP0 truncation in the lens sections isolated from older lenses may elucidate the proteases involved and their distribution in the human lens.

Effects of Protein Truncation on AQP0 Water Permeability

Even though partially proteolyzed proteins are present in aged lens fiber cells, the question arises as to whether these proteins continue to function or whether they are simply the remnants of once functional proteins. With respect to the fate of other lens proteins, connexin 50 loses pH and calcium sensitivity with fiber cell age resulting in gap junctions that may remain coupled (59), cleavage of α-A crystallin reduces the chaperone activity of the protein (60), and Na/K ATPase while detectable in aged fiber cells does not remain functional (12). As the only aquaporin in the lens fiber cells, AQP0 has been proposed to function as a water channel and contribute to the internal circulation within the lens. In the most recently published model of transport within the lens, it is suggested that water, driven by ion currents, moves paracellularly into the lens from the anterior and posterior surfaces. Then at some point, deeper into the lens, sodium leaks into the fiber cells and water follows through the AQP0 channels. The water then moves toward the equatorial poles through the gap junctional channels connecting adjacent cells carrying waste products out of the lens. The model of circulation implies that AQP0 remains a functionally active water channel in deeper lying fiber cells (5), however other studies

suggest that the membrane water permeability decreases with fiber cell age (7) and that a barrier to the diffusion of water into the lens nucleus develops in the aged human lens (6).

To assess the effects of age-related posttranslational modifications on the ability of AQP0 to transport water, the effect of backbone cleavage at three sites within the C-terminus was determined. To mimic posttranslational backbone cleavage of AQP0 observed in the lens, C-terminally truncated forms of AQP0, residues 1-234, 1-238, and 1-243 were heterologously expressed in a *Xenopus* oocyte expression system. The full-length human AQP0, residue 1-263, exhibited a water permeability similar to previously reported values of AQP0's from other species (Fig. 4.11). The truncated AQP0 proteins, 1-234 and 1-238, were synthesized but not trafficked to the oocyte plasma membrane thus impeding measurements of water permeability (Fig. 5.2). These data suggest that the C-terminus may be involved in routing the newly synthesized protein to the appropriate membrane as has been observed with AQP0 (2) and other aquaporins (142, 238). Although AQP0 1-243 was less efficiently routed and/or incorporated into the plasma membrane, the development of an assay to normalize permeability by the amount of protein expressed at the oocyte surface, permitted further assessment of the permeability of AQP0 1-243. These results indicated that at the same level of full-length or AQP 1-243 protein expression the membrane water permeability of AQP0 1-243 was indistinguishable from that of the full-length AQP0 1-263. This suggests that removal of the C-terminal twenty amino acids from AQP0, which may potentially alter the regulation of the channel, does not directly affect the ability of the protein to impart water permeability to the fiber cell membrane. Furthermore, since AQP0 in the lens is cleaved after insertion into the fiber cell membrane, these C-terminally truncated forms of AQP0

may continue to transport water and contribute to the internal circulation through the lens. These data are consistent with the role of AQP0 in the model of circulation as proposed by Donaldson *et al* (5).

The molecular basis for the previous observations of the age-related decrease in water permeability of vesicles generated from inner fiber cell membranes of a rabbit lens is still unknown. While this experiment has not been performed with human fiber cell membranes, the development of a barrier to water transport in the human lens by age 70 supported the idea that age-related changes in human AQP0 may result in a decreased water permeability. The decrease in fiber cell membrane permeability with age observed in these studies may be a result of a posttranslational modification of AQP0 not addressed in this study. In addition to the age-related changes in protein structure, there are other concurrent changes in the properties of the fiber cells and the possibility exists that other age-related alterations are responsible for the decreased membrane water permeability. For example, these changes could arise from the age-related change in membrane lipid composition. The impact of high levels of cholesterol and sphingomyelin on the water channel activity of AQP0 has not yet been addressed. The involvement of AQP0 in the proposed barrier to water movement, which was not observed in the younger 26 year old lens, may be elucidated by investigating age-related changes in AQP0 and the fiber cell membrane water permeability from the region of older human lenses in which the concentric barrier develops.

Based on the reproducible nature of the rate of deamidation, Robinson *et al* proposed that deamidation could serve as molecular clock signaling protein turnover or possibly introducing an altered protein function at a given time based on the age of the protein (75). The rate of formation and hydrolysis of a succinimide ring at susceptible residues, while dependent on many factors including pH, three dimensional structure, and the identity of adjacent residues, is predictable for a given residue in a protein assuming it remains under the same conditions. The reproducible nature of the rate of racemization of L-Asp to D-Asp has permitted the use of the L/D aspartic acid ratio in particular tissues as a determinant of age in forensics (77). Since deamidation, spontaneous protein truncation, and the isomerization/racemization of aspartic acid are all succinimide-linked reactions with reproducible reaction rates, Robinson's idea of molecular clocks could be further extended to include these reactions. As observed in other non-lens proteins following deamidation (81), age-related succinimide-linked changes could impart a new function, a loss protein function, or an alteration in the mechanism of regulation. It is conceivable that the incorporation of additional negative charges following deamidation, incorporation of an additional carbon into the peptide backbone following isomerization of aspartic acid, and spontaneous truncation of the C-terminus of AQP0 in a reproducible manner could affect protein-protein interactions thereby altering channel regulation. Once the role of the C-terminus of AQP0 has been defined the reality of succinimide-linked reactions in AQP0 serving as molecular clocks can be tested.

A Potential Protein Repair Mechanism in the Lens

Analysis of posttranslational modifications within the C-terminus of AQP0 has also revealed a potential protective mechanism utilized by the lens to repair damaged proteins. Studies characterizing the rates of spontaneous racemization and isomerization of L-aspartate in peptides and proteins, demonstrate that, while L-iso-Asp, D-Asp, and D-iso-Asp are formed, the primary product formed *in vitro* is L-iso-Asp (74). However, *in vivo,* AQP0 Asp 243 is isomerized and racemized predominately to D-iso-Asp. An age-related increase in the level of D-iso-Asp 243 was observed in lens sections prepared under the same conditions (Fig. 3.17). The formation of D-iso-Asp as the primary product of isomerization and racemization has also been observed in αA-crystallin (79) and other non-lens aged proteins (81). The formation of D-iso-Asp in αA-crystallin was postulated to be the result of environmental and structural constraints (79) although, the possibility exists that there is a repair mechanism responsible for the presence of predominately L-Asp and D-iso-Asp in aged tissue. Protein L-isoaspartate 0-methyltransferase (PIMT) has been demonstrated to enzymatically repair L-iso-Asp and D-Asp residues back to L-Asp in peptides and proteins (81, 213). D-iso-Asp is not a substrate for the enzyme (89), thus in aged tissues with endogenous PIMT the expected products would be L-Asp and D-iso-Asp (79, 81). PIMT activity has been observed in normal and cataractous human lenses (212) and the repair of proteins by PIMT has been shown to restore protein activity (81, 213). The elucidation of predominantly D-iso-Asp in AQP0 and other lens proteins in the aging lens is consistent with the idea that PIMT may be an active protein repair mechanism in the human lens.

The Role of AQP0 in the Lens

AQP0 has been proposed to serve dual roles within the lens, and based on previous studies and phenotypic characteristics of the AQP0 deficient animal, the most feasible roles appear to be that of a water permeable channel, maintaining osmotic balance, and that of a structural element, contributing to fiber cell shape through interactions with the cytoskeleton. Both of these roles are crucial to lens transparency. The ability of AQP0 to impart water permeability to the membrane is not contested in the field; whether this is the only role of AQP0 in the lens, however, is contested. As a structural protein, AQP0 may interact with the cytoskeleton contributing to the fiber cell flexibility, resiliency, and cell morphology. The phenotypic characteristics of the heterozygous transgenic AQP0 knock out mouse are consistent with both of these roles. These characteristics include decreased fiber cell membrane water permeability, a non-uniform cell shape, and a loss of interdigitations in the lateral membrane of the cells (121). It is very likely that if AQP0 interacts with the cytoskeletal elements to provide structural stability and maintain the shape of the fiber cells, that the intracellular C-terminus is involved. Interestingly, some of the same characteristics observed in the AQP0 knock out mouse occur as the fiber cells age. For example, as fiber cells age there is a decrease in membrane water permeability (7) and the well defined hexagonally shaped fibers become more rounded and lose the distinct lateral membrane interdigitations (25). Future elucidation of proteins that interact with AQP0 may provide insight into the involvement of AQP0 in these age-related changes.

CHAPTER 7

FUTURE DIRECTIONS

The findings in the present study, in conjunction with new developments in the field, have raised many questions warranting future investigation. Examination of the structure and function of the most abundant membrane protein in the lens, AQP0, will further the understanding of the role of this protein within the normal aging lens and in the development of congenital and maturity-onset cataract. The lens is uniquely suited to investigating age-related changes in protein structure and studies of AQP0 structure may reveal mechanisms involved in protein aging and protein repair that are also generally applicable to non-lens proteins. Further characterization of the water channel activity of AQP0 may provide insight into molecular determinants of water transport and the regulation of membrane water permeability. This information will contribute to the elucidation of the putative role of AQP0 in the internal circulatory system and in maintaining osmotic balance within the lens.

Structural characterization of AQP0 from opaque and clear regions of a human lens:

The LC-MS approach presented permitted the characterization of posttranslational modifications of the C-terminus of AQP0 from dissected sections of a human lens. The current method is amenable to more finely dissected regions of the lens and could be used (i) to examine the distribution of posttranslationally modified products of the C-terminus of AQP0 within older lenses, (ii) to compare the occurrence of modifications in selected regions of the lens such as the anterior and posterior poles, or the concentric region in which the barrier to water develops, and (iii) to compare the modifications of AQP0 isolated from opaque and transparent tissue excised from the same lens. Characterization of the age-related changes that occur in the normal lens will permit determination of

structural changes that are unique to or are more abundant during the formation of opacities.

Age-related concentric dissection of the lens versus physiologically-related dissection of the anterior and posterior poles from the equatorial region:

In order to define the role of protein components involved in the proposed model of circulation, the activities and distribution of aquaporin, connexins, Na/K ATPases, chloride channels, sodium channels, and other channels, transporters, and junctions are being assayed as a function of fiber cell age (5, 12). Theoretically these data will provide a map of the channel activity spatially within the lens either supporting or altering ideas of the current model of circulation. Future investigation of the spatial distribution of posttranslationally modified products of AQP0 in lenses of varying age will provide a view of the normal aging process and will permit one to address whether the spatial distribution of posttranslationally modified products in the lens remains the same or changes with age. While concentric dissection permits assessment of changes that occur as a function of fiber cell age, differences in the distribution of modified AQP0 in the anterior, equatorial, and posterior regions of the lens may provide insight into the potential role of AQP0 in the axial to equatorial flow of water through the lens. An analysis of this type would be interesting with respect to the level of AQP0 phosphorylation, which did not increase in an age-related manner. The LC-MS method developed would be amenable to this type of analysis.

Is the C-terminus of AQP0 repaired by protein L-isoaspartate O-methyl transferase?

In finding that the primary product of isomerization/racemization of AQP0 Asp 243 was D-iso-Asp, an unanticipated result based on studies of *in vitro* aging of proteins and peptides (74, 81), the activity of a repair enzyme was hypothesized. The activity of protein L-isoaspartate O-methyl transferase (PIMT) has been observed in normal and cataractous human lenses and has been suggested to play a protective role (212). The repair of isomerized and racemized AQP0 by PIMT could be tested on peptides corresponding to residues 239-244 (GAKPDV) of AQP0 with L-Asp, L-iso-Asp, D-Asp, and D-iso-Asp at the position corresponding to 243 and/or on AQP0 isolated from the lens and aged *in vitro*. Examples of these types of studies can be found in the following references (74, 81, 212, 213).

Effects of age-related posttranslational modifications on the permeability of AQP0:

It is very likely that the age-related changes in the C-terminus of AQP0 abolish and/or alter regulatory control of the protein. The C-termini of aquaporins, proposed to regulate water permeability by several different mechanisms (139, 160), have been shown by atomic force microscopy to lie near the interface of each monomer and extend toward the central cavity of the tetrameric structure (125, 139). Current research in the lab, aimed at elucidating proteins that interact with AQP0, may provide potential leads to investigate the role of the C-terminus of AQP0 and more generally the function of the AQP0 within the lens.

While truncation of the last twenty amino acids from AQP0 did not directly affect the permeability, further truncation of the C-terminus could not be assessed in the

Xenopus oocyte permeability assay since these truncated proteins were not trafficked to the oocyte plasma membrane. To circumvent this problem, an alternative system has been established for the expression of mutant aquaporins in a temperature sensitive strain of *Sacchromyces cerevisiae* (217). As discussed in Chapter 4, synthesized mutant membrane protein can be isolated from yeast secretory vesicles and subsequently analyzed in a vesicle shrinking permeability assay (217).

With regard to the decrease in fiber cell membrane permeability with fiber cell age observed in previous studies, the effect of lipid composition on AQP0 permeability was not addressed (7). The lipid vesicles used were generated directly from outer or inner fiber cells and while there are more posttranslationally modified products of AQP0 in the inner fiber cells there is also a change in the membrane lipid composition with fiber cell age. The age-related increase in sphingomyelin, dihydrosphingomyelin, and cholesterol could potentially impact membrane protein function (49-52). If membrane lipid composition does impact AQP0 mediated membrane water permeability (15), this would have implications in the age-related decrease in membrane permeability observed by Mathias *et al.*, (7), the development of the barrier to water transport observed by Truscott *et al.*, and others (6, 15, 38, 239, 240), and the proposed role of AQP0 in the circulation of water throughout the lens (5).

Could AQP0 water permeability or some other, yet to be determined, function be regulated in a reciprocal manner by calmodulin and phosphorylation?

Thus far, the only proteins thought to interact with the C-terminus of AQP0 are calmodulin, kinases, and phosphatases. The predicted binding domain of calmodulin,

residues 225-241 (162), contains three known sites of Ser phosphorylation at residues 229, 231, and 235. While the effect of phosphorylation on AQP0 function is unknown, the water permeability of AQP0 expressed in oocytes increases in the presence of calmodulin inhibitors (161). This raises the possibility that calmodulin may modulate AQP0 water permeability in the lens fiber cells by direct interaction with AQP0. To address whether calmodulin interacts with the C-terminus of AQP0, original experiments compared changes in fluorescence upon incubation of calmodulin with a synthetic peptide of AQP0 containing a tryptophan residue (162). Similar experiments utilizing differentially phosphorylated versions of the C-terminal peptide may provide evidence for reciprocal regulation of AQP0 by calcium/calmodulin and phosphorylation.

What are the molecular determinants of the low water permeability of AQP0 as compared to other mammalian aquaporins?

Although it was not in the scope of this project, recent developments in the structural characterization of AQP1 (127, 128) provide an avenue for the investigation of the molecular determinants responsible for the difference in permeabilities between AQP1 and AQP0. While comparisons between aquaporin and aquaglyceroporins have yielded insight into the molecular determinants of channel selectivity (147), comparisons between two aquaporin channels with different rates of transport may provide insight into the mechanisms of water movement. For instance, one could speculate that the rate of water transport through the channel is slowed in AQP0 due to additional hydrogen binding imposed by a tyrosine residue, which is homologous to Phe^{24} in the center of the AQP1 channel (127). Another interesting site was recently proposed as being involved in

gating of AQP4 water permeability. AQP4 has one of the highest permeability coefficients of the mammalian aquaporins and phosphorylation of Ser^{180} decreases AQP4 membrane water permeability (156). Aquaporins with a lower water permeability, such as AQP0 and AQP2, have an aspartic acid at the homologous site. It is possible that the negative charge at this site within an intracellular loop decreases water permeability. These studies, ideally suited to the *Xenopus* oocyte permeability assay, may also lend insight into the determinants responsible for the exponential or linear rate of swelling observed in AQP1 or AQP0 expressing oocytes, respectively. Very few site-directed mutagenesis studies have been performed on AQP0 and there have not been any such studies published since the elucidation of the AQP1 structure.

Is AQP0 involved in the circulation of water through the lens?

Often multiple aquaporins found in the same tissue act in a concerted manner to maintain osmotic balance (221). This has been observed in the cornea where AQP5, found in the epithelial layer of the cornea, was shown to absorb water while AQP1, found in the corneal epithelium, extrudes water from the corneal stroma (41). In the lens, AQP1 in the anterior epithelium and AQP0 in the lens fiber cells may act in a concerted manner to transport water through the lens and maintain osmotic balance. Since there has been a long standing debate concerning the role of AQP0 in the lens, it would be intriguing to investigate the transport properties of lenses obtained from wild type, AQP1 deficient animal, and AQP0 deficient animals. Lenses in culture have been shown to swell in response to a hypotonic stress. After several days the lens adapts and returns to the normal size even in the continued presence of the osmotic stress. It would be very

interesting to compare the rate of swelling and the rate of recovery among lenses obtained from wild type, AQP0, and AQP1 knockout mice. In addition, the ability of these lenses to transport water could be assessed in a trans-lens flux assay. Although this assay does not address the efflux at the equator, it may provide insight into whether the trans-lens flux measured in Fischbarg's studies (27) are mediated by AQP1 and/or AQP0.

In summary, the methods developed and the discoveries made in this study have laid the ground work for future investigation of the structure and function of AQP0 in the normal aging lens and in the cataractous lens. Future studies will provide insight into the (i) role of AQP0 in the developing lens and how mutations in AQP0 result in congenital cataract, (ii) the effect of typical and age-related posttranslational modifications on the function and regulation of AQP0 function in the normal lens, (iii) the involvement of AQP0 in maintaining osmotic balance in the lens, and (iv) the role of AQP0 in preserving lens transparency.

APPENDIX: LABVIEW SOFTWARE

Programs were developed using LabView (Laboratory Virtual Instrument Engineering Workbench) software from National Instruments (Austin, TX). Versions 5.1 of the LabView and IMAC Vision software were used. LabView allows graphical progamming in language G and the following appendix contains two programs. The first program described is entitled Basic Particle Example Lauren 080801 and was utilized for data processing of *Xenopus* oocyte images as discussed in Chapter 4. The second program presented, KS.HL.Seq.vi, was developed to acquire oocyte images at regularly timed intervals.

The first program, an adaptation of the basic particle virtual instrument, expedites the acquisition of pixel count of each oocyte in an image file. The raw data were collected in jpeg files that contained images of 5-8 oocyte silhouettes per file. If images were recorded every five seconds for 60 seconds there would be 13 files per assay. LabView was programmed to extract data from the images and download the pixel count for each oocyte into columns of a spreadsheet. Data from files of subsequent time points were entered into subsequent rows. The software maintained the oocyte position in consecutive images resulting in a column of pixel counts for each oocyte as it increased in area with time. The raw data were then downloaded into an Excel spreadsheet and the relative volume and permeability calculations made automatically according to the equations given in Chapter 4. This program was used extensively and the automated data processing program yielded results that were consistent with those obtained manually by Adobe Photoshop. The results generated were also consistent with permeability values obtained in the literature.

From the front panel of the basic particle program the user can open an image file by pressing "load image file" and threshold the image and get the pixel counts by pressing "process" followed by "stop". The threshold values typically used to define the area of the oocyte were 0 and 127. The oocyte images were visually inspected after the threshold step to ensure that each oocyte was individually represented and background signals did not interfere with the oocyte areas of interest. The data was saved as a .txt file and the file path selected. The data from each image file were sequentially opened using simple text and the table of values were copied and pasted into an Excel spreadsheet.

A program for acquiring and recording images of oocytes, KS.HL.Seq.vi, was also developed. This program while intended for use in this study has not yet been tested for accuracy and reproducibility of results. From the front panel the user can enter the number of images to collect. The program will automatically collect images at a rate of 30 frames per second. To capture one image every 5 seconds enter "149" into the skip table.

For each program the user interface (front panel) to the software, wire diagrams illustrating the connectivity of the virtual instruments (vi) in the program, and a hierarchy scheme of the virtual instruments used are shown.

The program Basic Particle Example Lauren 080801 is shown on pages 205-218.

The front panel is on page 205.

The wire diagram is on pages 206-217.

The hierarchy diagram is on page 218.

The program KS.HL.Seq.vi is shown on pages 219-221.

The front panel is on page 219.

The wire diagram is on page 220.

The hierarchy diagram is on page 221.

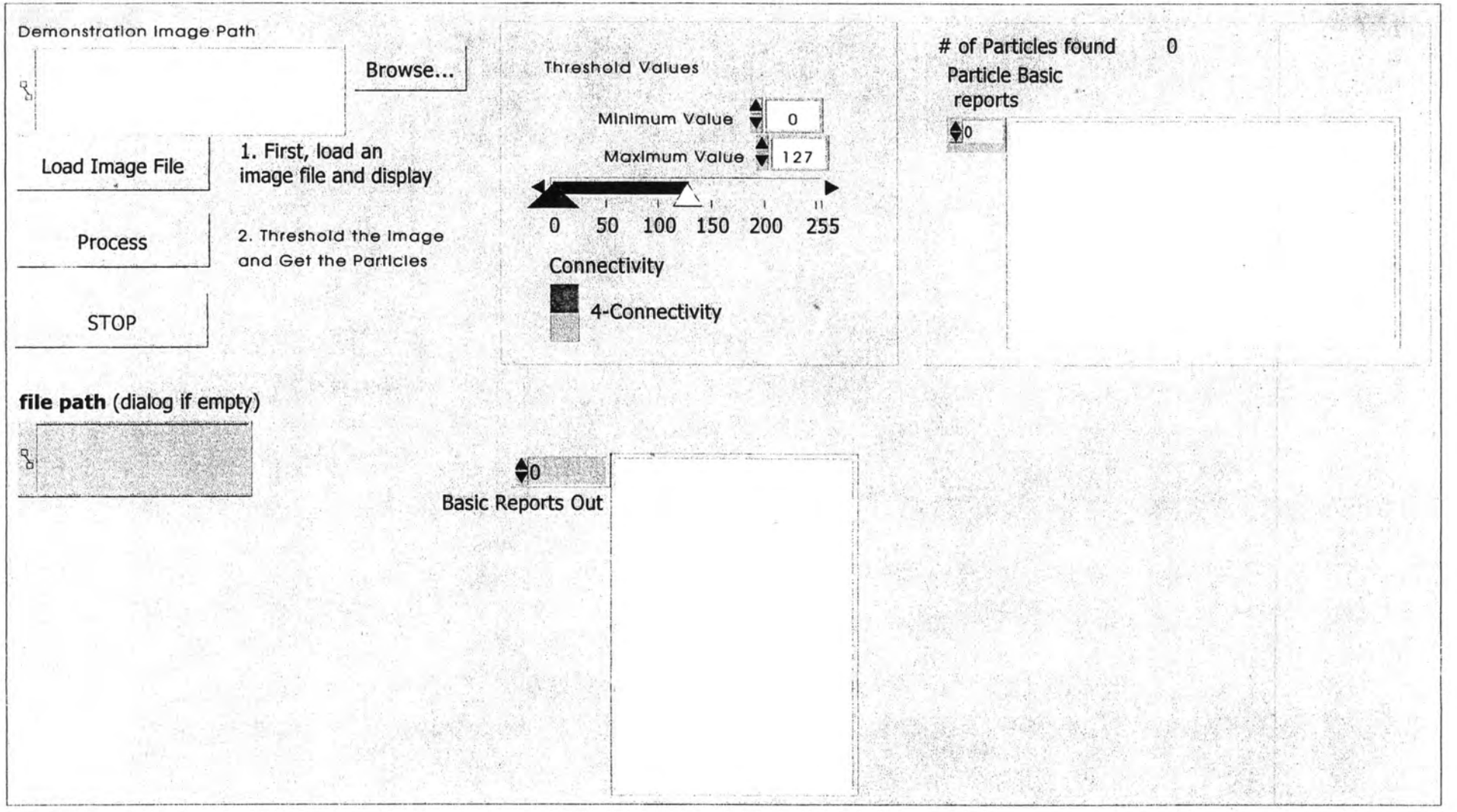
Demonstration Image Path
Browse...
Load Image File
1. First, load an image file and display
Process
2. Threshold the Image and Get the Particles
STOP
Threshold Values
Minimum Value
0
Maximum Value
127
0 50 100 150 200 255
Connectivity
4-Connectivity
# of Particles found
0
Particle Basic reports
0
file path (dialog if empty)
0
Basic Reports Out

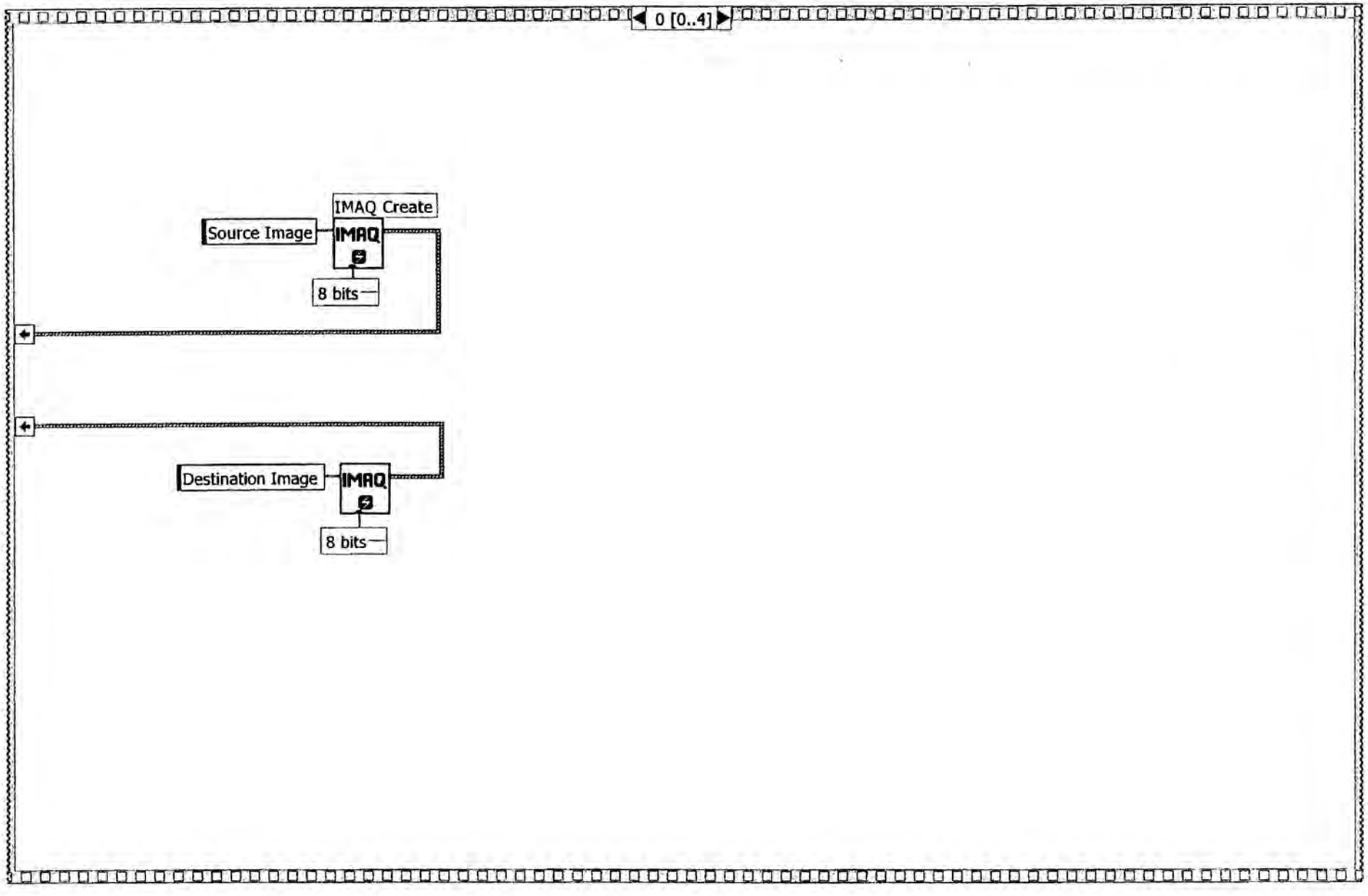
0 [0..4]
IMAQ Create
Source Image
IMAQ
8 bits
Destination Image
IMAQ
8 bits

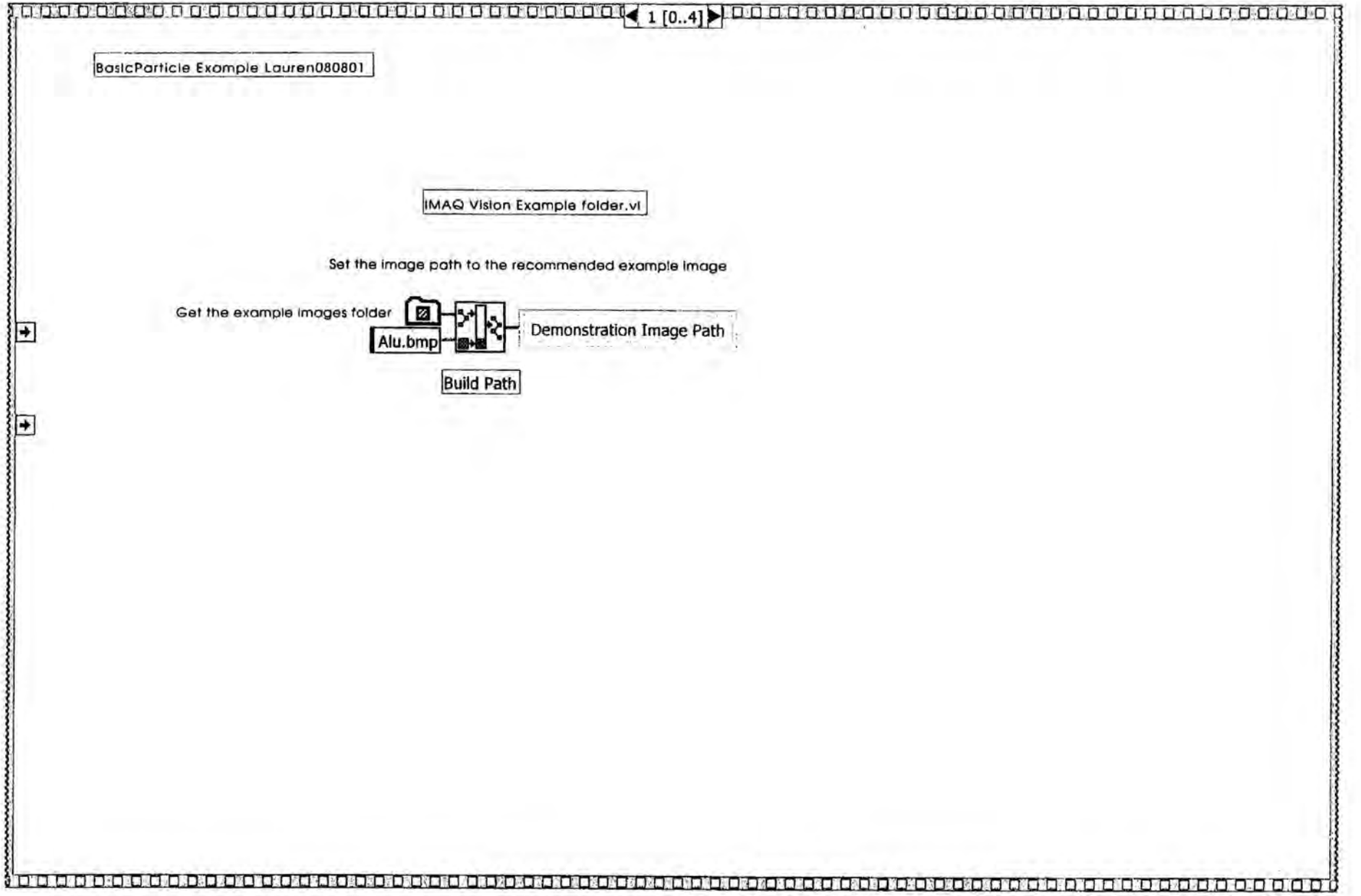
1 [0..4]
BasicParticle Example Lauren080801
IMAQ Vision Example folder.vi
Set the image path to the recommended example image
Get the example images folder
Alu.bmp
Demonstration Image Path
Build Path

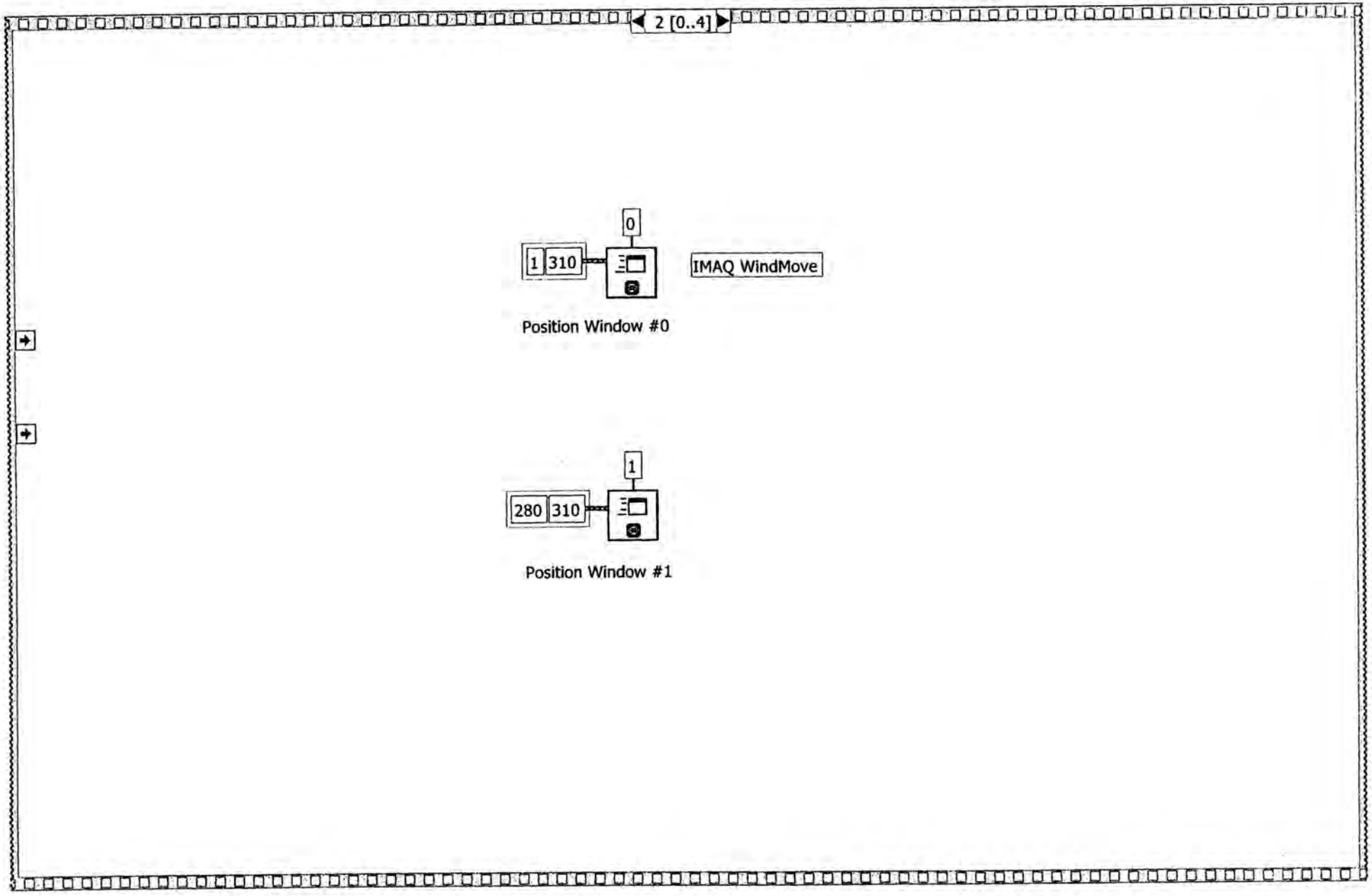
2 [0..4]
0
1
310
IMAQ WindMove
Position Window #0
1
280
310
Position Window #1

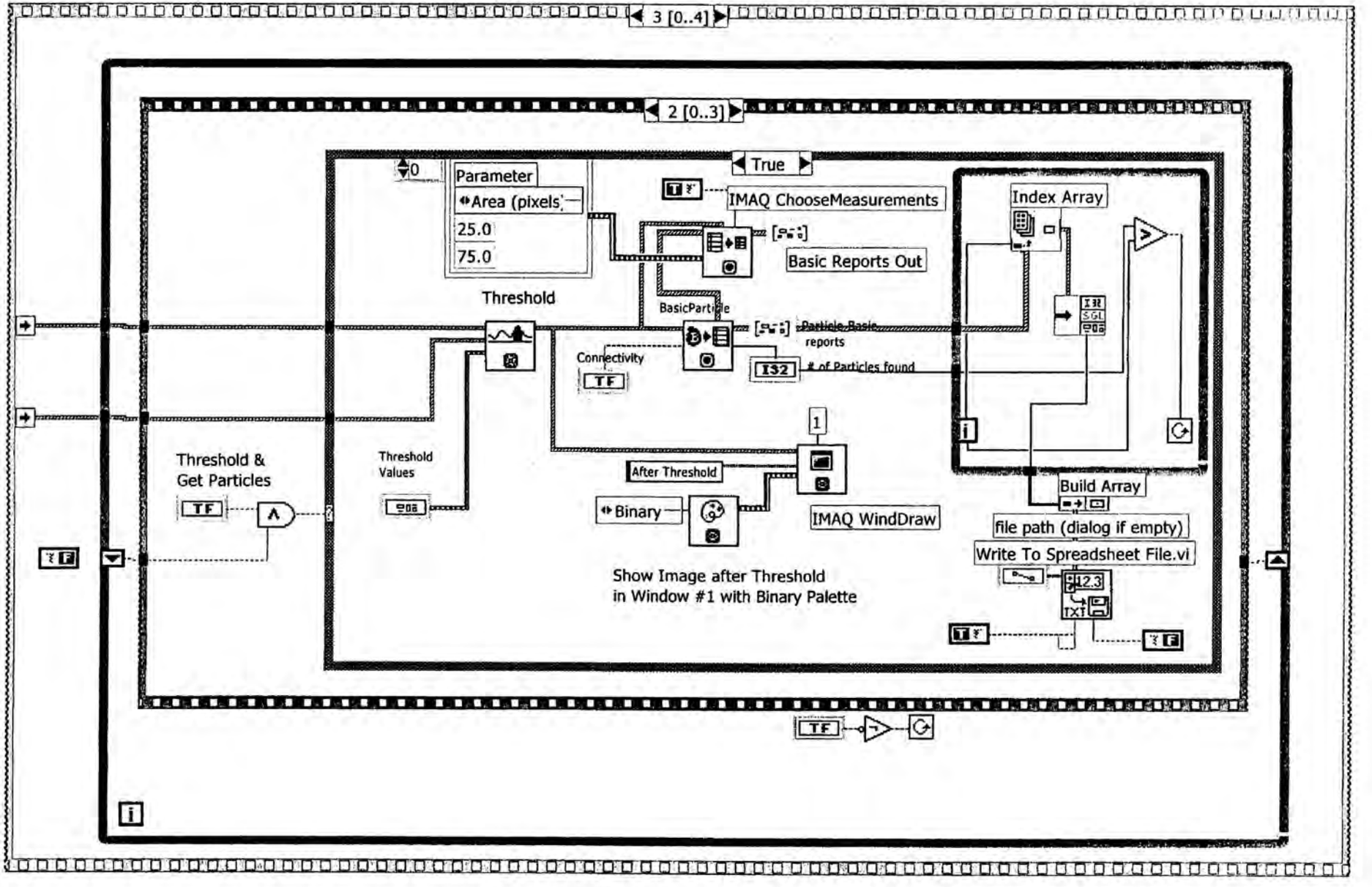
3 [0..4]
2 [0..3]
True
0
Parameter
Area (pixels)
25.0
75.0
Threshold
IMAQ ChooseMeasurements
Basic Reports Out
BasicParticle
Particle Basic reports
Connectivity
TF
I32
# of Particles found
Index Array
Threshold & Get Particles
Threshold Values
After Threshold
1
Binary
IMAQ WindDraw
Build Array
file path (dialog if empty)
Write To Spreadsheet File.vi
Show Image after Threshold in Window #1 with Binary Palette

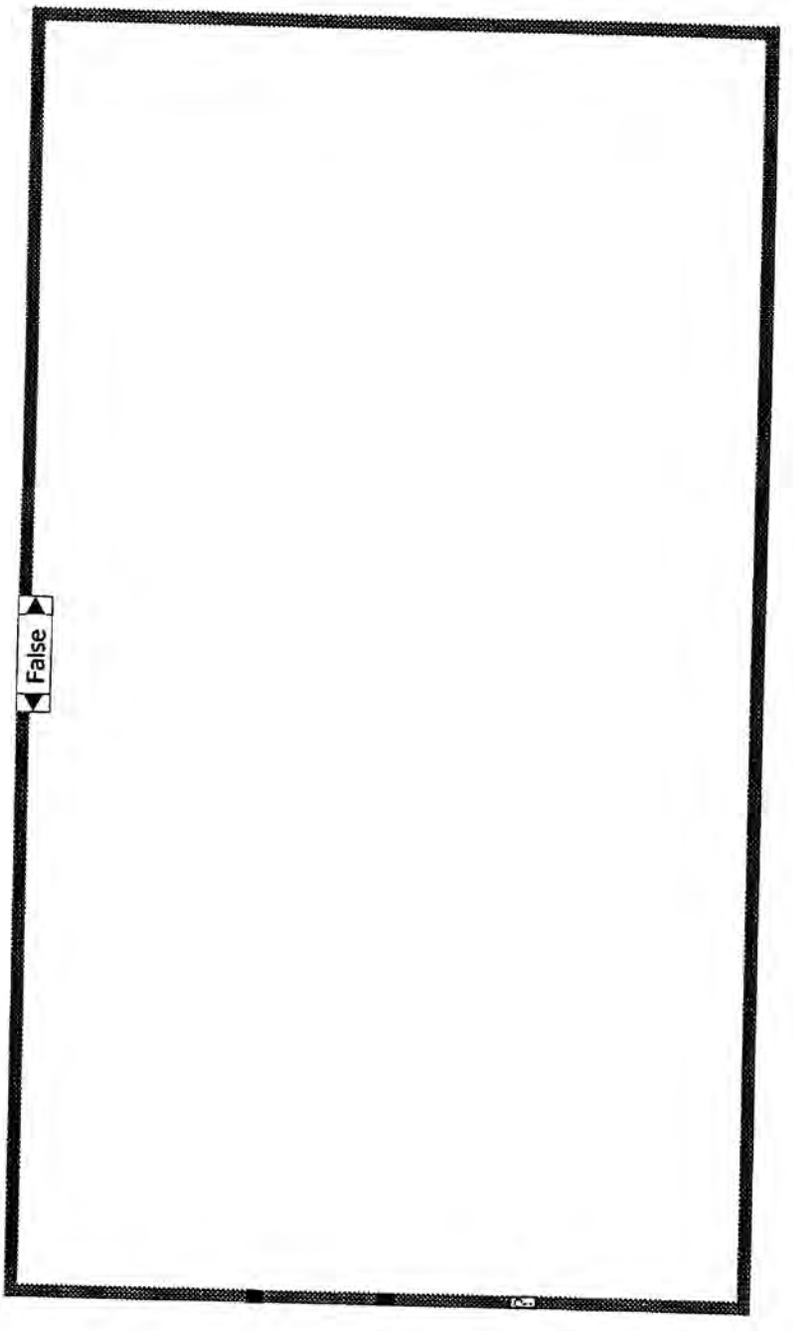
False

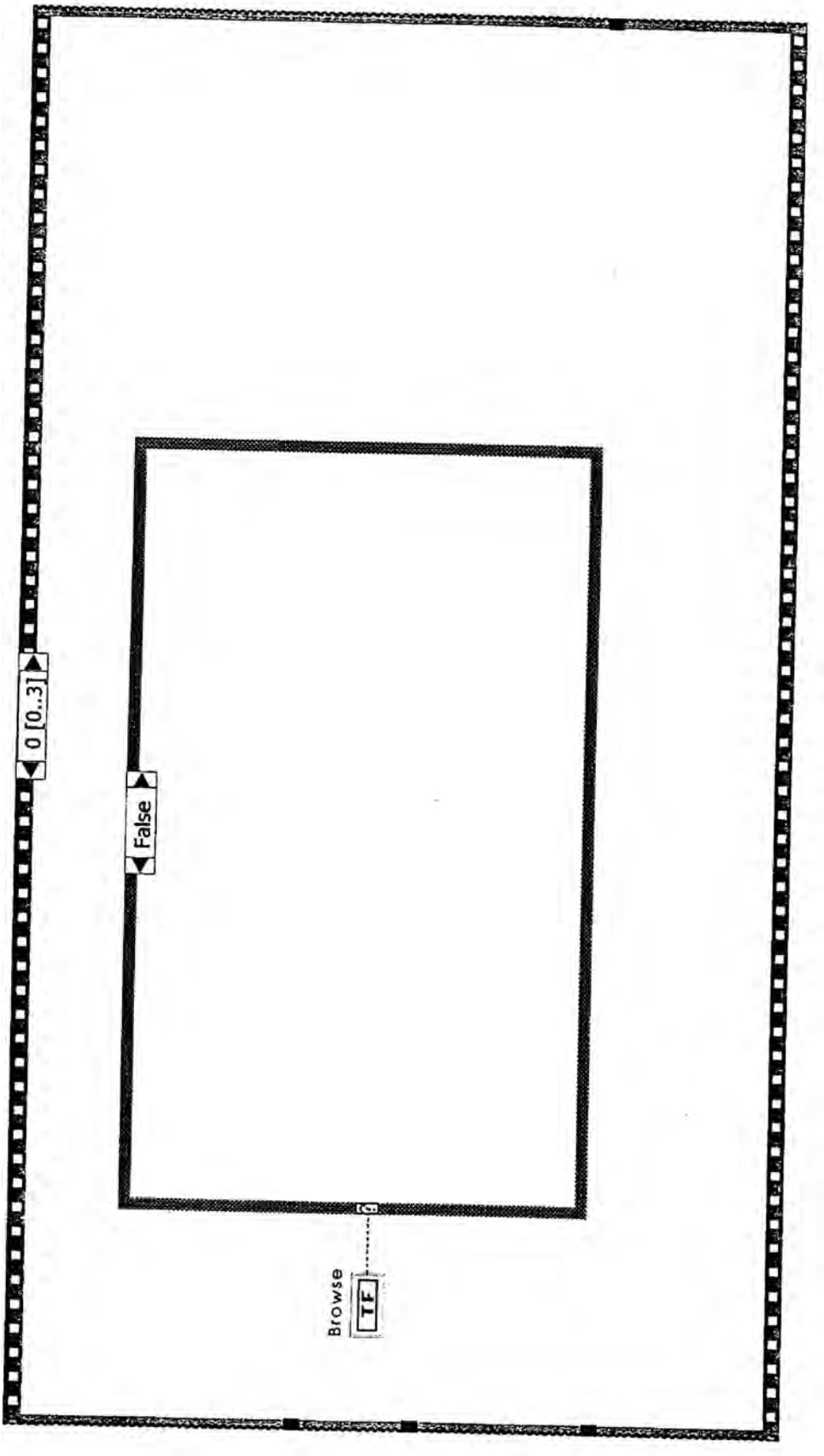
0 [0..3]
False
Browse
TF

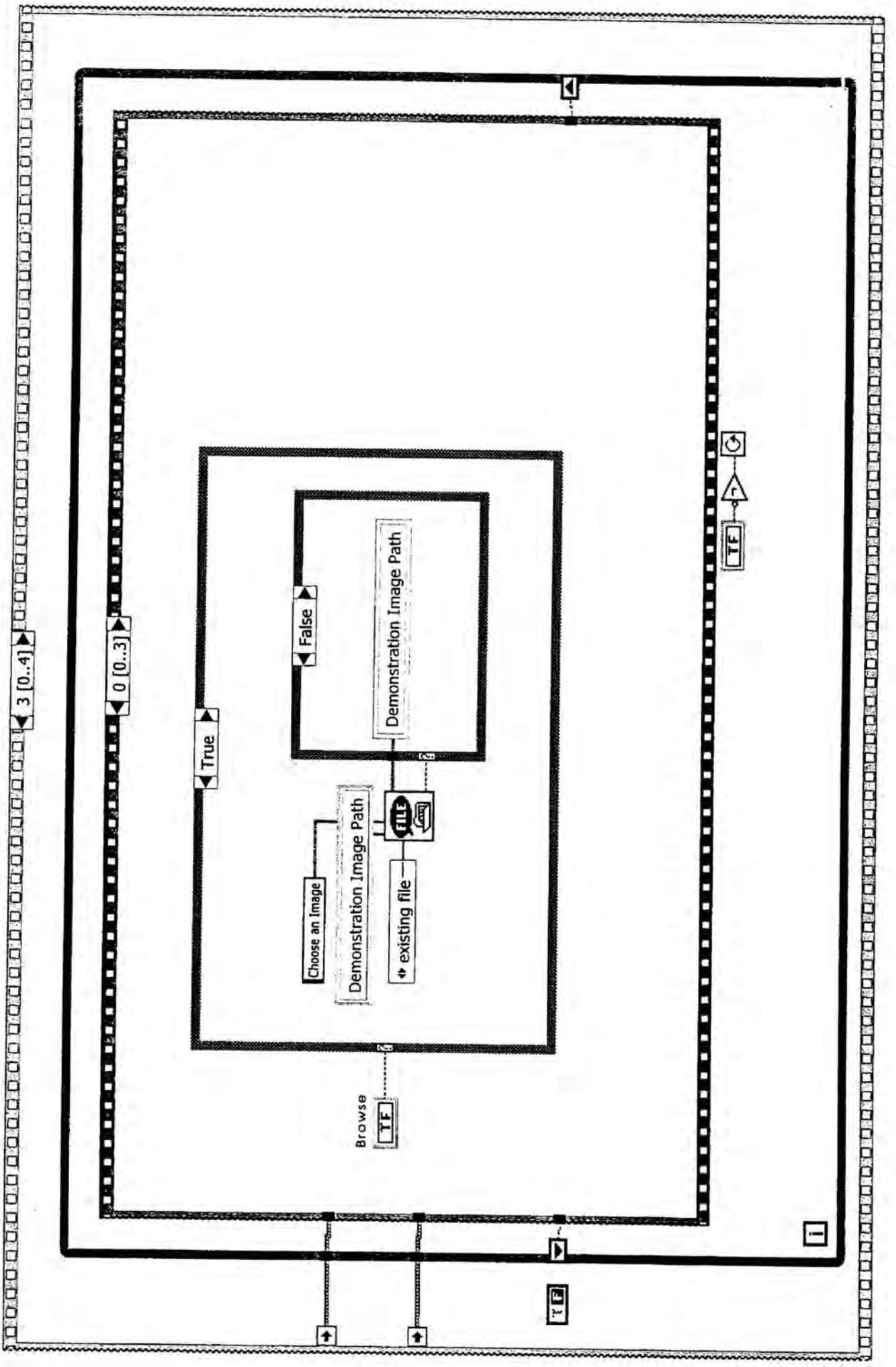
3 [0..4]
0 [0..3]
True
False
Demonstration Image Path
Choose an Image
Demonstration Image Path
existing file
Browse
TF
TF
i

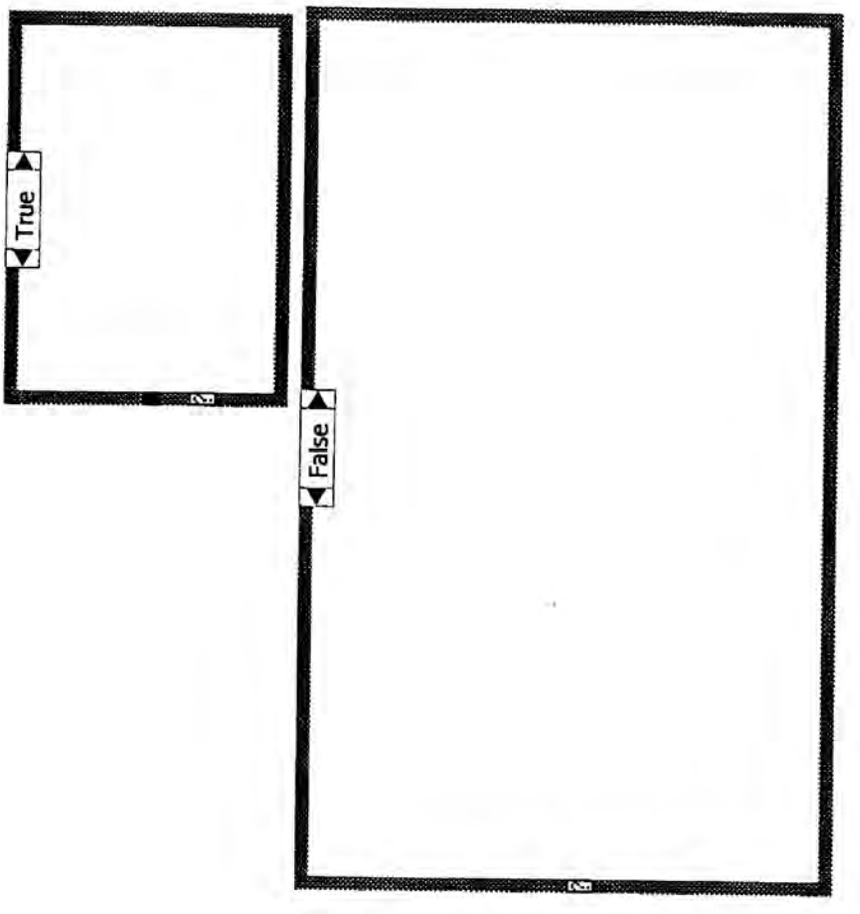
True
False

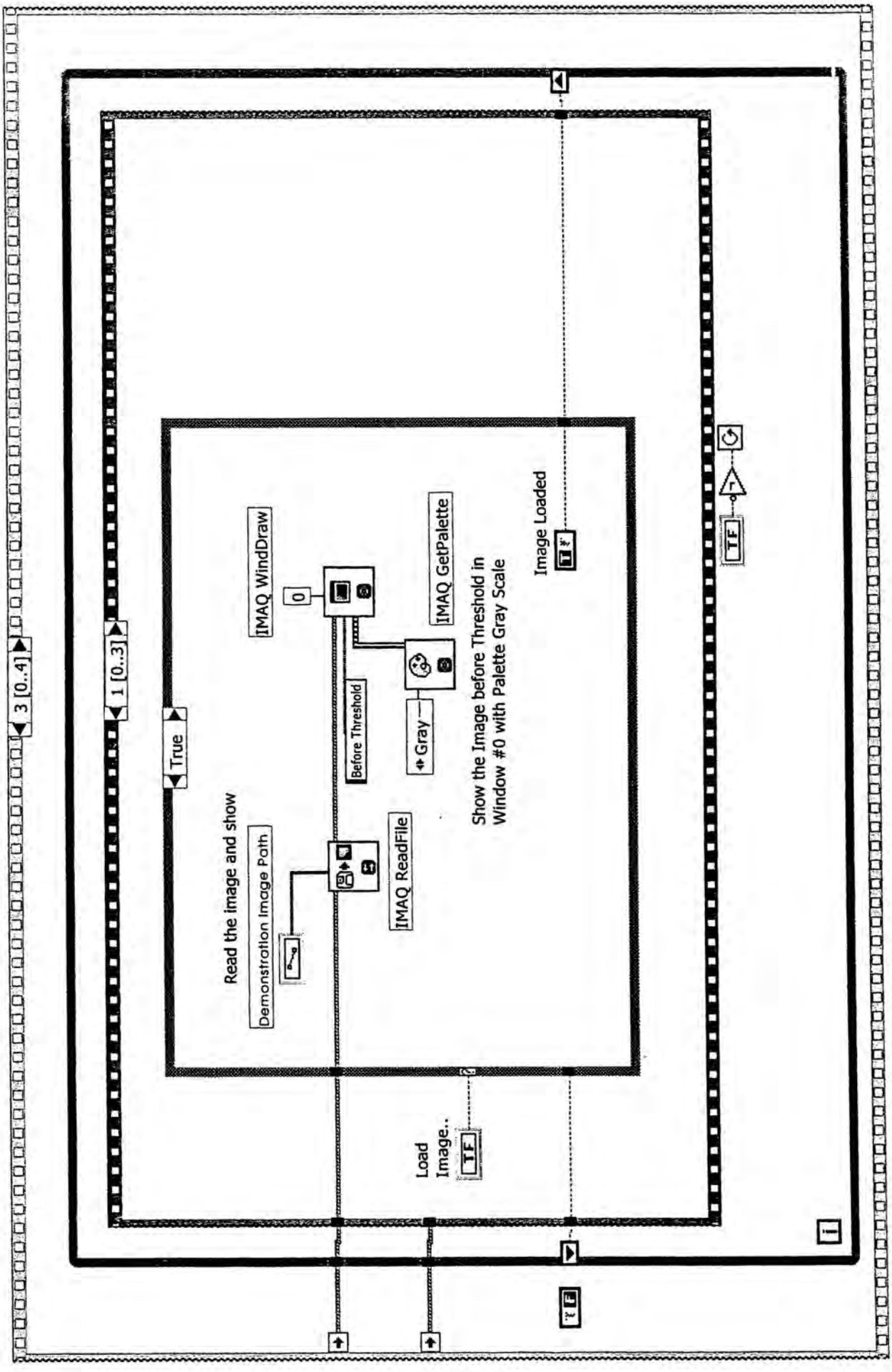
3 [0..4]
1 [0..3]
True
Read the image and show
Demonstration Image Path
IMAQ ReadFile
IMAQ WindDraw
0
Before Threshold
Gray
IMAQ GetPalette
Show the Image before Threshold in
Window #0 with Palette Gray Scale
Image Loaded
Load
Image..
TF
i

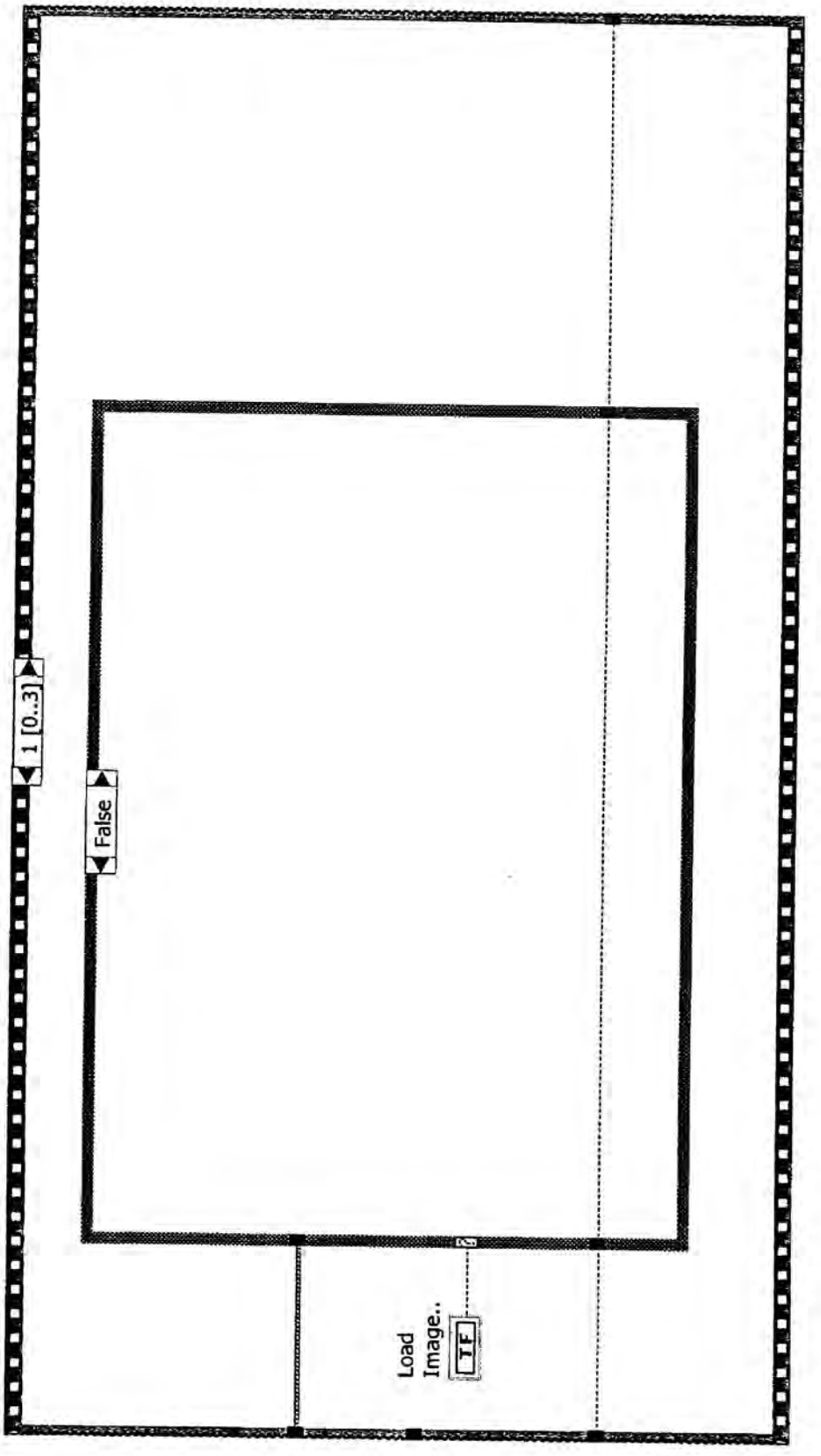
1 [0..3]
False
Load Image..
TF

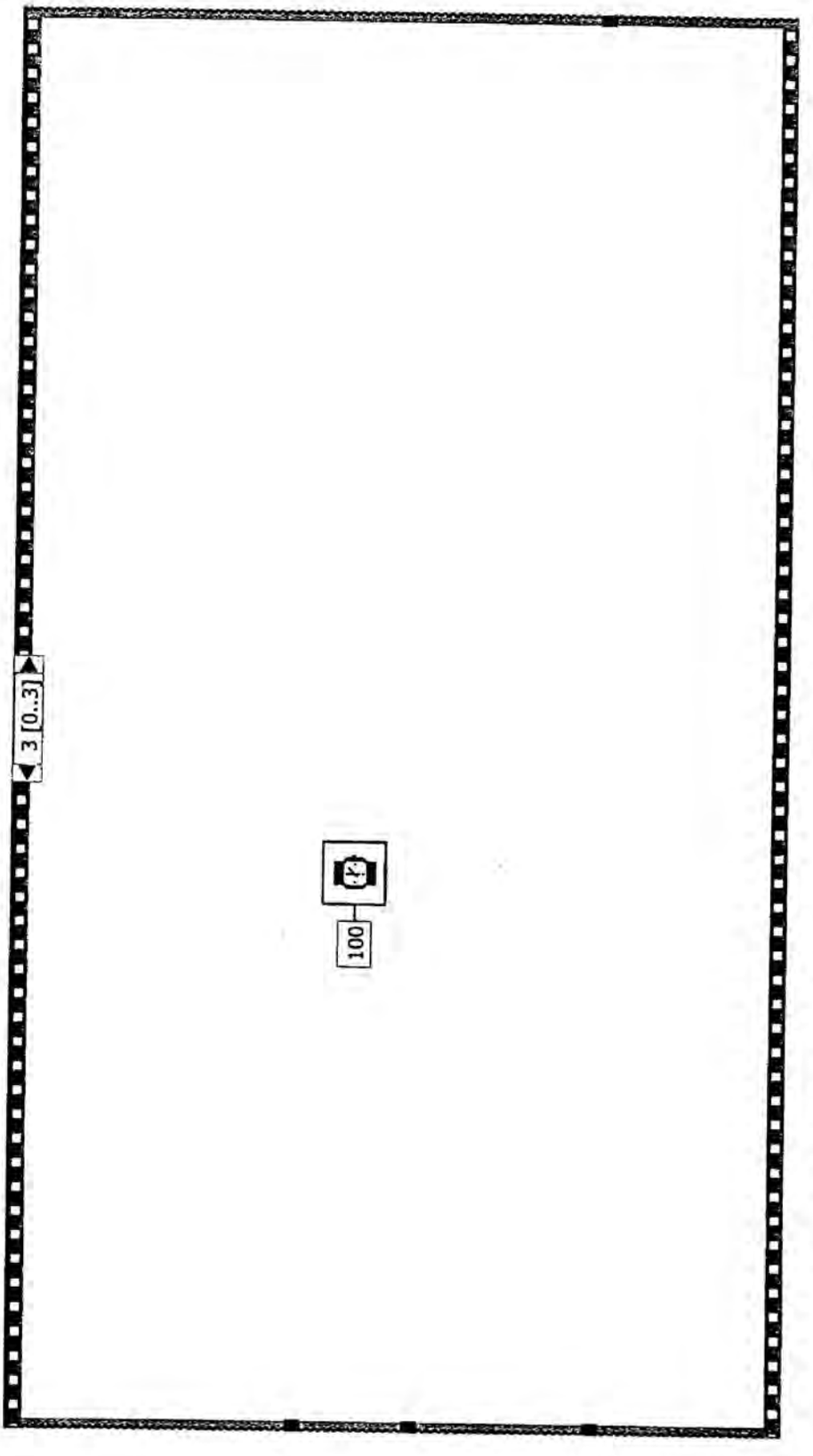
3 [0..3]
100

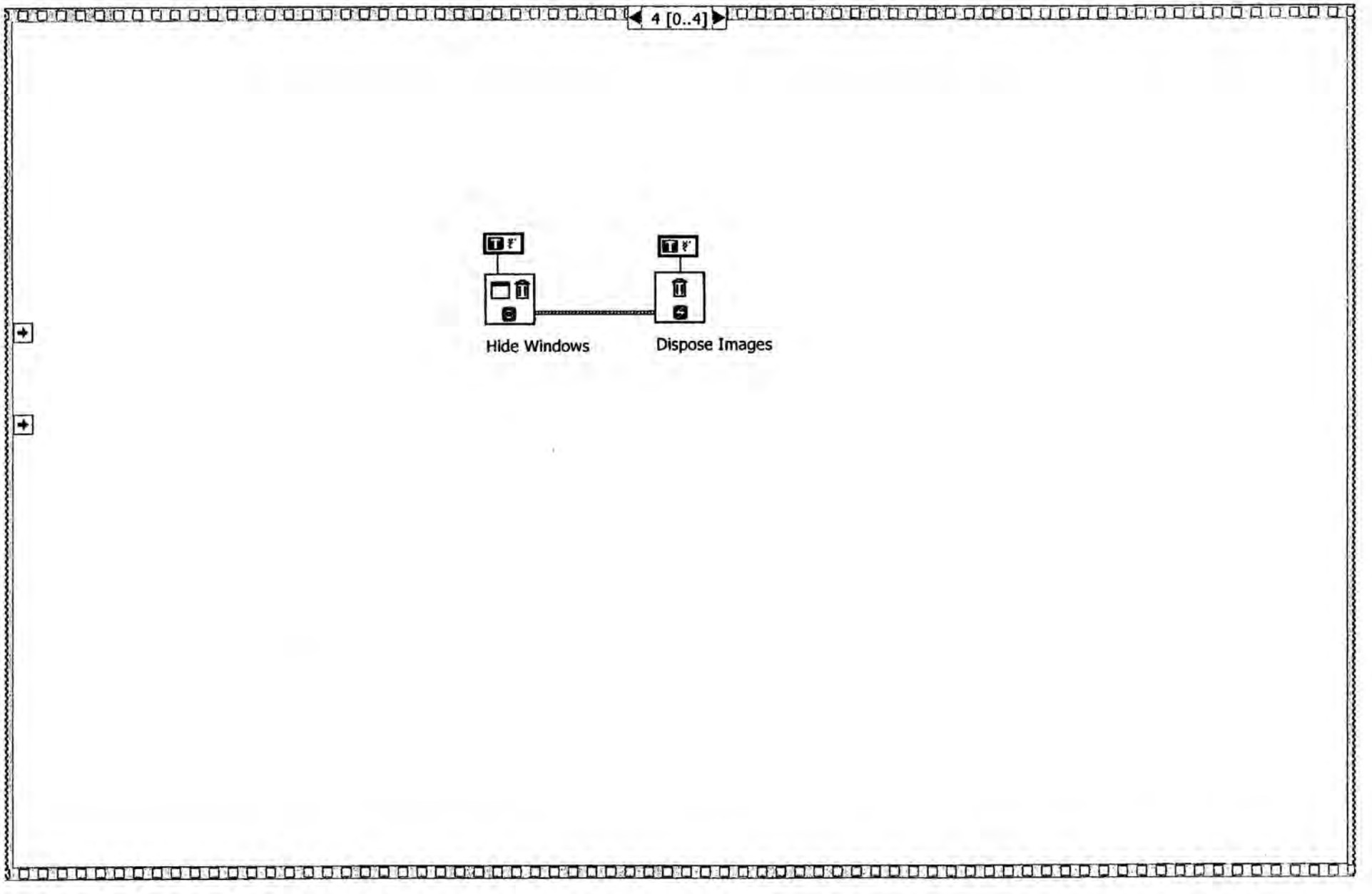
4 [0..4]
Hide Windows
Dispose Images

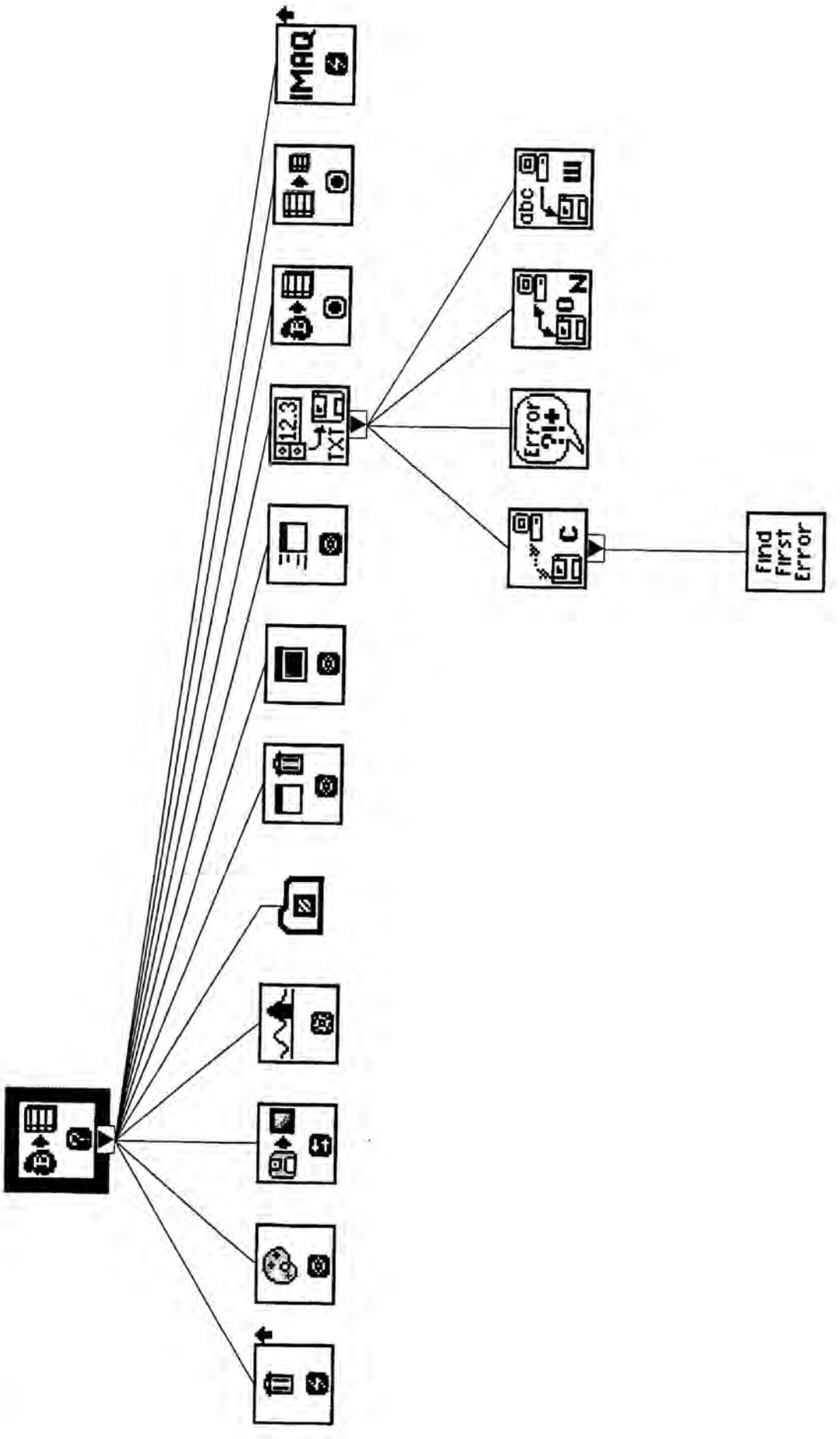
IMAQ
12.3
TXT
abc
Error
?!+
Find
First
Error

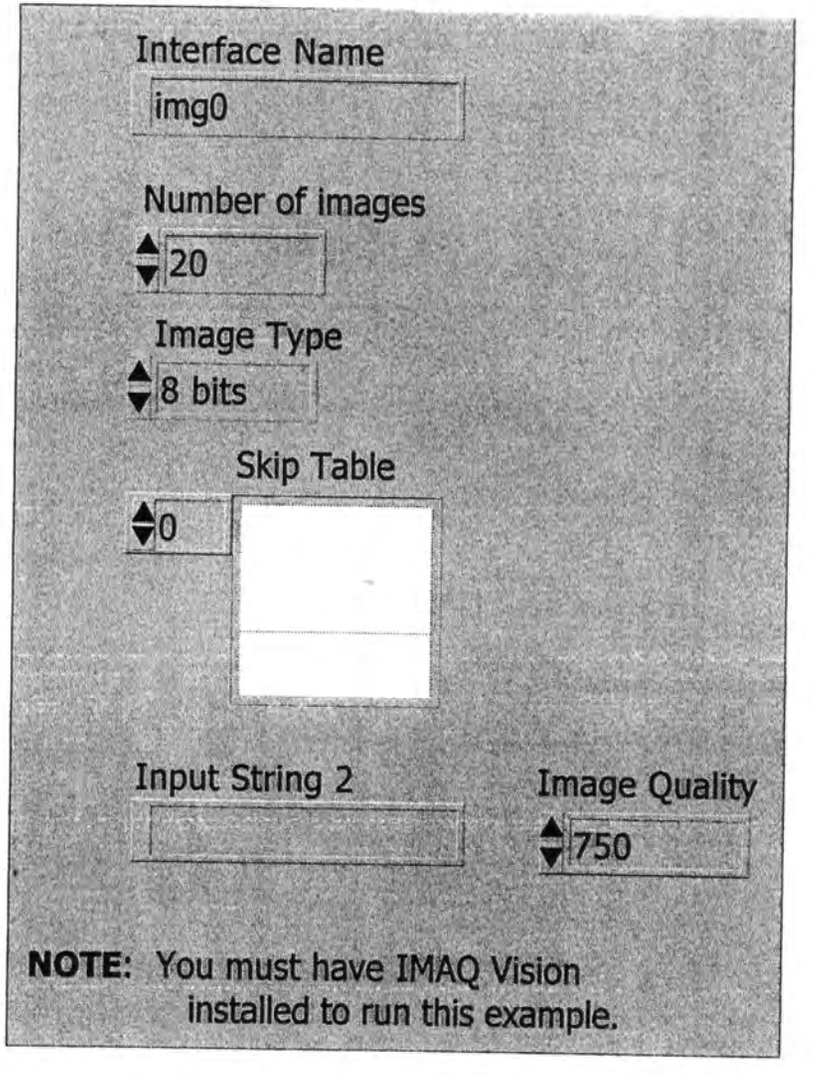
Interface Name
img0
Number of images
20
Image Type
8 bits
Skip Table
0
Input String 2
Image Quality
750
NOTE: You must have IMAQ Vision
installed to run this example.

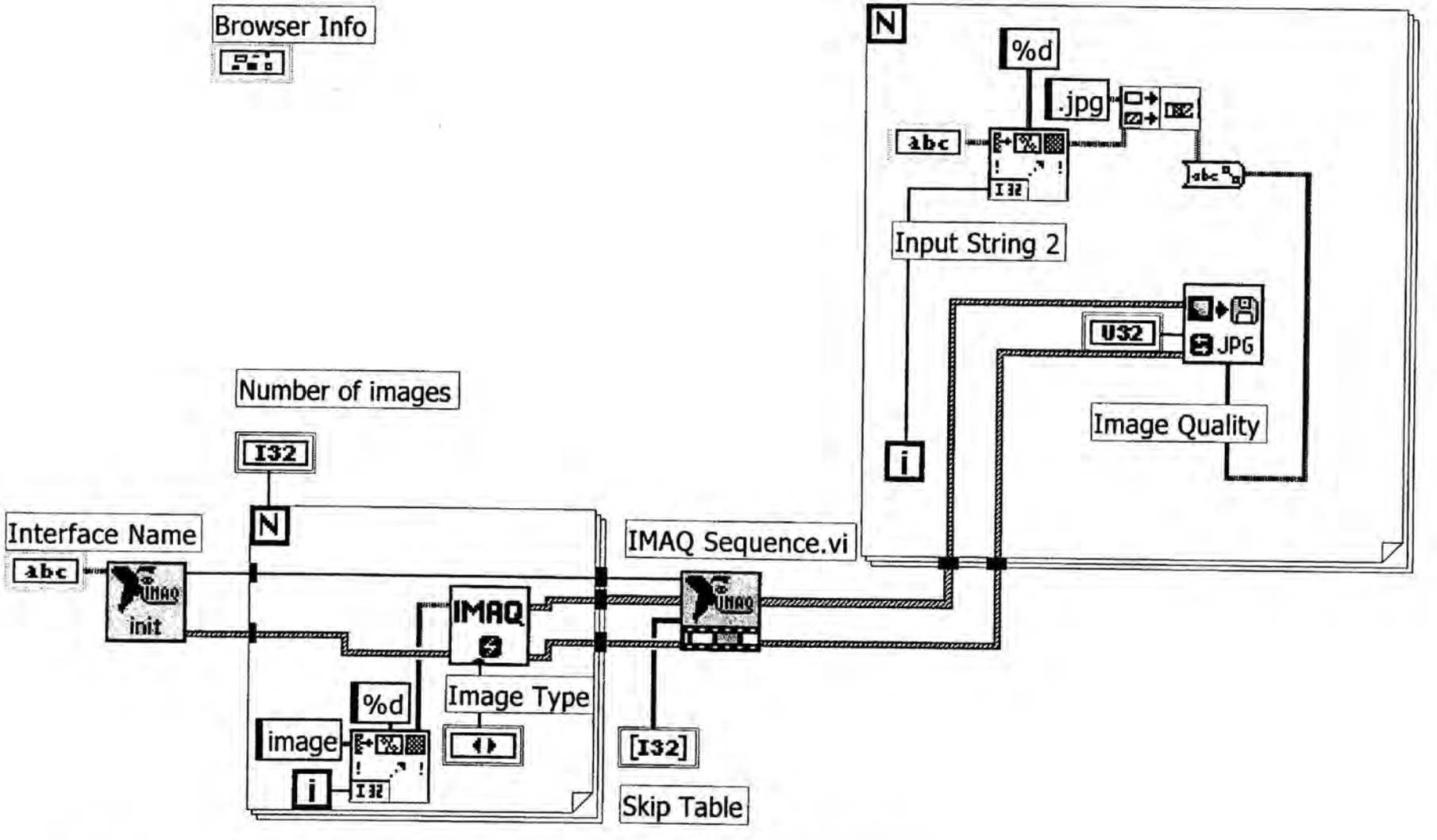

This example acquires 8 bit images. The IMAQ PCI-1424 can acquire from cameras with greater bit depths.
For 10-, 12-, 14- or 16-bit images :
-Modify the image type input in the IMAQ Create.vi to 16 bits
For color images:
-Modify the image type input in the IMAQ Create.vi to RGB Chunky

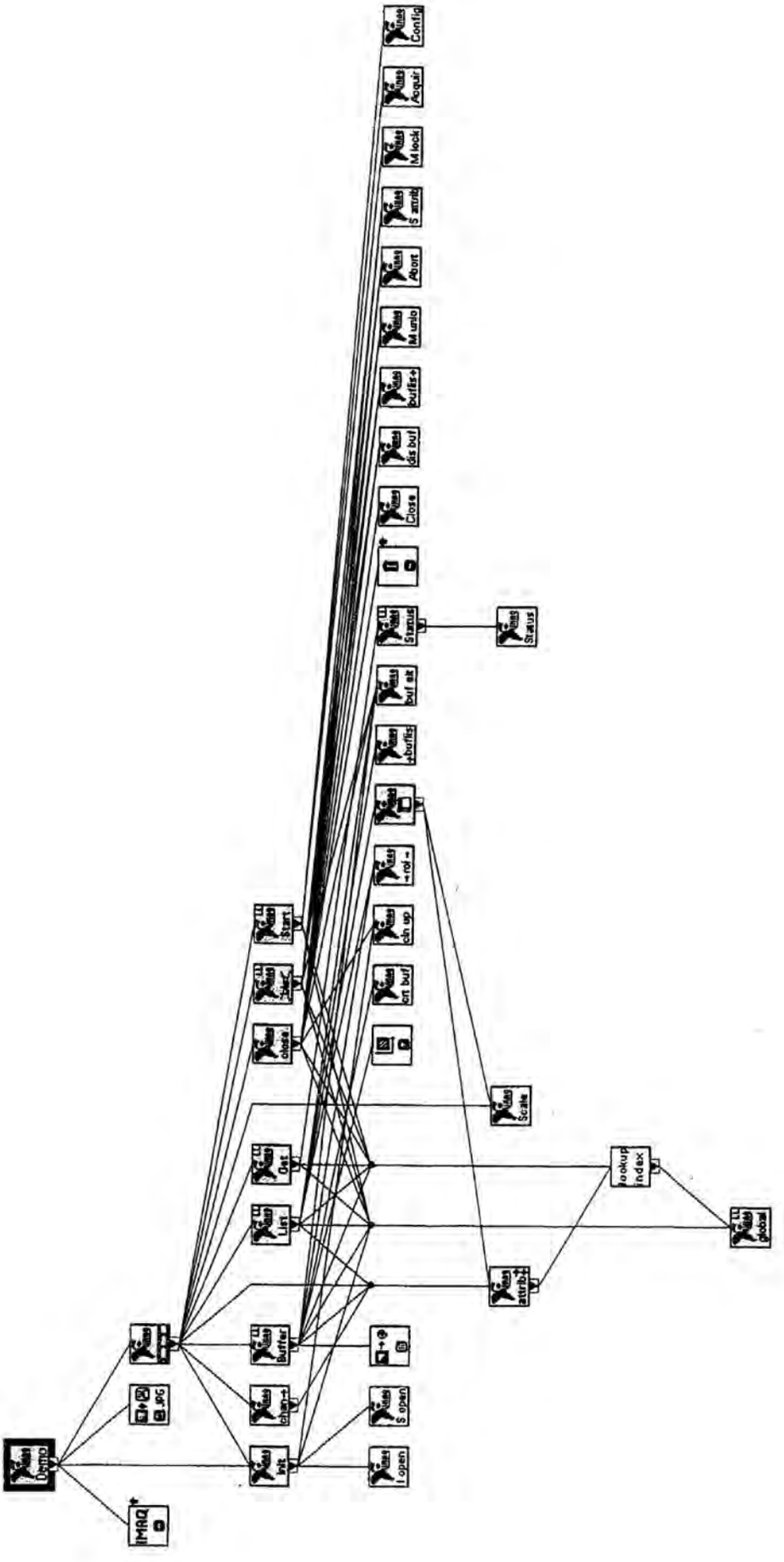
Config
Acquir
Mlock
S annlé
Abort
M unlo
buffs+
ds buf
Close
Status
buf str
+buffs
-rd-
cln up
cn buf
Scale
Start
Get
Lkup
Buffer
chan+
S open
I open
IMAQ
lookup
ndex
global
attrib+

REFERENCES

1. Francis, P., Chung, J. J., Yasui, M., Berry, V., Moore, A., Wyatt, M. K., Wistow, G., Bhattacharya, S. S., and Agre, P., Functional impairment of lens aquaporin in two families with dominantly inherited cataracts, *Hum. Mol. Genet., 9*, 2329-2334 (2000).

2. Shiels, A., and Bassnett, S., Mutations in the founder of the MIP gene family underlie cataract development in the mouse, *Nat. Genet., 12*, 212-5 (1996).

3. Gorin, M. B., Yancey, S. B., Cline, J., Revel, J. P., and Horwitz, J., The major intrinsic protein (MIP) of the bovine lens fiber membrane: characterization and structure based on cDNA cloning, *Cell, 39*, 49-59 (1984).

4. Preston, G. M., Carroll, T. P., Guggino, W. B., and Agre, P., Appearance of water channels in Xenopus oocytes expressing red cell CHIP28 protein, *Science, 256*, 385-7 (1992).

5. Donaldson, P., Kistler, J., and Mathias, R. T., Molecular solutions to mammalian lens transparency, *News Physiol. Sci., 16*, 118-123 (2001).

6. Moffat, B. A., Landman, K. A., Truscott, R. J. W., Sweeney, M. H. J., and Pope, J. M., Age-related changes in the kinetics of water transport in normal human lenses, *Exp. Eye Res., 69*, 663-669 (1999).

7. Varadaraj, K., Kushmerick, C., Baldo, G. J., Bassnett, S., Shiels, A., and Mathias, R. T., The role of MIP in lens fiber cell membrane transport, *J. Membr. Biol., 170*, 191-203 (1999).

8. Schey, K. L., Little, M., Fowler, J. G., and Crouch, R. K., Characterization of human lens major intrinsic protein structure, *Invest. Ophthalmol. Vis. Sci., 41*, 175-82 (2000).

9. Guyton, A., and Hall, J., *Textbook of Medical Physiology*, WB Saunders Company, Philadelphia (1996).

10. Maisel, H., *The Ocular Lens: Structure, Function, and Pathology*, Marcel Dekker, Inc., New York (1985).

11. Berman, E. R., *Biochemistry of the Eye*, Plenum Press, New York (1991).

12. Mathias, R. T., Rae, J. L., and Baldo, G. J., Physiological properties of the normal lens, *Physiol. Rev., 77*, 21-50 (1997).

13. Kuszak, J. R., The Development of Lens Sutures, *Prog. Retin. Eye Res., 14*, 567-591 (1995).

14. Al-Ghoul, K. J., Nordgren, R. K., Kuszak, A. J., Freel, C. D., Costello, M. J., and Kuszak, J. R., Structural evidence of human nuclear fiber compaction as a function of ageing and cataractogenesis, *Exp. Eye Res., 72*, 199-214 (2001).

15. Moffat, B. A., and Pope, J. M., Anisotropic Water Transport in the Human Eye Lens Studied by Diffusion Tensor NMR Micro-imaging, *Exp. Eye Res., 74*, 677-687 (2002).

16. Bassnett, S., and Beebe, D. C., Coincident loss of mitochondria and nuclei during lens fiber cell differentiation., *Dev. Dyn., 194*, 85-93 (1992).

17. Beebe, D. C., Vasiliev, O., Guo, J. L., Shui, Y. B., and Bassnett, S., Changes in adhesion complexes define stages in the differentiation of lens fiber cells, *Invest. Ophthalmol. Vis. Sci., 42*, 727-734 (2001).

18. Wride, M. A., Minireview: Apoptosis as seen through a lens, *Apoptosis, 5*, 203-209 (2000).

19. Wride, M. A., Parker, E., and Sanders, E. J., Members of time bcl-2 and caspase families regulate nuclear degeneration during chick lens fibre differentiation, *Dev. Biol., 213*, 142-156 (1999).

20. Ishizaki, Y., Jacobson, M. D., and Raff, M. C., Role For Caspases in Lens Fiber Differentiation, *J. Cell Biol., 140*, 153-158 (1998).

21. Dahm, R., Lens fibre cell differentiation - A link with apoptosis?, *Ophthalmic Res., 31*, 163-183 (1999).

22. Dahm, R., Gribbon, C., Quinlan, R. A., and Prescott, A. R., Changes in the nucleolar and coiled body compartments precede lamina and chromatin reorganization during fibre cell denucleation in the bovine lens, *Eur. J. Cell Biol., 75*, 237-46 (1998).

23. Koretz, J. F., Cook, C. A., and Kuszak, J. R., The zones of discontinuity in the human lens: Development and distribution with age, *Vis. Res., 34*, 2955-2962 (1994).

24. Garland, D. L., Duglas-Tabor, Y., Jimenez-Asensio, J., Datiles, M. B., and Magno, B., The nucleus of the human lens: demonstration of a highly characteristic protein pattern by two-dimensional electrophoresis and introduction of a new method of lens dissection, *Exp. Eye Res., 62*, 285-91 (1996).

25. Taylor, V. L., Alghoul, K. J., Lane, C. W., Davis, V. A., Kuszak, J. R., and Costello, M. J., Morphology of the Normal Human Lens, *Invest. Ophthalmol. Vis. Sci., 37*, 1396-1410 (1996).

26. Merriman-Smith, R., Donaldson, P., and Kistler, J., Differential expression of facilitative glucose transporters GLUT1 and GLUT3 in the lens, *Invest. Ophthalmol. Vis. Sci., 40*, 3224-3230 (1999).

27. Fischbarg, J., Diecke, F. P., Kuang, K., Yu, B., Kang, F., Iserovich, P., Li, Y., Rosskothen, H., and Koniarek, J. P., Transport of fluid by lens epithelium, *Am. J. Physiol., 276*, C548-57 (1999).

28. Goodenough, D. A., The crystalline lens. A system networked by gap junctional intercellular communication, *Semin. Cell Biol., 3*, 49-58 (1992).

29. Bassnett, S., Kuszak, J. R., Reinisch, L., Brown, H. G., and Beebe, D. C., Intercellular communication between epithelial and fiber cells of the eye lens, *J. Cell Sci., 107*, 799-811 (1994).

30. Kinsey, V., and Reddy, D., Studies of the crystalline lens. IX. The relative role of the epithelium and capsule in transport., *Invest. Ophthalmol. Vis. Sci., 4*, 104-116 (1965).

31. Robinson, K., and JW, P., Localization of steady currents in the lens, *Curr. Eye. Res., 2*, 843-847 (1983).

32. Zampighi, G. A., Eskandari, S., and Kreman, M., Epithelial organization of the mammalian lens, *Exp. Eye Res., 71*, 415-435 (2000).

33. Young, M. A., Tunstall, M. J., Kistler, J., and Donaldson, P. J., Blocking chloride channels in the rat lens: Localized changes in tissue hydration support the existence of a circulating chloride flux, *Invest. Ophthalmol. Vis. Sci., 41*, 3049-3055 (2000).

34. Paterson, C., Extracellular space of the cystalline lens, *Am. J. Physiol., 218*, 797-802 (1970).

35. Lahm, D., Lee, L., and Bettleheim, F., Age dependence of freezable and non-freezable water content of normal human lenses, *Invest. Ophthalmol. Vis. Sci., 26*, 1162-5 (1985).

36. Siebinga, I., Vrensen, F. J. M., De Mul, F. M., and Greve, J., Age-related changes in local water and protein content of human eye lenses measured by Raman microspectroscopy., *Exp. Eye. Res., 53*, 233-239 (1991).

37. Sweeney, M. H. J., and Truscott, R. J. W., An impediment to glutathione diffusion in older normal human lenses: a possible precondition for nuclear cataract, *Exp. Eye Res., 67*, 587-595 (1998).

38. Cheng, H. M., Water diffusion in the rabbit lens in vivo, *Progress In Lens And Cataract Research : In Honor Of Professor Kazuyuki Sasaki, 35*, 169-175 (2002).

39. Truscott, R. J. W., Age-related nuclear cataract: A lens transport problem, *Ophthalmic Res., 32*, 185-194 (2000).

40. Yang, B. X., and Verkman, A. S., Water and Glycerol Permeabilities of Aquaporins 1-5 and Mip Determined Quantitatively By Expression of Epitope-Tagged Constructs in Xenopus Oocytes, *J. Biol. Chem., 272*, 16140-16146 (1997).

41. Thiagarajah, J. R., and Verkman, A. S., Aquaporin deletion in mice reduces corneal water permeability and delays restoration of transparency after swelling, *J. Biol. Chem., 277*, 19139-44 (2002).

42. Alcala, L., Lieska, N., and Maisel, H., Protein component of the bovine lens cortical fiber cell membranes, *Exp. Eye Res., 21*, 581-95 (1975).

43. Gao, J., Sun, X., Yatsula, V., Wymore, R. S., and Mathias, R. T., Isoform-specific function and distribution of Na/K pumps in the frog lens epithelium, *J. Membr. Biol., 178*, 89-101 (2000).

44. Jacobs, M., Soeller, M., Cannell, M., and Donaldson, P., Quantifying changes in gap junction structure as a function of lens fiber cell differentiation, *Cell Commun. Adhes., 8*, 349-353 (2001).

45. Tunstall, M. J., Eckert, R., Donaldson, P., and Kistler, J., Localised fibre cell swelling characteristic of diabetic cataract can be induced in normal rat lens using the chloride channel blocker 5-nitro-2-(3-phenylpropylamino) benzoic acid, *Ophthalmic Res., 31*, 317-320 (1999).

46. Francis, P. J., Berry, V., Bhattacharya, S. S., and Moore, A. T., The genetics of childhood cataract, *J. Med. Genet., 37*, 481-8 (2000).

47. Francis, P. J., Berry, V., Moore, A. T., and Bhattacharya, S., Lens biology: development and human cataractogenesis, *Trends Genet., 15*, 191-6 (1999).

48. Berry, V., Francis, P., Kaushal, S., Moore, A. T., and Bhattacharya, S., MIP (AQP0) mutations in humans:associated with a novel locus for autosomal dominant congenital cataract, *ARVO, #507* (2000).

49. Borchman, D., Byrdwell, W. C., and Yappert, M. C., Regional and age-dependent differences in the phospholipid composition of human lens membranes, *Invest. Ophthalmol. Vis. Sci., 35*, 3938-42 (1994).

50. Zelenka, P. S., Lens lipids, *Curr. Eye Res., 3*, 1337-59 (1984).

51. Ferguson, S. R., Borchman, D., and Yappert, M. C., Confirmation of the identity of the major phospholipid in human lens membranes, *Invest. Ophthalmol. Vis. Sci., 37*, 1703-6 (1996).

52. Borchman, D., Byrdwell, W. C., and Yappert, M. C., Thermodynamic phase transition parameters of human lens dihydrosphingomyelin, *Ophthalmic Res., 28*, 81-5 (1996).

53. Finkelstein, A., *Water movement through lipid bilayers, pores, and plasma membranes*, Vol. 4, John Wiley & Sons, Bronx (1987).

54. Fettiplace, R., and Haydon, D. A., Water permeability of lipid membranes, *Physiol. Rev., 60*, 510-50 (1980).

55. Shang, F., Gong, X., McAvoy, J. W., Chamberlain, C., Nowell, T. R., and Taylor, A., Ubiquitin-dependent pathway is up-regulated in differentiating lens cells, *Exp. Eye Res., 68*, 179-192 (1999).

56. Hanson, S. R., Hasan, A., Smith, D. L., and Smith, J. B., The major in vivo modifications of the human water-insoluble lens crystallins are disulfide bonds, deamidation, methionine oxidation and backbone cleavage, *Exp. Eye Res., 71*, 195-207 (2000).

57. Takemoto, L., and Takehana, M., Major intrinsic polypeptide (MIP26K) from human lens membrane: characterization of low-molecular-weight forms in the aging human lens, *Exp. Eye Res., 43*, 661-7 (1986).

58. Lee, A., Morrow, J. S., and Fowler, V. M., Caspase remodeling of the spectrin membrane skeleton during lens development and aging, *J. Biol. Chem., 276*, 20735-20742 (2001).

59. Lin, J. S., Eckert, R., Kistler, J., and Donaldson, P., Spatial Differences in Gap Junction Gating in the Lens Are a Consequence of Connexin Cleavage, *Eur. J. Cell Biol., 76*, 246-250 (1998).

60. Takemoto, L., Release of α–A sequence 158-173 correlates with a decrease in the molecular chaperone properties of native α–crystallin, *Exp. Eye Res., 59*, 239-242 (1994).

61. Sharma, K. K., Elser, N. J., and Kester, K., Comparison of leucine aminopeptidase and aminopeptidase III activities in lens, *Curr. Eye Res., 15*, 774-81 (1996).

62. Kilby, G. W., Carver, J. A., Zhu, J. L., Sheil, M. M., and Truscott, R. J., Loss of the C-terminal serine residue from bovine beta B2-crystallin, *Exp. Eye Res., 60*, 465-9 (1995).

63. Harding, J., and Crabbe, M., *The lens: Development, protiens, metabolism and cataract.*, Vol. 1b, Academic Press, Orlando (1984).

64. Srivastava, O. P., and Ortwerth, B. J., Isolation and characterization of a 25K serine proteinase from bovine lens cortex, *Exp. Eye Res., 37*, 597-612 (1983).

65. Srivastava, O. P., and Srivastava, K., Human lens membrane proteinase: purification and age-related distributional changes in the water-soluble and insoluble protein fractions, *Exp. Eye Res., 48*, 161-75 (1989).

66. Srivastava, O. P., Characterization of a highly purified membrane proteinase from bovine lens, *Exp. Eye Res., 46*, 269-83 (1988).

67. Lin, J. S., Fitzgerald, S., Dong, Y. M., Knight, C., Donaldson, P., and Kistler, J., Processing of the Gap Junction Protein Connexin50 in the Ocular Lens Is Accomplished By Calpain, *Eur. J. Cell Biol., 73*, 141-149 (1997).

68. Ma, H., Fukiage, C., Kim, Y. H., Duncan, M. K., Reed, N. A., Shih, M., Azuma, M., and Shearer, T. R., Characterization and expression of calpain 10 - A novel ubiquitous calpain with nuclear localization, *J. Biol. Chem., 276*, 28525-28531 (2001).

69. Huang, Y., and Wang, K. K., The calpain family and human disease, *Trends Mol. Med., 7*, 355-62 (2001).

70. David, L. L., Varnum, M. D., Lampi, K. J., and Shearer, T. R., Calpain II in human lens, *Invest. Ophthalmol. Vis. Sci., 30*, 269-75 (1989).

71. Schey, K. L., Fowler, J. G., Shearer, T. R., and David, L., Modifications to rat lens major intrinsic protein in selenite-induced cataract, *Invest. Ophthalmol. Vis. Sci., 40*, 657-67 (1999).

72. Ueda, Y., Fukiage, C., Shih, M., Shearer, T., and David, L., Mass measurements of C-terminally truncated alpha-crystallin from two-dimensional gels identify Lp82 as a major endopeptidase in rat lens, *Mol. Cell. Proteomics, 1*, 357-365 (2002).

73. Earnshaw, W. C., Martins, L. M., and Kaufmann, S. H., Mammalian caspases: Structure, activation, substrates, and functions during apoptosis, *Annu. Rev. Biochem., 68*, 383-424 (1999).

74. Geiger, T., and Clarke, S., Deamidation, isomerization, and racemization at Asparginyl and Aspartyl residues in peptides, *J. Biol. Chem., 262*, 785-794 (1987).

75. Robinson, N. E., and Robinson, A. B., Molecular clocks, *Proc. Natl. Acad. Sci. USA., 98*, 944-949 (2001).

76. Wright, H. T., Nonenzymatic deamidation of asparaginyl and glutaminyl residues in proteins, *Crit. Rev. Biochem. Mol. Biol., 26*, 1-52 (1991).

77. Ritz-Timme, S., and Collins, M. J., Racemization of aspartic acid in human proteins, *Ageing Res. Rev., 1*, 43-59 (2002).

78. Masters, P., Bada, J., and Zigler, J., Aspartic acid racemization in the human lens during aging and in cataract formation, *Nature, 268*, 71-73 (1977).

79. Fujii, N., Matsumoto, S., Hiroki, K., and Takemoto, L., Inversion and isomerization of Asp-58 residue in human alpha A-crystallin from normal aged lenses and cataractous lenses, *Biochem. Biophys. Acta, 2*, 179-187 (2001).

80. Fujii, N., Takemoto, L. J., Momose, Y., Matsumoto, S., Hiroki, K., and Akaboshi, M., Formation of four isomers at the Asp-151 residue of aged human alpha A-crystallin by natural aging, *Biochem. Biophys. Res. Comm., 265*, 746-751 (1999).

81. Brennan, T. V., Anderson, J. W., Jia, Z., Waygood, E. B., and Clarke, S., Repair of spontaneously deamidated HPr phosphocarrier protein catalyzed by the L-isoaspartate-(D-aspartate) O-methyltransferase, *J. Biol. Chem., 269*, 24586-95 (1994).

82. Benedek, G. B., Cataract as a protein condensation disease: the Proctor Lecture, *Invest. Ophthalmol. Vis. Sci., 38*, 1911-21 (1997).

83. Kaneko, I., Morimoto, K., and Kubo, T., Drastic neuronal loss in vivo by beta-amyloid racemized at Ser(26) residue: conversion of non-toxic [D-Ser(26)]beta-amyloid 1-40 to toxic and proteinase-resistant fragments, *Neuroscience, 104*, 1003-11 (2001).

84. Takemoto, L., and Boyle, D., Increased deamidation of asparagine during human senile cataractogenesis, *Mol. Vis., 6*, 164-8 (2000).

85. Lapko, V. N., Purkiss, A. G., Smith, D. L., and Smith, J. B., Deamidation in human gamma S-crystallin from cataractous lenses is influenced by surface exposure, *Biochemistry, 41*, 8638-48 (2002).

86. Voorter, C., de Haard-Hoekman, W., van den Oetelaar, P., Bloemendal, H., and de Jong, W., Spontaneous peptide bond cleavage in aging alpha crystallin through a succinimide intermediate, *J. Biol. Chem., 263*, 19020-19023 (1988).

87. Robinson, N. E., Robinson, A. B., and Merrifield, R. B., Mass spectrometric evaluation of synthetic peptides as primary structure models for peptide and protein deamidation, *J. Pept. Res., 57*, 483-493 (2001).

88. Knapp, D. R., Chemical derivatization for mass spectrometry, *Methods Enzymol., 193*, 314-29 (1990).

89. Johnson, B. A., Murray, E. D., Jr., Clarke, S., Glass, D. B., and Aswad, D. W., Protein carboxyl methyltransferase facilitates conversion of atypical L-isoaspartyl peptides to normal L-aspartyl peptides, *J. Biol. Chem., 262*, 5622-9 (1987).

90. Lehmann, W. D., Schlosser, A., Erben, G., Pipkorn, R., Bossemeyer, D., and Kinzel, V., Analysis of isoaspartate in peptides by electrospray tandem mass spectrometry, *Protein Sci., 9*, 2260-2268 (2000).

91. Gonzalez, L. J., Shimizu, T., Satomi, Y., Betancourt, L., Besada, V., Padron, G., Orlando, R., Shirasawa, T., Shimonishi, Y., and Takao, T., Differentiating alpha- and beta-aspartic acids by electrospray ionization and low-energy tandem mass spectrometry, *Rapid Commun. Mass Spectrom., 14*, 2092-102 (2000).

92. Fujii, N., Takemoto, L. J., Matsumoto, S., Hiroki, K., Boyle, D., and Akaboshi, M., Comparison of D-aspartic acid contents in alpha A-crystallin from normal and age-matched cataractous human lenses, *Biochem. Biophys. Res. Comm., 278*, 408-413 (2000).

93. Roy, D., Spector, A., and Farnesworth, P., Human lens membrane: comparison of major intrinsic polypeptides from young and old lenses isolated by a new methodology, *Exp. Eye Res., 28*, 353-358 (1979).

94. Horwitz, J., and Wong, M. M., Peptide mapping by limited proteolysis in sodium dodecyl sulfate of the main intrinsic polypeptide isolated from human and bovine lens plasma membranes., *Biochem. Biophys. Acta., 622*, 124-143 (1980).

95. Takemoto, L., Takehana, M., and Horwitz, J., Antisera to synthetic peptides of MIP26K as probes of membrane changes during human cataractogenesis, *Exp. Eye Res., 42*, 497-501 (1986).

96. Takemoto, L., and Takehana, M., Covalent change of major intrinsic polypeptide (MIP26K) of lens membrane during human senile cataractogenesis, *Biochem. Biophys. Res. Comm., 135*, 965-71 (1986).

97. Takemoto, L., Takehana, M., and Horwitz, J., Covalent changes in MIP26K during aging of the human lens membrane, *Invest. Ophthalmol. Vis. Sci., 27*, 443-6 (1986).

98. Takemoto, L., Smith, J., and Kodama, T., Major intrinsic polypeptide (MIP26K) of the lens membrane: covalent change in an internal sequence during human senile cataractogenesis, *Biochem. Biophys. Res. Comm., 142*, 761-6 (1987).

99. Ma, Z., Hanson, S. R., Lampi, K. J., David, L. L., Smith, D. L., and Smith, J. B., Age-related changes in human lens crystallins identified by HPLC and mass spectrometry, *Exp. Eye Res.., 67*, 21-30 (1998).

100. MacCoss, M. J., McDonald, W. H., Saraf, A., Sadygov, R., Clark, J. M., Tasto, J. J., Gould, K. L., Wolters, D., Washburn, M., Weiss, A., Clark, J. I., and Yates, J. R.,

Shotgun identification of protein modifications from protein complexes and lens tissue, *Proc. Natl. Acad. Sci. USA., 99*, 7900-7905 (2002).

101. Hammond, C., The epidemilogy of cataract, *Optometry*, 24-29 (2001).

102. Berry, V., Francis, P., Kaushal, S., Moore, A., and Bhattacharya, S., Missense mutations in MIP underlie autosomal dominant 'polymorphic' and lamellar cataracts linked to 12q, *Nat. Genet., 25*, 15-7 (2000).

103. Bateman, J. B., Johannes, M., Flodman, P., Geyer, D. D., Clancy, K. P., Heinzmann, C., Kojis, T., Berry, R., Sparkes, R. S., and Spence, M. A., A new locus for autosomal dominant cataract on chromosome 12q13, *Invest. Ophthalmol. Vis. Sci., 41*, 2665-70 (2000).

104. Taylor, A., and Hobbs, M., 2001 assessment of nutritional influences on risk for cataract, *Nutrition, 17*, 845-57 (2001).

105. Sackett, C. S., and Schenning, S., The age-related eye disease study: the results of the clinical trial, *Insight, 27*, 5-7 (2002).

106. Gilmartin, B., The aetiology of presbyopia: a summary of the role of lenticular and extralenticular structures, *Ophthalmic Physiol. Opt., 15*, 431-7 (1995).

107. Atchison, D. A., Accommodation and presbyopia, *Ophthalmic Physiol. Opt, 15*, 255-72 (1995).

108. Sidel, V., and Solomon, A., Entrance of water into human red cells under an osmotic pressure gradient, *J. Gen. Physiol., 41*, 243-257 (1957).

109. Verkman, A. S., Water permeability measurement in living cells and complex tissues [Review], *J. Membr. Biol., 173*, 73-87 (2000).

110. Preston, G. M., and Agre, P., Isolation of the cDNA for erythrocyte integral membrane protein of 28 kilodaltons: member of an ancient channel family, *Proc. Natl. Acad. Sci. USA., 88*, 11110-4 (1991).

111. Zeidel, M. L., Ambudkar, S. V., Smith, B. L., and Agre, P., Reconstitution of functional water channels in liposomes containing purified red cell CHIP28 protein, *Biochemistry, 31*, 7436-40 (1992).

112. Mulders, S. M., Preston, G. M., Deen, P. M., Guggino, W. B., van Os, C. H., and Agre, P., Water channel properties of major intrinsic protein of lens, *J. Biol. Chem., 270*, 9010-16 (1995).

113. Park, J. H., and Saier, M. H., Phylogenetic characterization of the MIP family of transmembrane channel proteins, *J. Membr. Biol., 153*, 171-180 (1996).

114. Wistow, G. J., Pisano, M. M., and Chepelinsky, A. B., Tandem sequence repeats in transmembrane channel proteins, *Trends Biochem. Sci., 16*, 170-1 (1991).

115. Agre, P., King, L. S., Yasui, M., Guggino, W. B., Ottersen, O. P., Fujiyoshi, Y., Engel, A., and Nielsen, S., Aquaporin water channels - from atomic structure to clinical medicine, *J. Physiol. London, 542*, 3-16 (2002).

116. Verkman, A. S., van Hoek, A. N., Ma, T., Frigeri, A., Skach, W. R., Mitra, A., Tamarappoo, B. K., and Farinas, J., Water transport across mammalian cell membranes, *Am. J. Physiol., 270*, C12-30 (1996).

117. Hamann, S., Zeuthen, T., Lacour, M., Ottersen, O. P., Agre, P., and Nielsen, S., Aquaporins in Complex Tissues - Distribution of Aquaporins 1-5 in Human and Rat Eye, *Am. J. Physiol. Cell Physiol., 43*, C1332-C1345 (1998).

118. Nielsen, S., Frokiaer, J., Marples, D., Kwon, T. H., Agre, P., and Knepper, M. A., Aquaporins in the kidney: From molecules to medicine, *Physiol. Rev., 82*, 205-244 (2002).

119. Huebert, R. C., Splinter, P. L., Garcia, F., Marinelli, R. A., and LaRusso, N. F., Expression and localization of aquaporin water channels in rat hepatocytes - Evidence for a role in canalicular bile secretion, *J. Biol. Chem., 277*, 22710-22717 (2002).

120. Steinfeld, S., Cogan, E., King, L. S., Agre, P., Kiss, R., and Delporte, C., Abnormal distribution of aquaporin-5 water channel protein in salivary glands from Sjogren's syndrome patients, *Lab. Invest., 81*, 143-148 (2001).

121. Shiels, A., Bassnett, S., Varadaraj, K., Mathias, R., Al-Ghoul, K., Kuszak, J., Donoviel, D., Lilleberg, S., Friedrich, G., and Zambrowicz, B., Optical dysfunction of the crystalline lens in aquaporin-0-deficient mice, *Physiol. Genomics, 7*, 179-186 (2001).

122. Verkman, A. S., Yang, B. X., Song, Y. L., Manley, G. T., and Ma, T. H., Role of water channels in fluid transport studied by phenotype analysis of aquaporin knockout mice, *Exp. Physiol., 85* (2000).

123. Li, J., and Verkman, A. S., Impaired hearing in mice lacking aquaporin-4 water channels, *J. Biol. Chem., 276*, 31233-31237 (2001).

124. Tsubota, K., Hirai, S., King, L. S., Agre, P., and Ishida, N., Defective cellular trafficking of lacrimal gland aquaporin-5 in Sjogren's syndrome, *Lancet, 357*, 688-689 (2001).

125. Fotiadis, D., Hasler, L., Muller, D. J., Stahlberg, H., Kistler, J., and Engel, A., Surface tongue-and-groove contours on lens MIP facilitate cell-to-cell adherence, *J. Mol. Biol., 300*, 779-789 (2000).

126. Hasler, L., Walz, T., Tittmann, P., Gross, H., Kistler, J., and Engel, A., Purified Lens Major Intrinsic Protein (Mip) Forms Highly Ordered Tetragonal Two-Dimensional Arrays By Reconstitution, *J. Mol. Biol., 279*, 855-864 (1998).

127. de Groot, B. L., Engel, A., and Grubmuller, H., A refined structure of human aquaporin-1, *FEBS Lett., 504*, 206-211 (2001).

128. Sui, H. X., Han, B. G., Lee, J. K., Walian, P., and Jap, B. K., Structural basis of water-specific transport through the AQP1 water channel, *Nature, 414*, 872-878 (2001).

129. Cheng, A. C., Vanhoek, A. N., Yeager, M., Verkman, A. S., and Mitra, A. K., Three-Dimensional Organization of a Human Water Channel, *Nature, 387*, 627-630 (1997).

130. Jung, J. S., Preston, G. M., Smith, B. L., Guggino, W. B., and Agre, P., Molecular structure of the water channel through aquaporin CHIP. The hourglass model, *J. Biol. Chem., 269*, 14648-54 (1994).

131. Mitsuoka, K., Murata, K., Walz, T., Hirai, T., Agre, P., Heymann, J. B., Engel, A., and Fujiyoshi, Y., The structure of aquaporin-1 at 4.5-angstrom resolution reveals short alpha-helices in the center of the monomer, *J. Struct. Biol., 128*, 34-43 (1999).

132. Aerts, T., Xia, J. Z., Slegers, H., de Block, J., and Clauwaert, J., Hydrodynamic characterization of the major intrinsic protein from the bovine lens fiber membranes. Extraction in n-octyl-beta-D-glucopyranoside and evidence for a tetrameric structure, *J. Biol. Chem., 265*, 8675-80 (1990).

133. Konig, N., Zampighi, G. A., and Butler, P. J., Characterisation of the major intrinsic protein (MIP) from bovine lens fibre membranes by electron microscopy and hydrodynamics, *J. Mol. Biol., 265*, 590-602 (1997).

134. Smith, B., and Agre, P., Erythrocyte M_r 28,000 transmembrane protein exists as a multisubunit oligomer., *J. Biol. Chem., 266*, 6407-6415 (1991).

135. Fujiyoshi, Y., Mitsuoka, K., de Groot, B. L., Philippsen, A., Grubmuller, H., Agre, P., and Engel, A., Structure and function of water channels, *Curr. Opin. Struct. Biol., 12*, 509-515 (2002).

136. Preston, G. M., Jung, J. S., Guggino, W. B., and Agre, P., The mercury-sensitive residue at cysteine 189 in the CHIP28 water channel, *J. Biol. Chem., 268*, 17-20 (1993).

137. van Hoek, A. N., Hom, M. L., Luthjens, L. H., de Jong, M. D., Dempster, J. A., and van Os, C. H., Functional unit of 30 kDa for proximal tubule water channels as revealed by radiation inactivation, *J. Biol. Chem., 266*, 16633-16635 (1991).

138. Shi, L. B., Skach, W. R., and Verkman, A. S., Functional independence of monomeric CHIP28 water channels revealed by expression of wild-type mutant heterodimers, *J. Biol. Chem., 269*, 10417-22 (1994).

139. Fotiadis, D., Suda, K., Tittmann, P., Jeno, P., Philippsen, A., Muller, D. J., Gross, H., and Engel, A., Identification and structure of a putative Ca2+-binding domain at the C terminus of AQP1, *J. Mol. Biol., 318*, 1381-1394 (2002).

140. Shiels, A., MacKay, D., Bassnett, S., Al-Ghoul, K., and Kuszak, J., Disruption of lens fiber cell architecture in mice expressing a chimeric AQP0-LTR protein, *FASEB J., 14*, 2207-2212 (2000).

141. Mulders, S. M., Bichet, D. G., Rijss, J. P. L., Kamsteeg, E. J., Arthus, M. F., Lonergan, M., Fujiwara, M., Morgan, K., Leijendekker, R., Vandersluijs, P., Vanos, C. H., and Deen, P. M. T., An Aquaporin-2 Water Channel Mutant Which Causes

Autosomal Dominant Nephrogenic Diabetes Insipidus Is Retained in the Golgi Complex, *J. Clin. Invest., 102*, 57-66 (1998).

142. Kamsteeg, E. J., Wormhoudt, T. A. M., Rijss, J. P. L., van Os, C. H., and Deen, P. M. T., An impaired routing of wild-type aquaporin-2 after tetramerization with an aquaporin-2 mutant explains dominant nephrogenic diabetes insipidus, *EMBO J., 18*, 2394-2400 (1999).

143. Swamy-Mruthinti, S., Glycation decreases calmodulin binding to lens transmembrane protein, MIP, *Biochem. Biophys. Acta, 1536*, 64-72 (2001).

144. Fushimi, K., Sasaki, S., and Marumo, F., Phosphorylation of Serine 256 Is Required For Camp-Dependent Regulatory Exocytosis of the Aquaporin-2 Water Channel, *J. Biol. Chem., 272*, 14800-14804 (1997).

145. Heymann, J., and Engel, A., Aquaporins: Phylogeny, Structure, and Physiology of Water Channels, *News Physiol. Sci., 14*, 187-193 (1999).

146. Sansom, M. S. P., and Law, R. J., Membrane proteins: Aquaporins - channels without ions, *Curr. Biol., 11*, R71-R73 (2001).

147. de Groot, B. L., and Grubmuller, H., Water permeation across biological membranes: Mechanism and dynamics of aquaporin-1 and GlpF, *Science, 294*, 2353-2357 (2001).

148. Murata, K., Mitsuoka, K., Hirai, T., Walz, T., Agre, P., Heymann, J. B., Engel, A., and Fujiyoshi, Y., Structural determinants of water permeation through aquaporin-1, *Nature, 407*, 599-605 (2000).

149. Sansom, M. S., Shrivastava, I. H., Ranatunga, K. M., and Smith, G. R., Simulations of ion channels--watching ions and water move, *Trends Biochem. Sci., 25*, 368-74 (2000).

150. Meinild, A. K., Klaerke, D. A., and Zeuthen, T., Bidirectional water fluxes and specificity for small hydrophilic molecules in aquaporins 0-5, *J. Biol. Chem., 273*, 32446-51 (1998).

151. Leitch, V., Agre, P., and King, L. S., Altered ubiquitination and stability of aquaporin-1 in hypertonic stress, *Proc. Natl. Acad. Sci. USA, 98*, 2894-8 (2001).

152. Umenishi, F., and Schrier, R. W., Identification and characterization of a novel hypertonicity-responsive element in the human aquaporin-1 gene, *Biochem. Biophys. Res. Commun., 292*, 771-5 (2002).

153. Yamamoto, N., Sobue, K., Miyachi, T., Inagaki, M., Miura, Y., Katsuya, H., and Asai, K., Differential regulation of aquaporin expression in astrocytes by protein kinase C, *Mol. Brain Res., 95*, 110-116 (2001).

154. Yamamoto, N., Sobue, K., Fujita, M., Katsuya, H., and Asai, K., Differential regulation of aquaporin-5 and-9 expression in astrocytes by protein kinase A, *Mol. Brain Res., 104*, 96-102 (2002).

155. van Balkom, B. W., Savelkoul, P. J., Markovich, D., Hofman, E., Nielsen, S., van der Sluijs, P., and Deen, P. M., The role of putative phosphorylation sites in the targeting and shuttling of the aquaporin-2 water channel, *J. Biol. Chem., 277*, 41473-9 (2002).

156. Zelenina, M., Zelenin, S., Bondar, A. A., Brismar, H., and Aperia, A., Water permeability of aquaporin-4 is decreased by protein kinase C and dopamine, *Am. J. Physiol. Renal Physiol., 283* (2002).

157. Garcia, F., Kierbel, A., Larocca, M. C., Gradilone, S. A., Splinter, P., LaRusso, N. F., and Marinelli, R. A., The water channel aquaporin-8 is mainly intracellular in rat hepatocytes, and its plasma membrane insertion is stimulated by cyclic AMP, *J. Biol. Chem., 276*, 12147-12152 (2001).

158. Han, Z. Q., Wax, M. B., and Patil, R. V., Regulation of Aquaporin-4 Water Channels By Phorbol Ester-Dependent Protein Phosphorylation, *J. Biol. Chem., 273*, 6001-6004 (1998).

159. Hirsch, J. R., Loo, D. D. F., and Wright, E. M., Regulation of Na+/Glucose Cotransporter Expression By Protein Kinases in Xenopus Laevis Oocytes, *J. Biol. Chem., 271*, 14740-14746 (1996).

160. Chou, C. L., Yip, K. P., Michea, L., Kador, K., Ferraris, J. D., Wade, J. B., and Knepper, M. A., Regulation of aquaporin-2 trafficking by vasopressin in the renal collecting duct - Roles of ryanodine-sensitive Ca2+ stores and calmodulin, *J. Biol. Chem., 275*, 36839-36846 (2000).

161. Nemeth-Cahalan, K. L., and Hall, J. E., pH and calcium regulate the water permeability of Aquaporin 0, *J. Biol. Chem., 275*, 6777-6782 (2000).

162. Girsch, S. J., and Peracchia, C., Calmodulin interacts with a C-terminus peptide from the lens membrane protein MIP26, *Curr. Eye Res., 10*, 839-49 (1991).

163. Zeuthen, T., and Klaerke, D. A., Transport of water and glycerol in aquaporin 3 is gated by H(+), *J. Biol. Chem., 274*, 21631-6 (1999).

164. Virkki, L. V., Cooper, G. J., and Boron, W. F., Cloning and functional expression of an MIP (AQP0) homolog from killifish (Fundulus heteroclitus) lens, *Am. J. Physiol. Regul. Integr. Comp. Physiol., 281* (2001).

165. Mathias, R., Riquelme, G., and Rae, J., Cell to cell communication and pH in the frog lens, *J. Gen. Physiol., 98*, 1085-1103 (1991).

166. Zhou, L., Chen, T., and Church, R. L., Temporal expression of three mouse lens fiber cell membrane protein genes during early development, *Mol. Vis., 8*, 143-8 (2002).

167. Muggleton-Harris, A. L., Hardy, K., and Higbee, N., Rescue of developmental lens abnormalities in chimaeras of noncataractous and congenital cataractous mice, *Development, 99*, 473-80 (1987).

168. Chandy, G., Zampighi, G. A., Kreman, M., and Hall, J. E., Comparison of the Water Transporting Properties of Mip and Aqp1, *J. Membr. Biol., 159*, 29-39 (1997).

169. Kushmerick, C., Rice, S. J., Baldo, G. J., Haspel, H. C., and Mathias, R. T., Ion, water and small neutral solute transport in Xenopus oocytes expressing frog lens MIP, *Exp. Eye Res., 61*, 351-362 (1995).

170. Shiels, A., Griffin, C. S., and Muggleton-Harris, A. L., Immunochemical comparison of the major intrinsic protein of eye-lens fibre cell membranes in mice with hereditary cataracts, *Biochem. Biophys. Acta, 1097*, 318-24 (1991).

171. Sidjanin, D. J., Parker-Wilson, D. M., Neuhauser-Klaus, A., Pretsch, W., Favor, J., Deen, P. M. T., Ohtaka-Maruyama, C., Lu, Y., Bragin, A., Skach, W. R., Chepelinsky, A. B., Grimes, P. A., and Stambolian, D. E., A 76-bp deletion in the Mip gene causes autosomal dominant cataract in Hfi mice, *Genomics, 74*, 313-319 (2001).

172. Kuszak, J., Shiels, A., Kuszak, A., Kirk, T., and Novak, L., Freeze-etch analysis of lens cortical fiber membrane from aquaporin 0 or MIP knockout mice, *Invest. Ophthalmol. Vis. Sci., 42*, 4718 (2001).

173. Geyer, D. D., Flodman, P., Spence, M. A., and Bateman, J. B., Sequence analyses of the major intrinsic protein (MIP) candidate gene in an autosomal dominant cataract family, *ARVO, #3* (2000).

174. Zampighi, G. A., Kreman, M., Boorer, K. J., Loo, D. D. F., Bezanilla, F., Chandy, G., Hall, J. E., and Wright, E. M., A Method For Determining the Unitary Functional Capacity of Cloned Channels and Transporters Expressed in Xenopus Laevis Oocytes, *J. Membr. Biol., 148*, 65-78 (1995).

175. Mulders, S. M., Vanderkemp, A. J., Terlouw, S. A., Vanboxtel, H. A. F., Vanos, C. H., and Deen, P. M. T., The Exchange of Functional Domains Among Aquaporins With Different Transport Characteristics, *Pflugers Arch., 436*, 599-607 (1998).

176. Kuwahara, M., Shinbo, I., Sato, K., Terada, Y., Marumo, F., and Sasaki, S., Transmembrane helix 5 is critical for the high water permeability of aquaporin, *Biochemistry., 38*, 16340-6 (1999).

177. Zampighi, G., Hall, J., Ehring, G., and Simon, S., The structural organization and protein composition of lens fiber junctions, *J. Cell Biol, 108*, 2255-2274 (1989).

178. Dunia, I., Recouvreur, M., Nicolas, P., Kumar, N., Bloemendal, H., and Benedetti, E. L., Assembly of Connexins and Mp26 in Lens Fiber Plasma Membranes Studied By Sds-Fracture Immunolabeling, *J. Cell Sci., 111*, 2109-2120 (1998).

179. Michea, L. F., de la Fuente, M., and Lagos, N., Lens major intrinsic protein (MIP) promotes adhesion when reconstituted into large unilamellar liposomes, *Biochemistry, 33*, 7663-9 (1994).

180. Ehring, G. R., Lagos, N., Zampighi, G. A., and Hall, J. E., Phosphorylation modulates the voltage dependence of channels reconstituted from the major intrinsic protein of lens fiber membranes, *J. Membr. Biol., 126*, 75-88 (1992).

181. Ehring, G. R., Zampighi, G., Horwitz, J., Bok, D., and Hall, J. E., Properties of channels reconstituted from the major intrinsic protein of lens fiber membranes, *J. of Gen. Physiol., 96*, 631-64 (1990).

182. Swenson, K. I., Jordan, J. R., Beyer, E. C., and Paul, D. L., Formation of gap junctions by expression of connexins in Xenopus oocyte pairs, *Cell, 57*, 145-55 (1989).

183. Shen, L., Shrager, P., Girsch, S. J., Donaldson, P. J., and Peracchia, C., Channel reconstitution in liposomes and planar bilayers with HPLC-purified MIP26 of bovine lens, *J. Membr. Biol., 124*, 21-32 (1991).

184. Peracchia, C., and Girsch, S. J., Is the C-terminal arm of lens gap junction channel protein the channel gate?, *Biochem. Biophys. Res. Comm., 133*, 688-95 (1985).

185. Drake, K. D., Schuette, D., Chepelinsky, A. B., Jacob, T. J., and Crabbe, M. J., pH-Dependent channel activity of heterologously-expressed main intrinsic protein (MIP) from rat lens, *FEBS Lett., 512*, 199-204 (2002).

186. Goodenough, D. A., Lens gap junctions: a structural hypothesis for nonregulated low-resistance intercellular pathways, *Invest. Ophthalmol. Vis. Sci., 18*, 1104-22 (1979).

187. Lampe, P. D., and Johnson, R. G., Phosphorylation of MIP26, a lens junction protein, is enhanced by activators of protein kinase C, *J. Membr. Biol., 107*, 145-155 (1989).

188. Johnson, K., Lampe, P., Hur, K., Louis, C., and Johnson, R., A lens intercellular junction protein, MP26, is a phosphoprotein, *J. Cell Biol., 102*, 1334-43 (1986).

189. Garland, D., and Russell, P., Phosphorylation of lens fiber cell membranes, *Proc. Natl. Acad. Sci., 82*, 653-657 (1985).

190. Louis, C., Johnson, R., Johnson, K., and Turnquist, J., Characterization of the bovine lens plasma membrane substrates for cAMP-dependent protein kinase, *Eur. J. Biochem., 150*, 279-286 (1985).

191. Lampe, P., and Johnson, R., Amino acid sequence of in vivo phosphorylatin sites in the main intrinsic protein (MIP) of lens membranes, *Eur. J. Biochem., 194*, 541-547 (1990).

192. Schey, K. L., Fowler, J. G., Schwartz, J. C., Busman, M., Dillon, J., and Crouch, R. K., Complete map and identification of the phosphorylation site of bovine lens major intrinsic protein, *Invest. Ophthalmol. Vis. Sci., 38*, 2508-15 (1997).

193. Takemoto, L., and Emmons, T., Age-dependent deamidation of the major intrinsic polypeptide from lens membranes, *Curr. Eye Res., 10*, 865-9 (1991).

194. Horwitz, J., Robertson, N., Wong, M., Zigler, J., and Kinoshita, J., Some properties of lens plasma membrane polypeptides isolated from normal human lenses., *Exp. Eye Res., 28*, 359-365 (1979).

195. Roy, D., Age-dependent changes in the abundance of the major polypeptides of the human lens membrane, *Biochem. Biophys. Res. Commun., 88*, 30-31 (1979).

196. Alcala, J., and Maisel, H., Biochemsitry of lens plasma membranes and cytoskeleton., in *The Ocular Lens*, Maisel, H., Ed., Marcel Dekker, New York, pp. 169-222 (1984).

197. Paroutaud, P., Dunia, I., Benedetti, E. L., and Hoebeke, J., Sequence analysis of peptide fragments from the major intrinsic membrane protein of calf lens fibers MP26 and its natural maturation product MP22., *FEBS Lett., 181*, 74-78 (1985).

198. Takemoto, L. J., Gorthy, W. C., Morin, C. L., and Steward, D. E., Changes in lens membrane major intrinsic polypeptide during cataractogenesis in aged Hannover Wistar rats, *Invest. Ophthalmol. Vis. Sci., 32*, 556-61 (1991).

199. Granstrom, D., Swamy, M., Abraham, E., and Takemoto, L., Covalent change in the major intrinsic polypeptide (MIP26K) during cataract development in the streptozotocin-induced diabetic rat, *Curr. Eye Res., 8*, 589-93 (1989).

200. Takemoto, L., Kuck, J., and Kuck, K., Changes in the major intrinsic polypeptide (MIP26K) during opacification of the Emory mouse lens, *Exp. Eye Res., 47*, 329-36 (1988).

201. Padgaonkar, V. A., Lin, L. R., Leverenz, V. R., Rinke, A., Reddy, V. N., and Giblin, F. J., Hyperbaric oxygen in vivo accelerates the loss of cytoskeletal proteins and MIP26 in guinea pig lens nucleus, *Exp. Eye Res., 68*, 493-504 (1999).

202. Shearer, T. R., Ma, H., Fukiage, C., and Azuma, M., Selenite nuclear cataract: review of the model, *Mol. Vis., 3*, 8 (1997).

203. Beebe, D. C., Nuclear cataracts and nutrition: hope for intervention early and late in life [comment], *Invest. Ophthalmol. Vis. Sci., 39*, 1531-4 (1998).

204. Bassnett, S., Lens organelle degradation, *Exp. Eye Res., 74*, 1-6 (2002).

205. Lyon, M. F., Jarvis, S. E., Sayers, I., and Holmes, R. S., Lens opacity: a new gene for congenital cataract on chromosome 10 of the mouse, *Genet. Res., 38*, 337-341 (1981).

206. Muggleton-Harris, A. L., Festing, M. F. W., and Hall, M., A gene location for the inheritance of the cataract Fraser (Cat^{Fr}) mouse congenital cataract, *Genet. Res., 49*, 235-238 (1987).

207. Bradford, M. M., A rapid and sensitive method for the quantitation of microgram quantities of protein utilizing the principle of protein-dye binding, *Anal. Biochem., 72*, 248-254 (1976).

208. Schey, K. L., Hydrophobic proteins and peptides analyzed by matrix-assisted laser desorption/ionization, *Methods Mol. Biol., 61*, 227-30 (1996).

209. Voorter, C., and Kistler, J., cAMP-dependent protein kinase phosphorylates gap junction protein in lens cortex but not in lens nucleus, *Biochim. Biophys. Acta., 986*, 8-10 (1989).

210. Arneson, M., Cheng, H., and Louis, C., Characterization of the ovine-lens plasma-membrane protein-kinase substrate, *Eur. J. Biochem., 234*, 670-679 (1995).

211. McFadden, P. N., Horwitz, J., and Clarke, S., Protein carboxyl methyltransferase from cow eye lens, *Biochem. Biophys. Res. Comm., 113*, 418-24 (1983).

212. McFadden, P. N., and Clarke, S., Protein carboxyl methyltransferase and methyl acceptor proteins in aging and cataractous tissue of the human eye lens, *Mech. Age Dev., 34*, 91-105 (1986).

213. Young, A. L., Carter, W. G., Doyle, H. A., Mamula, M. J., and Aswad, D. W., Structural integrity of histone H2B in vivo requires the activity of protein L-isoaspartate O-methyltransferase, a putative protein repair enzyme, *J. Biol. Chem.., 276*, 37161-5 (2001).

214. Maric, K., Wiesner, B., Lorenz, D., Klussmann, E., Betz, T., and Rosenthal, W., Cell volume kinetics of adherent epithelial cells measured by laser scanning reflection microscopy: Determination of water permeability changes of renal principal cells, *Biophys. J., 80*, 1783-1790 (2001).

215. Zhang, R. B., and Verkman, A. S., Water and urea permeability properties of Xenopus oocytes: expression of mRNA from toad urinary bladder, *Am. J. Physiol., 260*, C26-34 (1991).

216. Quick, M. W., and Lester, H. A., Methods for expression of excitability proteins in *Xenopus* oocytes, *Methods Neurosci., 19*, 261-279 (1994).

217. Agre, P., Mathai, J. C., Smith, B. L., and Preston, G. M., Functional analyses of aquaporin water channel proteins, *Methods Enzymol., 294*, 550-72 (1999).

218. Ma, T., Frigeri, A., Tsai, S. T., Verbavatz, J. M., and Verkman, A. S., Localization and functional analysis of CHIP28k water channels in stably transfected Chinese hamster ovary cells, *J. Biol. Chem., 268*, 22756-64 (1993).

219. Farinas, J., Simanek, V., and Verkman, A. S., Cell volume measured by total internal reflection microfluorimetry: application to water and solute transport in cells transfected with water channel homologs, *Biophys. J., 68*, 1613-20 (1995).

220. Van Driessche, W., De Smet, P., and Raskin, G., An automatic monitoring system for epithelial cell height, *Pflugers Arch., 425*, 164-71 (1993).

221. Verkman, A. S., Aquaporin water channels and endothelial cell function, *J. Anat., 200*, 617-627 (2002).

222. Gradilone, S. A., Ochoa, J. E., Garcia, F., Larocca, M. C., Pellegrino, J. M., and Marinelli, R. A., Hepatocyte membrane water permeability measured by silicone layer filtering centrifugation, *Anal. Biochem., 302*, 104-107 (2002).

223. Solenov, E. I., Vetrivel, L., Oshio, K., Manley, G. T., and Verkman, A. S., Optical measurement of swelling and water transport in spinal cord slices from aquaporin null mice, *J. Neurosci. Methods, 113*, 85-90 (2002).

224. Nowak, M. W., Gallivan, J. P., Silverman, S. K., Labarca, C. G., Dougherty, D. A., and Lester, H. A., In vivo incorporation of unnatural amino acids into ion channels in Xenopus oocyte expression system, *Methods Enzymol., 293*, 504-29 (1998).

225. Pisano, M. M., and Chepelinsky, A. B., Genomic cloning, complete nucleotide sequence, and structure of the human gene encoding the major intrinsic protein (MIP) of the lens, *Genomics, 11*, 981-90 (1991).

226. Louis, C. F., Hur, K. C., Galvan, A. C., TenBroek, E. M., Jarvis, L. J., Eccelston, E. D., and Howard, J. B., Identifications of an 18,000 Dalton protein in mammalian lens fiber cell membranes, *J. Biol. Chem., 264*, 19967-19973 (1989).

227. Pfeuffer, J., Broer, S., Broer, A., Lechte, M., Flogel, U., and Leibfritz, D., Expression of aquaporins in Xenopus laevis oocytes and glial cells as detected by diffusion-weighted 1H NMR spectroscopy and photometric swelling assay, *Biochim. Biophys. Acta., 1448*, 27-36 (1998).

228. Iserovich, P., Kuang, K., Chun, T., and Fischbarg, J., A novel method to determine the diffusional water permeability of oocyte plasma membranes, *Biol. Cell, 89*, 293-7 (1997).

229. Traebert, M., Kohler, K., Lambert, G., Biber, J., Forster, I., and Murer, H., Investigating the surface expression of the renal type IIa Na+/P-i-cotransporter in Xenopus laevis oocytes, *J. Membr. Biol., 180*, 83-90 (2001).

230. Kamsteeg, E. J., and Deen, P. M. T., Detection of aquaporin-2 in the plasma membranes of oocytes: A novel isolation method with improved yield and purity, *Biochem. Biophys. Res. Comm., 282*, 683-690 (2001).

231. Stith, B. J., Hall, J., Ayres, P., Waggoner, L., Moore, J. D., and Shaw, W. A., Quantification of major classes of Xenopus phospholipids by high performance liquid chromatography with evaporative light scattering detection, *J. Lipid Res., 41*, 1448-54 (2000).

232. Valiyaveetil, F. I., Zhou, Y., and MacKinnon, R., Lipids in the structure, folding, and function of the KcsA K+ channel, *Biochemistry, 41*, 10771-7 (1077).

233. Brown, D., Targeting of membrane transporters in renal epithelia: when cell biology meets physiology, *Am. J. Physiol. Renal Fluid & Electrolyte Physiol., 278*, F192-201 (2000).

234. Shih, T., Smith, R., Toro, L., and Goldin, A., High-level expression and detection of ion channels in Xenopus oocytes., *Methods Enzymol., 293*, 529-555 (1998).

235. Kamsteeg, E. J., Heijnen, I., van Os, C. H., and Deen, P. M., The subcellular localization of an aquaporin-2 tetramer depends on the stoichiometry of phosphorylated and nonphosphorylated monomers, *J. Cell Biol., 151*, 919-30 (2000).

236. Knepper, M. A., and Inoue, T., Regulation of Aquaporin-2 Water Channel Trafficking By Vasopressin, *Curr. Opin. Cell Biol., 9*, 560-564 (1997).

237. Boyle, D. L., and Takemoto, L. J., Localization of MIP 26 in nuclear fiber cells from aged normal and age-related nuclear cataractous human lenses, *Exp. Eye Res., 68*, 41-49 (1999).

238. Deen, P. M., Van Balkom, B. W., Savelkoul, P. J., Kamsteeg, E. J., Van Raak, M., Jennings, M. L., Muth, T. R., Rajendran, V., and Caplan, M. J., Aquaporin-2: COOH terminus is necessary but not sufficient for routing to the apical membrane, *Am. J. Physiol. Renal Fluid & Electrolyte Physiol, 282* (2002).

239. Moffat, B. A., Atchison, D. A., and Pope, J. M., Age-related changes in refractive index distribution and power of the human lens as measured by magnetic resonance micro-imaging in vitro, *Vis. Res., 42*, 1683-1693 (2002).

240. Moffat, B. A., and Pope, J. M., The interpretation of multi-exponential water proton transverse relaxation in the human and porcine eye lens, *Magn. Reson. Imaging, 20*, 83-93 (2002).